JHR 57: 1–87 (2017)
doi: 10.3897/jhr.57.12892
http://jhr.pensoft.net

RESEARCH ARTICLE

JOURNAL OF Hymenoptera RESEARCH
A peer-reviewed open-access journal
The International Society of Hymenopterists

Eustochomorpha Girault, *Neotriadomerus* gen. n., and *Proarescon* gen. n. (Hymenoptera, Mymaridae), early extant lineages in evolution of the family

John T. Huber[1]

1 *Natural Resources Canada, c/o Canadian National Collection of Insects, AAFC, K.W. Neatby Building, 960 Carling Avenue, Ottawa, ON, K1A 0C6, Canada*

Corresponding author: *John T. Huber* (john.huber@agr.gc.ca)

Academic editor: *Petr Jansta* | Received 23 March 2017 | Accepted 8 May 2017 | Published 30 June 2017

http://zoobank.org/6201DACE-9900-4A2F-92C9-D3014851100D

Citation: Huber JT (2017) *Eustochomorpha* Girault, *Neotriadomerus* gen. n., and *Proarescon* gen. n. (Hymenoptera, Mymaridae), early extant lineages in evolution of the family. Journal of Hymenoptera Research 57: 1–87. https://doi.org/10.3897/jhr.57.12892

Abstract

Eustochomorpha Girault, with one described species, *E. haeckeli* Girault, from Australia is redescribed. *Neotriadomerus* Huber, **gen. n.**, is described, together with seven new species, all from Australia: *N. burwelli* Huber, **sp. n.**, *N. crassus* Huber, **sp. n.**, *N. darlingi* Huber, **sp. n.**, *N. gloriosus* Huber, **sp. n.**, *N. longiovipositor* Huber, **sp. n.**, *N. longissimus* Huber, **sp. n.** (one of the largest species of Mymaridae), and *N. powerae* Huber, **sp. n.** *Proarescon* Huber, **gen. n.**, is described for *P. primitivum* (Huber), **comb. n.**, transferred from *Borneomymar* Huber, and *P. similis* Huber, **sp. n.**, from Thailand. The previously unknown male of *Borneomymar madagascar* Huber is described and the genus is redescribed from critical point dried and slide mounted specimens. Triadomerini, **stat. n.**, is proposed to include six genera: *Borneomymar*, *Eustochomorpha* and *Neotriadomerus*, and the Cretaceous *Carpenteriana* Yoshimoto, *Macalpinia* Yoshimoto and *Triadomerus* Yoshimoto. Aresconini is proposed to include five (possibly six) genera: *Arescon* Enock, *Kikiki* Huber and Beardsley, *Proarescon* Huber and *Tinkerbella* Huber and Noyes, and the Cretaceous *Myanmymar* Huber and, tentatively, also *Enneagmus* Yoshimoto. The two tribes are proposed as being the earliest lineages in Mymaridae, with *Neotriadomerus* and *Triadomerus* being sister genera to the remaining extant and extinct genera, respectively.

Keywords

Taxonomy, Chalcidoidea, fairyfly, new genera, Australia, Thailand, earliest lineages

Copyright *John T. Huber*. This is an open access article distributed under the terms of the Creative Commons Attribution License (CC BY 4.0), which permits unrestricted use, distribution, and reproduction in any medium, provided the original author and source are credited.

Table of contents

Introduction 2
Methods 3
Results 4
Eustochomorpha Girault 1915 4
Eustochomorpha haeckeli Girault 6
Neotriadomerus Huber, gen. n. 14
Neotriadomerus burwelli Huber, sp. n. 25
Neotriadomerus crassus Huber, sp. n. 28
Neotriadomerus darlingi Huber, sp. n. 32
Neotriadomerus gloriosus Huber, sp. n. 40
Neotriadomerus longiovipositor Huber, sp. n. 43
Neotriadomerus longissimus Huber, sp. n. 51
Neotriadomerus powerae Huber, sp. n. 53
Neotriadomerus sp. 1. 60
Neotriadomerus sp. 2 60
Neotriadomerus sp. 3 60
Neotriadomerus sp. 4 62
Proarescon Huber, gen. n. 66
Proarescon primitivus (Huber), comb. n. 68
Proarescon similis Huber, sp. n. 69
Borneomymar Huber 77
Borneomymar madagascar Huber 81
Tribe Triadomerini, stat. n. 82
Tribe Aresconini 83
Discussion 84
Conclusions 85
Acknowledgements 85
References 86

Introduction

Eustochomorpha Girault (Hymenoptera: Mymaridae) includes a single species, *E. haeckeli* Girault (Girault 1915). Annecke and Doutt (1961) included *Eustochomorpha* in a world key, basing its placement in the key only on Girault'S, succinct but accurate original description; they did not locate the type. Dahms (1984) provided notes on the holotype and only known specimen but otherwise the genus remained unknown. Based mainly on two specimens collected in Western Australia *Eustochomorpha* is redescribed. Specimens of an undescribed genus, apparently related to *Eustochomorpha*, were found in various collections and are described. A third genus is proposed for *Borneomymar primitivum* Huber (Huber 2002). A key is given to these genera and their

included species. Several other genera are included because they may well be closely related. An attempt to place the Cretaceous fossils of Mymaridae in context with the extant fauna is made.

Methods

This study is based on about 35 specimens on card-mounts, point-mounts and slides. Slides of the specimens were prepared as described in Huber (2015). Morphological terms used in the descriptions are mostly as defined in Gibson (1997) and Huber (2012, 2015). All measurements of specimens are given in micrometers and, depending on specimen length and preparation, taken with an ocular micrometer attached to a Nikon compound microscope at 200× magnification or a Leitz-Wetzlar binocular microscope at 64× and 160× magnification. Because of rounding errors, it appears that the ratios are slightly incorrect compared to those calculated using the absolute measurements (micrometers) but, in fact, those calculated from the ocular micrometer readings before converting to micrometers are more accurate, so are given in the descriptions. Photographs of slide mounts were taken with a ProgRes C14^{plus} digital camera attached to a Nikon Eclipse E800 compound microscope, and a selection of the resulting layers combined electronically in Zerene Stacker™. Card- or point mounted specimens were photographed with a Leica DFC 500 camera mounted on a Leica Z16 APO Zoom macroscope or on the Nikon compound microscope. Abbreviations used in the descriptions are: fl_x for funicle segment, gt_x for gastral tergum and mps for multiporous plate sensilla. Because the number and position of setae and the type of sculpture on species within a given genus of Mymaridae is usually quite similar the sculpture and setation are described in detail under the single species in *Eustochomorpha*, the single new species under one of the new genera and, to avoid repetition, under the genus name for the new genus containing seven new species. The number and position of setae is described for one side of the body only. So when observing a specimen in dorsal view the total number of setae on a particular structure is twice that described. The setae of appendages (antenna, mouthparts, wings, legs, genitalia) are usually excluded because they are numerous and often similar; only obviously different ones are mentioned, where informative. In general, the position of body setae, particularly on the mesosoma, is fairly stable and consistent within and even among genera, though setal shape, length and thickness may vary. Specimens are deposited in the following institutions:

ANIC Australian National Insect Collection, Canberra, Australian Capital Territory, Australia;

CAS California Academy of Sciences, San Francisco, California, USA;

CNC Canadian National Collection of Insects, Arachnids and Nematodes, Ottawa, Ontario, Canada;

NZAC New Zealand Arthropod Collection, Auckland, New Zealand;

QMBA Queensland Museum, Queensland, Brisbane, Queensland, Australia;
QDPC Queensland Primary Industries Insect Collection, Brisbane, Queensland, Australia;
QSBG Queen Sirikit Botanic Garden, Chiang Mai, Chiang Mai, Thailand;
ROM Royal Ontario Museum, Toronto, Ontario, Canada;
UCRC Entomology Research Museum, University of California, Riverside, California, USA.

Results

Eustochomorpha Girault, 1915

Figs 1–31

Type species. *Eustochomorpha haeckeli* Girault, by monotypy.

Diagnosis. Female. Antenna with funicle 8-segmented and clava 2-segmented (Figs 3, 7, 14). Venation about 0.9× fore wing length. Postmarginal vein distinct, uniformly thick and about 0.7× marginal vein length, with at least 2 short, socketed setae (Fig. 8, apical one indicated by arrow, Fig. 20c). Hypochaeta possibly present (Fig. 20a), originating on the parastigma instead of on the costal cell. Ovipositor strongly extending posteriorly beyond gastral apex but not extending anteriorly under mesosoma (Figs 2, 4, 28, 30).

Description. Female. Body ≈1280–1290 μm in length, excluding section of ovipositor exserted beyond apex of hypopygium. **Colour.** Generally brown (Fig. 4), with a few metallic reflections (an artefact of lighting?) on gaster. Gaster at base and most parts of legs lighter brown to white. Wings hyaline, with venation light brown. **Head.** Head about 1.7× as wide as long, 1.3× as wide as high and 1.4× as high as long; in lateral view with anterior surface convex, receding strongly from ventral margin of eye to mouth opening, and bulging medially compared to laterally (at preorbital groove); posterior surface slightly, evenly convex (Fig. 4). Face about as wide as high (Fig. 5), without subantennal grooves; preorbital groove ventral to torulus straight then, more ventrally, slightly curving medially to ventrolateral margin of mouth opening. Torulus in slight triangular depression about 2.0× as high as torulus width and separated by 1.5× torulus width from transverse trabecula (Fig. 5). Vertex in lateral view (Fig. 11) sloping obliquely to transverse trabecula to form an obtuse angle with face, and vertex posteriorly merging smoothly into occiput medially but separated laterally from occiput by short transverse vertexal suture. Ocellar triangle raised slightly above level of rest of vertex, the mid ocellus almost vertical, the lateral ocelli oblique, facing posterolaterally; ocelli with POL about 2.0× LOL and about 1.26 OOL. Transverse trabecula separated at each apex from supraorbital trabecula (Fig. 5); preorbital trabecula (apparently absent because not sclerotized) short, extending to inner orbit at about dorsal margin of torulus (Fig. 5); supraorbital trabecula in 2 subequal sections, the posterior sections slightly converging and the sutures outside posterior sections continuing onto

occiput as the occipital grooves (short lines each appearing as posterior extension of supraorbital suture and strongly converging towards occipital foramen) (Fig. 6) separating occiput medially from temple dorsolaterally. Occiput separated from vertex by vertexal suture, this only present laterally behind lateral ocelli (Fig. 12). Eye large with numerous (about 100) small facets, in lateral view slightly higher than wide (10:9) and clearly separated dorsally from back of head (temple about 0.3× eye width). Ocular apodeme fairly long, crooked, needle-like. Malar sulcus absent (Fig. 11). Gena at level of ventral margin of eye wider than malar space. Occiput entire, not separated by transverse groove into upper and lower portions (Fig. 6a). **Mouthparts.** Labrum with 2? setae; mandible with 3 teeth. **Antenna.** Scape about 2.6× as long as wide, with radicle distinct from rest of scape and about 0.25× total scape length (Fig. 13); pedicel about 2.1× as long as wide, almost as wide and about 0.7× as long as entire scape; funicle 8-segmented; clava 2-segmented (Figs 3, 7, 14), 1.08× as wide as apical funicle segment and 0.32–0.36× as long as entire funicle. **Mesosoma.** Mesosoma about 2.2× as long as wide, 2.3× as long as high and 1.1× as wide as high. Pronotum entire (Figs 9, 12, 15), in dorsal view clearly visible, medially about 0.3× as long as mesoscutum; collar almost horizontal, with a shallow median longitudinal impression and prominent angular shoulders; neck shorter than collar, posteriorly strongly sloping up to collar; in lateral view, pronotum rectangular, slightly overlapping anterior margin of mesoscutum, with lateral surface merging smoothly into dorsal surface, with a shallow, oblique impression for femur. Spiracle (Figs 17, 18) apparently slightly stalked, at posterolateral angle of pronotum in a slight depression and facing dorsolaterally. Propleura near anterior apex not quite abutting, then gap widening slightly more anteriorly. Prosternum rhomboidal, incompletely divided medially by faint longitudinal groove posteriorly. Mesoscutum about 1.7× as long as scutellum, in dorsal view with shallow, thin, slightly diverging notauli apparently absent posteriorly (Figs 9, 15, 16), in lateral view mesoscutum (Fig. 4) almost flat except anteriorly. Scutellum slightly wider than long; anterior scutellum about 3× as long as narrowly trapezoidal, transverse frenum and separated from it by a shallow, curved frenal depression (Figs 9, 16); campaniform sensilla small, slightly closer to lateral margins of anterior scutellum than to each other, with apex of large, cone-shaped fenestra projecting anteriorly between them (Fig. 9). Axilla slightly advanced, the transscutal articulation laterally forming an obtuse angle with median section (Fig. 16); axillula long and narrow, separated from anterior scutellum by posteriorly recurved axillular groove; mesophragma widely convex posteriorly, extending to posterior apex of propodeum. Prepectus probably spindle-shaped (Fig. 17, partly hidden by fore leg); mesopleuron somewhat rectangular, with shallow depression separating mesepisternum from mesepimeron (Fig. 17). Metanotum with distinct lens-shaped dorsellum (only visible Fig. 9, a cleared, slide mount) and lateral panel length (toward hind wing articulation) about half length of dorsellum (Fig. 16). Metapleuron triangular, with a narrow anterior extension almost to base of hind wing, the margin at junction with mesopleuron deeply concave and posterior margin straight and vertical. Propodeum with a complete longitudinal groove medially, in lateral view weakly sloping, almost in same plane as dorsellum, in dorsal view with faint median

longitudinal groove. Propodeal spiracle facing dorsolaterally in a slight depression and separated from anterior margin of propodeum by about its own diameter. **Wings.** Fore wing (Figs 4, 8, 19) wide, with completely transparent membrane sparsely scattered with minute microtrichia. Venation complete; submarginal vein with 1 subbasal seta and about 16 bullae, the most apical one at level of proximal macrochaeta (Fig. 8); parastigma, 0.5× submarginal vein length; marginal vein present, its length (from distal macrochaeta) about 2.0× length of parastigma; stigmal vein short but distinct, curving away from wing margin (Fig. 20) then closely paralleling it, with 4 apical campaniform sensilla (Fig. 21b); postmarginal vein present, about 0.8× as long and as thick as marginal vein, with 4 microchaetae along anterior margin; hypochaeta absent (Fig. 8) but one similar to it originating on parastigma (Fig. 20a); proximal campaniform sensillum near posterior margin of marginal vein just beyond apical macrochaeta (far removed from the 4 campaniform sensilla on stigmal vein). Hind wing (Fig. 8) with membrane not extending to base of wing, relatively wide medially, tapering gradually almost to a point apically. Fore wing membrane with one irregular row of microtrichiae basally and two or three distally. **Legs.** Profemur and metafemur narrow (Fig. 17), metafemur widest, about 2× as wide as mesofemur. Tarsi 5-segmented. Calcar (moveable protibial spur) apparently without setae along outer margin, and with the inner tine about 0.5× as long as outer tine. Middle and hind legs with tarsomere 1 shorter than tarsomere 2. **Metasoma.** About 2.2× as long as wide, 2.3× as long as high and 0.9× as wide as high; its length, excluding exserted part of ovipositor, about 2.0× that of mesosoma (Fig. 4). Petiole ring-like, about 0.3× as long as wide. Gastral terga apparently with fine longitudinal wrinkles except gt_7; gt_1 shorter than remaining terga and apparently gt_6 the longest tergum, gt_7 apically acutely triangular. Cercus a distinctly raised, longer than wide, peg-like plate, with 4 setae (Figs 22, 25). Gt_6 with spiracle minute (apparently absent). Hypopygium extending posteriorly well beyond level of cercus (Figs 4, 23, 25). Ovipositor sheath exserted beyond gastral apex by about one third of its total length and abruptly upturned apically, apparently without subapical seta (Figs 22, 24).

Male. Unknown.

Hosts and habitat. Hosts are unknown. The holotype was collected in forest (Girault 1915).

Eustochomorpha haeckeli Girault

Figs 1–31

Eustochomorpha haeckeli Girault 1915: 156 (original description); Annecke and Doutt, 1961: 4, 14 (key, diagnosis); Dahms, 1984: 675 (holotype data); Lin et al., 2007: 33 (diagnosis in part, figs 129–131).

Type material. Holotype female (QMBA) on slide labelled as shown (Fig. 1). The holotype (Fig. 2) is in uncleared in Canada balsam under 1 coverslip fragment between two other fragments and is poorly mounted more or less dorsoventrally with legs

Figures 1–3. *Eustochomorpha haeckeli*, holotype female. **1** type slide, specimen under middle cover slip **2** body + legs **3** antenna. Scale bar = 100 µm.

mostly folded up against body; left antenna with clava missing; right antenna (Fig. 3) detached beyond pedicel and positioned next to left (very faint) hind wing; other hind wing detached and its membranous portion hidden under head; right fore wing folded over and partly hidden by legs. Except for estimated body length, measurements of the holotype are not given in the species description below (my measurements were inaccurate when I borrowed the specimen).

Diagnosis. Female. Among extant genera, *E. haeckeli* is distinguished from the first new genus described below, having a 2-segmented clava (3-segmented in the first new genus), and the ovipositor strongly exserted posteriorly beyond apex of gaster and not extending anteriorly under the mesosoma. It differs from the second new genus described below by the postmarginal vein shorter than the marginal vein (postmarginal vein longer than marginal vein in the second new genus), hypochaeta absent (hypochaeta present in the second new genus), and it differs from *Borneomymar* by its 2-segmented clava (1-segmented in *Borneomymar*).

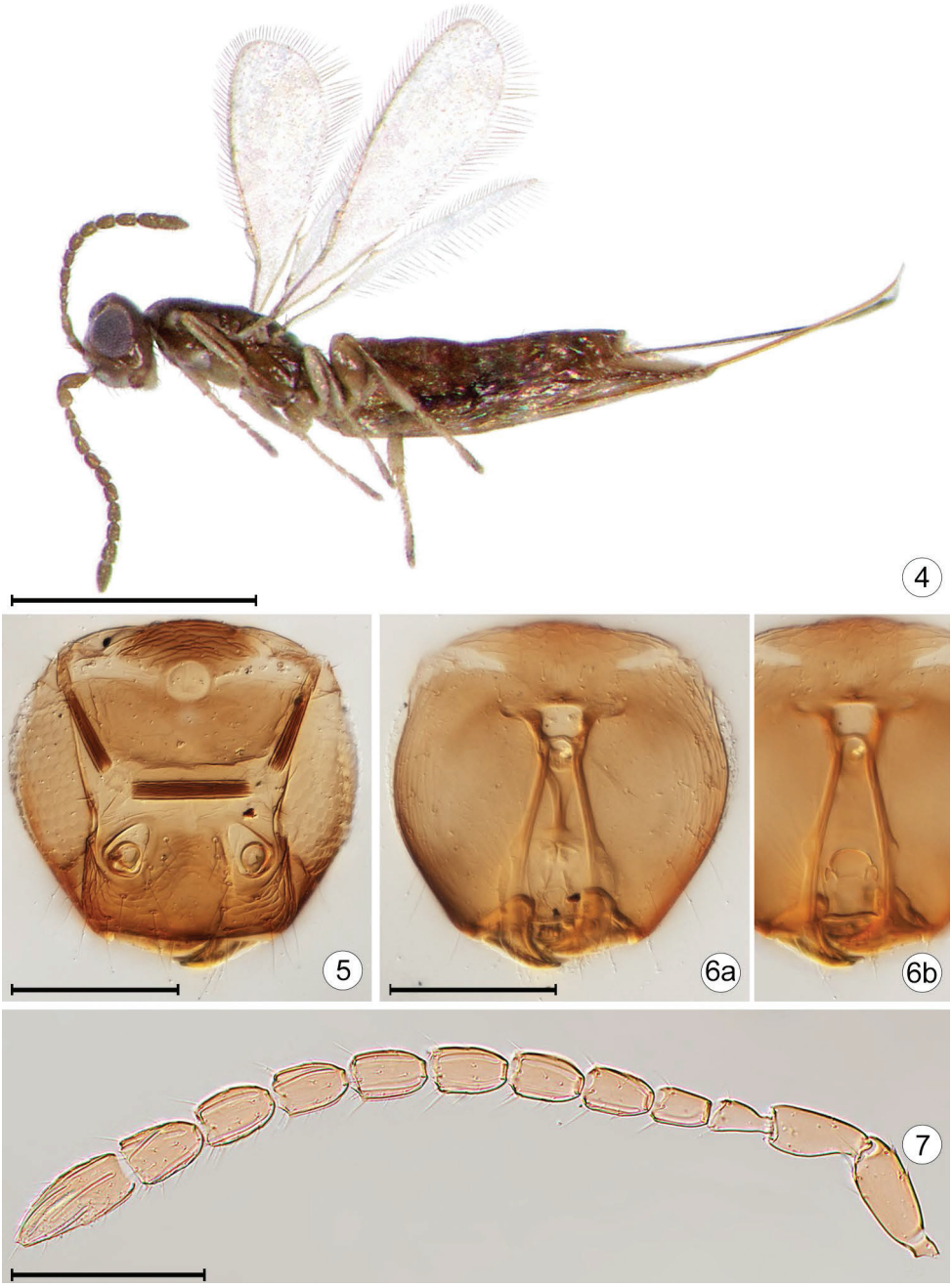

Figures 4–7. *Eustochomorpha haeckeli*, female. **4** habitus (Australia, WA, Stirling Range National Park) **5** head, anterior; **6a** head, posterior **6b** tentorium **7** antenna. Scale bar for **4** = 500 µm; **5–7** = 100 µm.

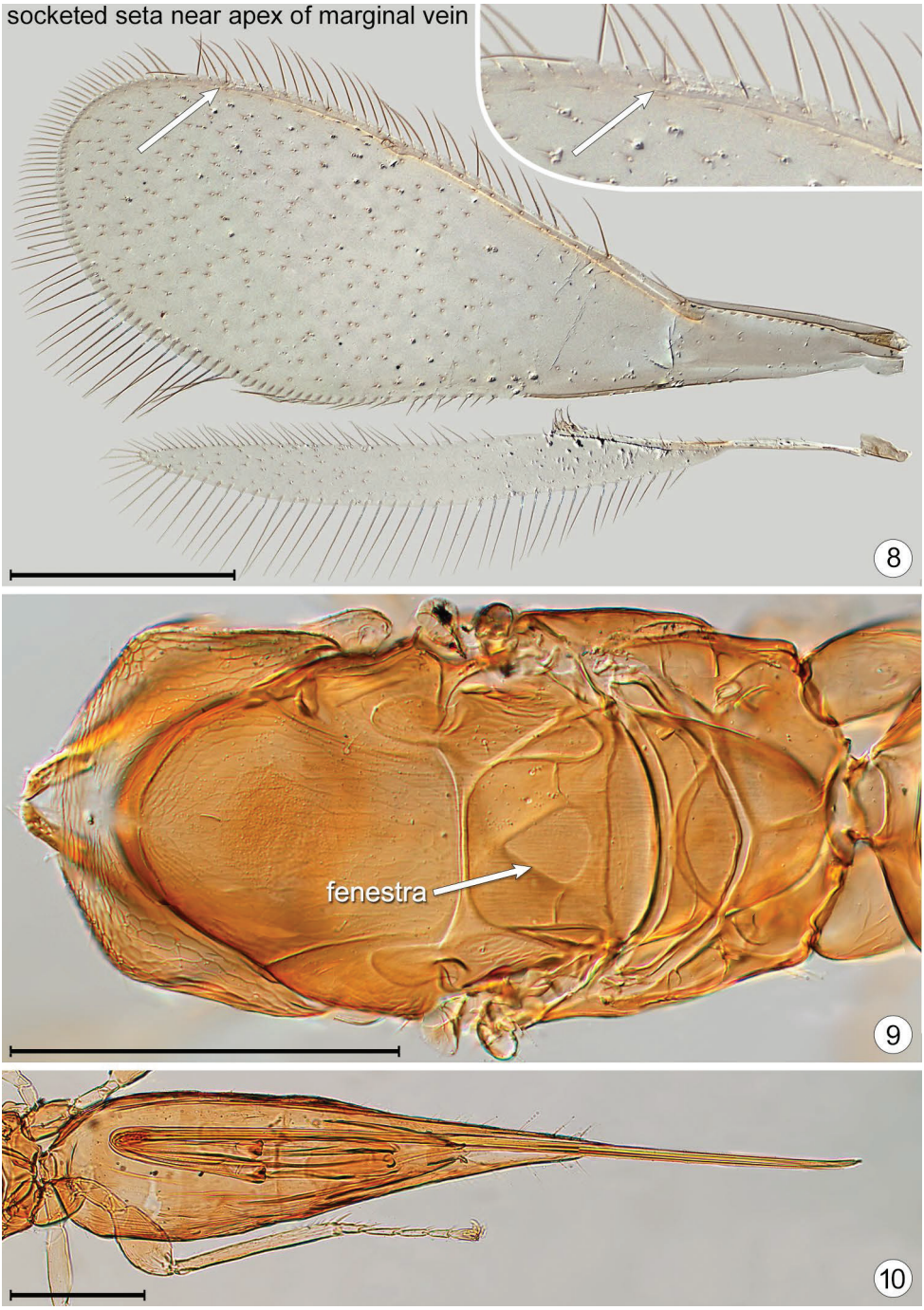

Figures 8–10. *Eustochomorpha haeckeli*, female. 8, wings **9** mesosoma, dorsal **10** metasoma, dorsal. Scale bar = 200 μm.

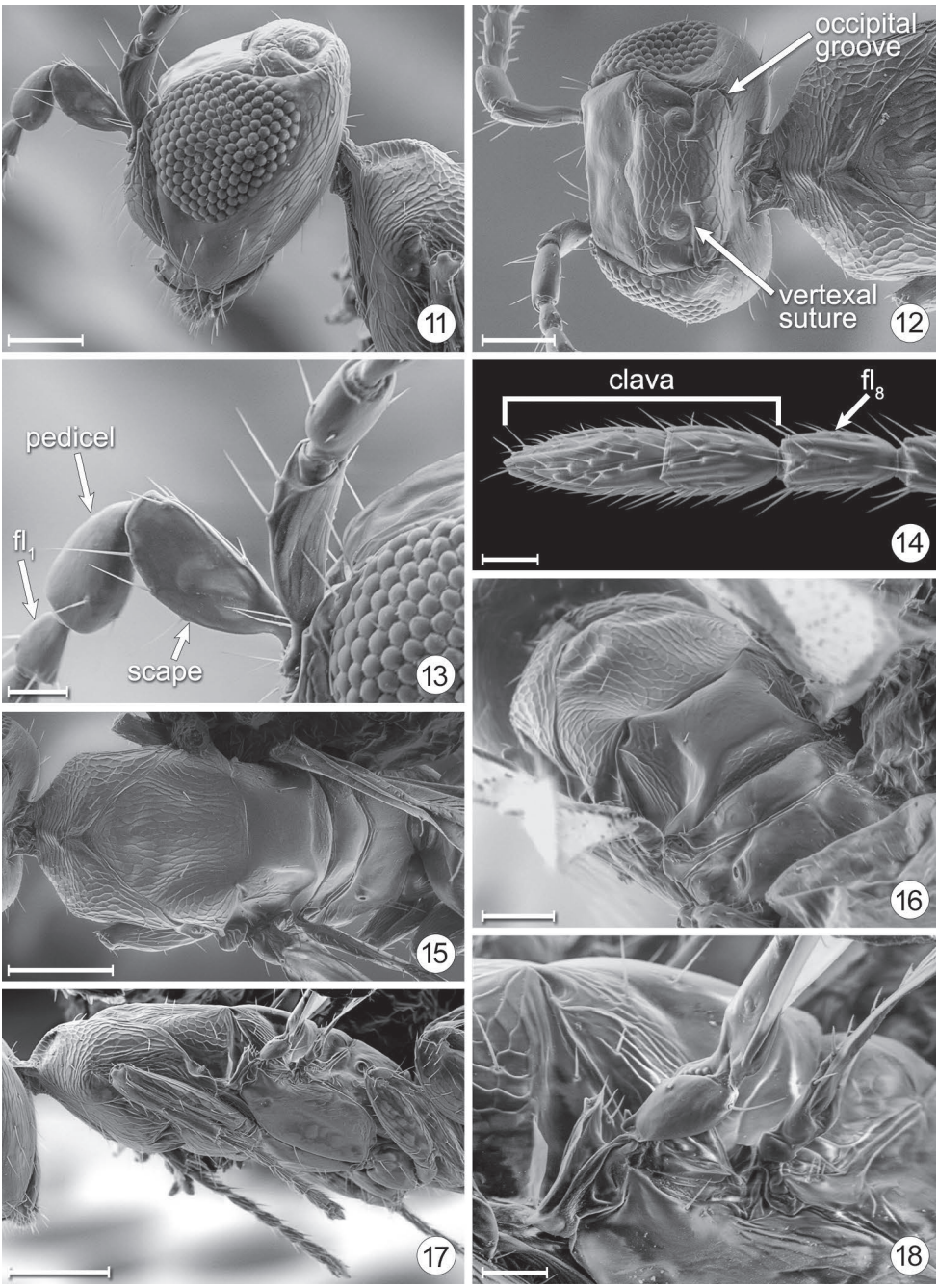

Figures 11–18. *Eustochomorpha haeckeli*, female. **11** head + prothorax, lateral **12** head + prothorax, dorsal **13** base of antenna, lateral (right antenna) and ventral (left antenna) **14** apex of antenna **15** mesosoma, dorsal **16** mesosoma, posterolaterodorsal **17** mesosoma, lateral **18** base of wings + mesosoma, lateral (medial portion). Scale bar for **11, 12, 16** = 50 μm; **13, 14, 18** = 20 μm; **15, 17** = 100 μm.

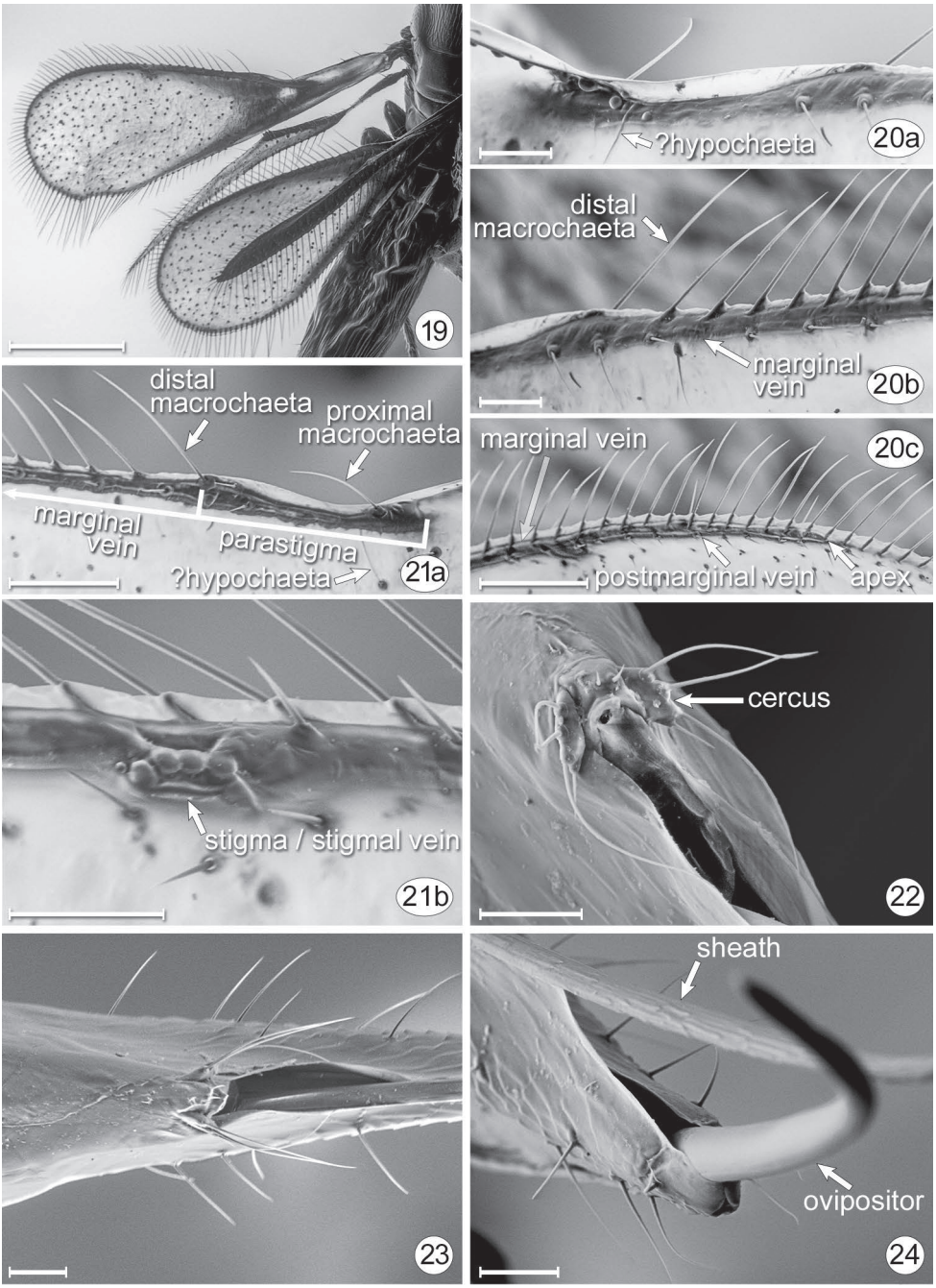

Figures 19–24. *Eustochomorpha haeckeli*, female. **19** wings **20a** parastigma, ventral **20b** base of marginal vein, ventral **20c** apex of marginal vein, stigma + postmarginal vein, ventral **21a** parastigma, dorsal **21b** stigma, dorsal **22** gaster apex showing cerci, posterolaterodorsal **23** gaster apex showing cerci, dorsal **24** gaster apex, posterolaterodorsal. Scale bar for **19** = 200 μm; **20a, 20b, 21b, 22–24** = 20 μm; **20c, 21a** = 50 μm.

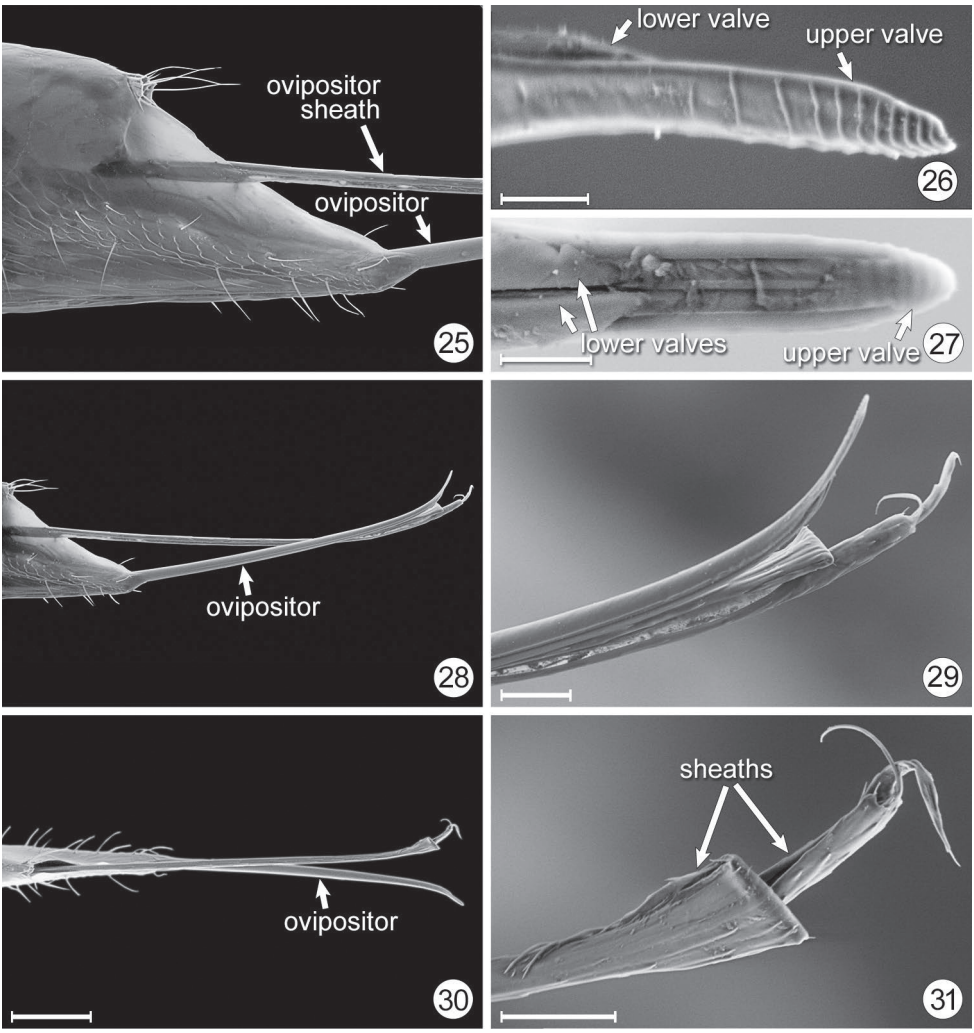

Figures 25–31. *Eustochomorpha haeckeli*, female. **25** gaster apex, lateral **26** ovipositor apex, dorsal **27** ovipositor apex, ventral **28** ovipositor + sheaths, lateral **29** apex of ovipositor + sheaths, lateral **30** ovipositor + sheaths, dorsal **31** apex of sheaths (one sheath folded over on itself). Scale bar for **25** = 50 µm; **26, 27** = 5 µm; **28, 30** = 100 µm; **29, 31** = 20 µm.

Description. Female. Body length ≈1280 (critical point dried specimen, Stirling Range National Park). **Colour**. Body mainly brown (Fig. 4). Ocellar triangle, mesothorax and fine longitudinal line laterally on gaster darker brown. Base of gaster, especially basal sterna, legs except metacoxa and metafemur and apical tarsomere of all legs, flagellum and mouthparts except mandibles, and a faint transverse band at level of anterior ocelli lighter brown to white. **Head**. Width 202. Face with weak reticulate sculpture medially, stronger laterally (Fig. 5), with setae distributed as follows: 3 medial to torulus and 8 ventral to torulus, the 2 submedially above mouth margin the shortest. Vertex smooth

anterior to mid ocellus and reticulate posterior to mid ocellus (Fig. 5), with 2 setae on anterior orbit lateral to transverse trabecula and 2 setae on dorsal orbit, in angle between eye and posterior section of supraorbital trabecula; ocellar triangle with 2 short setae lateral to mid ocellus and 1 short setae just posteromedial to lateral ocellus. Malar area apparently with 3 setae. Gena and occiput laterally longitudinally reticulate (Fig. 6a), the reticulations on occiput shallower and transverse medially; occiput with 2 short setae submedially above occipital foramen, about 9 setae sublaterally and laterally; tentorium with two very short dorsal arms (Fig. 6b). **Antenna.** Fl_1–fl_8 respectively with 0, 1, 2, 2, 2, 3, 3, 3 mps; clava 1 with 3 (4?) mps on first segment and 5 (6?) mps on second segment (Figs 3, 7). Length/width measurements (n=1): scape 70/27, pedicel 55/26, fl_1 33/18, fl_2 32/20, fl_3 39/25, fl_4 40/25, fl_5 44/25, fl_6 42/25, fl_7 42/24, fl_8 42/26, clava 112/31 (first segment 42, second segment 69). **Mesosoma.** Width 200 and length 415. Pronotum with reticulate sculpture, with 3 short setae along posterior margin and 3 towards anterior margin. Propleuron faintly, longitudinally reticulate, with 2 seta about midway between anterior and posterior apices. Prosternum smooth, with 1 seta submedially almost at anterior margin and 1 setae laterally midway between anterior and posterior margins. Mesoscutum faintly longitudinally reticulate, with 1 setae along inner margin midway between anterior and posterior apices of notaulus, and 1 setae at lateral angle of side lobe. Anterior scutellum smooth, with 1 setae on lateral margins level with campaniform sensillum; frenum faintly reticulate. Axilla reticulate, and with 1 seta at anteromedian angle and 1 dorsally on longitudinally reticulate lateral panel; axillula smooth. Metanotum smooth medially, faintly reticulate laterally, with 2 short setae along anterior margin of relatively wide lateral panel. Propodeum smooth, with 2 propodeal setae close together. **Wings.** Fore wing length (n=1) 723, width 259, length/width 2.98, longest marginal setae 72. Marginal vein with about 11 microchaetae along its length; cubital line with few setae extending to level of distal apex of retinaculum. Hind wing length 685, width 57, longest marginal setae 68. **Legs.** Femora and tibiae of all legs with faint longitudinal reticulation. Protibia at mid length with 2 short pegs. **Metasoma.** Petiole 54 wide, 18 long. Gaster 212 wide, 597 long (to apex of apical tergum), with a few short setae on most terga, the terga difficult to distinguish from one another (anterior and posterior margins not distinct) and apparently with fine longitudinal wrinkles at least laterally; gt_1 shorter than remaining terga, apparently with 1 lateral setae, gt_2 and gt_6 apparently with 1 submedian seta; gt_3 – gt_5 with about 4 submedian to sublateral setae in an irregular transverse row; gt_7 acutely triangular, with a small apical seta. Cercus with the first two cerci subequal in length, the third the longest and the fourth the shortest (Fig. 25). Hypopygium weakly sclerotized (almost transparent) dorsally and extending beyond gastral apex by ≈180, with a submedian and lateral row of about 8 setae. Ovipositor length 1074, its exserted part (posterior to hypopygium apex) 360.

Male. Unknown.

Material examined. Two females, collected in Malaise traps in combination with yellow pan traps underneath. AUSTRALIA. **Western Australia:** Yanchep National Park, 20–21.xii.1986, J.S. Noyes (1♀ on slide, CNC); Stirling Range National Park, 11–15.i.1987, J.S. Noyes (1♀ on point, BMNH).

***Neotriadomerus* Huber, gen. n.**
http://zoobank.org/5488307C-D58F-4E00-8DC9-C2ACB542A103
Figs 32–152

Eustochomorpha: Lin et al., 2007: 33 (diagnosis in part, figs 132–134).

Type species. *Neotriadomerus longiovipositor* Huber, by present designation.

Diagnosis. Female. Antenna with funicle 8-segmented and clava 3-segmented (Figs 39, 69). Venation about 0.85–0.90× fore wing length. Postmarginal vein distinct, uniformly thick and about 1.3–1.6× marginal vein length (Figs 70, 122). Hypochaeta present or, apparently, sometimes absent. Ovipositor strongly extending anteriorly under mesosoma (Figs 59, 74) at least to level of hind wing base but not or only slightly extending posteriorly beyond apex of gaster (Figs 75, 77). **Male.** Similar to female, but flagellum with 11 relatively wide segments (Figs 40–43, 82, 95), each with several mps; the segments progressively becoming narrower towards flagellar apex, fl_{11} sometimes only a little over half as wide as fl_1. Genitalia encapsulated, with thick walls (Figs 124, 143) and, in lateral view, paramere thick (Figs 65, 66).

Description. Female. Body 1380–5500 in length, excluding basal sac of gaster (enclosing anterior extension of ovipositor). **Colour.** Generally brown (Figs 81, 128, 144, 146, 147) to dark brown, scape and pedicel, legs in part and sometimes basal sac of gaster lighter brown to yellowish. Wings hyaline, the venation light brown. **Head.** Head about 2.0–2.9× as wide as long, about 1.2–1.6× as wide as high and about 1.3–2.3× as high as long; in lateral view with anterior surface almost flat, at most barely receding ventral to eye, slightly depressed medially compared to laterally at preorbital groove; posterior surface in lateral view slightly convex except slightly indented at postorbital groove (Figs 33, 45). Face about 1.2–1.3× as wide as high (Fig. 32), in lateral view almost flat, barely receding from ventral margin of eye to mouth opening; subantennal grooves absent; preorbital groove ventral to level of torulus straight all the way to lateral margin of mouth opening. Torulus in somewhat circular depression about 1.2× as high as torulus width and separated by less than 0.4× torulus width from transverse trabecula (Fig. 33). Vertex in lateral view usually almost in same plane as face, but sometimes almost horizontal and forming a right angle with face, and vertex posteriorly forming an almost right angle with occiput and separated from it laterally by a short transverse vertexal suture extending to or just medial to posterior ocellus but absent between posterior ocelli (Fig. 33). Ocellar triangle almost flat or raised slightly above level of rest of vertex, the mid ocellus oblique to almost vertical, lateral ocelli oblique, facing laterally or posterolaterally; ocelli with POL about 2.0× LOL and about 1.7–1.8× OOL (varying slightly with species); ocellar area (in cleared slide mounts) with frontofacial suture (seen as white lines) between mid and lateral ocellus, frontal suture (seen as white lines) from mid ocellus to corner of transverse trabecula, and sometimes also a median longitudinal line from mid ocellus to middle of transverse trabecula (Fig. 116). Transverse trabecula apparently separated (Fig. 67) or not (Figs 36, 37) from supraorbital trabecula; preorbital trabecula short, extending to about level of

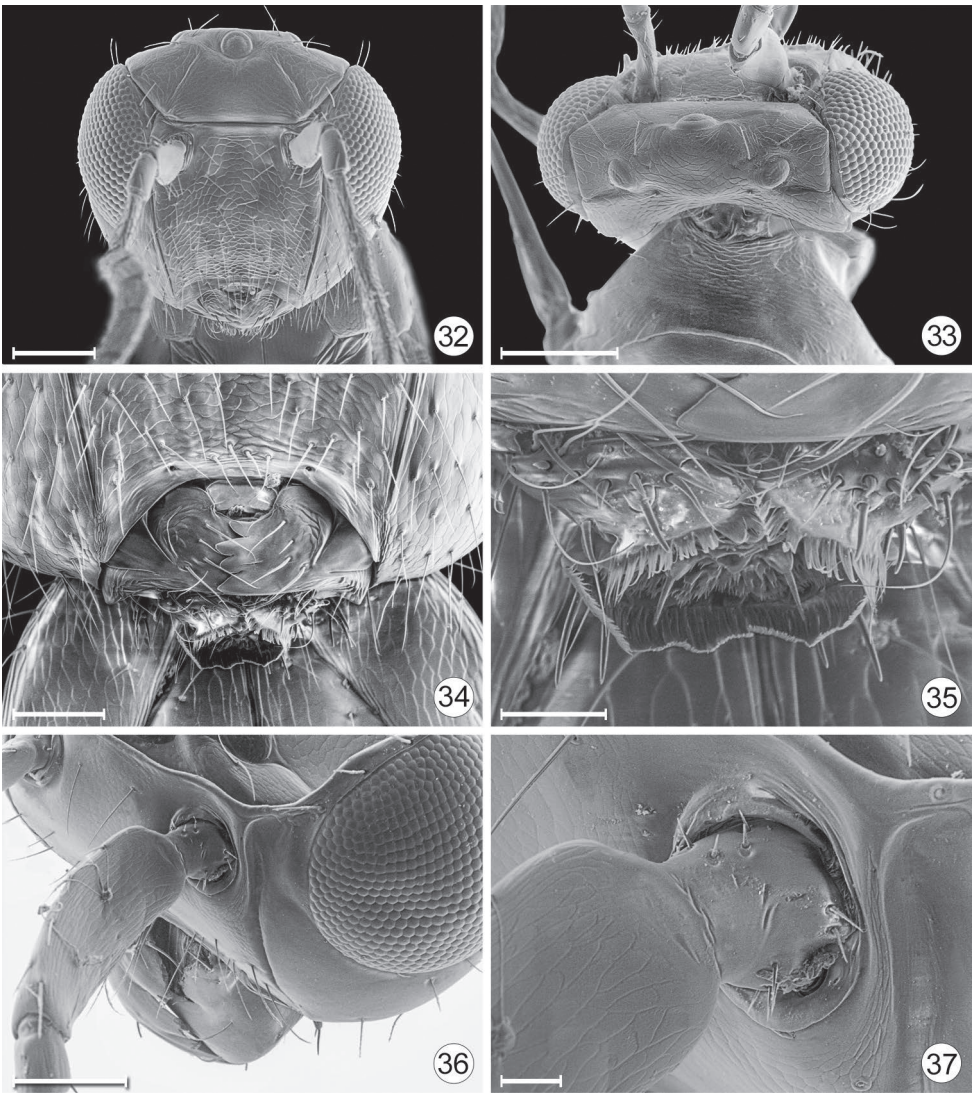

Figures 32–37. *Neotriadomerus* spp. **32** *N. gloriosus* female head, anterior **33** *N. darlingi* male head + pronotum, dorsal **34** *N. gloriosus* lower face + mouthparts, anterior **35** *N. gloriosus* maxillae + labium, anterior **36** *N. longissimus* head, scape and mandibles, dorsoanterolateral **37** *N. longissimus* radicle, anterolateral (and showing 3-way junction of transverse, supraorbital and preorbital trabeculae). Scale bar for **32, 33, 36** = 100 μm; **34** = 50 μm; **35, 37** = 20 μm.

dorsal margin of torulus; supraorbital trabecula in 2 equal or unequal sections, the anterior sections diverging posteriorly, the posterior, sometimes longer, sections slightly converging, and the sutures outside posterior sections continuing onto occiput as short, almost parallel lines, the occipital grooves, ventrally to level of foramen, thus separating occiput medially from temple laterally (Fig. 68). Eye large with numerous small facets,

in lateral view at most about 1.4× as high as wide and clearly but narrowly separated dorsally from back of head (temple in lateral view at most about 0.25× eye width). Ocular apodeme short, straight, and thin (Fig. 119, inset). Malar sulcus absent. Gena at level of ventral margin of eye at most as wide as length of malar space. Head posteriorly with curved postorbital groove extending across head above dorsal margin of occipital foramen to posterior margin of eye (Fig. 68) and separating occiput/temple dorsally from gena/postgena ventrally. **Mouthparts.** Labrum with 4 or 6 setae; mandible with 4 uneven teeth, the ventral one the longest (Fig. 34). **Antenna.** Scape about 3.0–3.9× as long as wide, with radicle distinct from rest of scape and about 0.24–0.29× total scape length; pedicel about 1.1–1.6× as long as wide, 0.72–1.09× as wide and about 0.36–0.42× as long as entire scape; funicle 8-segmented (Fig. 69); clava 3-segmented (Fig. 39), 1.07–1.22× as wide as apical funicle segment and 0.18–0.23× as long as entire funicle. **Mesosoma.** About 1.8–2.4× as long as wide, 2.4–2.8× as long as high and 1.0–1.3× as wide as high (card- or point-mounted specimens, air- or critical-point dried). Pronotum entire, in dorsal view clearly visible, medially about 0.3–0.6× as long as mesoscutum; collar almost horizontal, medially flat to slightly convex and without evident shoulders (Fig. 44); neck not or barely differentiated from collar; in lateral view, pronotum with lateral surface merging smoothly into dorsal surface, with a shallow, oblique ventroanterior impression margined by an oblique groove posteriorly for reception of femur (when fore leg folded against body). Spiracle (Fig. 46) very slightly stalked, at posterolateral angle of pronotum in a slight depression and facing posterodorsally. Propleura near anterior apex not quite abutting then widening more anteriorly towards the cervical sclerites (Fig. 141). Prosternum rhomboidal, almost completely divided medially by longitudinal groove (Fig. 141). Mesoscutum about 1.1–1.6× as long as scutellum, in dorsal view with narrow, distinctly diverging notauli (Fig. 44) appearing in slide mounts wider and shallower near transscutal articulation (Fig. 72), in lateral view almost flat except anteriorly (Figs 45, 81). Scutellum slightly longer than wide (at widest point on frenum), the anterior scutellum narrower and slightly shorter to slightly longer than transversely biconvex frenum and separated from it by an evenly curved frenal line; campaniform sensilla as far apart from each other as to lateral margin of anterior scutellum and slightly farther apart than their distance to transcutal articulation, with apex of cone-shaped fenestra not extending to level of campaniform sensilla. Axilla slightly advanced, the transscutal articulation laterally almost in line with median section, and about as wide anteriorly as width of anterior scutellum at transcutal articulation; axillar pit separated from anterior scutellum by curved axillular groove; mesophragma convex posteriorly, extending to posterior apex of propodeum (Fig. 72, faintly visible under propodeum). Prepectus rather rectangular, at widest point about 0.8× as wide as long. Mesopleuron somewhat spindle shaped, with shallow oblique depression separating mesepisternum from mesepimeron and almost straight groove extending from anterior margin to mesocoxal insertion (Fig. 92). Metanotum with distinct biconvex (slide mount, Fig. 87) or somewhat triangular (SEM, Figs 44, 48) dorsellum and lateral panel length at hind wing articulation about one-third to half length of dorsellum. Metapleuron quadrangular, with almost straight sides (Figs 56, 123). Propo-

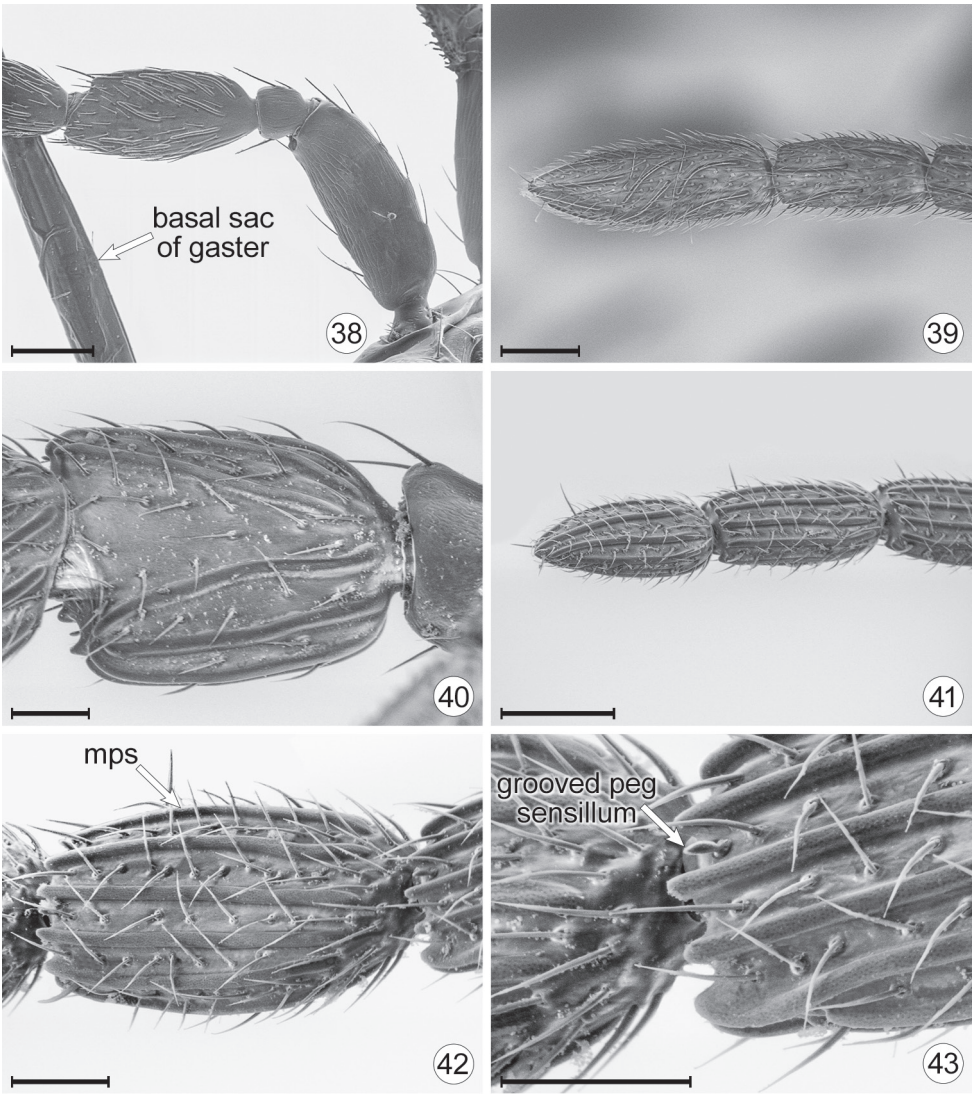

Figures 38–43. *Neotriadomerus* spp. **38** *N. longissimus* female scape–base of fl_2, lateral **39** *N.* sp. female fl_8 + clava, lateral **40** *N. darlingi* male apex of pedicel–base of fl_2, lateral **41** *N. darlingi* male fl_{11}–fl_{13}, lateral **42** *N. darlingi* male fl_{11}, lateral **43** *N. darlingi* male apex of fl_{11}, lateral. Scale bar for **38** = 100 μm; **39, 41** = 50 μm; **40, 42, 43** = 20 μm.

deum in lateral view weakly sloping, almost in same plane as dorsellum and in dorsal view flat medially, without median or submedian grooves or other ornamentation (Figs 44, 46, 56, 72). Propodeal spiracle facing dorsolaterally, separated from anterior margin of propodeum by much less than half its own diameter. **Wings.** Fore wing (Fig. 113) about 2.6–3.7× as long as wide, evenly and densely covered with microtrichia from wing apex proximally to at most about level of distal macrochaeta but almost without

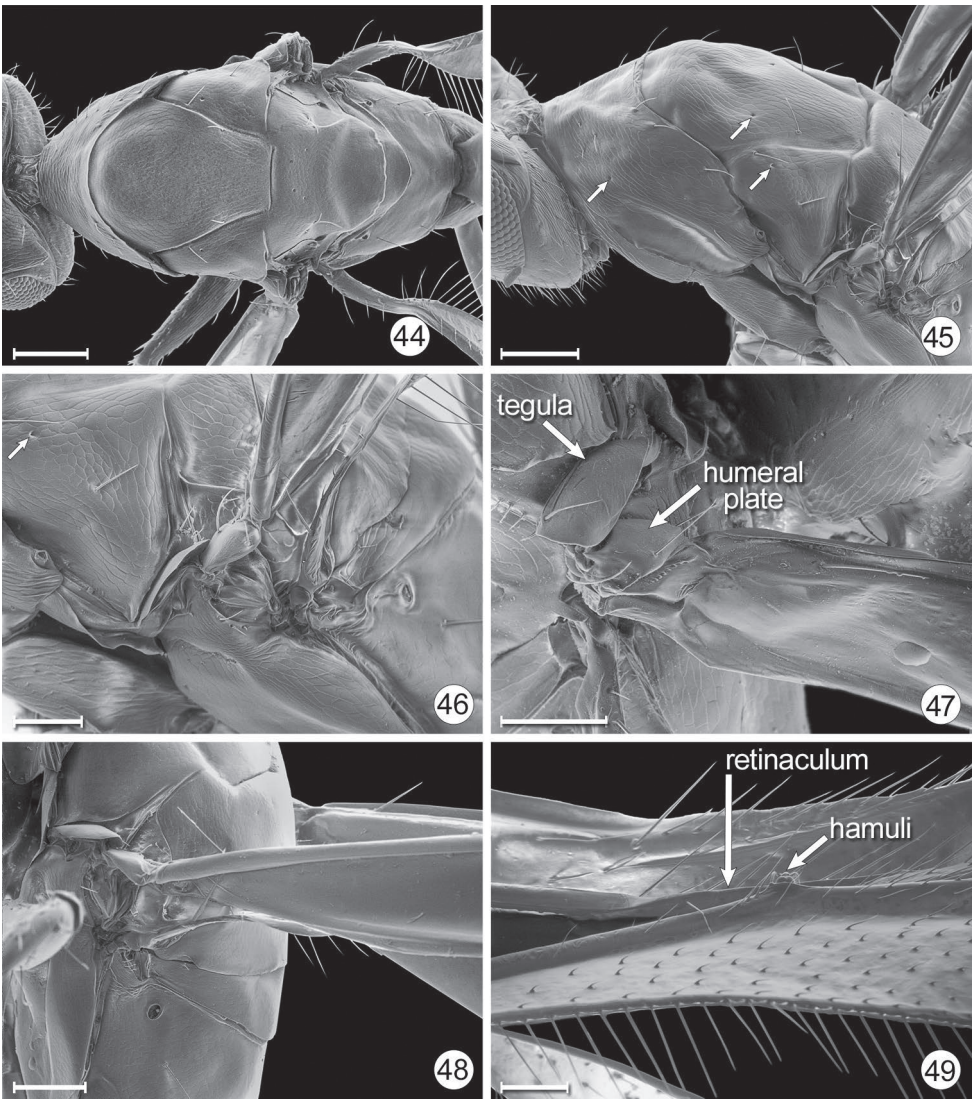

Figures 44–49. *Neotriadomerus* spp. **44** *N. darlingi* mesosoma, dorsal **45** *N.* sp. mesosoma, dorsolateral (arrows indicate pores) **46** *N.* sp. base of left wings (ventral) and surrounding mesosoma, dorsolateral **47** *N. darlingi* fore wing base, dorsal **48** *N. longissimus* fore wing base, ventral **49** *N.* sp., hind wing attachment to fore wing, ventral. Scale bar for **44, 45, 48** = 100 μm; **46, 47, 49** = 50 μm.

microtrichia behind submarginal vein (Figs 48, 113) and parastigma (Figs 50, 51) and just behind much or all of marginal vein (Fig. 70); an oblique and usually distinct setal line extending more or less horizontally from apical margin of wing to about halfway towards base of marginal vein; cubital line ending proximally either at about same level as remaining mictrotrichiae or extending to base of parastigma; marginal setae short, the longest not more than about 0.13× wing width (Fig. 70). Venation complete (Fig.

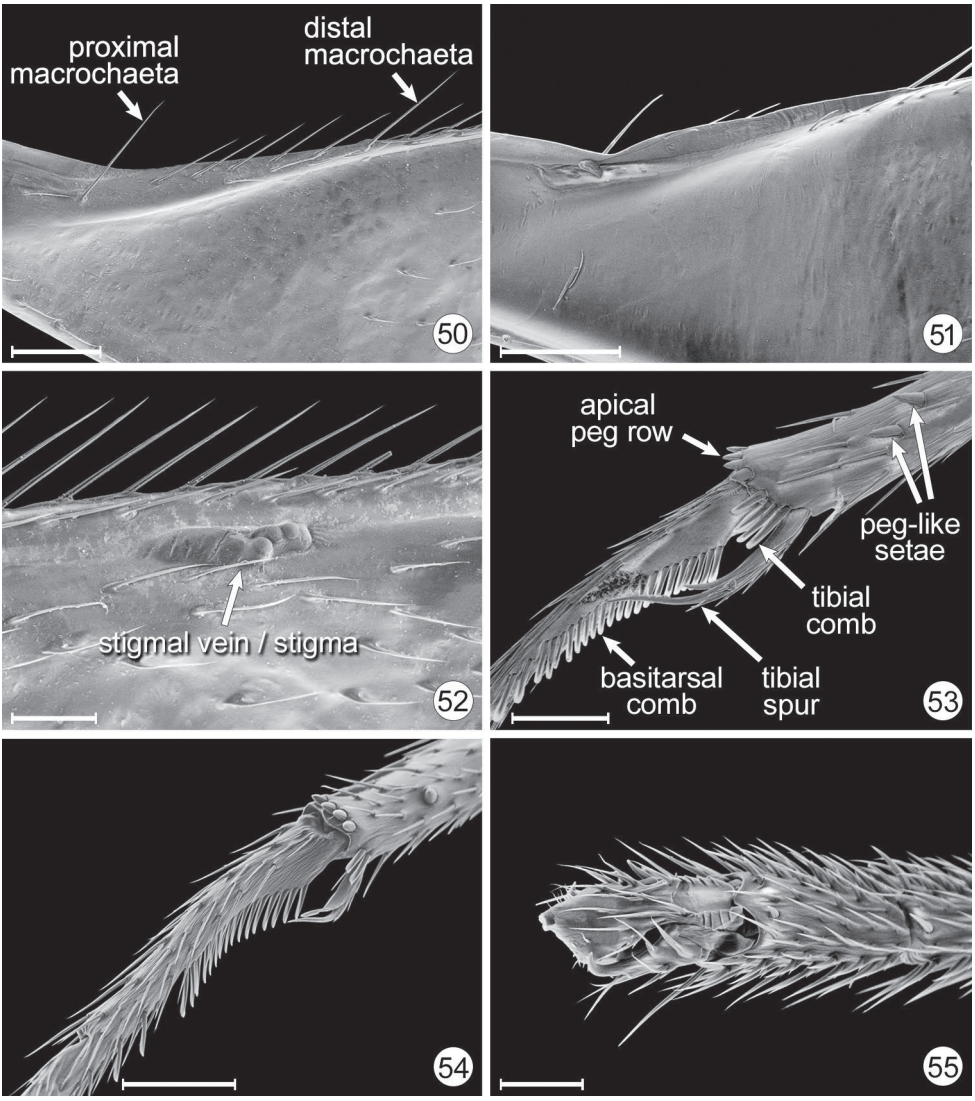

Figures 50–55. *Neotriadomerus* spp. **50** *N. darlingi* male parastigma, dorsal **51** *N. longissimus* female parastigma, ventral **52** *N. darlingi* male stigmal vein, dorsal **53** *N. longissimus* female calcar, lateral **54** *N.* sp. female calcar, dorsolateral **55** *N.* sp. female pretarsus, dorsolateral. Scale bar for **50, 53, 54** = 50 μm; **51** = 100 μm; **52, 55** = 20 μm.

122); submarginal vein with 1 proximal seta; parastigma (from distal macrochaeta to base) about 0.5–0.7× submarginal vein length; marginal vein length (from distal macrochaeta to junction of stigmal and postmarginal veins) about 1.2–1.5× parastigma length; stigmal vein short but distinct, about 0.15–0.17× marginal vein length, curving away from wing margin then closely paralleling it (Fig. 122), with 4 apical campaniform sensilla (Fig. 52); postmarginal vein about 1.3–1.6× as long and as thick as mar-

ginal vein, with a few microchaetae along anterior margin; hypochaeta usually present, occasionally apparently absent (broken off?), much closer to proximal than distal macrochaeta; proximal campaniform sensillum near posterior margin of marginal vein just apical to distal macrochaeta. Hind wing with membrane not extending to base of wing, relatively wide medially, with a rounded apex, uniformly covered with microtrichia almost to base of membrane (Figs 49, 70). **Legs.** Profemur and mesofemur narrow; metafemur widest, about 1.4× as wide as mesofemur (Figs 77, 92). Tarsi 5-segmented. Calcar (moveable protibial spur) with setae along outer margin, and with inner tine about 0.4× as long as outer tine (Figs 53, 54). Pretarsus normal (Fig. 55). Mid and hind legs with tarsomere 1 at least as long as tarsomeres 2 + 3. **Metasoma.** Petiole usually ring-like, about 0.4–0.5× as long as wide (Fig. 72) but in one (the largest) species 0.7–1.0× as long as wide. Gaster 1.18–3.25× as long as mesosoma. Gaster with gt_1 and gt_6 usually slightly the longest terga (Figs 56, 73, 89, 92). Cercus distinctly raied as a thin flap above surface of gt_7 (Fig. 62) with 4 setae about equal in length (Fig. 65). Hypopygium distinct (Fig 56), extending about 0.3–0.6× length of gaster, sometimes as far as level of spiracle. Ovipositor sheath barely projecting posteriorly beyond apex of gaster but strongly projecting anteriorly (inside basal sac of gaster) from at least middle of mesosoma (Fig. 74) to well in front of head (Fig. 126), apparently with 1 subapical seta. **Body sculpture and setation.** Sculpture generally uniform and so faint that body often appearing almost smooth and shiny (Figs 81, 82, 126–129, 144–147). Head with engraved, slightly transverse (longitudinal on gena and postgena) or almost isodiametric reticulations becoming raised and slightly imbricate ventrally on face and on occiput (Figs 32–34). Mesosoma with faint isodiametric to elongate reticulations either transverse, mainly on pronotum, or longitudinal, mainly on scutellum. Metasoma apparently without sculpture (Figs 56–62) except anterior apex of basal sac of gaster in at least one species. Head with few to numerous setae on face ventral to toruli, and on gena (Figs 32–34) but one (Fig. 36) or two (Fig. 32) just medial to torulus. Vertex with 2 setae, 1 between mid and lateral ocelli and 1 more laterally. Eye orbit with 3 setae dorsoanteriorly and 3 dorsally and posterodorsally. Occiput with 1 submedial seta dorsally and, more ventrally, 1 seta sublaterally and 1 seta submedially. Gena/postgena with several setae. Pronotum with about 3 setae along posterior margin and about 5 shorter setae anteriorly. Propleuron with a few small scattered setae (Figs 44, 116). Prosternum (Fig. 141) with 1–3 setae mainly in anterior half. Mesosoma with a few short setae (not treated here) around insertions of wings and some longer setae as follows. Mesoscutum with 1 adnotaular seta in posterior half of midlobe, 1 anteromedial and 1 posterolateral seta on lateral lobe and a few small pits (Figs 44–46). Anterior scutellum with 1 seta at lateral margin just anterior to axillular groove (represented by a curved medial edge at junction with frenum). Axilla with 1 anteromedial seta and 1 lateral seta. Propodeum with 2 or, occasionally, 3 propodeal setae laterally behind spiracle. Petiole apparently with 1 minute seta ventrally on anterior margin. Gaster with setae on terga increasing in number from gt_1 to gt_6 but apparently none on sterna except 1 or 2 short ones laterally on basal sac of gaster and longer ones on hypopygium (Fig. 56). Gt_1 with about 3 lateral and 1 dorsal in 1 row; gt_2 and gt_3 with a few more lateral and dorsal in 1 row;

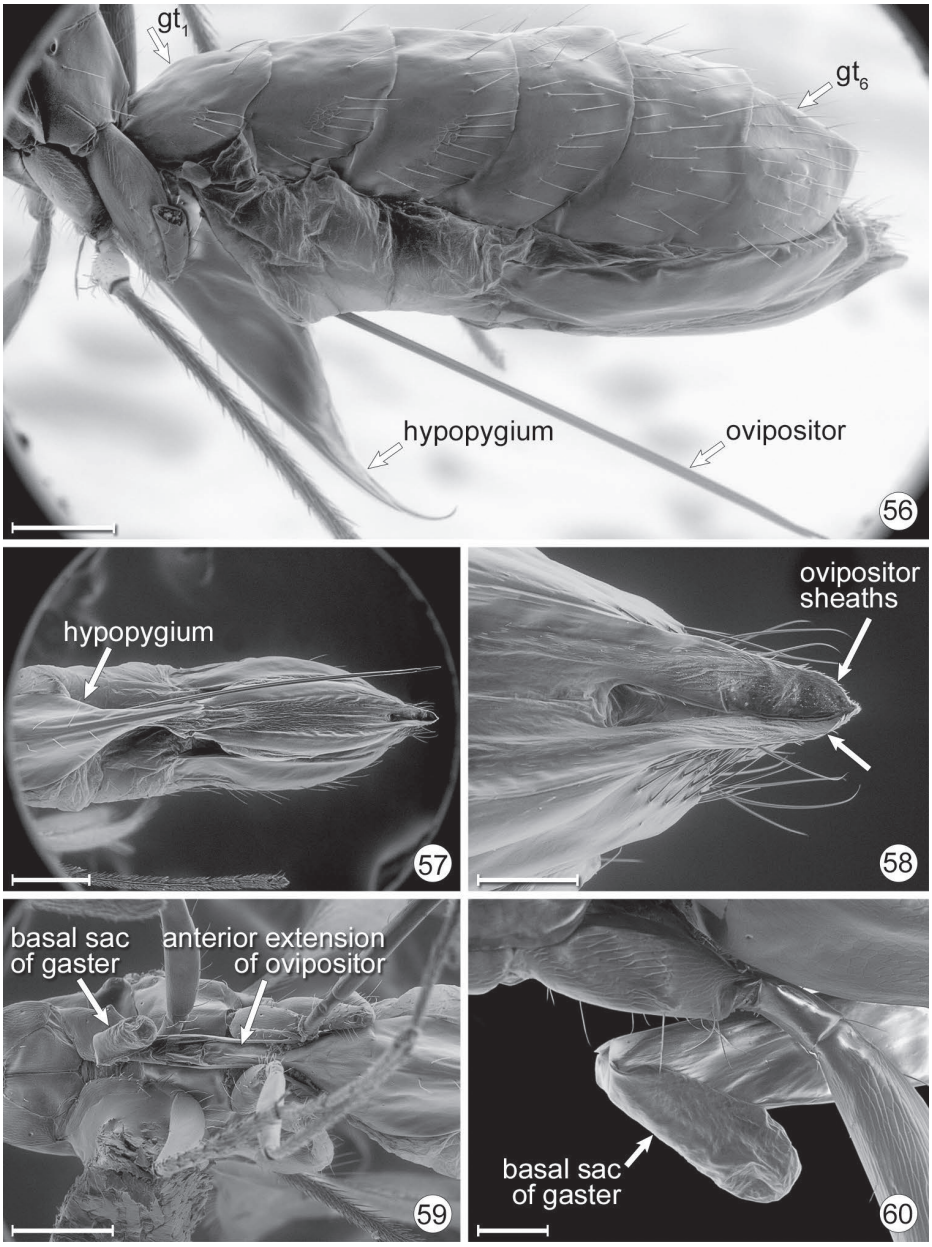

Figures 56–60. *Neotriadomerus* spp. **56** *N.* sp. metasoma, lateral **57** *N.* sp. metasoma, ventral **58** *N.* sp. apex of metasoma, ventral **59** *N.* sp. mesosoma and ovipositor sac, ventral **60** *N.* sp. apex of ovipositor sac, lateral. Scale bar for **56, 57, 59** = 200 μm; **58, 60** = 50 μm.

gt_4–gt_6 with even more in 2 or more irregular rows, those around spiracle often shorter; gt_7 with about 10 setae in one row. Hypopygium with about 4 ventral setae. Cerci with 4 fairly long curved setae.

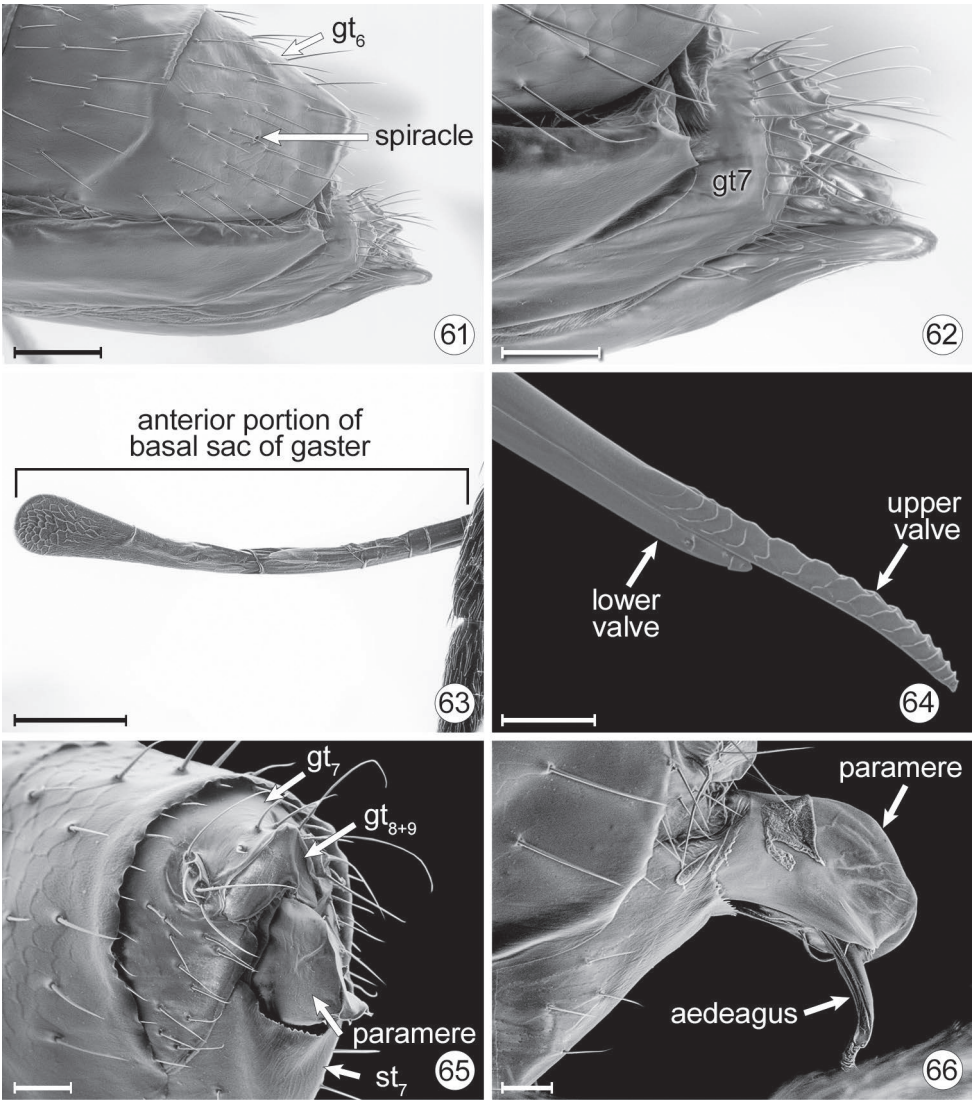

Figures 61–66. *Neotriadomerus* spp. **61** *N.* sp. apex of gaster, lateral **62** *N.* sp. gt_7 + ovipositor apex, lateral **63** *N. longissimus* ovipositor sac, lateral **64** *N.* sp. male ovipositor apex, lateral **65** *N. darlingi* apex of gaster, posterolateral **66** *N. powerae* male genitalia, lateral. Scale bar for **61** = 100 µm; **62** = 50 µm; **63** = 200 µm; **64–66** = 20 µm.

Male. Similar to female. Body 1280–2560 in length (males still unknown for the largest species). Flagellum with 11 relatively wide segments (Figs 40–43, 95). Gaster (card- or point mounted specimens) narrower than mesosoma, laterally compressed, with posterior apex in dorsal view wider and in lateral view usually higher than anterior apex (at petiole). Sculpture and setation of male similar to female but with fewer setae

on gt_6. Genitalia encapsulated, with thick walls; aedeagal apodemes evenly curved anteriorly towards each other, and shorter than aedeagus; paramere shorter than aedeagus and high in lateral view, with 3 or 4 short apical and ventral setae.

Etymology. The name is masculine. The prefix *Neo* is Greek for new or recent, young, + *Triadomerus*, apparently the closest related genus.

Distribution. *Neotriadomerus* species occur only in Australia where seven are described (below) and as many as four others are illustrated (Figs 144–152) but not named. No fossil species are known.

Hosts and habitat. Hosts are unknown. The estimated ovipositor length, when fully extended, is about 12 mm for the largest species of *Neotriadomerus*. This suggests that its host might be eggs of Orthoptera laid quite deeply inside plant tissue or in soil. Perhaps only Orthoptera, but possibly Coleoptera or Cicadidae, would have eggs long enough to host a developing female parasitoid (5.9 mm long) of this species. Specimens of *Neotriadomerus* have been collected in a variety of habitats in all Australian states except Victoria and Tasmania. Some specimens have been collected at light, suggesting they may be active at night. Noyes and Valentine (1989: 28, and figs 49, 50) discussed *Australomymar* Girault, illustrated two of the largest species, and suggested that eggs of Orthoptera or Cicadidae might be their hosts. Several specimens (NZAC, UCRC) of the species shown in Noyes and Valentine fig. 50, are ≈55 mm long excluding the posteriorly exserted section of the ovipositor and the longest one is 6.9 mm (NZAC) (S. Triapitsyn, D. Ward, personal communication). A much smaller, undescribed specimen (CNC) of *Australomymar*, was reared from an unidentified taxon of Tettigoniidae from *Pinus radiata* D. Don (Pinaceae) in Chile. I suggest here that Orthoptera might also be the hosts of *Neotriadomerus*.

Key to species of *Neotriadomerus*. Females.

1 Body 5000 long; ovipositor at least 5900 long, extending anteriorly under mesosoma to well beyond level of head (Fig. 126); mandible massive (Fig. 36) ..... ***N. longissimus* sp. n.**

– Body at most about 2600 long; ovipositor at most 2240 long, extending under mesosoma at most to level of head (Figs 114, 115); mandible much smaller (Figs 32, 33, 67) **2**

2(1) Fore wing with cubital line of setae extending proximally to base of parastigma, i.e., clearly proximal to other microtrichia on wing surface (Figs 70, 79, 103, 132) **3**

– Fore wing with cubital line of setae extending proximally only to apex of parastigma, about level with other microtrichia on wing surface (Figs 86, 113) **9**

3(2) Fl_1 with 2 mps; fl_2 with about 4 (5?) mps (Fig 69) ..... ***N. burwelli* sp. n.**

– Fl_1 with at least 4 mps; fl_2 with at least 6 mps (Figs 78, 102, 131) **4**

(3) Fl_2 with 2 barely overlapping whorls of mps (Figs 144, 147) **5**

– Fl_2 with 1 whorl of mps (Fig. 102) **6**

5(4) Fl_8 length/width 2.6 (Fig. 144) ..... ***N.* sp. 1**
– Fl_8 length/width 2.2 (Fig. 147) ..... ***N.* sp. 3**
6(4) Fl_1 about 0.7× as long as fl_2 (Fig. 102); remaining funicle segments longer and narrower, with fl_2 and fl_8, respectively, 2.5× and 2.0× as long as wide .... ***N. gloriosus* sp. n.**
– Fl_1 at least 0.9× as long as fl_2 (Figs 78, 131); remaining funicle segments shorter and wider, with fl_2 and fl_8, respectively, at most 2.1× and 1.9× as long as wide **7**
7(6) Fl_2–fl_7 each slightly more than 2.0 × as long as wide; clava about 3.2× as long as wide ..... ***N. powerae* sp. n.**
– Fl_2–fl_7 each at most 1.6× as long as wide; clava about 2.6× as long as wide (Fig. 78) 8
8(7) Fl_2–fl_3 each about 1.6× as long as wide ..... ***N. crassus* sp. n.**
– Fl_2–fl_3 each almost quadrate ..... *N.* sp. 2
9(2) Ovipositor extending anteriorly under mesosoma to level of head (Figs 114, 115), at least . about 3.6× as long as metatibia; funicle with at least 9 mps on each segment (Fig. 112) ..... ***N. longiovipositor* sp. n.**
– Ovipositor extending anteriorly under mesosoma to level of apex of procoxa (Fig. 92), at most about 2.8× as long as metatibia; funicle with 6 mps on each segment (Fig. 85) ..... ***N. darlingi* sp. n.**

Key to species of *Neotriadomerus*. Males.

Males of *darlingi*, *longiovipositor* and *powerae* are known and almost certainly correctly associated with the corresponding females; males are unknown for *N. burwelli*, *N. crassus*, *N. gloriosus* and *N. longissimus*. Two unnamed males are also keyed; one (sp. 4) is not definitely associated with a female and the other (sp. 1) is definitely associated with a female.

1 Fore wing with cubital line of setae extending at least to base of parastigma, clearly proximal to other microtrichia on wing surface (Fig. 139) **2**
– Fore wing with cubital line of setae extending at most to apex of parastigma (level with distal macrochaeta), about level with other microtrichia on wing surface (Fig. 95) **4**
2(1) Fl_6 wider, its length/width about 1.8 (Fig. 150)..... ***Neotriadomerus* sp. 4**
– Fl_6 narrower, its length/width at least 2.0 (Fig. 138)..... **3**
3(2) Fl_6 about 2.0 ..... ***N. powerae* sp. n.**
– Fl_6 about 3.5 ..... ***N.* sp. 1**
4(1) Flagellomeres each with 2 barely overlapping whorls of shorter mps (Fig. 121)..... ***N. longiovipositor* sp. n.**
– Flagellomeres each with 1 whorl of longer mps (Fig. 95)..... ***N.* ?*darlingi* sp. n.**

***Neotriadomerus burwelli* Huber, sp. n.**
http://zoobank.org/B09A3418-3623-42B6-B88F-62C9729617E3
Figs 67–75

Type material. Holotype female (QMBA) on slide (Fig. 71) labelled: 1."Mahogany forest, 1200m Mt Moffatt Nat. Pk, C. Qld 24°56'S, 148°04'E 24-26 Feb 1996 C.J. Burwell mv lamp". 2. "Holotype Neotriadomerus burwelli Huber ♀".

Diagnosis. *Neotriadomerus burwelli* differs from the other small (body length less than 2600) species of *Neotriadomerus*, as follows: fore wing with cubital line extending proximally to base of parastigma (Fig. 70); fl_1 with 2 mps, fl_2 with 4 mps and almost 2× as long as fl_1, and fl_2–fl_5 each at least 2.0× as long as wide and with at most 6 long mps in 1 whorl (Fig.69); ovipositor 2.7× as long as metatibia and extending anteriorly under mesosoma as far as apex of procoxa (Fig. 74).

Description. Female. Body length ≈ 1590 (holotype). **Colour.** Holotype body almost uniformly dark brown; legs brown, with trochantelli, base and apex of femora and entire protibia, base and apex of meso- and metatibiae, and tarsi except tarsomere 5 paler, almost white; tarsomere 5 brown. **Head.** Head width 305 (Figs 67, 68). **Antenna.** Fl_1 about 0.5 as long as fl_2, with 2 mps; fl_2 the longest funicle segment, with 4 mps; fl_3–fl_7 with 4–6 mps; fl_8 with 7? mps. Clava with about 12 mps, 5 on first, 2 on second and 5 on third segment (Fig. 69). Antennal measurements (n=1), length/width (ratio of flagellar segments): scape 119/20 (3.91), pedicel 50/31 (1.62), fl_1 63/27 (2.32), fl_2 82/29 (2.82/3.10 [left and right antenna different]), fl_3 77/28 (2.80), fl_4 73/30 (2.46), fl_5 79/28 (2.79/2.36 [left and right antenna different]), fl_6 70/30 (2.38), fl_7 70/31 (2.27), fl_8 69/34 (2.00); entire clava 118/41 (2.89), with segments 1–3 length [measured along dorsal margin] 44, 21, and 54. **Mesosoma.** Width 250, length 514. **Wings.** Fore wing length 1074, width 386, length/width 2.78, longest marginal setae 60; cubital line extending to just proximal to base of parastigma (Fig. 70). Hind wing length 862, width 118, longest marginal setae ≈ 66. **Legs.** Protibia with 5 short pegs along its length and a transverse row of 4 abutting pegs apically (as in Fig. 53). **Metasoma.** Metasoma in dorsal view 300 at widest point, gradually widening from petiole to about 0.6 of gaster length towards apex, then more abruptly narrowing to cerci (Fig. 73). Gaster length 745, about 1.45× as long as mesosoma; gt_1–gt_7 lengths about 220: 105: 100: 100; 130: 98 (Fig. 73); hypopygium (apex difficult to see) extending about 0.7× length of gaster. Ovipositor sheath length 1041, 2.64× metatibia length (394) and extending anteriorly to just anterior apex of procoxae (Fig. 74) and posteriorly slightly beyond apex of gaster (Figs 73, 75).

Male. Unknown.

Etymology. The species is named after Chris Burwell, curator of insects at the Queensland Museum, who collected the only known specimen of this species.

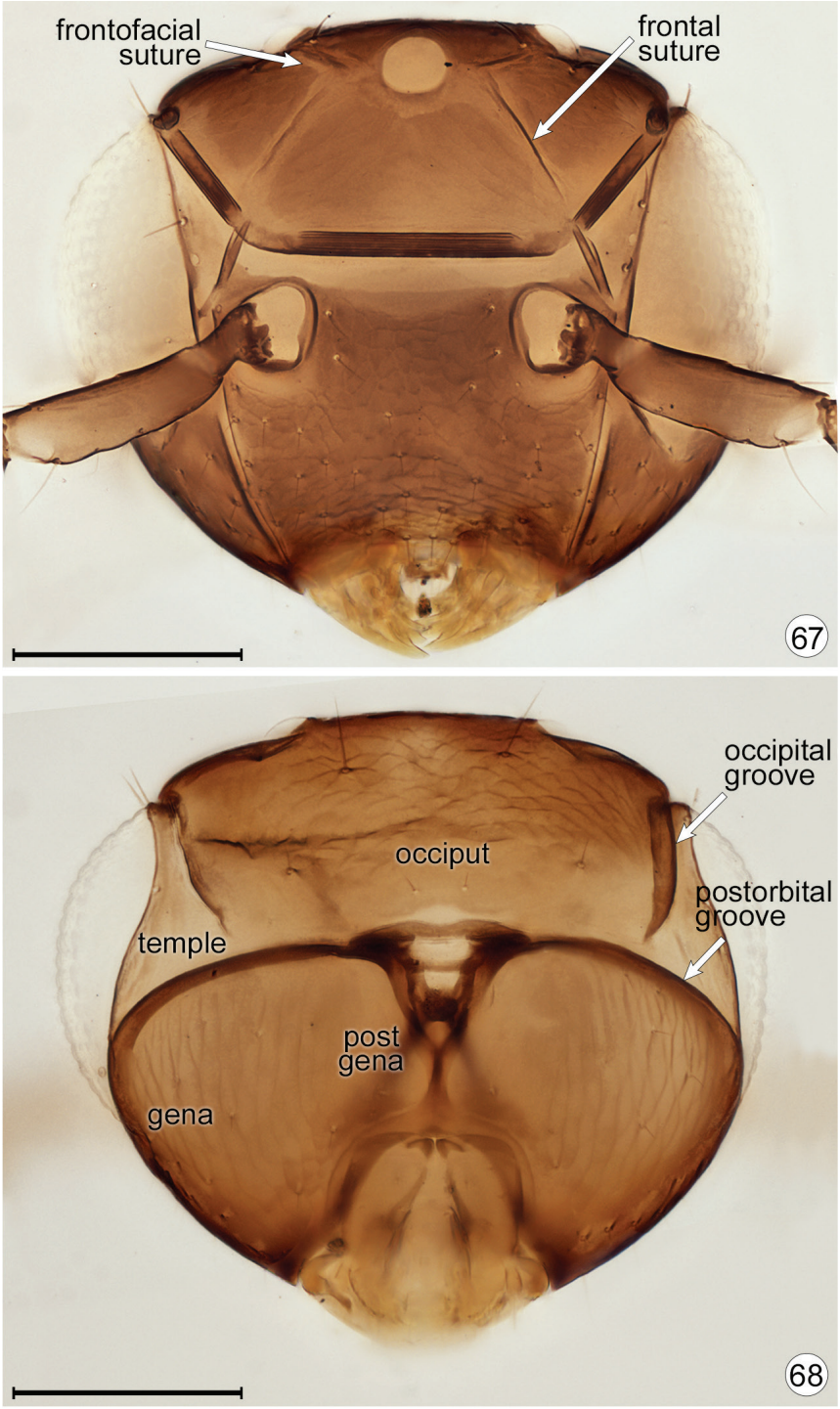

Figures 67, 68. *Neotriadomerus burwelli*, holotype. **67** head, anterior **68** head, posterior. Scale bar = 100 µm.

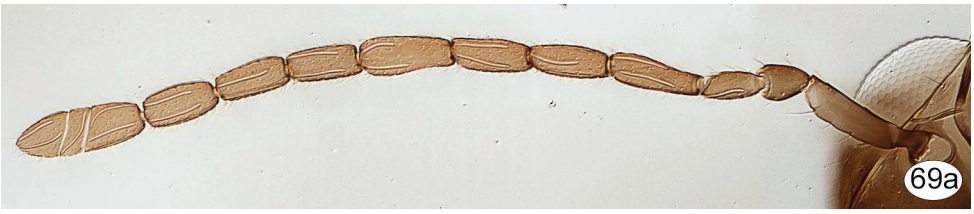

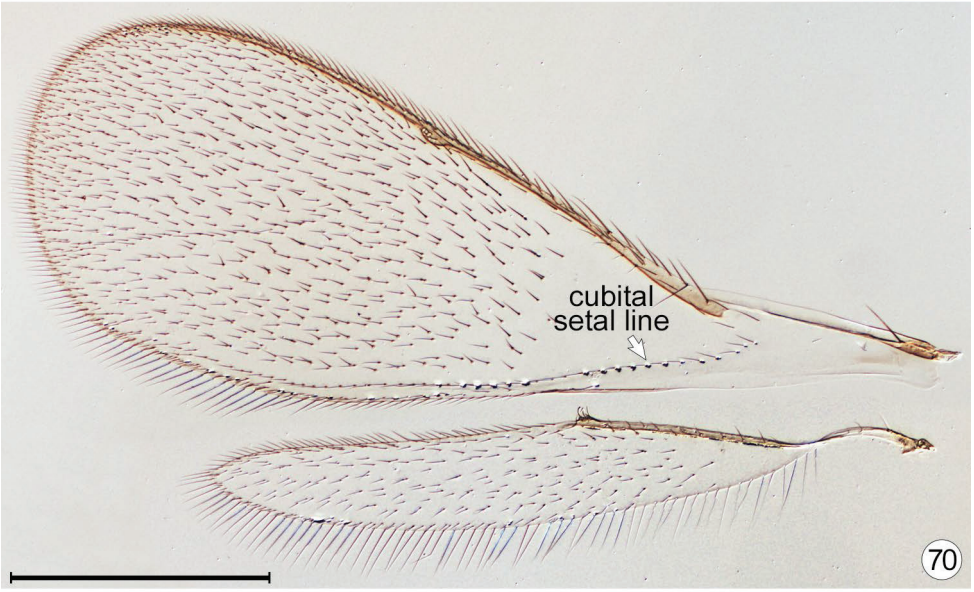

Figures 69–71. *Neotriadomerus burwelli*, holotype. **69a** right antenna, medial **69b** same antenna, lateral (as seen through antenna) **70** wings **71** holotype slide. Scale bar = 300 µm.

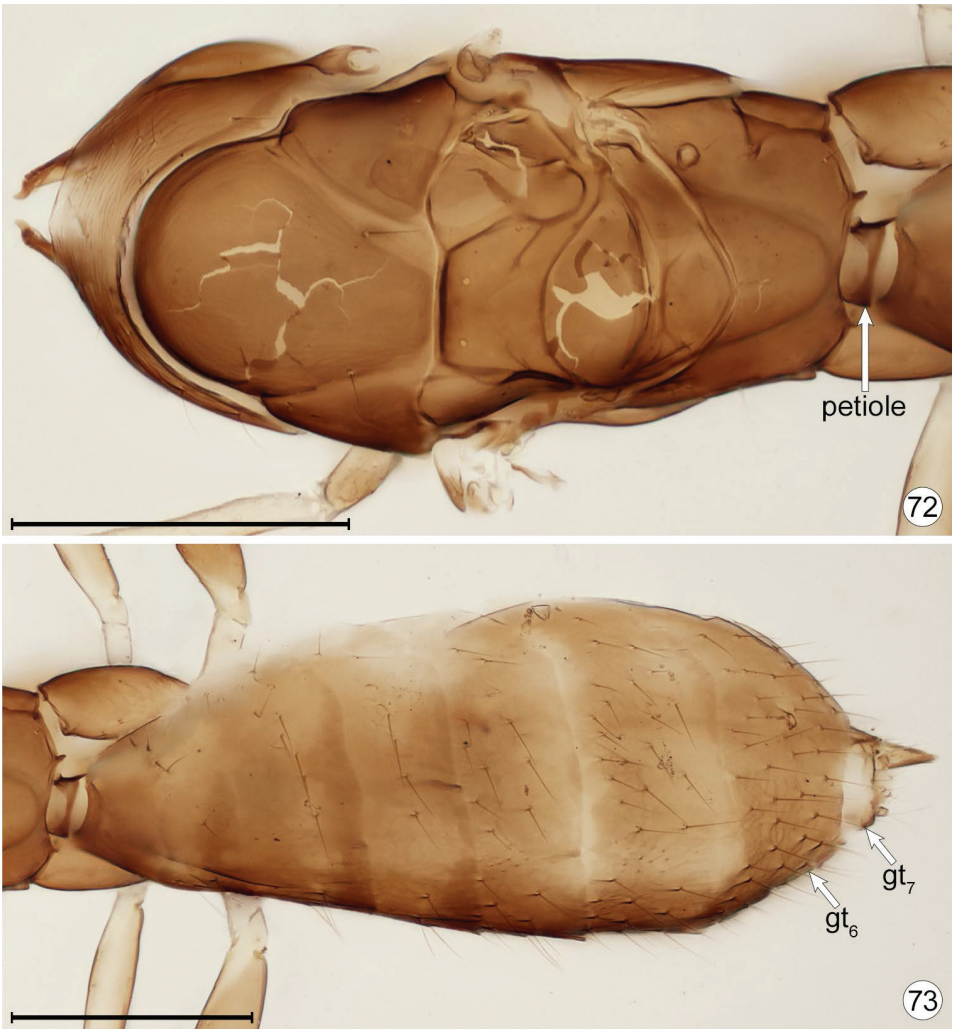

Figures 72, 73. *Neotriadomerus burwelli*, holotype. **72** mesosoma, dorsal **73** metasoma, dorsal. Scale bar = 300 μm.

***Neotriadomerus crassus* Huber, sp. n.**
http://zoobank.org/DC4DB59A-207D-4DBD-9234-C944B9FD71AA
Figs 76–80

Type material. Holotype female (ANIC) on slide (Fig. 80) labelled: 1. "Black Mountain, ACT 28-29 Mar. 1968 light trap". 2. "Neotriadomerus crassus ♀ lateral holotype".

Diagnosis. *Neotriadomerus crassus* differs from the other small (body length less than 2600) species of *Neotriadomerus* as follows: fore wing with cubital line extending proximally to about base of parastigma (Fig. 79); fl_1–fl_8 relatively short, each at most 1.65× as long as wide and with at least 8 mps (Fig. 78).

Figures 74, 75. *Neotriadomerus burwelli*, holotype. **74** mesosoma, ventral **75** metasoma, ventral (seen through body). Scale bar = 300 μm.

Description. Female. Body length ≈ 1685 (holotype). **Colour.** Body almost uniformly dark brown; legs brown, with trochantelli, base and apex of femora and entire protibia, base and apex of meso- and metatibiae, and tarsi except tarsomere 5 of all legs and metatarsomere 1 paler, almost white; tarsomere 5 brown and metatarsomere 1

Figures 76, 77. *Neotriadomerus crassus*, holotype. **76** head + anterior of mesosoma, dorsolateral **77** mesosoma + metasoma (ovipositor broken off near base of hypopygium), dorsolateral. Scale bar for **76** = 200 μm; **77** = 500 μm.

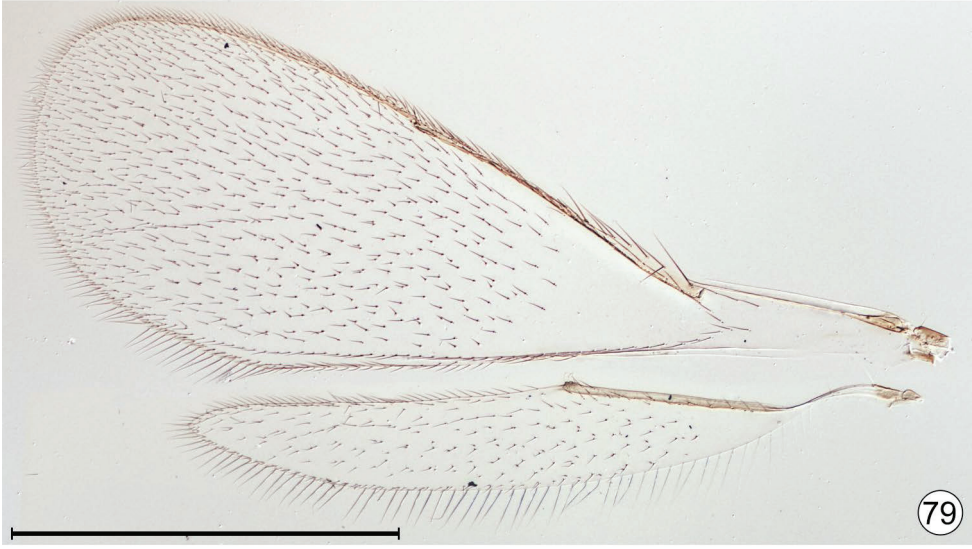

Figures 78–80. *Neotriadomerus crassus*, holotype. **78** antenna **79** wings **80** type slide. Scale bar = 500 µm.

light brown. **Head.** Width not measurable (Fig. 76). **Antenna.** Fl_1 slightly longer than fl_2, apparently with 8 mps; fl_2–fl_8 with 8 mps (possibly 9 or 10 on fl_7 and fl_8); clava with about 22 mps, 8 on first, 6 on second and 8 on third segment (Fig. 78). Antennal measurements (n=1), length/width (ratio of flagellar segments): scape 145/47 (3.10), pedicel 58/42 (1.37), fl_1 86/56 (1.53), fl_2 84/52 (1.60), fl_3 82/50 (1.63), fl_4 81/50 (1.63), fl_5 86/53 (1.62), fl_6 82/51 (1.59), fl_7 78/50 (1.57), fl_8 76/48 (1.58); entire clava 143/55 (2.59), with segments 1–3 length [measured along dorsal margin], 46, 35, and 64. **Mesosoma.** Width not measurable, length 580. **Wings.** Fore wing length 1154, width 397, length/width 2.91, longest marginal setae 46; cubital line extending to just proximal to base of parastigma (Fig. 79). Hind wing length 942, width 130, longest marginal setae 66. **Legs.** Protibia with 6 short, thick pegs along its length and transverse row of 4 abutting pegs apically (as in Fig. 53). **Metasoma.** Metasoma (Fig. 77) in lateral view 224 at highest point, gradually widening from petiole to about 0.6 of

gaster length towards apex, then more abruptly narrowing to cerci. Gaster length 765, about 1.63× as long as mesosoma; gt_1–gt_6 lengths about ≈ 156, ≈ 94, 87, 112, 118, 152; hypopygium (Fig. 77, positioned at right angle to metasoma) extending about 0.7× length of gaster, extending to about halfway towards apex of tergum 5. Ovipositor broken and partly missing, with estimated length (from basal loop to posterior apex of sheath) ≈ 864, about 2.11× metatibia length (410), extending anteriorly to about level of apex of mesocoxae and extending posteriorly slightly beyond apex of gaster (Fig. 77).

Male. Unknown.

Etymology. The species name, *crassus*, is Latin for thick or stout, referring to the fairly short, thick funicle segments in females.

***Neotriadomerus darlingi* Huber, sp. n.**
http://zoobank.org/12B05D86-1539-4CA9-B5F8-6895EA2E6952
Figs 33, 40–44, 47, 50, 52, 65, 81–99

Type material. Holotype female (ANIC) on slide (Fig. 84), labelled: 1. "Australia: Sth Aust. 32 km N. Renmark, 263m 33°53'S, 140°43'E, 15.ii-15.iv.2000, DC Darling". 2. "Bookmark Biosphere Rsv. Malaise trps (4) Amalia Dam xeric mallee scrub ROM 2000040". 3. "Neotriadomerus darlingi Huber Holotype ♀ dorsal".

Paratypes. 3 females, 1 male. AUSTRALIA. **South Australia:** Same locality data as holotype (1 ♀ and 1♂, ROM, CNC); 35 km N Renmark, 263m, 33°52'48"S; 140°43'30"E, 11-14.ii.2000, D.C. Darling, Bookmark Biosphere Reserve, Malaise trap, Amalia Dam, mallee vegetation, ROM 2000030 (1♀, ANIC). **Western Australia:** 85 km E. Southern Cross, Boorabbin National Park, 28.xii.1986, J.S. Noyes (1♀, BMNH)

Two males with the following data questionably belong to this species so are not labelled as paratypes. They were collected from South Australia, Brookfield Conservation Park, 34.21°S, 139.29°E, 17 & 18.ii.1992, J. Cardale, A. Roach, light trap (2♂, ANIC) and one is illustrated (Figs 93–99). Both sexes need to be collected together from Brookfield Conservation Area to be more certain of their conspecificity with the holotype.

Diagnosis. *Neotriadomerus darlingi* differs from the other small (body length less than 2600) species of *Neotriadomerus* as follows: fore wing with cubital line extending proximally to about level of other microtrichia (Fig. 86); funicle segments with at most 6 mps (Fig. 85); ovipositor 2.57–2.74× as long as metatibia (Fig. 92).

Description. Female. Body length 1420–1560 (n=2, card-mounted paratypes). **Colour**. Body (Fig. 81) almost uniformly dark brown; fore leg yellow except procoxa brownish basally, ventral surface of profemur and tarsomere 5 brown; middle and hind legs lighter brown with trochantelli, base and apex of femora and entire protibia, base and apex of meso- and metatibiae, and tarsi except tarsomere 5 paler, almost white; metafemur medially and tarsomere 5 brown; ovipositor sheath with lighter band subapically (Figs 81, 88, 89). **Head.** Width ≈ 320–346 (card-mounted) and 358 (slide

Figure 81. *Neotriadomerus darlingi*, paratype female, habitus lateral (35 km N. Renmark, 263 m, 11–14. ii.2000). Scale bar = 1000 μm.

mounted specimen from WA, Figs 90, 91). **Antenna.** Fl_1 slightly shorter than to almost equal to fl_2, with 5 mps (Fig. 85); fl_2–fl_8 with 6 mps. Clava with 10 or 11 mps, 5 or 6 on first, 2 on second and 4 on third segment. Antennal measurements (n=2, first

Figure 82. *Neotriadomerus darlingi*, paratype male, habitus dorsal (35 km N. Renmark, 263 m, 15.ii–15.iv.2000). Scale bar = 1000 μm.

number is for the holotype, a slightly smaller specimen), length/width (ratio of flagellar segments): scape 124–126/37–40 (3.37–2.51), pedicel 50–56/39–41 (1.29–1.36), fl_1 70–74/38–45 (1.85–1.65), fl_2 80–75/34–40 (2.36–1.88), fl_3 77–76/34–38 (2.26–1.97), fl_4 78–75/35–38 (2.24–1.96), fl_5 79–76/33–38 (2.39–2.01), fl_6 76–74/33–37 (2.28–2.20), fl_7 77–78/34–39 (2.23–2.13), fl_8 76/34–40 (2.25–1.89); entire clava 141–142/39–42 (3.63–3.40), with segments 1–3 length [measured along dorsal margin], 48–50, 25, and 67–68. **Mesosoma.** Width 225 (holotype), length 628–656, with 2 propodeal setae (Fig. 87). **Wings.** Fore wing length 1045–1118, width 383–412, length/width 2.71–2.73, longest marginal setae ≈ 51–61; cubital line extending to just proximal to base of parastigma (Fig. 86). Hind wing length ≈ 870–890, width 121–140, longest marginal setae ≈ 58–62. **Legs.** Protibia with 4 or 5 short, thick pegs along its length and a transverse row of 2 or 3 abutting pegs apically. **Metasoma.** Metasoma in lateral view 255–360 at highest point, gradually widening from petiole to about 0.4–0.7 of gaster length towards apex, then more abruptly narrowing to cerci (Fig. 89). Gaster length (holotype, second measurement) 776–858, 1.18–1.36× as long as mesosoma; gt_1–gt_7 lengths about ≈ 162–170, ≈ 136–144, 98–126, 113–177, 132–186,

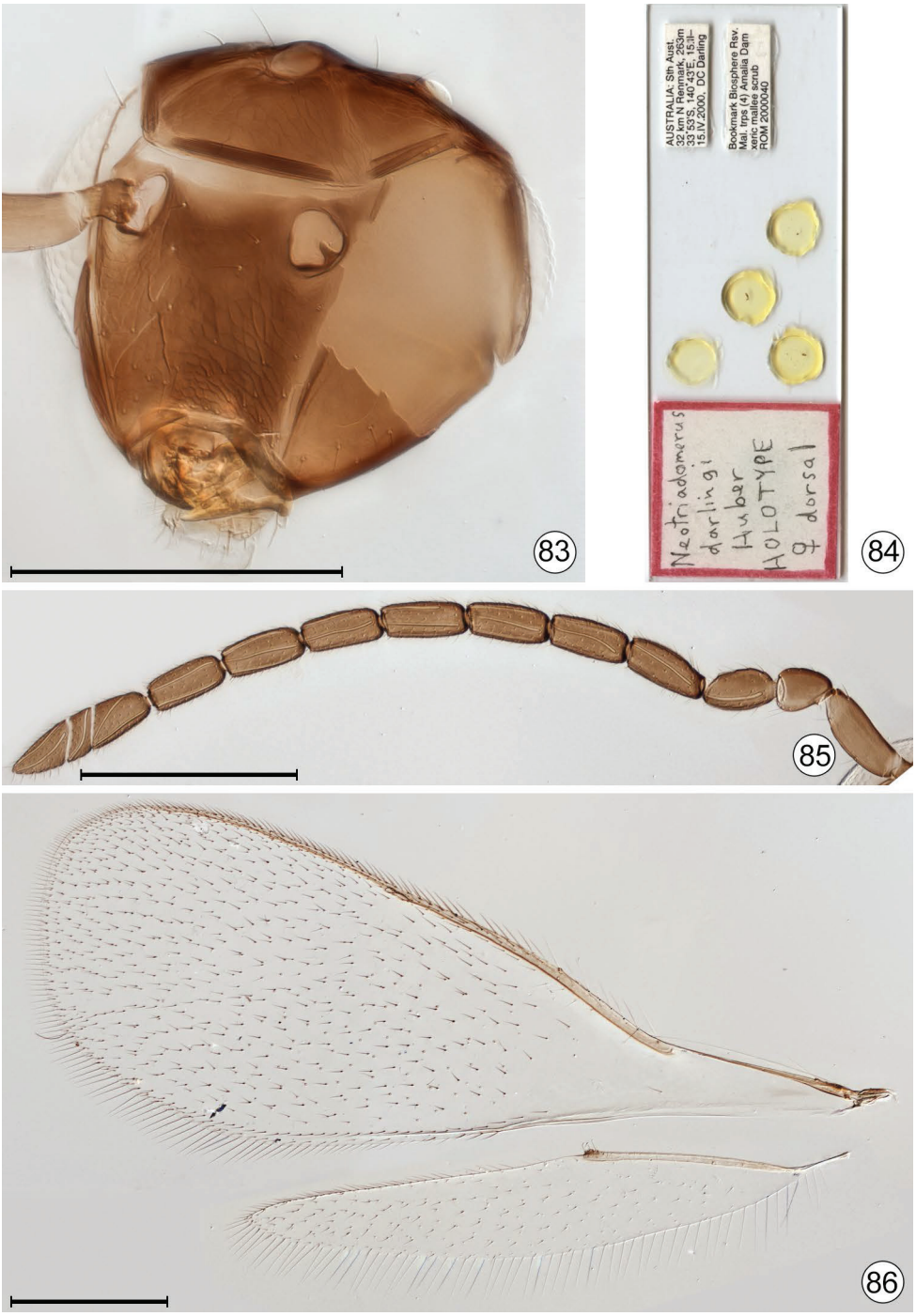

Figures 83–86. *Neotriadomerus darlingi*, holotype. **83** head, anterolateral **84** type slide **85** antenna **86** wings. Scale bar = 200 µm.

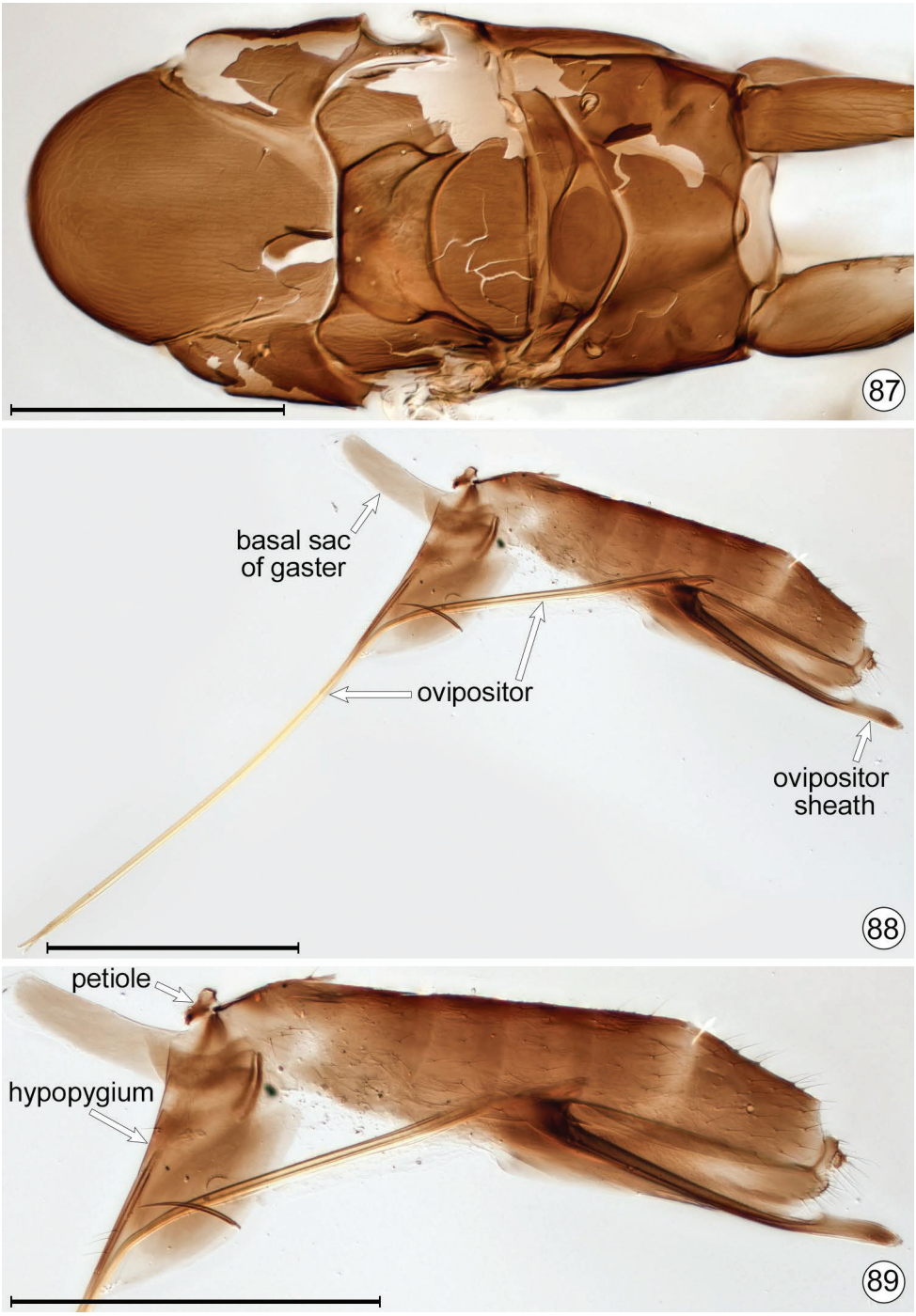

Figures 87–89. *Neotriadomerus darlingi*, holotype. **87** mesosoma, dorsal **88** metasoma, lateral, with ovipositor unsheathed **89** metasoma enlarged, lateral. Scale bar for **87** = 200 µm; **88, 89** = 500 µm. Note: 88 and 89 are flipped horizontally (gaster apex pointing left in holotype slide).

Figures 90–92. *Neotriadomerus darlingi*, paratype female (Boorabbin National Park). **90** head, anterior **91** head, posterior **92** mesosoma, legs and metasoma, lateral. Scale bar for **90, 91** = 200 μm; **92** = 500 μm.

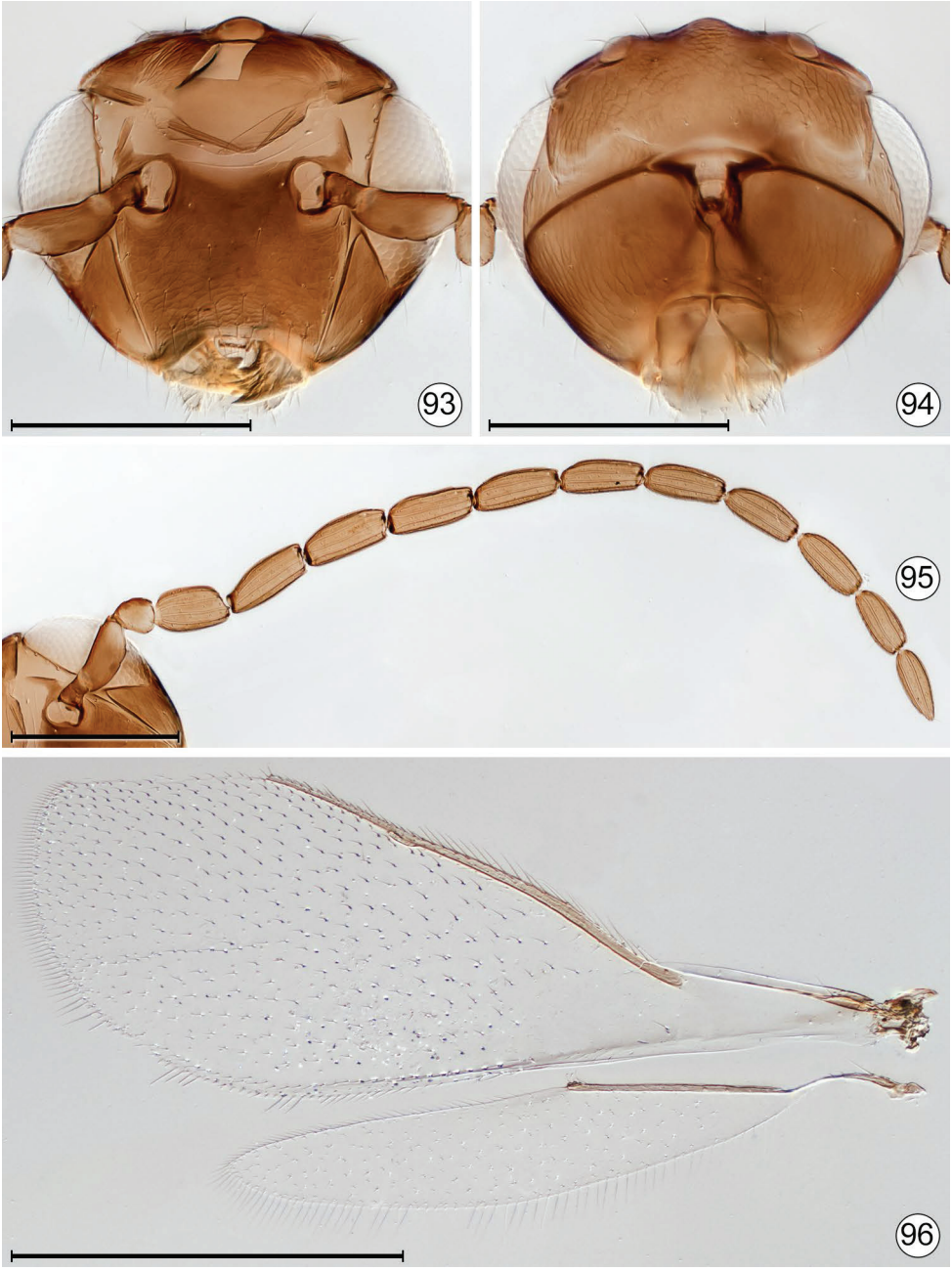

Figures 93–96. *Neotriadomerus ?darlingi*, paratype male (Brookfield Conservation Area). **93** head, anterior **94** head, posterior **95** antenna **96** wings. Scale bar for **93–95** = 200 µm; **96** = 500 µm.

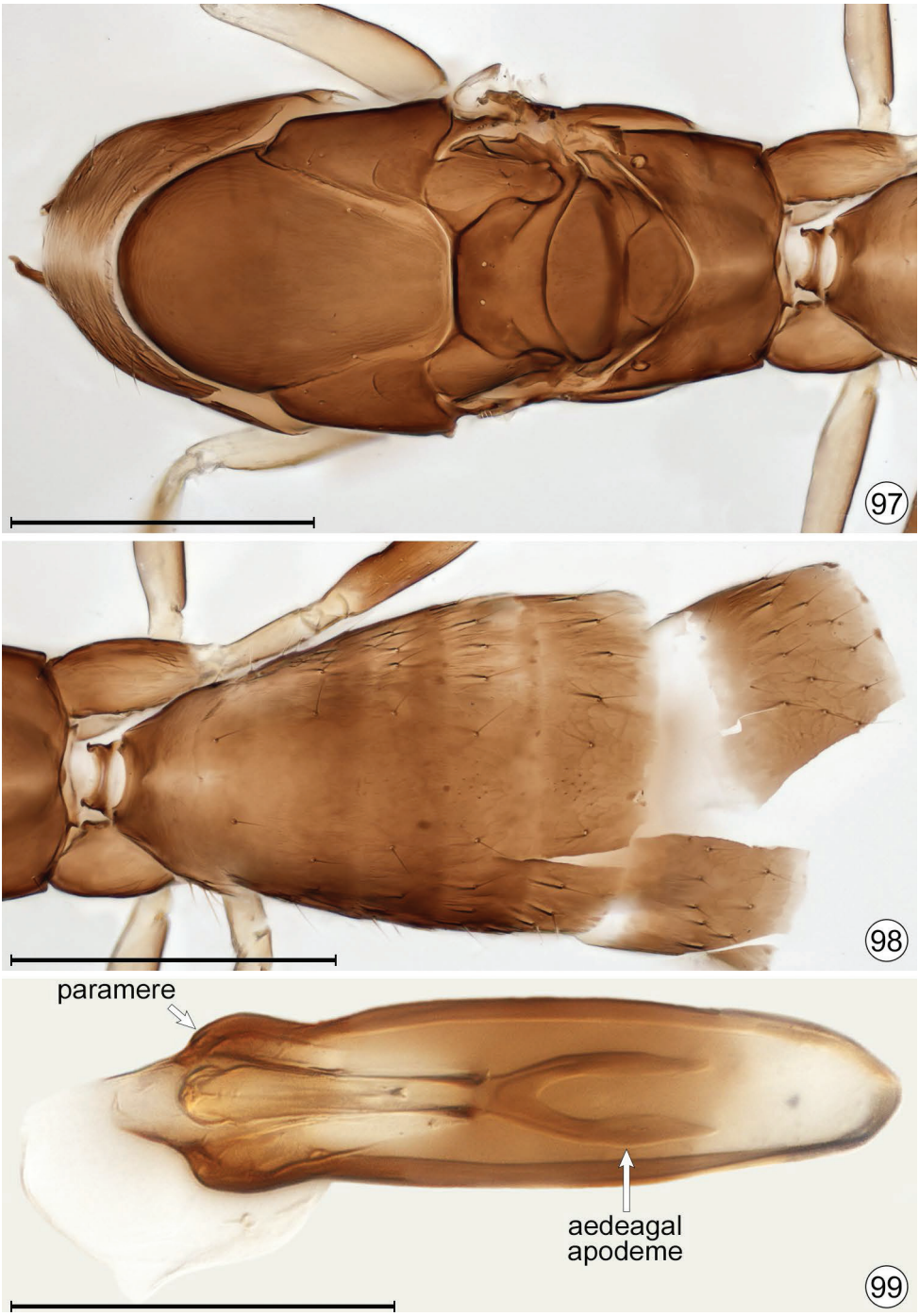

Figures 97–99. *Neotriadomerus* ?*darlingi*, paratype male (Brookfield Conservation Area). **97** mesosoma, dorsal **98** metasoma, dorsal (gt_7 broken off) **99** genitalia, dorsal. Scale bar for **97, 98** = 300 μm; **99** = 100 μm.

209–146, 53–58; hypopygium extending about 0.6× length of gaster, about to apex of tergum 4. Ovipositor sheath length ≈ 946–1050, about 2.57–2.74× metatibia length (368–383), extending anteriorly to apex of procoxa (or anterior margin of frenum) and extending posteriorly to a little beyond apex of gaster (Figs 88, 89, 92).

Male. Body length 1330 (point-mounted paratype) and 1230 (slide-mounted specimen, Brookfield Conservation Area). Colour as for female but with legs almost entirely brown (Fig. 82). **Head.** If correctly associated, as for female (Figs 93, 94). **Antenna.** Fl_1 with about 13 mps and about 1.5× as wide as fl_{11} with about 7 mps (Fig. 95); total length of flagellum 475. Antennal measurements length/width (slide-mounted specimen): scape 120/41 (2.90), pedicel 47/43 (1.09), fl_1 92/53 (1.75), fl_2 105/48 (2.24), fl_3 108/48 (2.24), fl_4 104/44 (2.38), fl_5 109/43 (2.54), fl_6 100/42 (2.41), fl_7 98/41 (2.39), fl_8 97/43 (2.24), fl_9, 96/41 (2.35), fl_{10} 86/39 (2.22), fl_{11} 92/35 (2.64); fl_6 with about 11 mps. **Mesosoma.** Length 620, width 290 (Fig. 97). **Wings.** If correctly associated, as for female (Fig. 96). **Metasoma.** Pedicel length/width 30/75 (Fig. 98). Gaster length ≈ 785. Genitalia with capsule thick-walled, aedeagal apodeme thick and shorter than aedeagus; paramere thick and apically curved medially (Fig. 99).

Etymology. The species is named after Chris Darling, curator of Entomology at the Royal Ontario Museum, Toronto, who collected the type series.

Neotriadomerus gloriosus Huber, sp. n.

http://zoobank.org/33067489-E0B9-488E-9AAD-591B903E3F00
Figs 32, 34, 35, 100–107

Type material. Holotype female (QMBA) on slide (Fig. 107), labelled: 1. "Mt. Glorious, S.E. Qld. Hiller March 1982 Malaise trap". 2. "Neotriadomerus gloriosus Huber ♀ dorsal holotype".

Diagnosis. *Neotriadomerus gloriosus* differs from the other small (body length less than 2600) species of *Neotriadomerus*, as follows: fore wing with cubital line extending to just proximal to base of parastigma (Fig. 103); fl_2–fl_5 each at least 2.0× as long as wide and with at most 6 long mps in 1 whorl (Fig. 102).

Description. Female. Body length ≈ 1840 (holotype). **Colour**. Holotype body almost uniformly dark brown; legs brown, with trochantelli, base and apex of femora and entire protibia, and base and apex of meso- and metatibiae, and tarsi except tarsomere 5 paler, almost white; tarsomere 5 brown. **Head.** Head width 374 (Figs 100, 101). **Antenna.** Fl_1 about 0.7× as long as fl_2, with 4 mps; fl_2 slightly the longest funicle segment, with 8 mps; fl_3–fl_8 with 8 (9? on fl_8) mps; clava with about 18 mps, 8 on first, 4 on second and 6 (8?) on third segment (Fig. 102). Antennal measurements (n=1), length/width (ratios of flagellar segments, different for each antenna so left antenna, except scape of right antenna, measured—the left antenna has narrower funicle segments): scape 152/49 (3.10), pedicel 57/43 (1.32), fl_1 91/50 (1.84), fl_2 118/48 (2.47), fl_3 114/46 (2.48), fl_4 111/46 (2.43), fl_5 105/46 (2.29), fl_6 99/45 (2.21), fl_7 99/47 (2.09), fl_8 92/46 (1.98); entire clava 148/52 (2.82), with segments 1–3 length

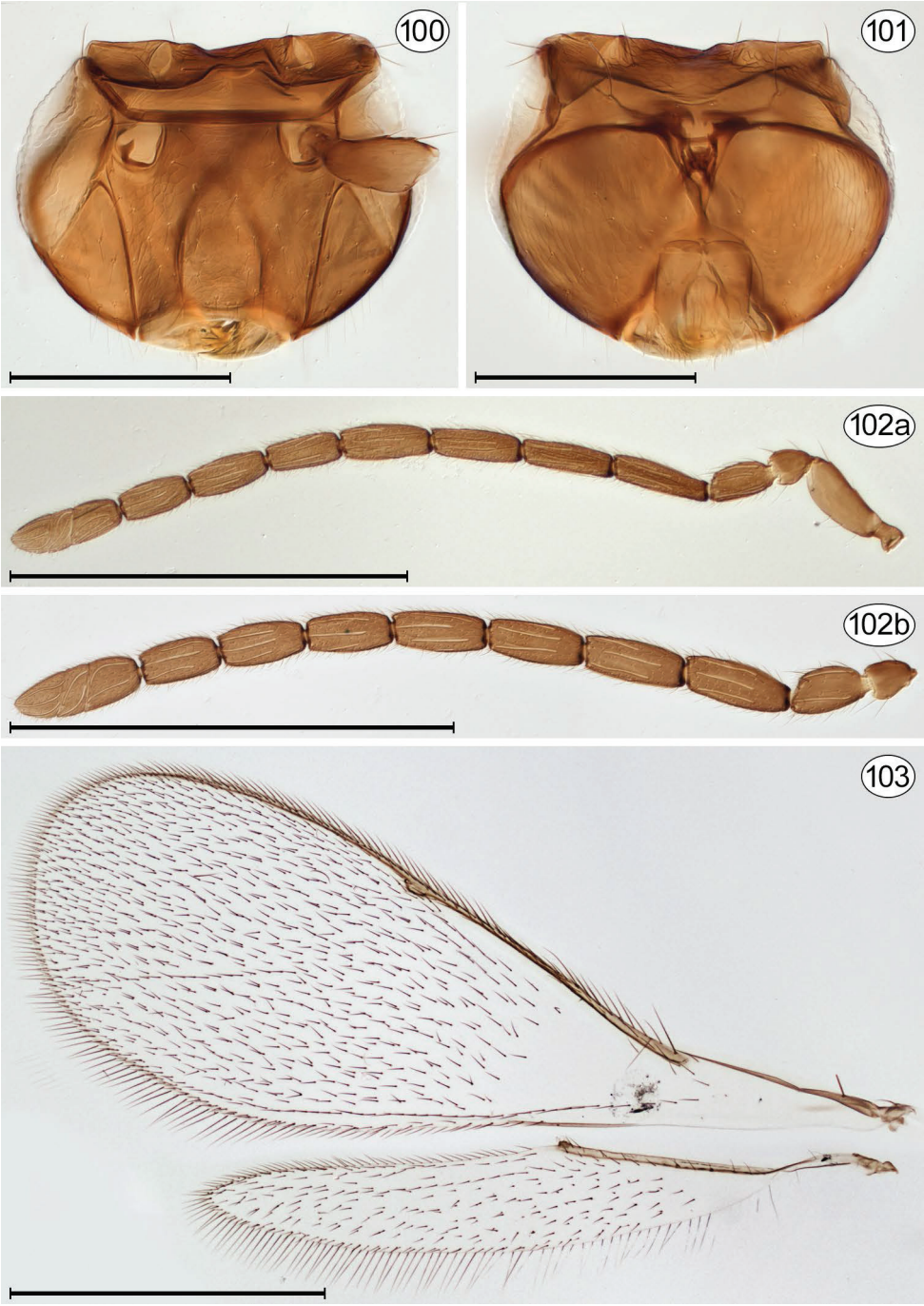

Figures 100–103. *Neotriadomerus gloriosus*, holotype. **100** head, anterior **101** head, posterior **102a** right antenna **102b** left antenna **103** wings. Scale bar for **100, 101** = 200 µm; **102, 103** = 500 µm.

Figures 104–107. *Neotriadomerus gloriosus*, holotype. **104** mesosoma, dorsal **105** metasoma, lateral **106** metasoma, median plane **107** type slide. Scale bar = 200 µm.

[measured along dorsal margin] 56, 28, and 64. **Mesosoma.** Width 324, length 711, with 2 propodeal setae (Fig. 104). **Wings.** Fore wing length 1367, width 486, length/width 2.81, longest marginal setae 77; cubital line extending to just proximal to base of

parastigma (Fig. 103). Hind wing length 1109, width 157, longest marginal setae 78. **Legs.** Protibia with 6 or 7 short, thick pegs along its length and a transverse row of 4 abutting pegs apically (as in Fig. 53). **Metasoma.** Metasoma height in lateral view 225 (excluding lowered hypopygium) (Figs 105, 106). Gaster length 1002, about 1.41× as long as mesosoma; gt_1–gt_7 lengths about 170: 166: 151: 118: 130: 209 [measurement of a tergum excludes the telescoped portion inside another (more anterior) tergum]; hypopygium extending posteriorly to about level of spiracle. Ovipositor sheath length 1274, ≈ 2.54× metatibia length (≈ 502), extending anteriorly to about level of apex of procoxa and extending posteriorly only slightly beyond apex of gaster (Fig. 105, 106) [apparently extending more than normal because ovipositor not at its normal resting position, i.e., filling entire length of basal sac of gaster, whose almost membranous apex is distinctly folded over (Fig. 105, arrow)].

Male. Unknown.

Etymology. The species is named after the type locality, Mt. Glorious National Park.

Neotriadomerus longiovipositor **Huber, sp. n.**
http://zoobank.org/1CDB865F-9F10-446D-913D-C76B7E6501C2
Figs 108–125

Type material. Holotype female (ANIC) on slide (Fig. 111) labelled: 1. "15.17S 145.10E 5Km WbyN Rounded Hill nr Hope Vale Mission Q 7 Oct. 1980 J.C. Cardale ex ethanol". 2. "Neotriadomerus longiovipositor Huber Holotype ♀ dorsal".

Paratypes. 4 females, 4 males, 1 deformed male (gynandromorph?). AUSTRALIA. **Queensland:** Batavia Downs, 12.40°S; 142.39°E, 22.vi–23.viii.1992, P. Zborowski & J. Cardale, flight interception trap (1♂, ANIC); NW of Chillagoe near historical mine site, 17°08'40"S; 144°30'16"E, 30.iii.1992, E.C. Dahms & G. Sarnes (1♂, QMBA); 18.5 km W. Gordonvale, 13.xi.1979, E.C. Dahms, J.B. Woolley & J. LaSalle, open forest (1♀, QDPC); Heathlands, 11.45°S; 142.35°E, 15–26.i.1992, I. Naumann, T. Weir, at light (1♀, ANIC); Millstream Falls National Park, 17.41°S; 145.26°E, 24–25.v.1980, I.D. Naumann, J.C. Cardale (1 deformed ♂, ANIC); 5 km W. by N. Rounded Hill near Hope Vale Mission, 15.17°S, 145.10°E; 7-10.v.1981, I.D. Naumann (1♀, ANIC); 15.16°S; 144.59°E 14 km W. by N. Hope Vale Mission. 8-18.x.1980, J.C. Cardale, collected at light (1♂, ANIC); Ross River resevoir, 10 km S. Townsville, 19° 27'S; 146° 44'E, 27.xi.1991, C.J. Burwell (1♂, QMBA); near Swamp Mitchell Plateau airfield, 14.47°S; 125.49°E, 18.v.1983, I.D. Naumann, J.C. Cardale (1♀, ANIC).

Diagnosis. *Neotriadomerus longiovipositor* differs from the other small (body length less than 2600) species of *Neotriadomerus*, as follows: fore wing with cubital line extending proximally to about level of other microtrichia (Fig. 113); ovipositor extending anteriorly under mesosoma at least to level of head (Figs 114, 115); funicle segments with mps in two widely overlapping whorls (Fig. 112). Male flagellomeres with mps in two scarcely overlapping whorls (Fig 121).

Figures 108–111. *Neotriadomerus longiovipositor*, holotype. **108** head, anterior **109** mouthparts and tentorium **110** head, posterior **111** holotype slide. Scale bar = 200 µm.

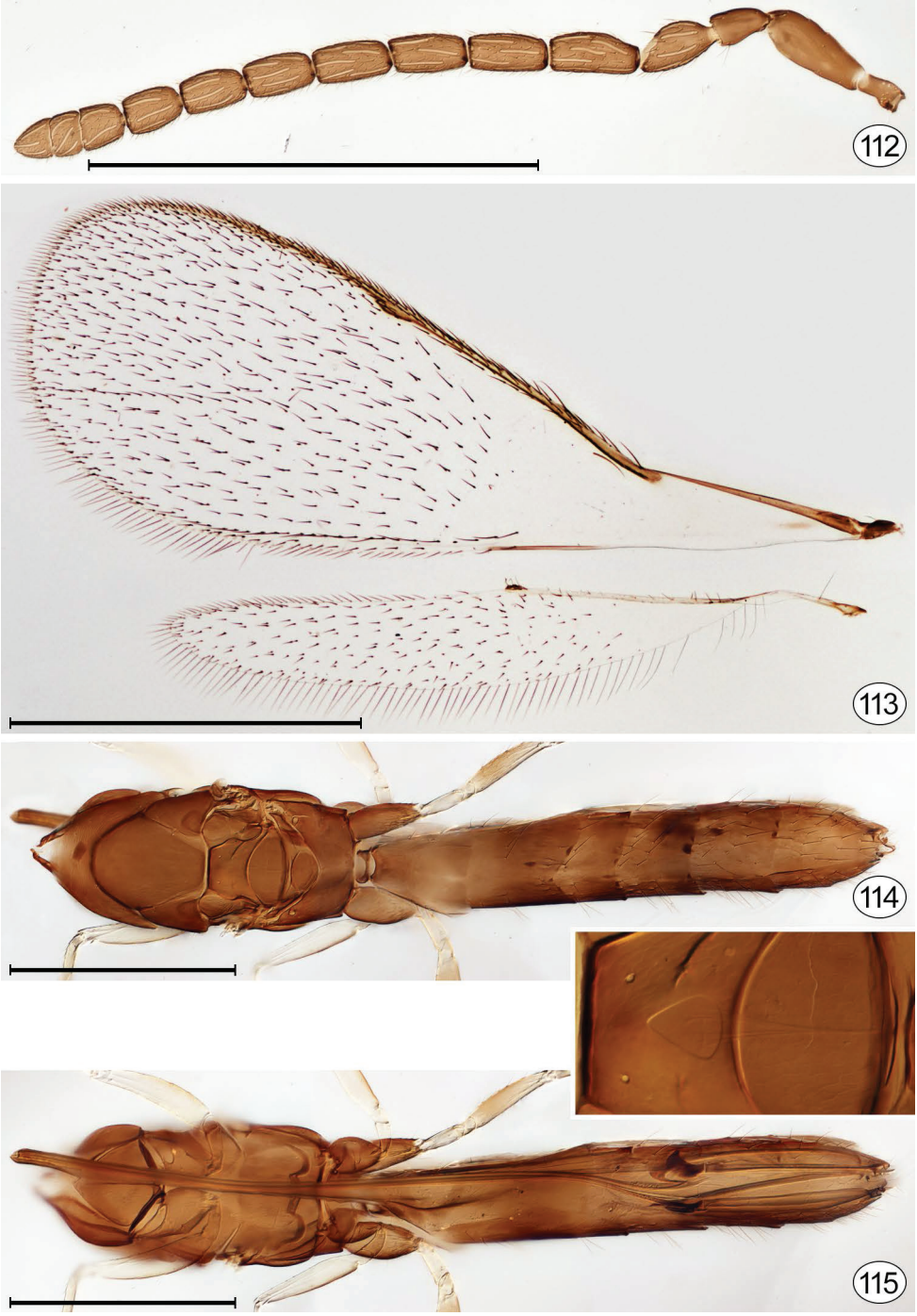

Figures 112–115. *Neotriadomerus longiovipositor*, holotype. **112** antenna **113** wings **114** mesosoma + metasoma, dorsal (inset shows fenestra of scutellum) **115** mesosoma + metasoma, ventral as seen dorsally through body. Scale bar = 500 µm.

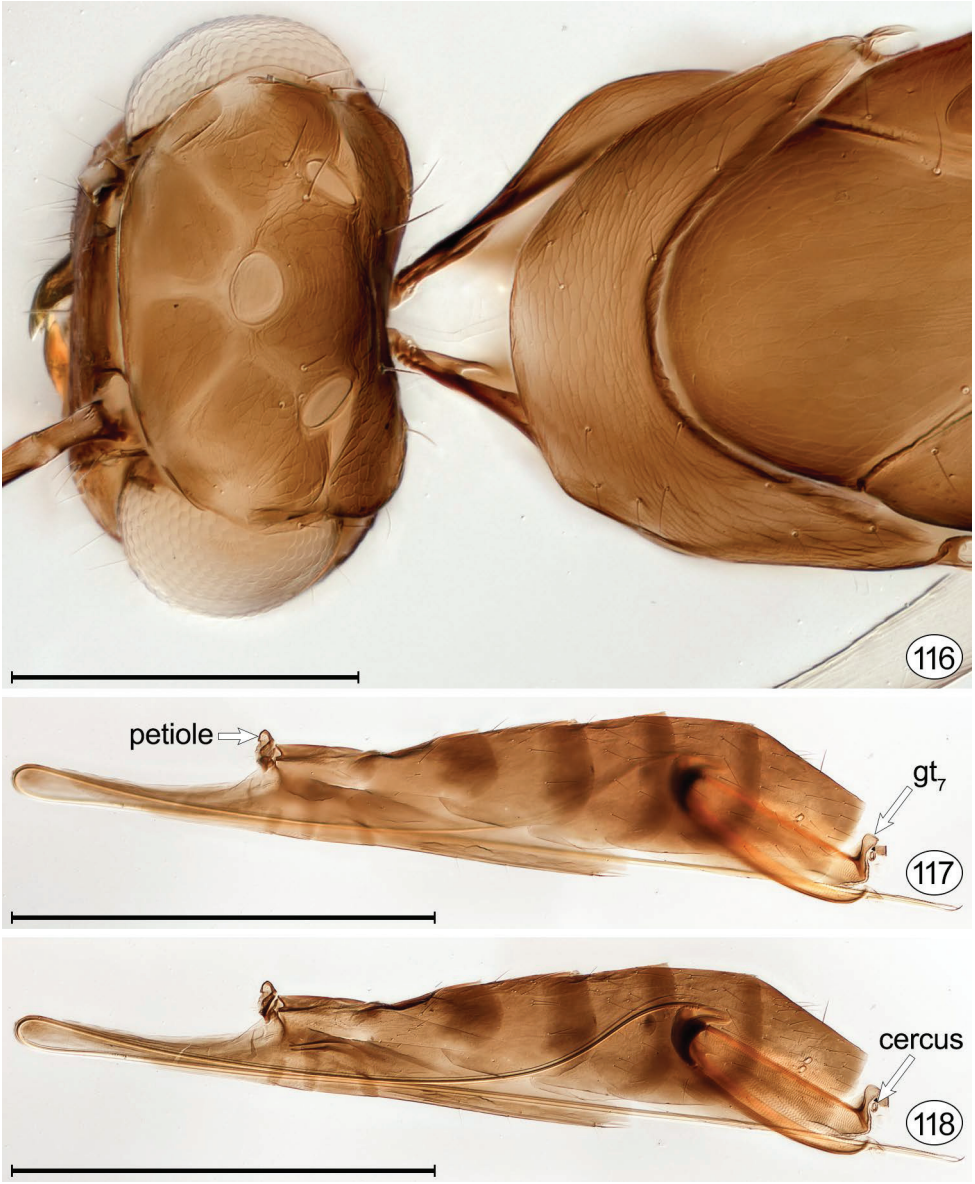

Figures 116–118. *Neotriadomerus longiovipositor*, female paratypes. **116** head + anterior of mesosoma, dorsal (near Swamp Mitchell Plateau Airfield) **116** metasoma, lateral (18.5 km W. Gordonvale) **117** metasoma, median plane **118** metasoma, lateral. Scale bar for **116** = 200 μm; **117, 118** = 1000 μm.

Description. Female. Body length ≈ 1700–2250 (n=6). **Colour.** Body (before slide mounting one specimen) uniformly shiny black except mouthparts brown; antenna dark brown but scape and pedicel ventrally slightly lighter; pro- and mesocoxa dark brown except extreme apices yellowish, metacoxa dorsally almost black; the rest of each leg yellowish except for femur ventrally of fore- and mid leg, entire femur ex-

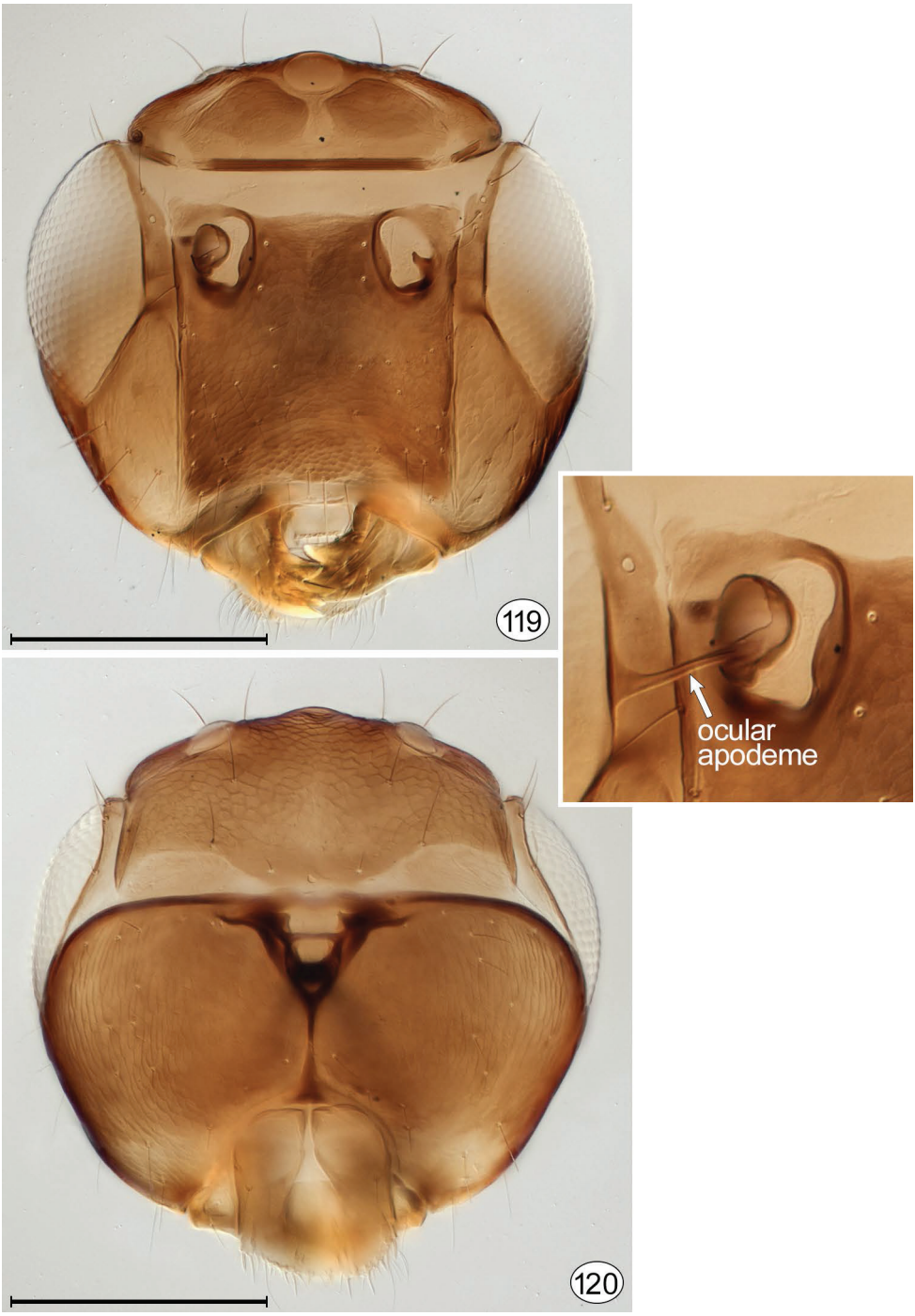

Figures 119, 120. *Neotriadomerus longiovipositor*, male paratype (14 km W. by N. Hope Vale Mission). **119** head, anterior (inset shows ocular apophysis or apodeme) **120** head, posterior. Scale bar = 200 µm.

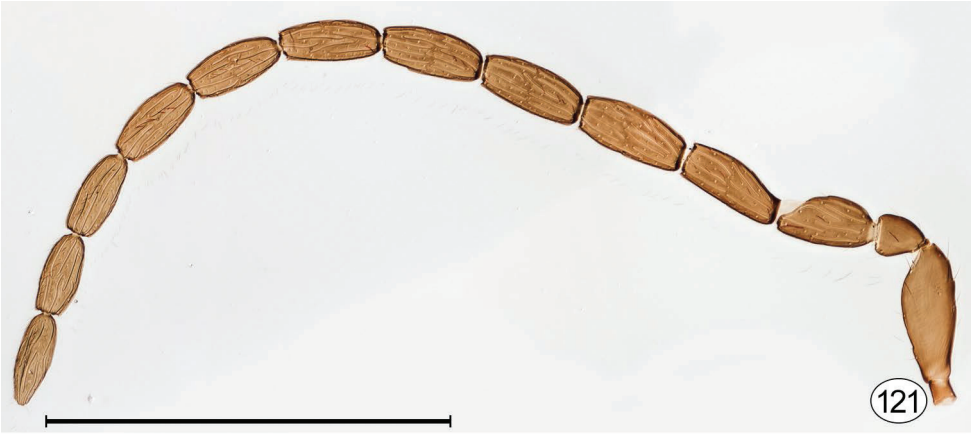

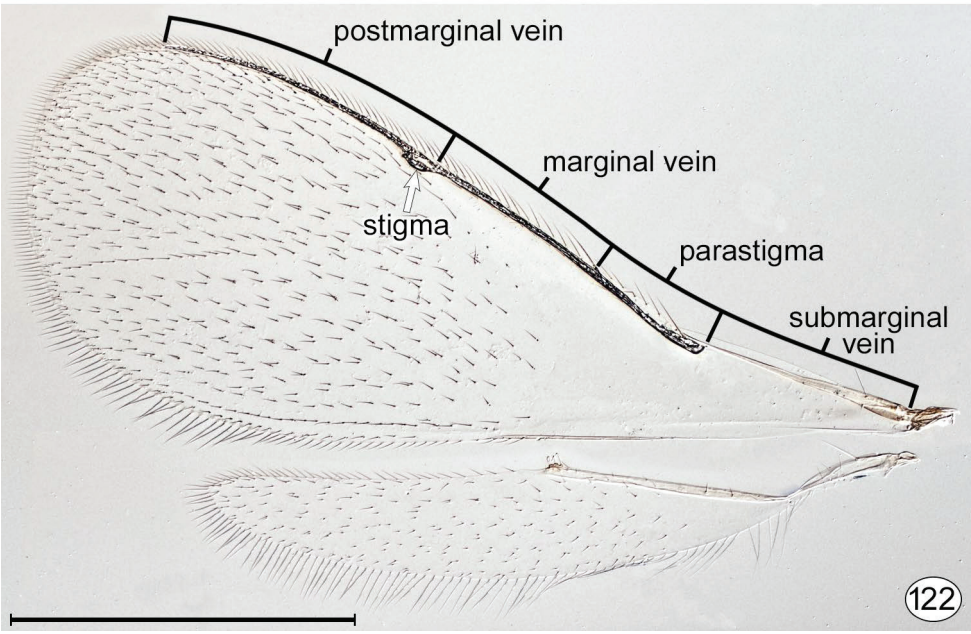

Figures 121, 122. *Neotriadomerus longiovipositor*. **121** male antenna, paratype (14 km W. by N. Hope Vale Mission) **122** wings. Scale bar = 500 μm.

cept extremities of hind leg, and apical tarsomere of all legs brown. **Head.** Head width 344–412 (Figs 108, 110). **Antenna.** Fl_1 slightly shorter than fl_2, with 8 (9?) mps; fl_2 slightly the longest funicle segment, with 9–12 mps; fl_3–fl_8 with 9–12 (13?) mps; clava with 22 mps, 8 on first, 6 on second and 8 on third segment (Fig. 112). Antennal measurements (n=4), length/width (ratio of flagellar segments): scape 174–194/47–65 (2.99–3.78), pedicel 57–66/40–46 (1.30–1.67), fl_1 85–104/44–57 (1.83–1.95), fl_2 88–108/45–52 (1.88–2.19), fl_3 80–109/43–52 (1.72–2.11), fl_4 72–84/44–47 (1.65–1.97), fl_5 70–102/42–47 (1.66–2.19), fl_6 68–97/43–50 (1.56–1.94), fl_7 65–96/41–44 (1.54–2.17), fl_8 63–64/42–46 (1.41–1.49); entire clava 126–128/49/53 (2.43–2.59),

Figures 123, 124. *Neotriadomerus longiovipositor*, male paratype (14 km W. by N. Hope Vale Mission). **123** mesosoma, legs + metasoma, lateral **124** genitalia, lateral. Scale bar for **123** = 1000 µm; **124** = 200 µm.

with segments 1–3 length [measured along dorsal margin] 40–46, 29–31, and 50–60 (the paratype from 18.5 km W. Gordonvale was the largest specimen but had fl_8 and clava missing from both antennae so the maximum lengths in the ranges given above

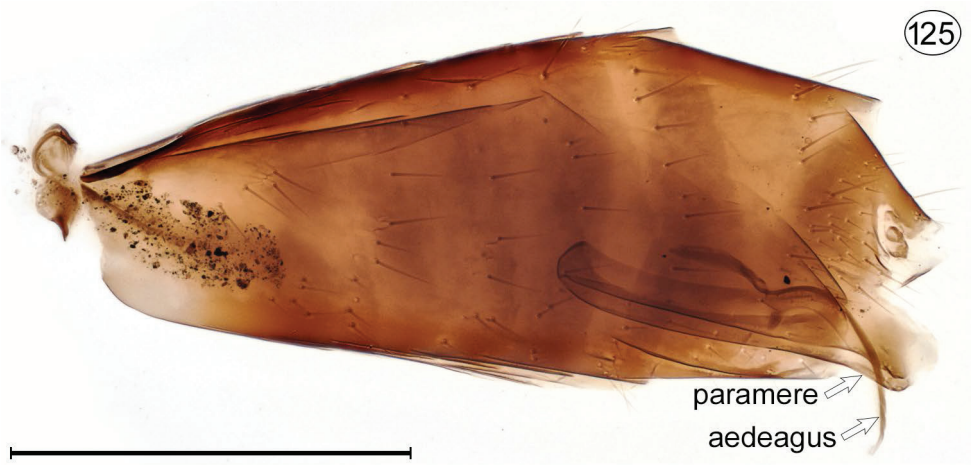

Figure 125. *Neotriadomerus longiovipositor*, male paratype (near historical mine site, NW of Chillagoe). Gaster, median plane showing genitalia. Scale bar = 300 µm.

for those segments are smaller than they should be). **Mesosoma.** Mesosoma length 617–678, width 317–327 (n=3, slide mounts), height ≈ 280 (critical point dried paratype). **Wings.** Fore wing length (n=3) 1118–1208, width 407–432, length/width 2.71–2.80, longest marginal setae ≈ 54–62; cubital line extending to just proximal to base of parastigma (Fig. 113). Hind wing length ≈ 914–1052, width 120–136, longest marginal setae ≈ 50–67. **Legs.** Protibia with 5 or 6 (on specimen with only 2 on one leg) short, thick pegs along its length and a transverse row of 3 or 4 abutting pegs apically (as in Fig. 53). **Metasoma.** Metasoma height in lateral view ≈ 480 (including slightly lowered hypopygium, critical point dried paratype) or 320–400 (three slide mounted paratypes). Gaster length 918–1453, about 1.49–2.12× as long as mesosoma; gt_1–gt_7 lengths about 204–244, 190–236, 136–266, 130–207, 114–209, 218–320, ≈ 24–59 [measurement of a tergum excludes the telescoped portion inside another (more anterior) tergum]; hypopygium extending posteriorly to about apex of gt_3 to halfway between anterior and posterior margin of gt_4. Ovipositor length 1445–2238, ≈ 3.58–4.82× metatibia length (≈ 380–472) and extending anteriorly to level of head or beyond (Figs 114, 115) and not extending posteriorly beyond apex of gaster (Figs 114, 115), except in one paratype (Figs 117, 118).

Male. Colour. As for female. **Head.** Head (Figs 119, 120) width 380–436 (n=4). **Antenna.** Measurements, length/width (n=3): scape 170–214/56–67, pedicel 57–68/46–52, flagellar segments: fl_1 117–122/55–63, fl_2 109–134/52–58, fl_3 103–136/50–62, fl_4 105–130/47–56, fl_5 102–125/48–55, fl_6 98–127/50, fl_7 96–120/48–52, fl_8 89–120/44–53, fl_9 84–112/45–48, fl_{10} 76–104/42–48, fl_{11} 90–118/36–43; total flagellar length 1068–1349; fl_6 length/width ratio 1.98–2.54, with about 17–19 mps in two slightly overlapping whorls (Fig. 121). **Mesosoma.** Mesosoma length 780–860, about 0.80–1.22× as long as metasoma length (680–1020); propodeum with 2 propodeal setae, rarely 3 on one side. **Wings.** Fore wing (Fig. 122) length (n=3) 1191–1320, width

446–495, length/width, 2.56–2.67, longest marginal setae 58–68; cubital line extending to about level of other microtrichia. Hind wing length 921–1024, width 132–158, longest marginal setae 52–65. **Metasoma.** Petiole length 35–36, width 70–76 (n=2). Gaster length 780–860; gt_1–gt_5 each with a row of about 5 lateral and dorsal setae on each side (apparently without dorsal setae on gt_1), and gt_6 with about 6 long dorsal setae on each side and about 20 short lateral setae (Fig. 123). Genitalia (Fig 124, 125) with paramere in lateral view higher than wide and blunt apically, with 2 short apicoventral setae close together and 2 or 3 short subapical setae more widely spaced.

Etymology. The name is a noun in apposition, referring to the long ovipositor (the second longest in the genus) that extends anteriorly to the head.

***Neotriadomerus longissimus* Huber, sp. n.**
http://zoobank.org/B79EB1F3-8092-4382-96C7-A966E9549C50
Figs 36–38, 48, 51, 53, 63, 126, 127

Type material. Holotype female (ANIC) on point labelled: 1. "Blundells ACT 27 Feb 1951 H M Cage". 2. "Holotype Neotriadomerus longissimus Huber ♀".

Paratype. 1 female. AUSTRALIA. **Queensland:** Brisbane Forest Park, 27°25'04"S; 152°49'48"E, 23–29.x.1998, N. Power, dry sclerophyll, MT (1♀, CNC).

Diagnosis. *Neotriadomerus longissimus* differs from other species of *Neotriadomerus* as follows: body 5000—almost twice the length of any other species (Fig. 126); head cuboidal, with vertex horizontal, almost at right angle to the face (Fig. 126); mid ocellus almost in contact with the transverse trabecula; mandible massive (Fig. 36); gaster with basal sac extending anteriorly well anterior to head (Figs 38, 63, 126, 127).

Description. Female. Body length 5000–5450 (n=2, card and point-mounted holotype and paratype), excluding basal sac of gaster (5900–6300 if this included). **Colour.** Holotype body black except for brown mandibles, scutellum, and most of middle segments of metasoma; legs and apex of anterior extension of ovipositor brownish yellow; paratype body (Figs 126, 127) uniformly brown, except for almost black head and scape brown, legs mostly yellow except for partly or almost entirely brown coxae and metafemur, anterior extension of ovipositor from level of head almost white (Figs 126, 127). **Head.** Head width 640–690. Vertex horizontal, forming almost right angle with face, with ocelli in anterior half and mid ocellus in contact with transverse trabecula. Eye almost circular, slightly narrower ventrally than dorsally. Gena at dorsal and ventral margins of eye almost equally wide. Mandible massive, extending ventral to head by at least half face height. **Antenna.** Each funicle segment in lateral view at least twice its width as in dorsal view, with about 25–30 short mps in 3 more or less overlapping whorls (Fig. 38). Clava with about 10 mps on each segment. Antennal measurements (n=2), length/width (ratio of flagellar segments): scape 297-317/109–119 (2.58–2.91), pedicel 54–69/59–69 (1.08–1.07), fl_1 228/109–119 (1.92–2.09), fl_2 262–267/89–109 (2.45–2.94), fl_3 248–257/89–99 (2.60–2.78), fl_4 238–248/79 (3.00–3.13), fl_5 228/69–74 (3.07–3.29), fl_6 198–218/69 (2.86–3.14), fl_7 178–198/69

Figures 126, 127. *Neotriadomerus longissimus*, paratype, lateral (Brisbane Forest Park). **126** habitus, lateral **127** anterior body, enlarged. Scale bar for **126** = 2000 µm; **127** = 1000 µm.

(2.57–2.86), fl_8 168–178/69 (2.23–2.57), entire clava 267/64–69 (3.86–4.05), with segments 1–3, respectively, 109, 69 and 89–99 long. **Mesosoma.** Mesosoma length 110–120. **Wings.** Fore wing length (n=2) 2460–2790, width 670–845, length/width 3.30–3.72, longest marginal setae 100; cubital line of setae extending halfway between apex and base of parastigma (about midway between level of proximal and distal macrochaetae). Hind wing length 1970–1790, width 205–230, longest marginal setae 100–130. **Metasoma.** Metasoma (paratype only) in dorsal view thin, 260 at its widest (near apex) and 80 at its narrowest, its length (near middle) 345 and 390 (holotype and paratype), 3.18–3.25× as long as mesosoma; in lateral view 435 high (near apex) and 205 (near middle); gt_1–gt_7 lengths (paratype only) 715: 690: 155: 715: 740: 435: 80; hypopygium extending about 0.3× length of gaster. Ovipositor sheath length (n=2) 5900–6300, 6.23–7.9× metatibia length (795–950) and extending anteriorly to well in front of head but barely extending posterior to apex of gaster (Fig. 126).

Male. Unknown.

Etymology. The species name, *longissimus*, is Latin for longest, referring the extremely long gaster.

***Neotriadomerus powerae* Huber, sp. n.**
http://zoobank.org/AEDF1141-A5A7-48EF-935A-A47373FE4329
Figs 128–143

Type material. Holotype female (ANIC) on slide (Fig. 130) labelled: 1. "Australia: Qld. Brisbane Forest Park, 27°25'04"S 152°49'48"E 29.xi-5.xii.1997, dry sclerophyll, N. Power, Mt". 2. "Neotriadomerus powerae Huber ♀ dorsal holotype".

Paratypes. 1 female, 3 males. AUSTRALIA. **Queensland:** Same data as holotype but 14–20.iii.1998 (1♀ and 1♂, CNC), 28.xi.1998 (1♂, ANIC), 26.ix-2.x.1999 (1♂, ANIC). The collector stated that the specimens were collected in a Malaise trap set across a creek bed running through the base of an occasionally flooded gully between two sections of dry sclerophyll.

Diagnosis. *Neotriadomerus powerae* differs from other small (body length less than 2600) species of *Neotriadomerus* as follows: fore wing with cubital line extending to just proximal to base of parastigma (Fig. 132); fl_2–fl_7 each just over twice as long as wide, with at least 8 mps and clava with 6 mps on each segment (Fig. 131).

Description. Female. Body length ≈ 1560 (holotype). **Colour.** Body (Fig. 128) almost uniformly dark brown; legs brown, with trochantelli, base and apex of femora and entire protibia, and base and apex of meso- and metatibiae, and tarsi except tarsomere 5 paler, almost white; tarsomere 5 brown. **Head.** Head width 363 (holotype). **Antenna.** Fl_1 almost as long as fl_2, with 8 mps; fl_2 about equal to fl_3 or following funicle segments except fl_7 or fl_8, with 8 mps; fl_3–fl_6 with 8 mps, fl_7 and fl_8 apparently with 9 or 10 mps. Clava with 18 mps, 6 on first, 6 on second and 6 on third segment (Fig. 131). Antennal measurements (n=1), length/width (ratio of flagellar segments):

Figure 128. *Neotriadomerus powerae*, paratype female habitus, dorsal (Brisbane Forest Park). Scale bar = 1000 µm.

scape ≈ 138/44 (≈ 3.15), pedicel 54/43 (1.27), fl_1 84/48 (1.77), fl_2 88/43 (2.07), fl_3 90/44 (2.06), fl_4 88/42 (2.10), fl_5 88/40 (2.19), fl_6 89/40 (2.23), fl_7 86/42 (2.05), fl_8 82/43 (1.91); entire clava 151/47 (3.23), with segments 1–3 length [measured along dorsal margin] 50, 37, and 64. **Mesosoma.** Width 284, length 578, with 3 propodeal setae (Fig. 133). **Wings.** Fore wing length 1173, width 417, length/width 2.81, longest marginal setae 52. Hind wing length 940, width 130, longest marginal setae 62. **Legs.** Protibia with 5 short, thick pegs along its length and a transverse row of 4 abutting pegs apically (as in Fig. 53). **Metasoma.** Metasoma height in lateral view 270. Gaster length 865, about 1.5× as long as mesosoma; gt_1–gt_7 lengths about 169: 106: 99: 113: 162: 170 (Figs 134, 135) [measurement of a tergum excludes the telescoped portion inside another (more anterior) tergum]; hypopygium (difficult to see) extending posteriorly to level of apex of tergum 5. Ovipositor sheath length 1113, ≈ 2.73× metatibia

Figure 129. *Neotriadomerus powerae*, paratype male habitus, lateral (Brisbane Forest Park). Scale bar = 1000 μm.

length (≈ 51), extending anteriorly to about level of apex of procoxa and extending posteriorly slightly beyond apex of gaster (Figs 134, 135).

Male. Colour. As for female (Fig. 129). **Head.** Head (Figs 136, 137) width 346 (n=1). **Antenna.** Measurements, length/width: scape 124/45, pedicel 49/43, flagellar segments: fl_1 97/62, fl_2 108/54, fl_3 104/56, fl_4 102/50, fl_5 108/50, fl_6 102/50, fl_7 98/53, fl_8 99/51, fl_9 94/50, fl_{10} 86/47, fl_{11} 90/45; total flagellar length 1089; fl_6 length/width

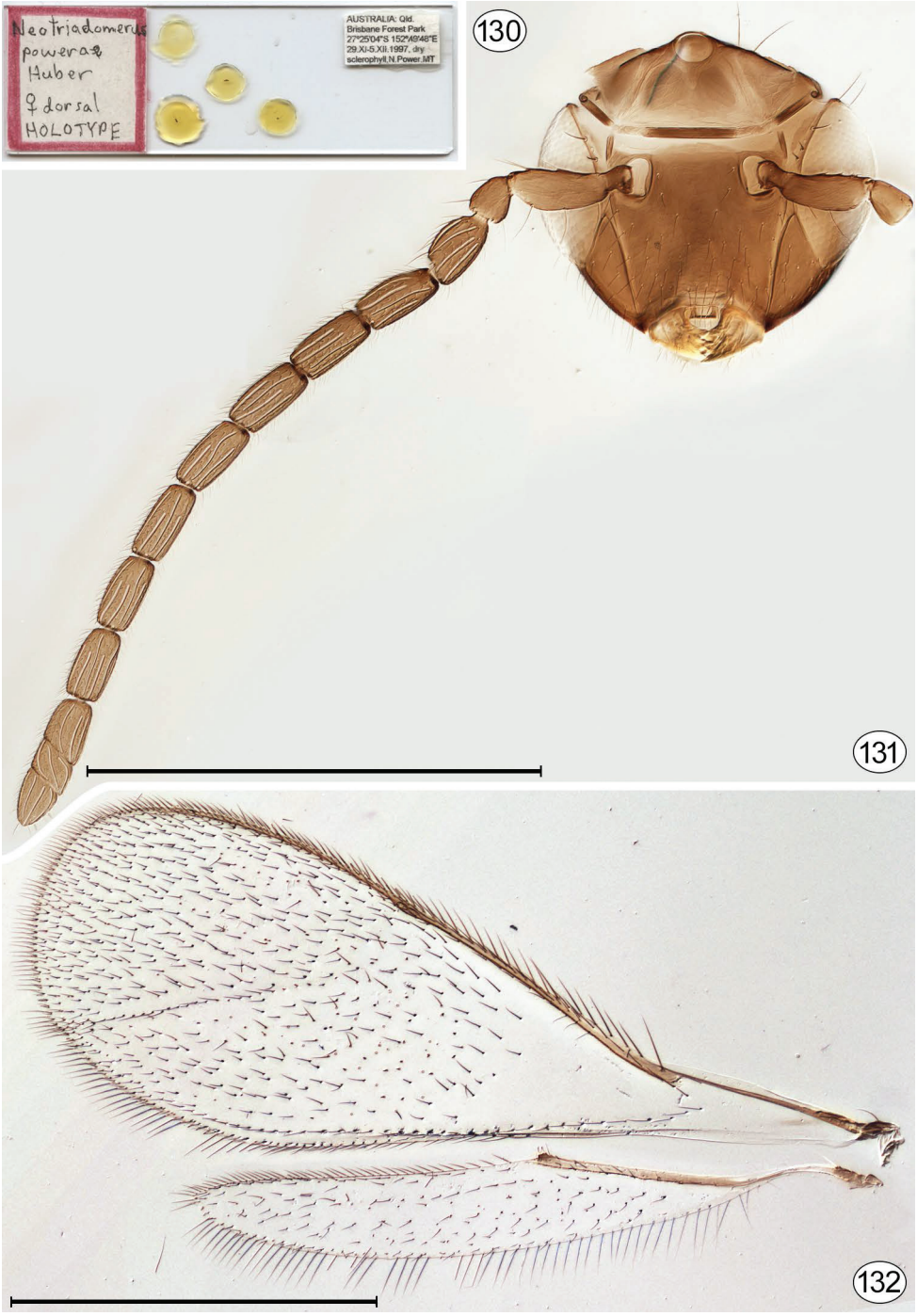

Figures 130–132. *Neotriadomerus powerae*, holotype. **130** type slide **131** head + antenna, anterior **132** wings. Scale bar = 500 µm.

Figures 133–135. *Neotriadomerus powerae*, holotype. **133** mesosoma, dorsal **134** mesosoma, lateral **135** mesosoma, median plane. Scale bar for **133** = 200 µm; **134, 135** = 500 µm.

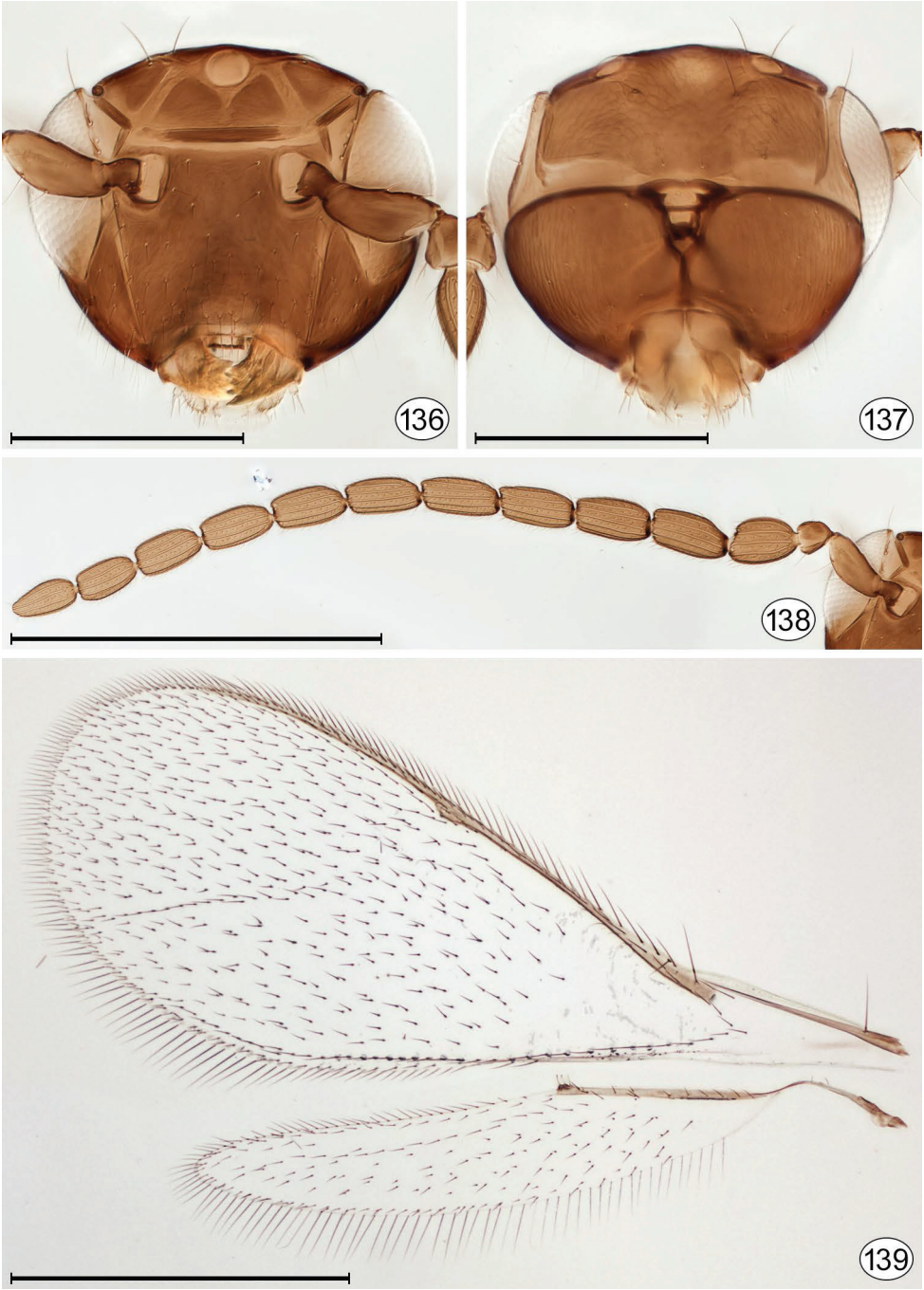

Figures 136–139. *Neotriadomerus powerae*, male paratype (Brisbane Forest Park). **136** head, anterior **137** head, posterior **138** antenna **139** wings. Scale bar for **136, 137** = 200 µm; **138, 139** = 500 µm.

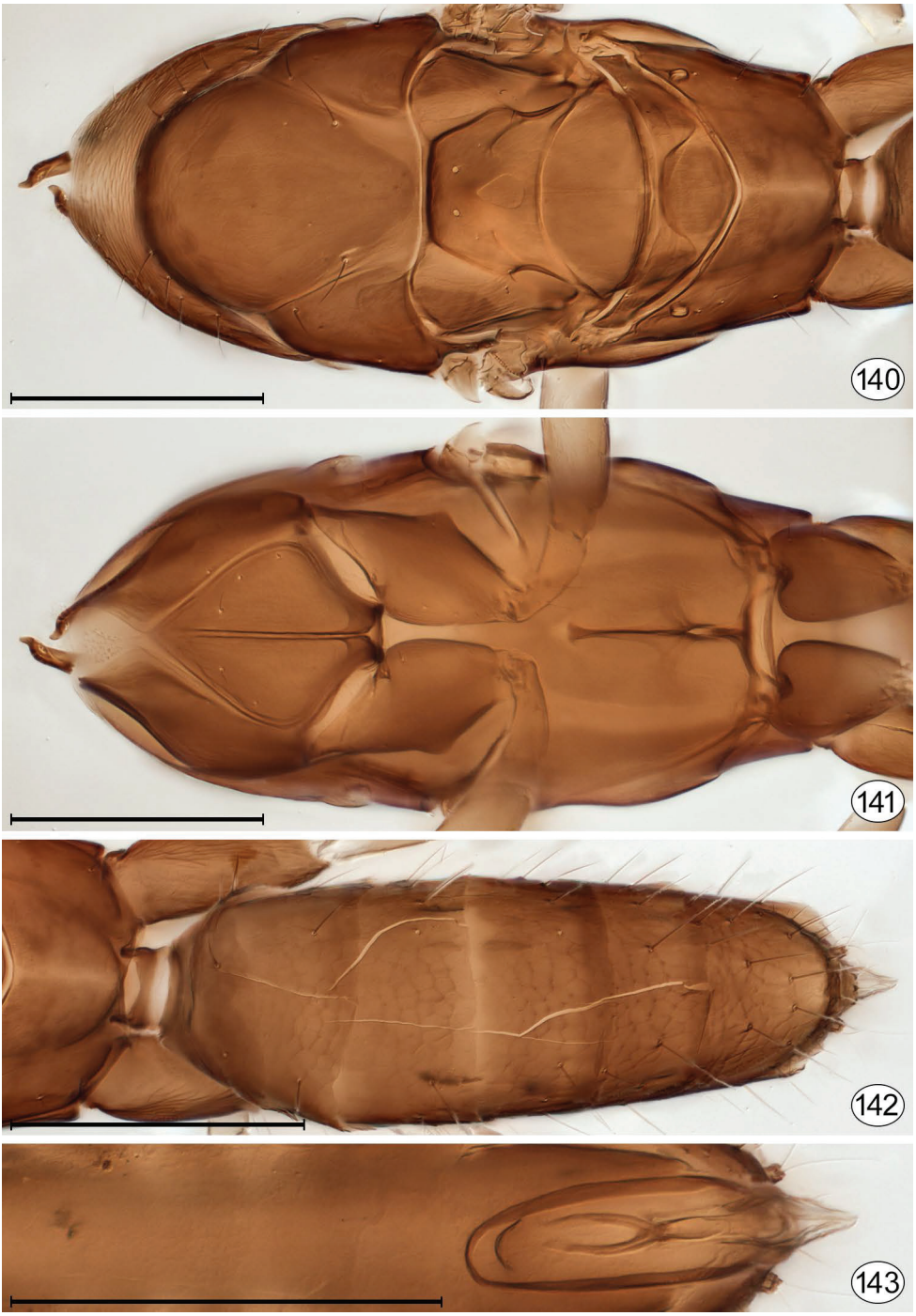

Figures 140–143. *Neotriadomerus powerae*, male paratype (Brisbane Forest Park). **140** mesosoma, dorsal **141** mesosoma, ventral **142** metasoma, dorsal **143** genitalia, dorsal seen through gaster. Scale bar = 200 μm.

2.04, with 12 mps (Fig. 138). **Mesosoma.** Mesosoma length 610, about 1.24× as long as metasoma length (494); propodeum with 3 propodeal setae (Fig. 140). **Wings.** Fore wing length (n=1) 1043, width 386, length/width 2.70, longest marginal setae 76; cubital line extending to just proximal to base of parastigma (Fig. 129). Hind wing length 834, width 132, longest marginal setae 62. **Metasoma.** Petiole length 13, width 29. Gaster length 468; gt_1–gt_5 with 1 long dorsal setae and 4 long lateral setae on each side and gt_6 with about 5 long dorsal setae, 3 long lateral setae, and about 20 short lateral setae on each side (Fig. 142). Genitalia as in Fig. 143.

Etymology. The species is named after Narelle Power, who ran a Malaise trap for many months in Brisbane Forest Park.

***Neotriadomerus* sp. 1.**
Figs 144, 145

Material examined. AUSTRALIA. **Australian Capital Territory:** 3 km E. Piccadilly Circus, Blundells Creek, 35.22°S, 148.50°E, 850m, xii.1984, Weir, Lawrence, Johnson (1♀ and 1♂, ANIC).

Comment. The female (Fig. 144) and male (Fig. 45) almost certainly are conspecific, with body lengths 2460 and 2480, respectively. Female antenna with 2 widely overlapping whorls of mps (each segment with about 10? mps); male antenna with 2 narrowly overlapping whorls of mps (each segment with about 20? mps). This species most resembles *N. longiovipositor* but differs in that the cubital line of setae extends proximal to base of parastigma, unlike in *N. longiovipositor*.

***Neotriadomerus* sp. 2**
Fig. 146

Material examined. AUSTRALIA. **Western Australia:** 29 km SE by E of Coolgardie, 31.07°S, 121.24°E, 5.v.1983, E.S. Nielsen, E.D. Edwards (1♀, ANIC).

Comment. Body length 1380. Female antenna with 1whorl of mps on each segment and the shortest and widest funicle segments (Fig. 146) of any *Neotriadomerus* species; fore wing with cubital line of setae extending to base of parastigma.

***Neotriadomerus* sp. 3**
Fig. 147

Material examined. AUSTRALIA. **New South Wales:** Kosciusko National Park, Leather Barrel Creek, 0.8 km SW. Picnic Area, 36°32'S, 148°11'E, 1080m, 7–21. ii.1993, A. Newton, M. Thayer, open Eucalyptus forest (gum + *delegatensis*) with shrubby understory, window trap (1♀, ANIC).

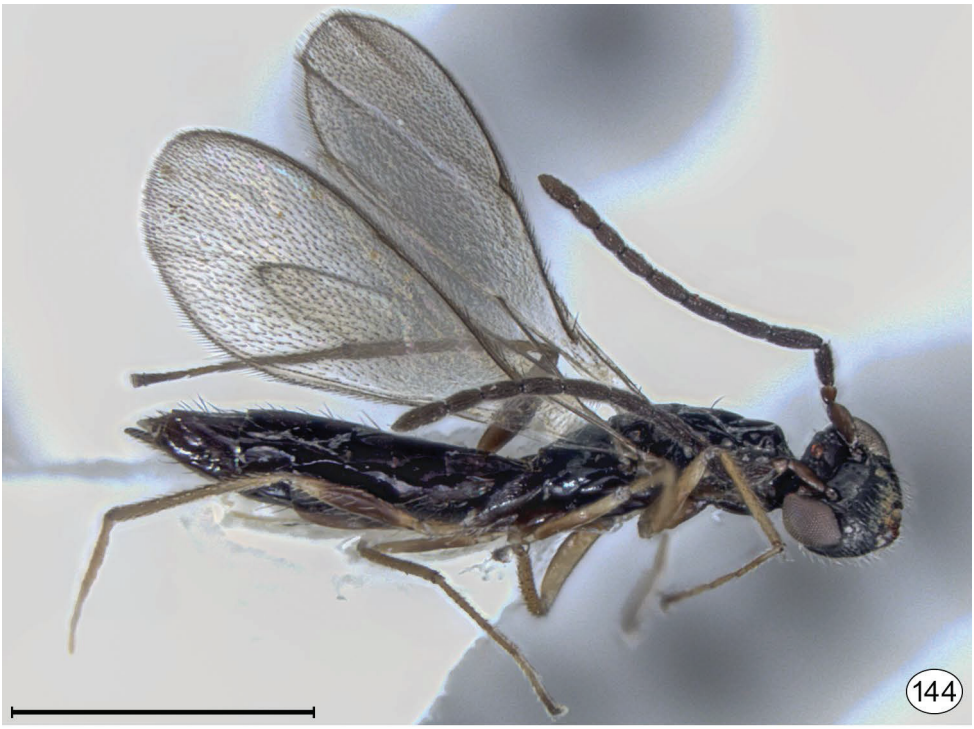

Figures 144, 145. *Neotriadomerus* sp. 1 (Australia, ACT, 3 km E. Piccadilly Circus, Blundells Creek, 35.22°S, 148.50°E, 850m, xii.1984. **144** female habitus, dorsolateral **145** male habitus, dorsal. Scale bar = 1000 μm.

Figure 146. *Neotriadomerus* sp. 2, female habitus, lateral (Australia, WA, 29 km SE by E of Coolgardie, 31.07°S, 121.24°E, 5.v.1983). Scale bar = 1000 µm.

Comment. Body length 1920; fore wing with cubital line of setae extending to base of parastigma. This specimen is similar to the female from Blundells Creek but fl_1 is even shorter than fl_2 so it is provisionally treated as distinct.

***Neotriadomerus* sp. 4**
Figs 148–152

Material examined. AUSTRALIA. **Northern Territory:** 12 km WNW Ross River, Tourist Camp, 23.32°S, 134.23°E, 13.v.1978, J.C. Cardale (1♂, ANIC).

Description. Male. Body length ≈ 1330**. Colour.** Body almost uniformly dark brown; legs brown, with trochantelli, base and apex of femora and tibiae, and tarsi except tarsomere 5 paler; tarsomere 5 brown. **Antenna.** Measurements, length/width: scape 139/46, pedicel length/width 52/46, flagellar segment length: fl_1 100/68, fl_2 94/67, fl_3 97/61, fl_4 100/56, fl_5 100/56, fl_6 98/54, fl_7 96/54, fl_8 96/53, fl_9 92/50, fl_{10} 87/46, fl_{11} 94/37; total flagellar length 1053; fl_6 length/width 1.81, with 11 (12?) mps

Figure 147. *Neotriadomerus* sp. 3, female habitus, lateral (Australia, NSW, Kosciusko National Park, Leather Barrel Creek, 0.8 km SW. Picnic Area, 36°32'S, 148°11'E, 1080m, 7–21.ii.1993). Scale bar = 1000 μm.

(Fig. 150). **Mesosoma.** Mesosoma (Figs 148, 149) length 640, 1.16× as long as metasoma length; propodeum with 3 propodeal setae (Fig. 149). **Wings.** Fore wing length 1077, width 398, length/width 2.71, longest marginal setae 60; cubital line extending to just proximal to base of parastigma (Fig. 151). Hind wing length 900, width 138,

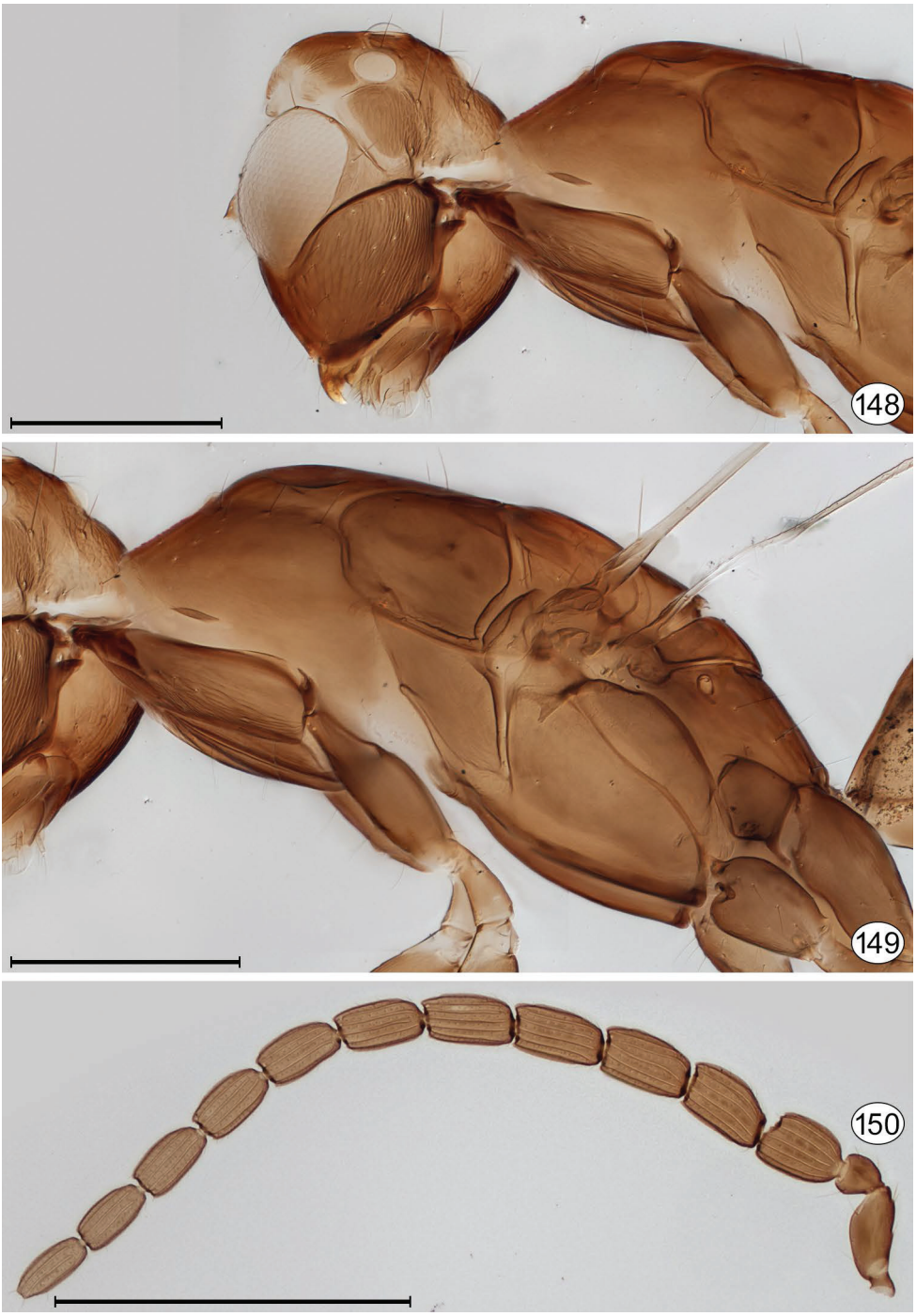

Figures 148–150. *Neotriadomerus* sp. 4, male (Australia, NT, 12 km WNW Ross River, Tourist Camp). **148** head and anterior mesosoma, lateral **149** mesosoma, lateral **150** antenna. Scale bar for **148, 149** = 200 µm; **150** = 400 µm.

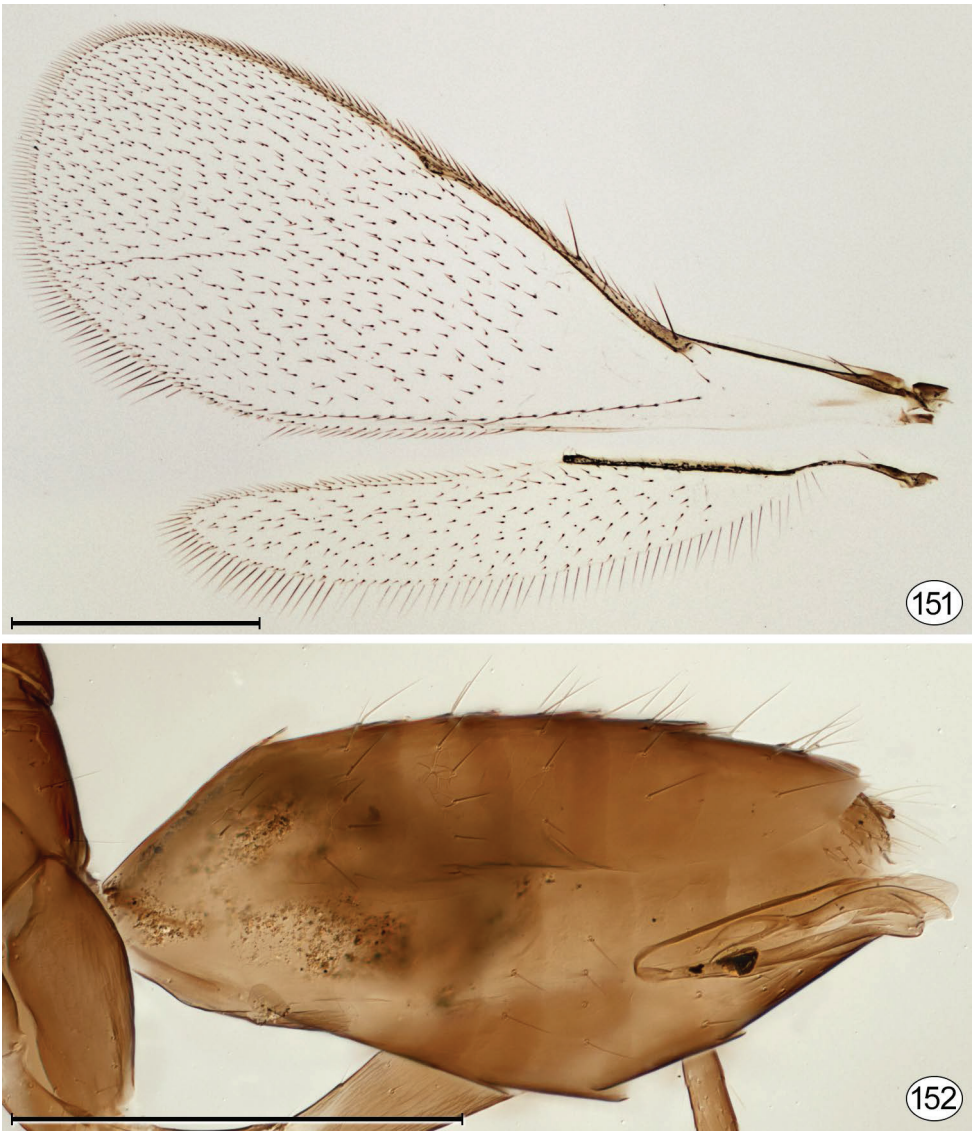

Figures 151–152. *Neotriadomerus* sp. 4, male (same data as **148–150**). **151** wings **152** metasoma, lateral. Scale bar = 300 μm.

longest marginal setae 64. **Metasoma.** Gaster length 517, with setae present on sterna but fewer than on terga (Fig. 152). Genitalia length 220 (Fig. 152).

Comment. The flagellar segments are wider than those of *N. darlingi* (Figs 82, 95?), *N. longiovipositor* (Fig. 121), and *N. powerae* (Figs 129, 138) and *N.* sp. 1; the number and distribution of mps are most similar to *N. darlingi* or *N. powerae* and the propodeum has 3 setae as in *N. powerae*. The condensed description given above may help associate the male with a conspecific female when they are collected, preferably together with more males.

***Proarescon* Huber, gen. n.**
http://zoobank.org/9D52630E-F7D4-4DE0-A3D1-0469F28531E2
Figs 153–176

Type species. *Borneomymar primitivum* Huber, by present designation.

Diagnosis. Female. Antenna with funicle 8-segmented (in *Arescon* 5-segmented) and clava 1-segmented, gradually narrowing apically to a point (Figs 156, 166). **Both sexes.** Fore wing with microtrichia more densely spaced except for oval area along posterior margin (in *Arescon* with microtrichia usualy more sparsely spaced, as shown in Triapitsyn [2016]).

Description. Female. Body 635–720 in length (critical point dried). **Colour.** Body generally light brown with some areas yellow to creamy white; darker brown are mouth margin, trabeculae, ocellar triangle, clava except apex, dorsellum, meso- and metapleuron, propodeum, and gt_4–gt_5 (Figs 165, 168, 170). Wings hyaline except for light brown behind venation (Fig. 169 and Huber 2002, fig. 5). **Head.** Head about 1.50–1.59× as wide as long, about 1.29–1.35× as wide as high, and 1.17–1.18× as high as long; in lateral view with anterior surface slightly convex, flat at level of toruli, then evenly curved to mouth margin; posterior surfaces convex and evenly curved from vertex to mouth margin. Face about 0.9× as wide as high; subantennal groove absent; preorbital groove ventral to level of torulus straight then more ventrally curving slightly medially to lateral margin of mouth opening (Figs 153, 171–male). Torulus in slight triangular depression about 1.7× as high as torulus width and separated by about 2.0× its width from transverse trabecula (Fig. 171–male). Vertex in lateral view horizontal, forming a right angle with face, posteriorly almost at right angle with occiput and separated from it by medially divided tranverse vertexal suture extending behind posterior ocelli almost from eye to eye; occiput separated from gena by a short, oblique posterior extension of supraorbital suture extending from lateral apex of vertexal suture and curving ventrally to dorsolateral corner of occipital foramen. Ocellar triangle small, slightly raised, with mid ocellus almost vertical and lateral ocelli oblique and facing posteriorly; ocelli with POL about 1.0× LOL and about 0.67× LOL; ocelli on stemmaticum (Fig. 154)—seen as white lines in cleared slide mounts (Fig. 165)—these are, respectively, a short, transverse groove in front of mid ocellus, continuing anterolaterally as the frontal suture to midpoint of supraorbital trabecula (apparently divided medially by an unscletotized area), a groove between the lateral margins of mid and lateral ocelli—the frontofacial suture, and a medially divided transverse groove behind the lateral ocelli, the vertexal suture, extending almost from eye to eye. Transverse trabecula darkly sclerotized medially and at each apex apparently not separated from supraorbital trabecula; preorbital trabecula extending ventrally about halfway between dorsal and ventral margins of torulus to where torulus nearest to eye; supraorbital trabecula in 2 almost equal sections, the anterior sections diverging posteriorly, the posterior sections parallel (Fig. 165). Eye large with numerous small facets, in lateral view about as high as wide and clearly separated dorsally from back of head (temple about 0.3× eye width). Ocular apodeme long and straight, needle-like. Malar sulcus present. Gena at level of ventral margin of eye slightly wider than malar space. Occiput separated from temple by occipital groove

(Fig. 165) but otherwise not separated from gena/postgena. **Mouthparts**. Labrum with 1? seta; mandible with 4 uneven teeth (Fig. 153). **Antenna.** Scape 3.4–4.7× as long as wide, with radicle distinct from rest of scape and about 0.36–0.37× total scape length; pedicel about 2.0× as long as wide, almost as wide as and 0.26–0.27× as long as entire scape; funicle 8-segmented; clava 1-segmented, 0.98–1.10× as wide as apical funicle segment and 0.41–0.63× as long as entire funicle (Figs 156, 166, and Huber 2002, fig. 6). **Mesosoma.** About 1.7× as long as wide, 1.8× as long as high and 1.2× as wide as high. Pronotum entire (Fig. 157), in dorsal view clearly visible, medially about 0.5× as long as mesoscutum, with collar bell-shaped in lateral view pronotum sloping down towards junction with head and neck almost absent (not separable), and lateral panel somewhat rectangular and overlapping anterior margin of mesoscutum, with lateral surface merging smoothly into dorsal surface, with a shallow, oblique groove for femur. Spiracle (Fig. 157) flat with surface of pronotum, facing posterodorsally, and apparently slightly closer to anterior apex of notaulus than to posterolateral angle of pronotum. Propleura near anterior apex not quite abutting, then gap widening slightly more anteriorly. Prosternum rhomboidal and completely divided medially by faint longitudinal groove. Mesoscutum about 1.8× as long as scutellum, in dorsal view with shallow, thin, slightly diverging notauli a little wider and shallower posteriorly (Figs 157, 158, 168), in lateral view almost flat. Scutellum slightly wider than long, the anterior scutellum about 0.9× as long as frenum and separated from it by a shallow, medially straight frenal depression (Fig. 157); campaniform sensilla about as far from each other as to lateral margin of anterior scutellum; fenestra small, almost circular, and posterior to campaniform sensilla (Fig. 168, inset). Axilla distinctly advanced, the transscutal articulation laterally forming a distinct angle with median section (Fig. 168); axillula short, separated from anterior scutellum by concave axillular groove; mesophragma fairly narrowly convex posteriorly, extending to posterior apex of propodeum. Prepectus apparently narrowly triangular; mesopleuron somewhat rectangular, with shallow depression separating mesepisternum from mesepimeron. Metanotum with distinct triangular (Fig. 159) or lens-shaped (Fig. 168, in cleared slide mounts) dorsellum and lateral panel length toward hind wing articulation about one third length of dorsellum. Metapleuron triangular, the margin at junction with mesopleuron almost straight and posterior margin straight and vertical. Propodeum without carinae, with 1 propodeal seta (Fig. 159). **Wings.** Fore wing wide, with microtrichia on most of membrane beyond and partly behind venation to level of second macrochaeta except for a bare area medially along posterior margin (Fig. 169). Venation complete; submarginal vein with 1 proximal macrochaeta but no distal seta; parastigma 0.73× submarginal vein length; marginal vein present, its length about 1.42× parastigma length, with a second macrochaeta about midway between first distal macrochaeta and stigmal vein; stigmal vein distinct, about 0.28× length of marginal vein, with anterior margin of stigma parallel or converging with wing margin and with 4? apical campaniform sensilla in a line; postmarginal vein present, apparently about 1.1× as long and almost as thick as marginal vein; hypochaeta fairly close (about 0.3× length of parastigma) to proximal macrochaeta; proximal campaniform sensillum near posterior margin of parastigma just next to first distal macrochata. Hind wing normal (Fig. 169). **Legs.** Profemur slightly wider than meso-and metafemora; metafemur

about 1.2× mesofemur width. Tarsi 5-segmented. Calcar (moveable protibial spur) with about 2 setae along outer margin, and with inner tine about 0.45× outer tine length. Middle and hind legs with tarsomere 1 as long as tarsomere 2. **Metasoma.** 1.95× as long as wide, 2.18× as long as high and 1.12× as wide as high; its length, excluding exserted part of ovipositor, about 1.37× that of mesosoma. Petiole ring-like, about 0.36× as long as wide. Gastral terga about equal in length except gt_6 slightly longer (Figs 162, 170). Cercus flat, with 4 setae, the second-most dorsal one longest (Figs 162, 170). Hypopygium short, extending about one-third ovipositor length (Fig. 170). Ovipositor sheath exserted beyond gastral apex by about 0.2× total sheath length, with 1 subapical seta.

Male. Body length ≈ 585 (slide mounted paratype). **Colour.** Similar to female but with slightly more extensive brown on mesosoma (Fig. 173), and metasoma with brown apically instead of medially (Fig. 175). **Head.** As for female, mandible with 4 teeth (Fig. 171). **Antenna.** Scape (n=1) about 3.00× as long as wide, with radicle about 0.35× scape; pedicel 1.28× as long as wide; flagellum 11-segemented, with fl_1 shorter and wider than other segments, fl_2–fl_{11} subequal, each flagellomere with 4 mps (Fig. 172). **Mesosoma.** As for female (Figs 159, 160, 173). **Wings.** Fore wing (Fig. 174) with proximal campaniform sensillum near posterior margin of marginal vein about midway between first and second distal macrochata. **Metasoma.** Petiole length/width 0.38; gaster about 0.82× as long as mesosoma (Fig. 162). Genitalia with long parameres and apparently no digiti (Figs 163, 164, 176).

Etymology. The genus is masculine. The prefix, *pro-* is Latin for in front of, earlier or first, + *Arescon*, apparently the most closely related genus.

Key to species of *Proarescon*. Females.

1 Clava 4.7× times as long as wide, with ventral margin distinctly concave (Figs 156, 166); fore wing with cubital line extending proximally to about level of second distal macrochaeta (Fig. 169), not much further towards wing base than remaining microtrichia on wing surface.... ***P. similis* Huber, sp. n.**

– Clava less than 3.5× as long as wide, with ventral margin almost straight (Huber 2002, fig. 6); fore wing with cubital line extending proximally almost to level of proximal macrochaeta, distinctly further towards wing base than remaining microtrichia on wing surface (Huber 2002, fig. 5)..... .....***P. primitivus* (Huber)**

***Proarescon primitivus* (Huber), comb. n.**
Figs 153–176

Borneomymar primitivum Huber, 2002: 49 (description, figs 5, 6).

Comment. In Huber (2002) the female and male symbols in the material examined sections were inadvertently either deleted or were replaced by a question mark. All

the specimens of the three species mentioned in that chapter were females except for 2 males on points and 2 males on slides of *Borneomymar discus* Huber from Malaysia, Sarawak, Gunung Buda. The brief description below complements the original description, which did not include antennal segment widths or hind wing measurements.

Description. Female. Body length 634 (paratype). **Antenna.** Length/width measurements (holotype): scape 184/35, pedicel 50/26, fl_1 16/13, fl_2 16/12, fl_3 23/16, fl_4 26/16, fl_5 29/18, fl_6 62/25, fl_7 59/26, fl_8 63/31, clava 120/35.**Wings.** Fore wing length 583, width 154, length/width 3.78, longest marginal setae 122. Hind wing length 560, width 23, longest marginal setae 90.

Material examined. THAILAND: Chanthaburi, Khao Kitchakut Nat. Park, Khao Prabaht Peak, 12°50.45'N 102°9.81'E, 875m, 27.ii-6.ii.2009, MT, Suthida and Charoenchai, #4046 (1♀, CNC).

***Proarescon similis* Huber, sp. n.**
http://zoobank.org/7CEE8233-FC3D-4B9D-AB79-CCEFA137E27D
Figs 153–176

Type material. Holotype female (QSBG) on slide (Fig. 167) labelled: 1. "Proarescon similis Huber ♀ dorsal Holotype". 2. "Thailand: Surat Thani, Khao Sok Nat. Park, Klong Morg Unit, 87 m, 8°53.725'N 99°38.025'E, MT 10-17.ii.2009, Phongphan, #3937".

Paratypes. 1 female and male. **THAILAND. Nakhon Si Thammarat.** Namtok Yong Nat. Park, TV aerial, 966m 8°14.262'N; 99°48.289'E, 15-22.ix.2008, Malaise trap, Paiboon, #3540 (1♂ on slide, QSBG); Namtok Yong Nat. Park, Klong Jang waterfall, 8°16.283'N; 99°38.702'E, 154m, Malaise trap, 23.ii-2.iii.2009, S. Samnaokan, #4665 (1♂, CNC). **Surat Thani.** Khao Sok Nat. Park, 122m, 8°54.555'N; 98°30.522'E, Malaise trap, 13-20.i.2009, Pongphan, #3914 (1♀, CNC).

Diagnosis. Female. Clava 4.7× times as long as wide, with ventral margin distinctly concave (in *P. primitivus*, clava about 3.4× as long as wide, with ventral margin almost straight); fore wing with cubital line not extending proximally beyond first apical macrochaeta, barely proximal to remainder of microtrichia (in *P. primitivus*, cubital line extending proximally almost to level of proximal macrochaeta, distinctly proximal to other microtrichia).

Description. Female. Body length 740 (holotype), 634 (paratype on card). **Head.** Head width 182 (holotype). Face with weak elongate reticulate sculpture, vertical laterally becoming horizontal medially, with thin setae distributed on each side as follows: 2 medial to torulus and 7 ventral to torulus, the 2 setae submedially above mouth margin longer and thicker than the others (Fig. 153). Vertex with transverse elongate reticulate sculpture, with 1 or 2 setae on orbit of eye lateral to transverse trabecula and 2 setae between eye and posterior section of supraorbital trabecula and 1 seta lateral to posterior apex of vertexal suture; ocellar triangle (inside stemmaticum) with 1 seta between mid and lateral ocelli and 1 setae lateral to mid ocellus but outside triangle

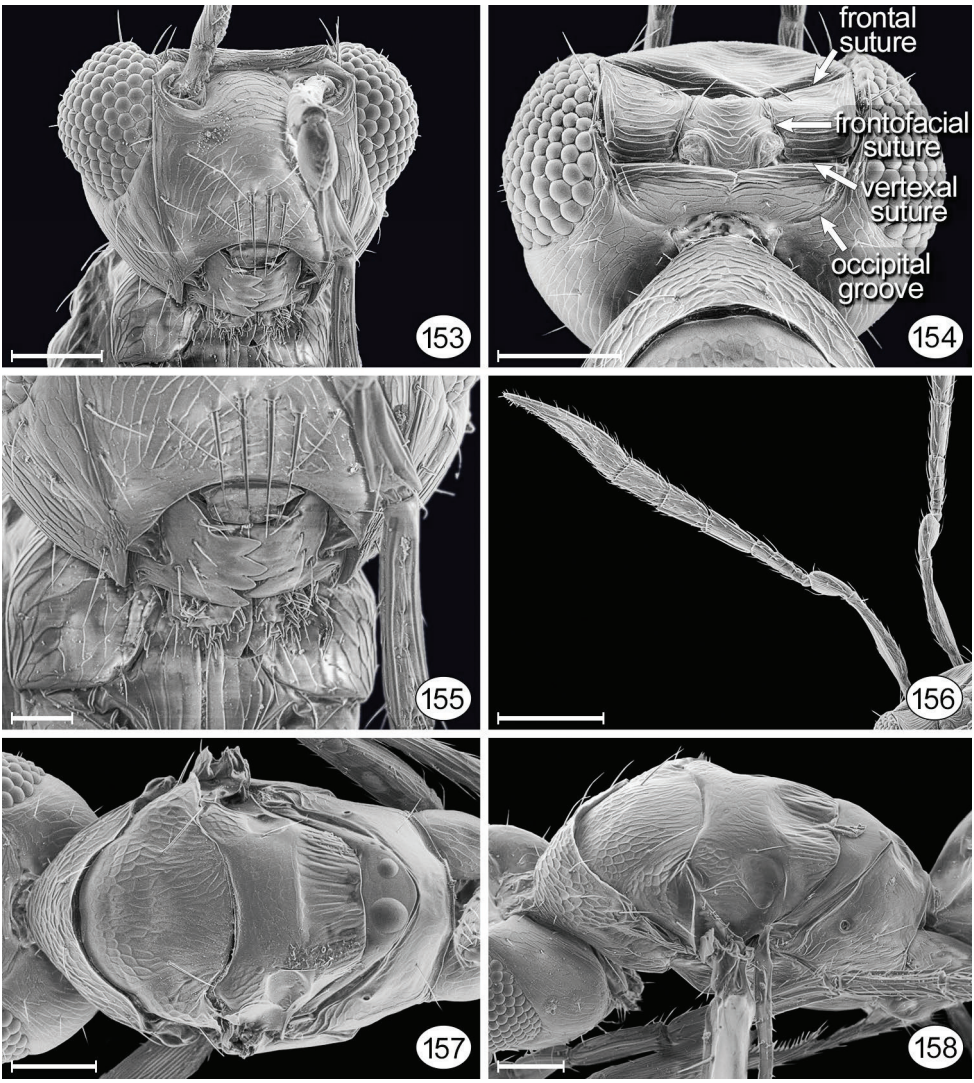

Figures 153–158. *Proarescon similis*. **153** male head, ventroanterior **154** female head and pronotum, posterodorsal **155** male lower face and prosternum **156** female antennae **157** female mesosoma, dorsal **158** male mesosoma, dorsolateral. Scale bar for **153, 154, 157, 158** = 50 µm; **155**= 20 µm; **156** = 100 µm.

(Fig. 165). Malar space with 2 setae. Occiput with engraved transverse reticulate sculpture, with 1 short setae submedially and 1 sublaterally above occipital foramen. Gena with longitudinally reticulate sculpture laterally, becoming isodiametric around foramen, and with about 5 setae sublaterally and laterally. **Antenna.** Fl_1–fl_5 without mps, Fl_6–fl_8 each with 2 mps; clava with 6 mps. Length/width measurements: scape 166/-, pedicel 39/-, fl_1 11/12, fl_2 13/12, fl_3 12/13, fl_4 15/14, fl_5 18/16, fl_6 50/16, fl_7 51/21, fl_8 54/31, clava 143/30. **Mesosoma.** Width 156 and length 287. Pronotum with raised transverse to isodiametric reticulate sculpture, with 3 long setae near posterior margin

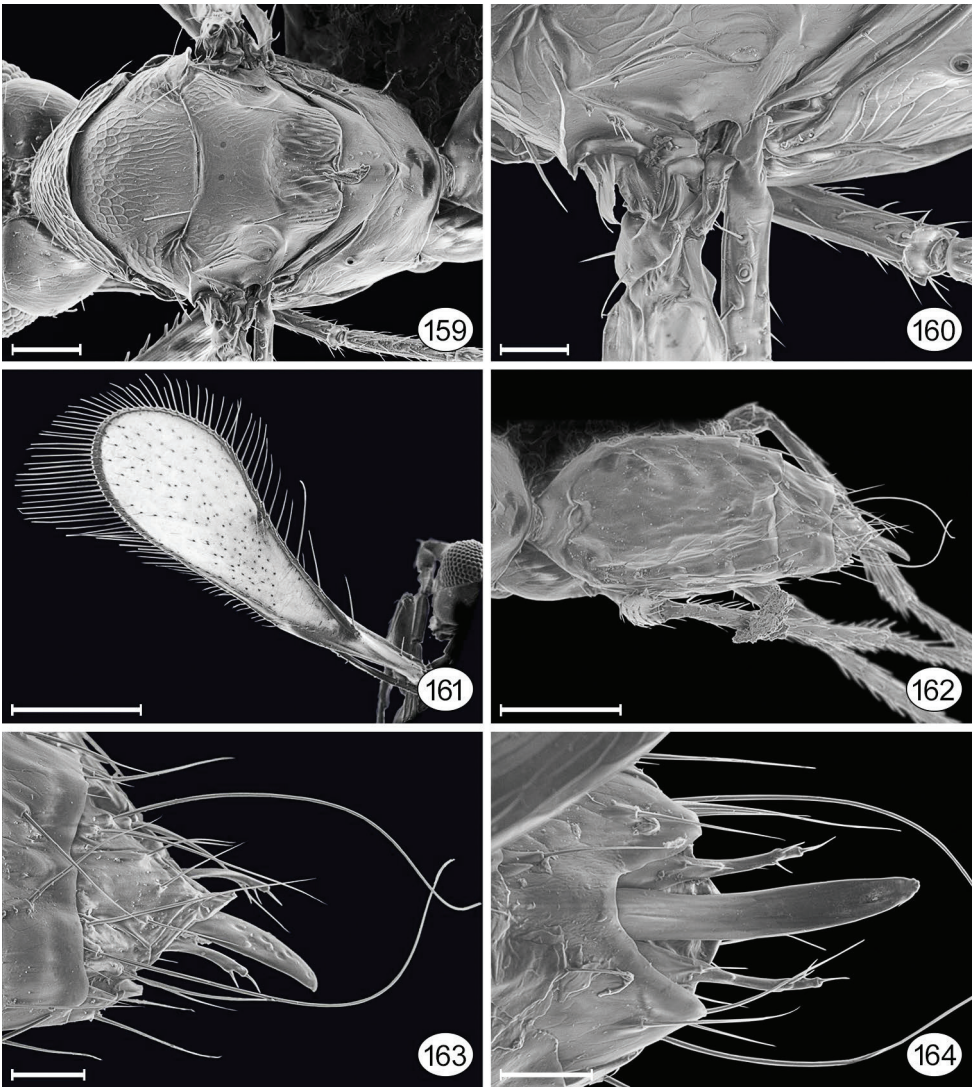

Figures 159–164. *Proarescon similis*, male. **159** mesosoma, dorsal **160** base of wings + axilla, dorsal **161** fore wing, dorsal **162** mesosoma, laterodorsal **163** apex of gaster + genitalia, dorsolateral **164** apex of gaster + genitalia, ventral. Scale bar for **159** = 50 μm; **160, 163, 164** = 20 μm; **161** = 200 μm; **162** = 100 μm.

and 2 short setae towards anterior margin. Propleuron faintly, longitudinally reticulate, with 1 seta medially and 1 seta laterally about midway between anterior and posterior apices. Prosternum apparently smooth, with 1 seta submedially almost at anterior margin. Mesoscutum with sculpture isodiametric anteriorly and on lateral lobes to longitudinally reticulate posteriorly on midlobe, with 1 setae along inner margin midway between anterior and posterior apices of notaulus, and 1 setae at lateral angle of lateral lobe. Anterior scutellum smooth, with 1 setae laterally at dorsal margin of axillula, and with campaniform sensilla about 2× their diameter from transscutal articulation

Figures 165–167. *Proarescon similis*, holotype. **165** head, dorsal **166a** antenna without scape, lateral **166b** antenna, dorsal **167** type slide. Scale bar = 100 µm.

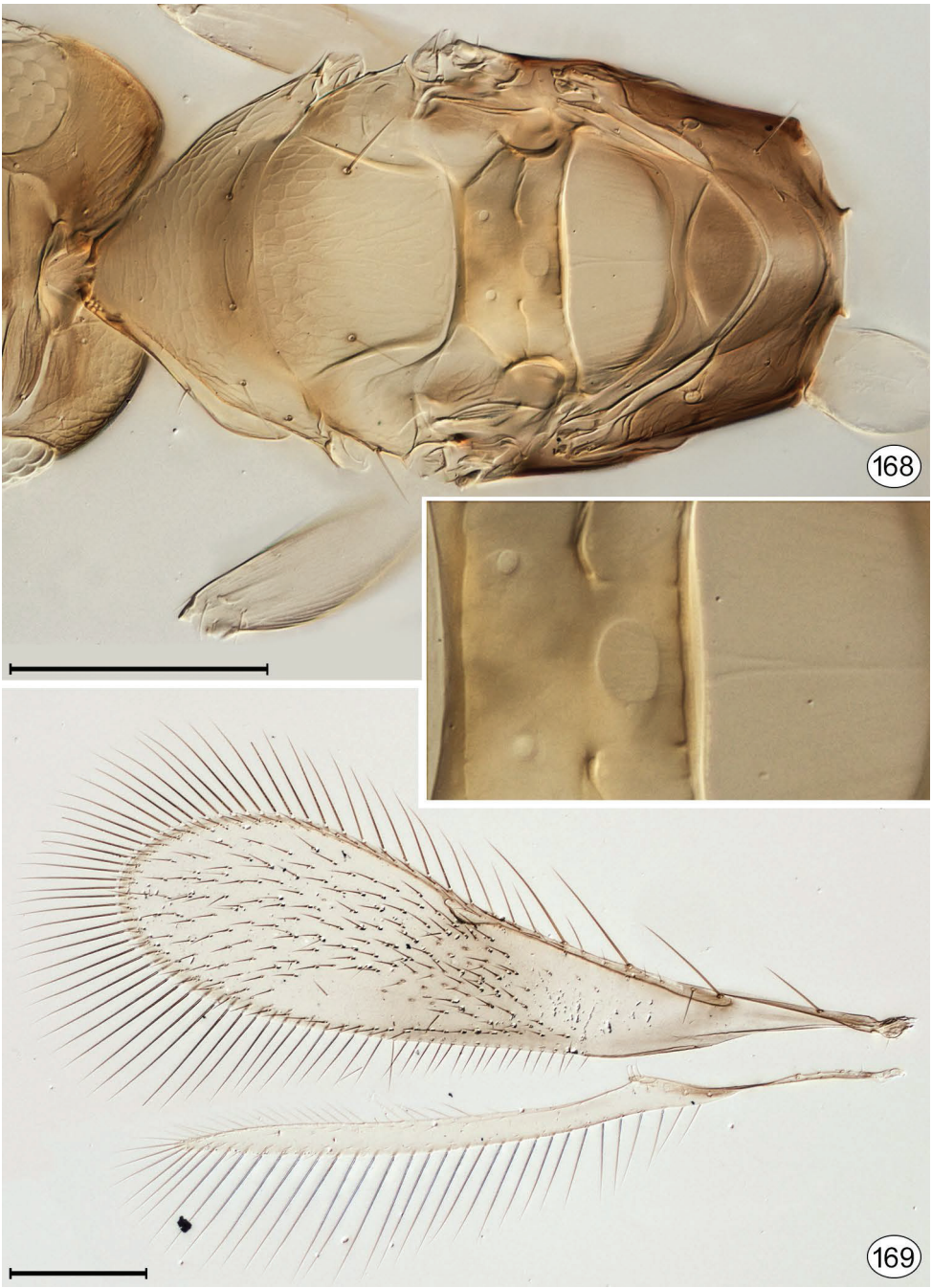

Figures 168, 169. *Proarescon similis*, holotype. **168** metasoma, dorsal (inset: enlargment of central area of scutellum showing fenestra) **169** wings. Scale bar = 100 μm.

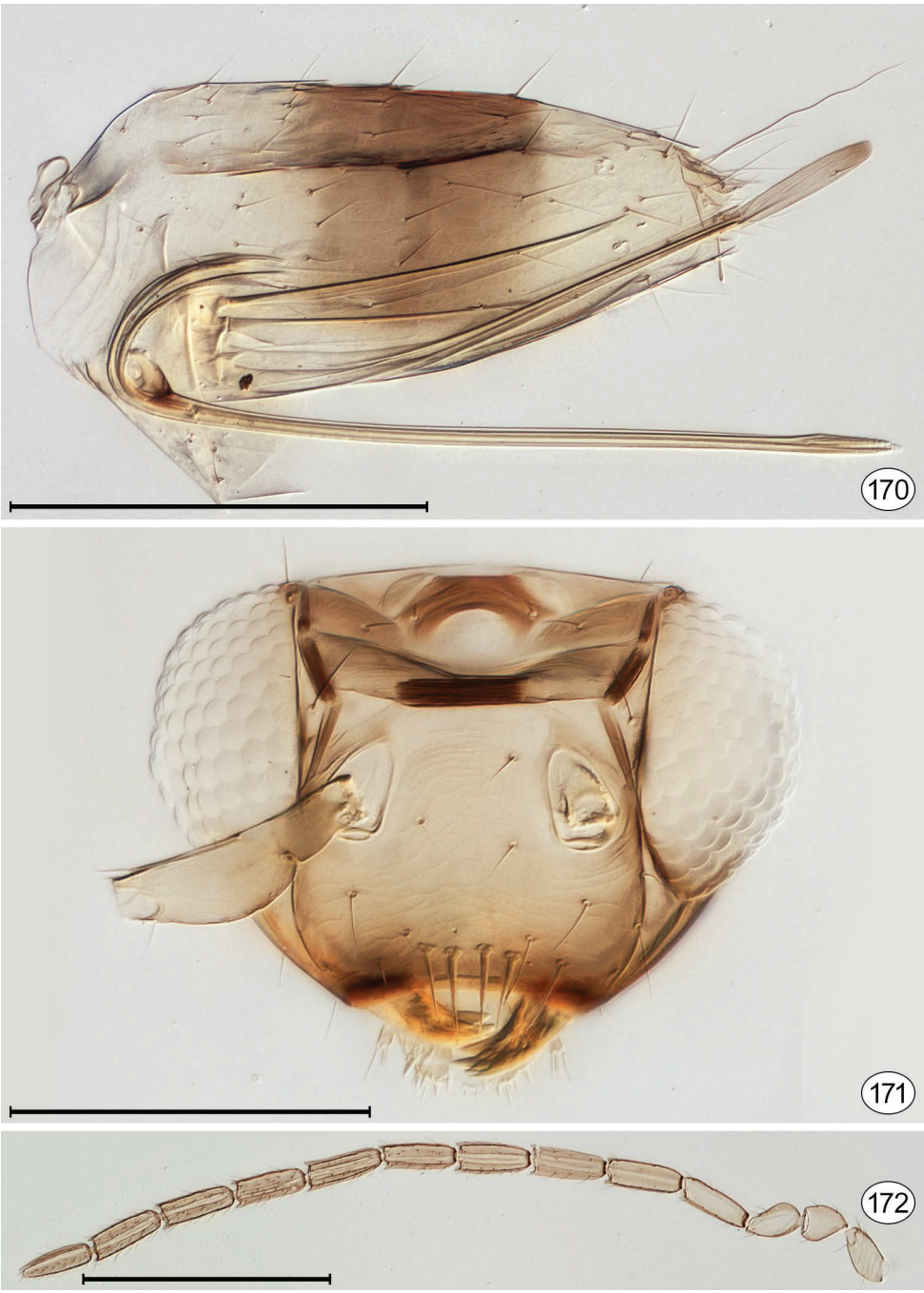

Figures 170–172. *Proarescon similis*. **170** holotype metasoma, lateral **171** male paratype head, anterior **172** male paratype antenna. Scale bar for **170, 172** =200 μm; **171** =100 μm.

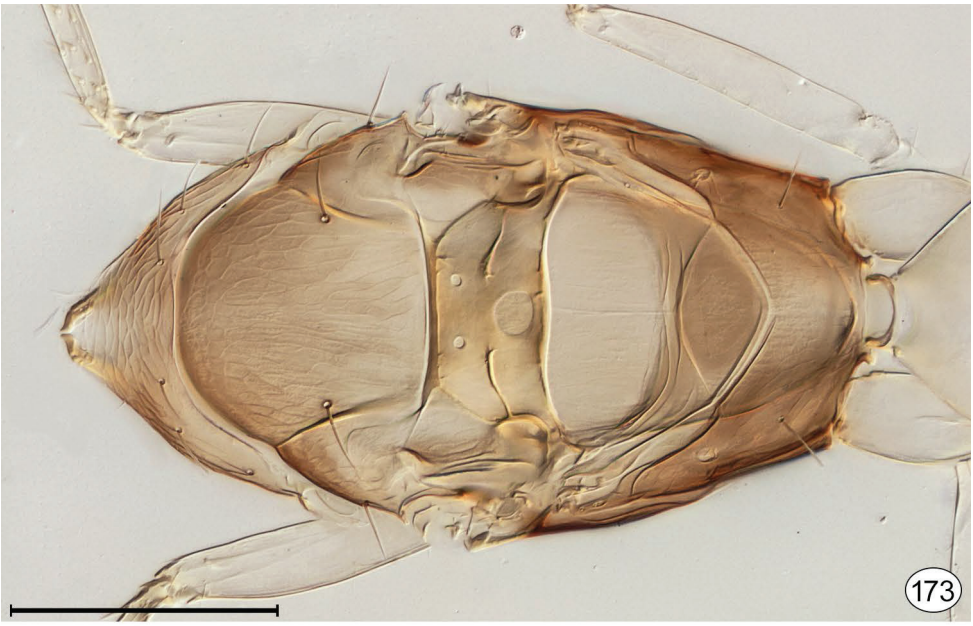

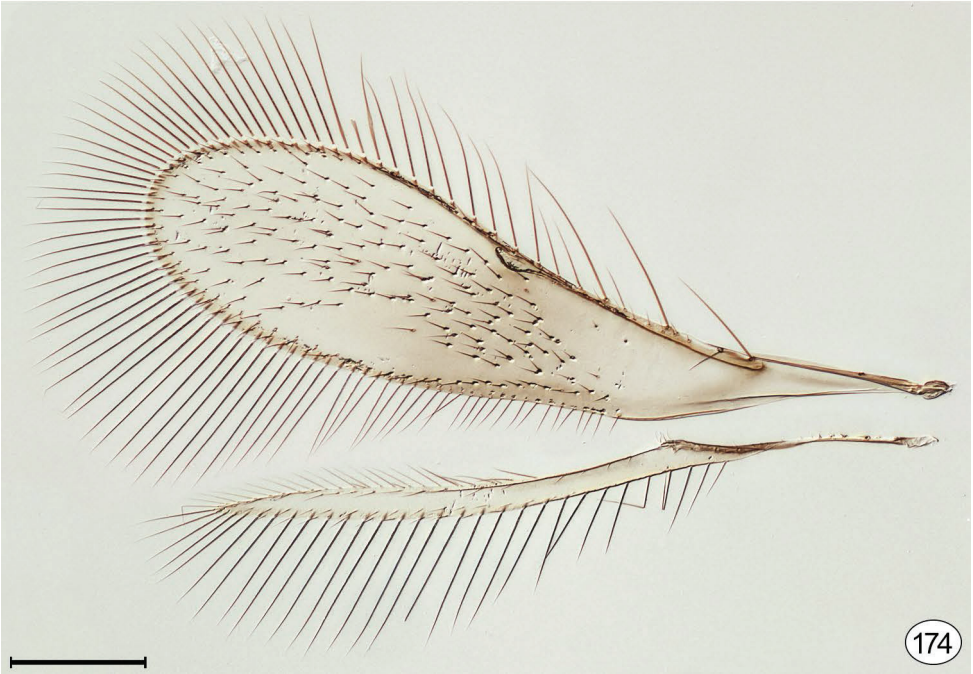

Figures 173, 174. *Proarescon similis*, male paratype. **173** mesosoma, dorsal **174** wings. Scale bar = 100 μm.

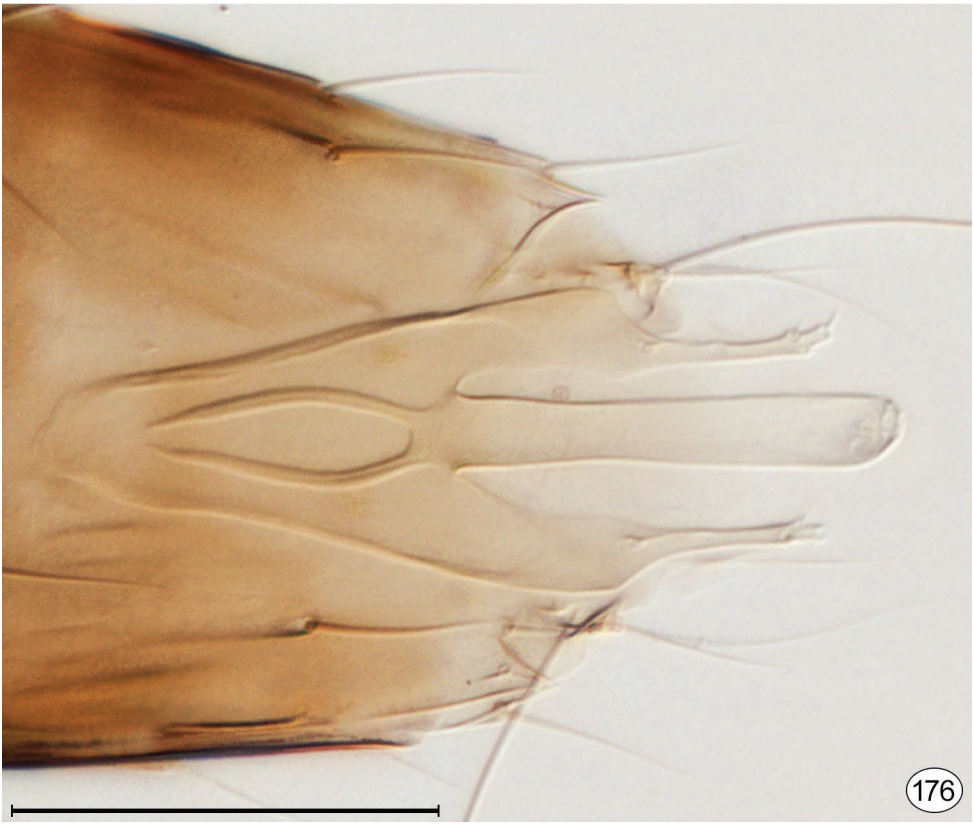

Figures 175, 176. *Proarescon similis*, male paratype. **175** metasoma, dorsal **176** genitalia, dorsal (seen through body). Scale bar for **175** = 100 μm; **176** = 50 μm.

and about 7× their diameter from each other; fenestra small, transversely oval and posterior to campaniform sensilla; frenum with faint, longitudinal wrinkles. Axilla with isodiametric reticulations and with 1 seta dorsally on apparently smooth lateral panel; axillula smooth. Metanotum smooth with 1 short seta on anterior margin closer to lateral apex of lateral panel than to dorsellum and 2 minute seta on anterior margin at apex of lateral panel. Propodeum apparently smooth medially, with faint engraved longitudinal reticulations laterally, with 1 propodeal setae midway between spiracle and posterior margin. **Wings.** Fore wing length (n=1) 563, width 146, length/width 3.86, longest marginal setae 107; cubital line of setae extending halfway towards base of parastigma, about midway between level of proximal and distal macrochaetae. Hind wing length 542, width 26, longest marginal setae 104. **Legs.** Femora and tibiae of all legs at most with faint longitudinal reticulation. Protibia with about 14 short, thick pegs along its length. **Metasoma.** Petiole width 26, length 11. Gaster (Fig. 170) height 155, length 352, apparently without sculpture (Figs 162, 163) and with 2 short setae on gt_1 and 3–6 longer lateral and dorsal setae on remaining terga. Cercus with 4 setae, the first seta about 2× as long as the remaining setae. Hypopygium about 0.35× gaster length. Ovipositor 380 long, its exserted part (56) about 0.2× entire sheath length, with 1 subapical seta.

Male. Colour. As in generic description. **Head.** Head width 192 (n=1). **Wings.** Fore wing length (n=1) 563, width 146, length/width, 3.88, longest marginal setae 107. Hind wing length 542, width 26, longest marginal setae 114. **Antenna.** Measurements (n=1): scape length/width 74/22, pedicel length/width 30/37, flagellar segment length: fl_1 44, fl_2 59, fl_3 62, fl_4 61, fl_5 60, fl_6 60, fl_7 64, fl_8 61, fl_9 61, fl_{10} 62, fl_{11} 58; total flagellar length 652; fl_6 length/width 2.73, with 4 mps (Fig. 172). **Metasoma.** Gaster (Fig. 175) apparently without sculpture, with setae dorsolaterally and laterally and a few minute spicules medially on gt_4 and gt_5. Genitalia (Figs 163, 164, 176) with curved aedeagal apodeme about 0.6× as long as aedeagus; paramere thin, with 3 subapical and apical setae.

Etymology. The species name, *similis*, is Latin for similar, referring to the similarity of this species to the only other described species in *Proarescon*.

Borneomymar Huber

Figs 176–187

Type species. *Borneomymar discus* Huber 2002: 45, by original designation.

Diagnosis. Female. Head without stemmaticum (Fig. 178); occipital groove almost transverse (Fig. 178). Antenna with funicle 8-segemented, only fl_4–fl_8 with mps, and clava 1-segmented (Fig. 179); mandible with 3 teeth; fore wing length 1006, width 235, length/width 4.28, longest marginal setae 203 (Fig. 180); venation ≈ 0.75× wing length (apex of postmarginal vein difficult to determine); submarginal vein 2.03 × as long as parastigma, parastigma with hypochaeta much closer to proximal than to distal macrochaeta; marginal vein 1.94× as long as parastigma; postmar-

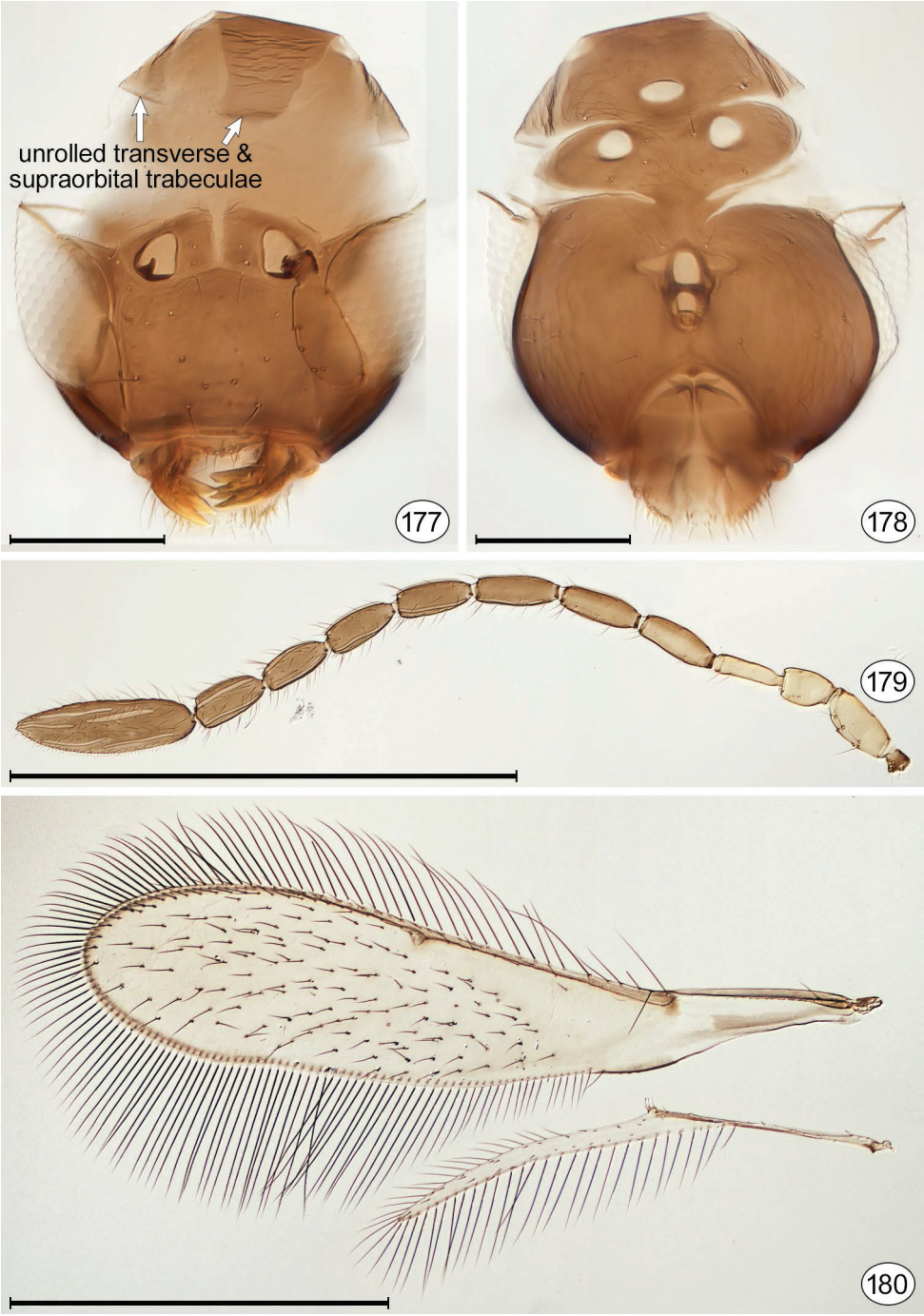

Figures 177–180. *Borneomymar madagascar*, female. **177** head, anterior (vertex detached anteriorly, with trabeculae unrolled) **178** head, posterior **179** antenna **180** wings. Scale bar for **177, 178** = 100 µm; **179, 180** = 500 µm.

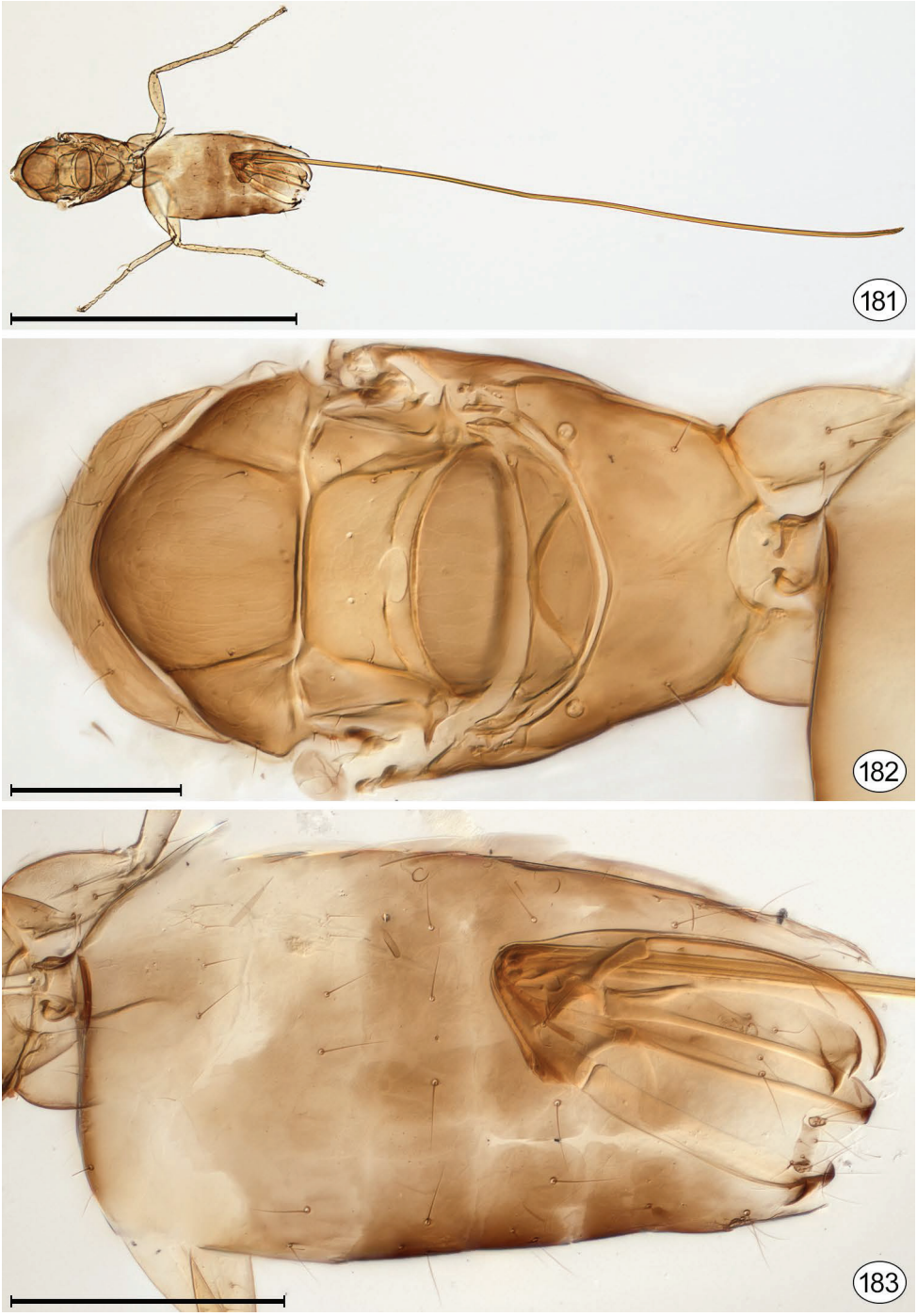

Figures 181–183. *Borneomymar madagascar*, female. **181** body (without head), habitus, dorsal **182** mesosoma, dorsal **183** metasoma, dorsal (slightly twisted). Scale bar for **181** = 1000 µm; **182, 183** = 100 µm.

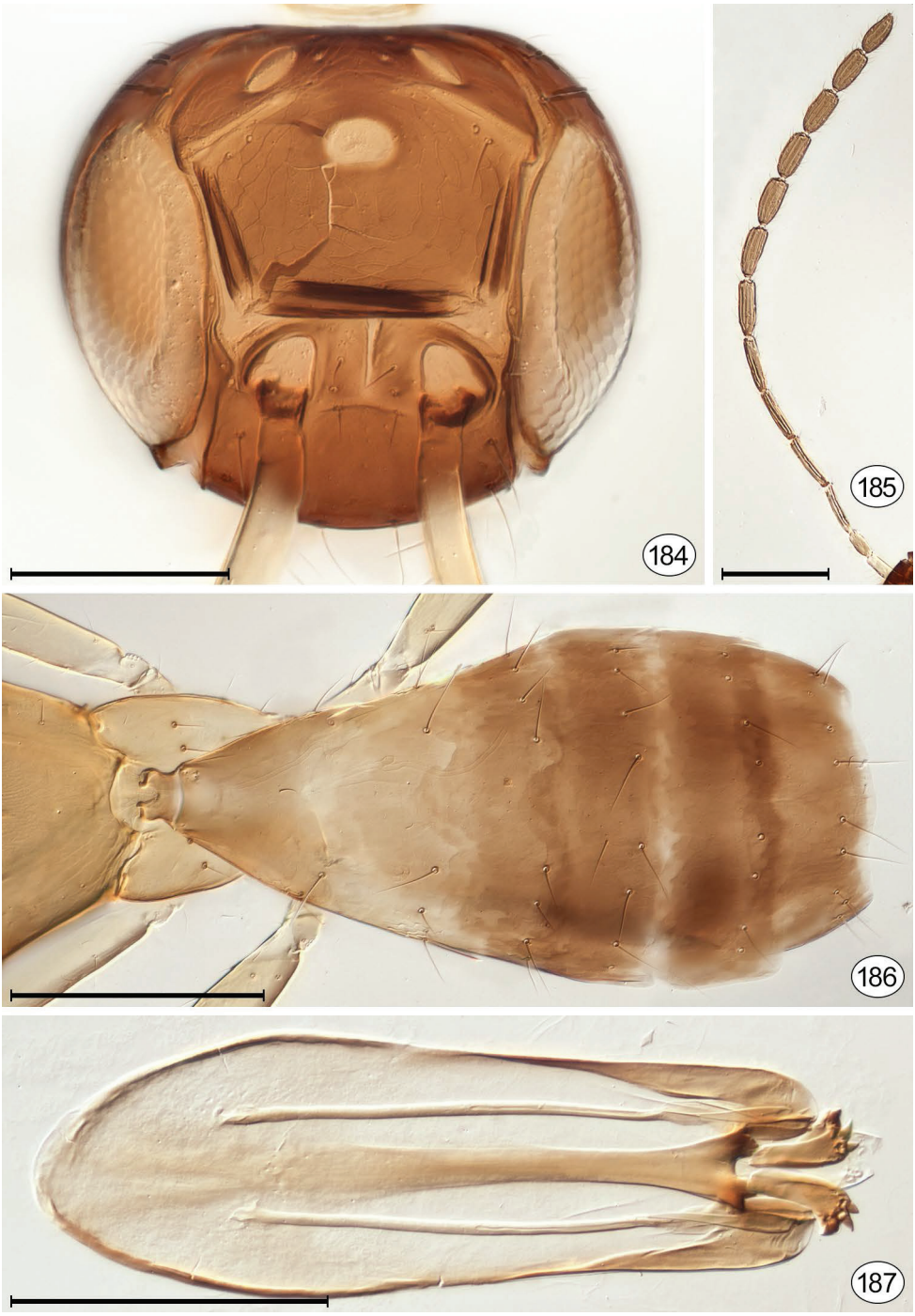

Figures 184–187. *Borneomymar madagascar*, male. **184** head, dorsal **185** antenna, dorsal, twisted laterally after fl_4 **186** metasoma (gt_7 missing) **187** genitalia, dorsal. Scale bar for **184, 187** = 100 μm; **185, 186** = 200 μm.

ginal vein ≈ 0.95× as long as marginal vein; hind wing length 648, width 32, longest marginal setae 122; ovipositor extremely long, projecting posterior to apex of hypopygium by ≈ 2.2–2.4× body length (Fig. 181). **Male.** Similar to female except for gaster (Fig. 186) and antenna. Head (Fig. 184). Fore wing length 1134, width 303, length/width 3.74, longest marginal setae 220; hind wing length 797, width 32, longest marginal setae 32. Antenna with flagellum 11-segmented, all segments with several mps (Fig. 185); genitalia (Fig. 187), encapsulated, with long aedeagal apodeme and digitus with 3 teeth.

Borneomymar madagascar **Huber**

Figs 176–187

Borneomymar madagascar: Huber, 2002: 48 (original description); Engel et al. 2013: 2 (comparison with a fossil species).

Diagnosis. This species differs from, *B. discus* Huber, the only other extant species now included in the genus, as follows: radicle about as long as wide, scape 2.84× as long as wide (in *B. discus* radicle much longer than wide, scape 5.86× as long as wide); fore wing uniformly hyaline (Fig. 180) (in *B. discus* fore wing with distinct brown areas); gaster in lateral view about as 0.5× as high as long (almost circular in *B. discus*).

Description. Female. Body length 922–998 (n = 4, critical point dried specimens, measured to apex of hypopygium), ovipositor length ≈ 2022–2330 (not completely straight so probably slightly longer). Head (Fig. 184) width 266. Antenna measurements (n = 1), length/width (ratio): scape 101/36 (2.84), pedicel 56/35 (1.59), fl_1 68/20 (3.35), fl_2 81/30 (2.73), fl_3 82/29 (2.81), fl_4 86/30 (2.85), fl_5 79/32 (2.43), fl_6 76/34 (2.25), fl_7 72/32 (2.27), fl_8 74/34 (2.20), clava 176/52 (3.40); fl_2–fl_8 each apparently with 3 mps, clava with 12 mps (Fig. 179; hypopygium extending distinctly beyond posterior apex of gaster. **Male.** Body length ≈ 1315 (excluding gt_7, removed to extract genitalia). Head (Fig. 184) width 262. Antenna measurements (n= 1, slide mounted), length/width [scape–fl_4 are vertical so width cannot be measured]: scape 104/ - , pedicel 56/ -, fl_1 106/ -, $fl_2$108/ -, fl_3 106/ -, fl_4 108/ - , fl_5 111/≈ 35, fl_6 101/38, fl_7 92/42, fl_8 96/41, fl_9 94/41, fl_{10} 91/39, fl_{11} 88/35; total flagellar length 1102; fl_6 length/width 2.66, with 9? mps.

Material examined. MADAGASCAR. **Antananarivo.** Botanic garden near entrance to Andasibe National Park, 1025 m, 18°55.58'S; 48°24.47'E, 1-5.xi.2001, R. Harin'Hala, tropical forest, Malaise trap, lot # 007164 (1♀ on slide, CAS). **Diego-Suarez.** Montagne d'Ambre National Park, 975 m, 12°31'S; 49°11'E, 4–19.iii.2001, M. Irwin, E. Schlinger, R. Harin'Hala, Malaise trap, lot # 007149 (1♂ on slide, CAS). **Fianarantsoa.** Massif de Andringitra, 975m, 21°57'50"S; 46°55'59"E, 7–19.xii.1999, M.E. Irwin et al., Malaise trap (4♀ on cards, CNC, UCRC).

Tribe Triadomerini stat. n.

Notes. Yoshimoto (1975) treated the Cretaceous amber fossils from Canada and classified *Triadomerus* Yoshimoto in his new subfamily Triadomerinae, *Carpenteriana* Yoshimoto and *Macalpinia* Yoshimoto in Mymarinae, and *Enneagmus* Yoshimoto in Trichogrammatidae. He defined his Triadomerinae as "having the submarginal and marginal veins distinctly separated at the junction of the fore wing and antennae 13-segmented in the female". Poinar and Huber (2011) keyed the Cretaceous genera of Mymaridae, adding only *Myanmymar* Huber from Burmese amber to bring the number of genera to five, including *Enneagmus*, which Huber (2005) had reclassified in Mymaridae.

I treat Yoshimoto's Triadomerinae as a tribe, defined as follows, based mainly on extant genera and species: mandible with 3 (*Borneomymar*, *Eustochomorpha*) or 4 teeth; pronotum entire; fore wing wide, with marginal setae much shorter than wing width; venation more than 85% of wing length, with marginal vein present and longer than submarginal vein, and with postmarginal vein present and longer than marginal vein; hypochaeta, when present, closer to proximal than to distal macrochata; hind wing wide with marginal setae shorter than wing width; tarsi 5-segmented, with tarsomere 1 distinctly longer than any of the others; petiole clearly shorter than wide, ring like. **Female.** Antenna with flagellum at most 11 segmented (funicle 8-segmented and clava 1–3-segmented); ovipositor usually greatly exserted beyond either posterior (*Borneomymar*, *Eustochomorpha*) or anterior (*Neotriadomerus*) apex of body but in the extinct genera not projecting either anteriorly or posteriorly. **Male.** Antenna 11-segmented, the flagellomeres each with several mps; genitalia encapsulated, with short, thick parameres, apparently without digiti (in *Neotriadomerus*) but thinner walled and with digiti (in *Borneomymar*)

Triadomerini is treated here as the sister clade to the remainder of Mymaridae. The only apomorphy that defines the tribe is reduction in number of flagellar segments (at most 11) relative to Rotoitidae, whose species have a 12-segmented flagellum in females of both included extant genera. An additional diagnostic feature of the extant species of Triadomerini is the exserted cerci on a distinct prominence, similar to that of Torymidae. The occurrence of elevated cerci, number of teeth in mandibles, and several other features cannot definitely be determined from the fossil specimens studied. The lack of a hypochaeta apparently occurs in *Triadomerus* and *Eustochomorpha* and apparently also in at least one of the *Neotriadomerus* species.

Triadomerus is known only from Cretaceous amber from present day western Canada (Yoshimoto 1975). *Eustochomorpha* and *Neotriadomerus* species are confined to Australia, and extant *Borneomymar* species occur in the islands of Borneo and Madagascar whereas the one extinct *Borneomymar* species is from Eocene amber from the Baltic region (Engel et al. 2013). *Macalpinia* and especially *Carpenteriana* doubtfully belong in Triadomerini but perhaps are better classified here than elsewhere. Even though *Carpenteriana* has 7-segmented funicle and an entire clava its fore wing vena-

tion appears to be similar to *Macalpinia*. *Macalpinia* has an 8-segmented funicle and 3-segmented clava, as in *Triadomerus* and *Neotriadomerus*, so on the basis of this feature is classified fairly well in the tribe even though it appears to have no postmarginal vein and apparently only 4-segmented tarsi (tarsi are difficult to see; they may, in fact, be 5-segmented). Thus, I classify six genera in Triadomerini: four genera definitely—*Borneomymar*, *Eustochomorpha*, *Neotriadomerus*, *Triadomerus*, and two genera tentatively—*Carpenteriana* and *Macalpinia*.

Tribe Aresconini

Notes. Viggiani (1988) proposed Aresconini for *Arescon* Walker and defined the tribe on the characteristic male genitalia, i.e., encapsulated, with relatively long, narrow parameres but apparently no digiti. Based on mainly extant genera and species, Aresconini is defined by the following features: mandible with 4 teeth; pronotum entire; venation long but postmarginal vein usually short; funicle in females 4-, 5- or 8-segmented; clava entire or 2-segmented; male genitalia usually with long parallel-sided parameres. I classify members of the extant genera *Kikiki* Huber and Beardsley (Huber and Beardsley 2000), *Tinkerbella* Huber & Noyes (Huber & Noyes 2013), *Proarescon* (this paper), and the extinct genus *Myanmymar* (Poinar and Huber 2011) in the tribe based on similarities in head features, fore wing shape or venation, and male genitalia where known.

Arescon is almost worldwide (Triapitsyn 2016) whereas *Proarescon* is only in southeastern Asia. Lin et al. (2007) and Huber (2009) had first classified *Kikiki* in the *Alaptus* group of genera then, with *Tinkerbella* described as a separate genus (Huber and Noyes 2013), in the *Anagrus* group of genera. In both cases, similarities in various features were used to justify their placement. Now, however, I believe these two genera are best classified in Aresconini. The male genitalia of *Kikiki* have fairly long and thick parameres (Huber and Noyes 2013, fig. 35), the vertex has a distinct stemmaticum (Huber and Noyes 2013, figs 12, 41), the fore wing has a long venation, and the mandible has 4 teeth, all features that occur also in *Arescon* and *Proarescon*. *Kikiki* may be almost worldwide (Australia, India, northern South America, Hawaiian Islands) and *Tinkerbella* is so far known only from Costa Rica (Huber and Noyes 2013). *Enneagmus* may fit in Aresconini better than in Triadomerini because of its apparently short venation, and 4-segmented funicle and 3-segmented tarsi as in *Kikiki*. The 3-segmented clava may simply be an ancestral feature, reduced to two segments in *Kikiki* and *Tinkerbella*. However, the short venation, apparently much less than half the wing length is unlike the other genera in Aresconini. Thus, six genera are here classified in Aresconini: *Arescon*, *Enneagmus*, *Kikiki*, *Myanmymar*, *Proarescon*, and *Tinkerbella*. If *Minutoma* Kaddumi (Kaddumi 2005) is indeed a mymarid, it may also belong here; its small body length is comparable to that of *Tinkerbella*.

Key to extant genera of *Aresconini* and *Triadomerini*. Females.

See Poinar and Huber (2011) for key to the extinct Cretaceous genera.

1 Clava 2 or 3-segmented; propodeum with 2 or 3 setae **2**
– Clava 1-segmented (i.e., entire); propodeum with 1 seta **5**
2(1) Clava 2-segmented **3**
– Clava 3-segmented [ovipositor extending anteriorly well under mesosoma but not exserted posteriorly much beyond gastral apex (Figs 105, 126)] .... ***Neotriadomerus* Huber, gen. n.**
3(2) Ovipositor extending posteriorly well beyond posterior apex of gaster (Figs 2, 4); tarsi 5-segmented; funicle 8-segmented ..... ***Eustochomorpha haeckeli* Girault**
– Ovipositor not or barely exserted beyond posterior apex of gaster; tarsi 3- or 4-segmented; funicle 4- or 5-segmented **4**
4(3) Tarsi 4-segmented; funicle 5-segmented ..... ***Tinkerbella* Huber & Noyes**
– Tarsi 3-segmented; funicle 4-segmented ..... ***Kikiki* Huber & Beardsley**
5(1) Funicle 5-segmented ..... ***Arescon* Walker**
– Funicle 8-segmented **6**
6(5) Fl_1–fl_5 each much shorter than fl_6–fl_8 (Fig. 166) ..... ***Proarescon* Huber, gen. n.**
– Fl_1–fl_5 as long as fl_6–fl_8 (Huber 2002, figs 2, 4) ..... ***Borneomymar* Huber**

Discussion

Huber (2002) treated *Triadomerus* (extinct) and *Eustochomorpha* (extant) as sister genera to the remaining extant genera of Mymaridae based, in females (males are unknown), on an 8-segmented funicle and 3- or 2-segmented clava, respectively, i.e., 11 or 10 flagellar segments in total. In *Neotriadomerus*, males are known and have the same number of flagellar segments as in females, i.e., 11, and this is considered to be as the most plesiomorphic feature possible in Mymaridae. *Macalpinia* and *Triadomerus* also have an 8-segmented funicle and 3-segmented clava. Species in all other genera (all extant only, except for one fossil *Borneomymar* species) whose males are known have a different number of segments between females and males, with at least one less segment in females compared to males. But because males of the species of most extant genera have an 11-segmented flagellum, it is probably safe to assume that males in the extinct genera also have an 11-segmented flagellum, as in females. On this basis, *Triadomerus*, *Macalpinia* and *Neotriadomerus* are treated as the sister clade to other genera within Triadomerini and to all remaining genera of Mymaridae, both extinct and extant. At present the relationships among these three genera cannot be determined but, among extant genera only, *Neotriadomerus* is clearly the sister genus to the all remaining genera, including *Eustochomorpha*. Loss of one claval segment in *Eustochomorpha*, to give a 10-segmented flagellum in its females, makes this the sister genus to the remaining genera of extant Mymaridae other than *Neotriadomerus*.

Conclusions

The distribution of the extinct and extant genera that can definitely be placed in Mymaridae encompasses a time span of almost 100 my. Kaddumi (2005) classified *Minutoma*, found in 120–135 my Cretaceous amber from the Zarqa River basin, in Mymaridae but Huber in Heraty et al. (2013: 2) suggested it might be better placed in Tetracampidae; its clava appears to be 4-segmented. But if it is a member of Mymaridae then the family extends back into the early Cretaceous, well after the beginning of the breakup of Pangea into Laurasia in the north and Gondwana in the south, beginning 200 million years ago. The present centre of diversity of Mymaridae is in the Australasian region, particularly Australia and New Zealand, but the fossil evidence shows that the family was already quite diverse in the Cretaceous and that the origin of Mymaridae is not necessarily there. In Triadomerini, all the Cretaceous genera (known only from Laurasia) eventually became extinct whereas *Eustochomorpha* and *Neotriadomerus* are extant in Australia (part of Gondwana). *Borneomymar*, in contrast, is represented by two extant species in the islands of Borneo and Madagascar (both part of Gondwana) and one extinct species from Baltic amber, i.e., from Laurasia (Engel et al. 2013). In Aresconini, the only extinct genus is *Myanmymar* (Laurasia?); all the rest are extant and, except for *Proarescon* and *Tinkerbella*, widespread.

The widespread distribution of Mymaridae already existed at least 80 my ago (described taxa from Canadian and Burmese Cretaceous amber) and the family is currently worldwide, except for Antarctica. Two scenarios may explain this: 1) The family may have evolved before the breakup of Pangaea, 200–180 million years ago, and was already widespread throughout the supercontinent wherever suitable hosts occurred, which would suggest a Jurassic origin; 2) The family is more recent, having originated in only part of Pangea, probably Gondwana, and some species then spread to Laurasia after the two parts became well separated from each other. This is quite possible because Mymaridae are small and easily carried long distances on wind and some would have survived the trip. Mymaridae as a recognizable taxon may therefore be a lot older than the present evidence shows, going back well into the early Cretaceous.

Acknowledgements

The following curators and collectors are thanked for sending specimens for study: J. Cardale (ANIC), C. Burwell and G. Daniels (QMBA), C. Darling (ROM), J.F. Donaldson (QDPC), and S. Triapitsyn (UCRC). I thank particularly J. Read (CNC, now retired) for proof reading, taking the scanning electron micrographs and digital images, and arranging them into plates.

References

Annecke DP, Doutt RL (1961) The genera of the Mymaridae. Hymenoptera: Chalcidoidea. Republic of South Africa, Department of Agricultural Technical Services, Entomology Memoirs 5: 1–71.

Dahms EC (1984) A checklist of the types of Australian Hymenoptera described by Alexandre Arsene Girault: III. Chalcidoidea species F-M with advisory notes. Memoirs of the Queensland Museum 21(3): 579–842.

Engel MS, McKellar RC, Huber JT (2013) A fossil species of the primitive mymarid genus *Borneomymar* (Hymenoptera: Mymaridae) in Eocene Baltic amber. Novitates Paleoentomologicae 5: 1–8. https://doi.org/10.17161/np.v0i5.4651

Gibson GAP (1997) Chapter 2. Morphology and terminology. In: Gibson GAP, Huber JT, Woolley JB (Eds) Annotated keys to the genera of Nearctic Chalcidoidea (Hymenoptera). NRC Research Press, Ottawa, Ontario, Canada, 16–44.

Girault AA (1915) Australian Hymenoptera Chalcidoidea — II. Second supplement. Memoirs of the Queensland Museum 3: 154–169.

Heraty JM, Burks BD, Cruaud A, Gibson G, Liljeblad J, Munro J, Rasplus J-Y, Delvare G, Janšta P, Gumovsky AV, Huber JT, Woolley JB, Krogmann L, Heydon S, Polaszek A, Schmidt S, Darling DC, Gates MW, Mottern JL, Murray E, Dal Molin A, Triapitsyn S, Baur H, Pinto JD, van Noort S, George J, Yoder M (2013) A phylogenetic analysis of the megadiverse Chalcidoidea (Hymenoptera). Cladistics 29: 466–542. https://doi.org/10.1111/cla.12006

Huber JT (2002) The basal lineages of Mymaridae (Hymenoptera) and description of a new genus, *Borneomymar*. In: Melika G, Thuróczy C (Eds) Parasitic wasps. Evolution, systematics, biodiversity and biological control. Agroinform, Kiadó & Nyomba Kft., Budapest, 44–53.

Huber JT (2005) The gender and derivation of genus-group names in Mymaridae and Mymarommatidae. Acta Societatis Zoologicae Bohemicae 69: 167–183.

Huber JT (2012) Revision of *Ooctonus* (Hymenoptera: Mymaridae) in the Nearctic region. Journal of the Entomological Society of Ontario 143: 15–105.

Huber JT (2015) World reclassification of the *Gonatocerus* group of genera (Hymenoptera: Mymaridae). Zootaxa 3967: 1–184. https://doi.org/10.11646/zootaxa.3967.1.1

Huber JT, Beardsley JW (2000) A new genus of fairyfly, *Kikiki*, from the Hawaiian Islands (Hymenoptera: Mymaridae). Proceedings of the Hawaiian Entomological Society 34: 65–70.

Huber JT, Noyes JS (2013) A new genus and species of fairyfly, *Tinkerbella nana* (Hymenoptera: Mymaridae), with comments on its sister genus *Kikiki*, and discussion on small size limits in arthropods. Journal of Hymenoptera Research 32: 17–44. https://doi.org/10.3897/jhr.32.4663

Kaddumi HF (2005) Amber of Jordan. The oldest prehistoric insects in fossilized resin. 2nd edition. Eternal Rivers Museum of Natural History, Amman, Jordan. 168 pp. [privately printed]

Lin N-Q, Huber JT, LaSalle J (2007) The Australian genera of Mymaridae (Hymenoptera: Chalcidoidea). Zootaxa 1596: 1–111.

Noyes JS, Valentine EW (1989) Mymaridae (Insecta: Hymenoptera) – introduction, and review of genera. Fauna of New Zealand 17: 1–95.

Poinar G Jr., Huber JT (2011) A new genus of fossil Mymaridae (Hymenoptera) from Cretaceous amber and key to Cretaceous mymarid genera. ZooKeys 130: 461–472. https://doi.org/10.3897/zookeys.130.1241

Triapitsyn SV (2016) Review of the Oriental species of the genus *Arescon* Walker, 1846 (Hymenoptera: Mymaridae). Euroasian Entomological Journal 15 (Supplement 1): 137–151.

Viggiani G (1988) A preliminary classification of the Mymaridae (Hymenoptera: Chalcidoidea) based on the external male genitalic characters. Bollettino del Laboratorio di Entomologia Agraria "Filippo Silvestri" 45: 141–148.

Yoshimoto CM (1975) Cretaceous chalcidoid fossils from Canadian amber. The Canadian Entomologist 107: 499–528. https://doi.org/10.4039/Ent107499-5

JHR 57: 89–101 (2017)
doi: 10.3897/jhr.57.12510
http://jhr.pensoft.net

RESEARCH ARTICLE

JOURNAL OF Hymenoptera RESEARCH
A peer-reviewed open-access journal
The International Society of Hymenopterists

Stiff upper lip: Labrum deformity and functionality in bees (Hymenoptera, Apoidea)

Michael C. Orr[1], Amber D. Tripodi[2]

1 *Biology Department, Utah State University, 5305 Old Main Hill, Logan, Utah, 84322, USA* **2** *USDA-ARS Pollinating Insects Research Unit, Utah State University, 5310 Old Main Hill, Logan, Utah, 84322, USA*

Corresponding author: *Michael C. Orr* (michael.christopher.orr@gmail.com)

Academic editor: *Jack Neff* | Received 4 March 2017 | Accepted 14 April 2017 | Published 30 June 2017

http://zoobank.org/31C32185-46FF-4690-BDED-8519C83AE73C

Citation: Orr MC, Tripodi AD (2017) Stiff upper lip: Labrum deformity and functionality in bees (Hymenoptera, Apoidea). Journal of Hymenoptera Research 57: 89–101. https://doi.org/10.3897/jhr.57.12510

Abstract

In hyper-diverse groups such as Hymenoptera, a variety of structures with different, complementary functions are used for feeding. Although the function of the parts such as the mandibles is obvious, the use of others, like the labrum, are more difficult to discern. Here, we discuss the labrum's function in bees, as well as the implications of deformities to this and associated characteristics.

Keywords

Anthophora, Apidae, *Heliophila*, *Micranthophora*, morphology, physiology

Introduction

As one of the oldest groups of terrestrial organisms, invertebrates employ an exceptional diversity of feeding and sensory strategies (Grimaldi and Engel 2005). The structures related to the sensation and manipulation of food are most often found on the head (Chapman 1998; Chapman and de Boer 1995; Snodgrass 1993). Although the evolutionary origins of some parts of the insect head remain contested, it is clear that each major component plays a role in the overall functioning of the head and, therefore, the survival of the organism (Frase and Richter 2013; Ortega-Hernández and Budd 2016; Posnien et al. 2009; Smith et al. 2014; Smith and Goldstein In press).

Copyright *Michael C. Orr, Amber D. Tripodi.* This is an open access article distributed under the terms of the Creative Commons Attribution License (CC BY 4.0), which permits unrestricted use, distribution, and reproduction in any medium, provided the original author and source are credited.

The primary uses of many of the parts of the head are generally obvious (e.g., eyes or mandibles), but those of others, such as the labrum, are more obscure. This is in part due to the frequent conflation of the labrum with the associated epipharynx (Dellacasa et al. 2010; Snodgrass 1993). Although these two components function in tandem, it is important to differentiate between them because failure to do so may obscure the individual functions of each of these structures.

The insect labrum is typically a sclerotized plate found below the clypeus, either articulated there or fused to it, and it is generally innervated and connected to frons musculature (Chapman 1998; Snodgrass 1985; 1993). Often referred to as the "upper lip" based on the Latin origin of the term, it is considered an important element of insect food manipulation (Rebora et al. 2014; Snodgrass 1985). The labrum is also a site of attachment for the epipharyngeal wall, a soft membrane found on the inner face of the labrum that often has a medial projection called the epipharynx (the epipharyngeal wall is also called the membranous inner face of the labrum or similar terms, we will generally consider the epipharynx as a specific part of the epipharyngeal wall (Chapman 1998; Dellacasa et al. 2010; Snodgrass 1993; Vilhelmsen 1996). The epipharyngeal wall is more generally associated with sensory functions, especially chemo- and mechano-sensation, likely because it often continues internally from the labrum, along the inner face of the clypeus, to the mouth (Snodgrass 1985; 1993). Together, the labrum and epipharyngeal wall form a functional unit that assists insect feeding in many different ways.

Interestingly, the labrum appears to be more frequently modified for secondary, non-feeding purposes than the epipharyngeal wall. This may be either a consequence of observer effort, given the fact that the epipharyngeal wall is typically hidden and overlooked in favor of the readily apparent labrum, or simply because the labrum is exposed and can more easily interface with the external environment. Regardless, insects use the labrum in many novel ways. For example, labral sensillae commonly used for more benign purposes are now part of the trigger and lock mechanism used by some trap-jaw ants to spring their powerful mandibles (Larabee and Suarez, 2014). Not all uses of the labrum are tied to such exceptional behaviors, however, as the labrum has many forms and functions across insects and even within orders such as Hymenoptera, making definitive identification of labrum function a surprisingly challenging task.

Even in some economically important groups like bees, the labrum's general role is relatively poorly understood. Similar to insects at large, there is also a great diversity of bee labrum forms (Fig. 1; Michener 1944; Michener 2007), but the function of only relatively few of these forms has been investigated, and labral use remains obscure even in closely-studied groups (Walker 1995). Even the most dramatic labral modifications in the bees, such as the elaborate keels seen in many female Halictidae, have unknown functionality, though they are absent in males and much reduced in parasitic members of the family (Michener 1978; Michener 2007; Walker 1995; Fig. 1A). Conversely, many of the apid bees which have unusually long labrums are cleptoparasitic, though the functionality of this trait is again unknown, these structures are perhaps related to nest cell penetration or protection of the mouthparts (Michener 2007; Fig. 1B).

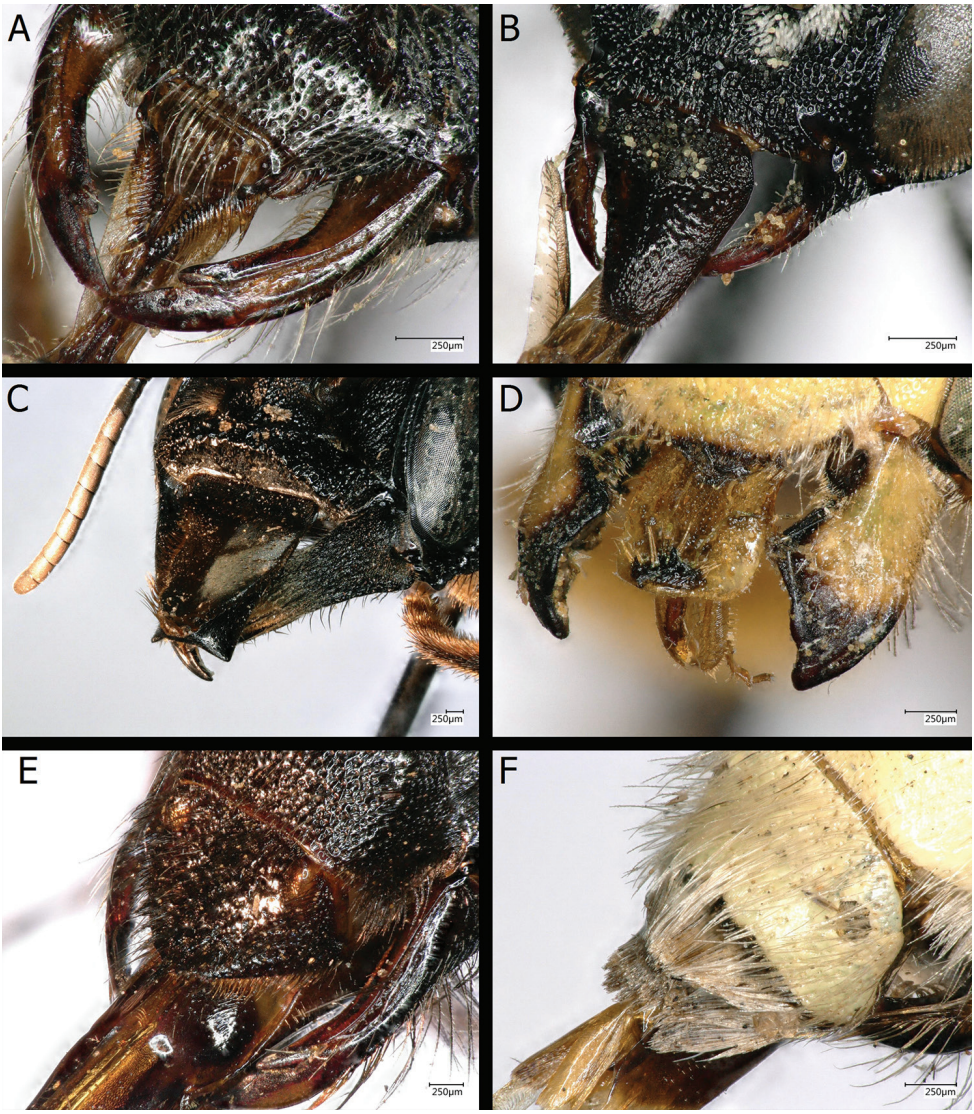

Figure 1. Labrum form diversity in bees. **A** *Halictus ligatus* Say 1837 female (NPIC:87530) **B** *Holcopasites insoletus* (Linsley, 1942) male (NPIC:BBSL211611) **C** *Megachile sculpturalis* Smith 1853 female (NPIC:BBSL1030971) **D** *Trachusa larreae* (Cockerell, 1897) female (NPIC:94880) **E** *Habropoda laboriosa* (Fabricius, 1804) female (NPIC:BBSL253733) **F** *Anthophora abrupta* Say, 1838 male (NPIC:BBSL231004). Scale bars indicate 250µm for each image independently.

However, long labrums are linked to resource transport in some nest-building species. For example, the largest bee in the world (*Megachile pluto* Smith, 1860) and some of its relatives (Fig. 1C) are known to carry nesting materials (resin, wood) between their mandibles and labrum (Messer 1984). Similarly, *Trachusa larreae* females (Fig. 1D) have a shock of setae on the labral apex that facilitates resin collection (Cane 1996),

and *Habropoda laboriosa* females (Fig. 1E) may use labral setae to aide in pollen collection (Cane and Payne 1988; Thorp 2000). Rather more fascinating, *Anthophora abrupta* males (Fig. 1F) are known to use a labral "moustache" to paint floral fragrances onto mating areas to attract females (Lee 1998; Norden and Batra 1985; Whitten et al. 1989). However, relatively few bee species are known to use the labrum in these particular ways, and it appears safe to assume that such non-feeding related functions are secondary.

It is reasonable to state that the labrum serves some broader function in bees, given that it is obviously articulated and connected to both musculature and nerves (Ellis and Hepburn 2006; Erickson Jr et al. 1986; Snodgrass 1985). Reports of bee lice (Braulidae) tickling the labrum of honey bees to induce regurgitation, and the presence of sensillae there, clearly suggest mechano-sensory function at a minimum (Grimaldi and Underwood 1986), although the existence of chemo-sensory labral or epipharyngeal sensillae in bees is debated (de Brito Sanchez 2011; Mitchell et al. 1999; Sandoz et al. 2002; Whitehead and Larsen 1976). The labrum is also apparently used to press the epipharyngeal wall against the proboscis to create an airtight seal during ingestion, giving it an additional function beyond mere sensation (Carreck et al. 2013). Interestingly, the epipharyngeal wall has apparently lost the gustatory functions seen in many other insects, such tasks are instead thought to be managed by bees with the antennae, other mouthparts, and forelegs (de Brito Sanchez 2011; Mitchell et al. 1999). This makes sense when considering that the epipharyngeal wall is less likely to directly touch food that bees are initially handling, in comparison to groups with gustatory labral sensillae (*e.g.*, Orthoptera: Cook 1972; Zaim et al. 2013).

The larval labrum's function also appears to be linked to sensation and feeding, as many bees and other Hymenoptera have conspicuous setae there (Murao and Tadauchi 2005; O'Donnell 1989; Pitts and Matthews 2000; Rozen 2001). However, complications arise in that sensillae can change form, and possibly even function, between instars (Garófalo and Rozen Jr 2001), and the distribution of sensillae is highly variable both across and within groups (Rozen 2001; Rozen Jr and Kamel 2006). Cleptoparasitic larvae are especially interesting, often featuring high numbers of labral sensillae and unusual integumental modifications (e.g., sharp apical tubercles, setae-derived spines; Rozen Jr and Kamel 2006; Straka and Bogusch 2007). It may be that cleptoparasites use their sensillae to locate hosts and competitors, and the broadly flattened labral form of some instars also appears to be used to create a seal on host eggs during feeding (Alves-dos-Santos et al. 2002). Rozen Jr and Kamel (2006) suggest that such enlarged forms are also used in conjunction with the mandibles to crush their opponents. These seemingly antagonistic forms revert to the unmodified type seen in most non-cleptoparasites, supporting the idea that they are likely involved with the belligerent life history typical of early-instar cleptoparasites (Baker 1971). Whatever primary and secondary functions the labrum may serve, it clearly serves purposes in both adults and larvae.

In light of the functional importance of the labrum and epipharyngeal wall, selection should strictly regulate their presence and form. Even if these components do

not serve chemo-sensory functions, the loss of mechano-sensory function could easily hinder food manipulation (Carreck et al. 2013). The discovery of a deformed adult bee without a functional labrum was, then, a surprise. Here, we describe an aberrant specimen of *Anthophora* (*Heliophila*) *petrophila* Cockerell, 1905, compare it to typical specimens of the genus, and discuss the implications of its labral reduction.

Methods

A single bee specimen with an aberrant labrum was found among the >30,000 *Anthophora* that the first author has passed under a microscope. This specimen belongs to *A. petrophila*, a xeric bee that is found commonly throughout much of the western United States. It was collected by P.H. Timberlake at Olancha, California on May 2nd, 1927 off of *Salix exigua* Nuttall 1842, and is held in the University of California, Riverside's Entomology Research Museum (UCRCENT407176). Many typical specimens of *A. petrophila* have also been examined during the first author's studies (n>3000), and the epipharyngeal wall's morphology when dried was also observed in five specimens (NPIC: BBSL482833, BBSL510382, BBSL510415, BBSL516410, BBSL918735 from NPIC). Images were taken with a VHX-5000 Digital Microscope. Terminology follows Michener (2007).

Results

Examination of typical specimens of *Anthophora petrophila* versus the aberrant specimen enabled confirmation of labral reduction, rather than absence (Fig. 2). The darkened clypeal border seen in typical *A. petrophila* is clearly present in the aberrant specimen, surrounding the nozzle-like sclerite which we assert is the reduced labrum. The absence of other sclerites in this area further supports the homology of this sclerite with the labrum of typical *A. petrophila*. The clypeus is correspondingly enlarged, descending and encircling the labrum as it normally does to a lesser extent, which suggests that the growth of these two areas may be linked in some way. Notably, in comparison to normal specimens, this also reduces the protuberance of the deviant's clypeal rim, and the deformed labrum is entirely bare of setae.

Upon further examination, it was determined that the epipharyngeal wall was also greatly reduced. As the aberrant specimen was collected in 1927, it was decided that internal features would not be examined through dissection, in order to avoid unnecessary damage to this apparently unique specimen. Nonetheless, examination of the inner face of the labrum in five normal, pinned specimens of *Anthophora petrophila* confirmed that the epipharyngeal wall would have been distinguishable in the deviant specimen if it were unmodified.

No additional abnormalities were evident in this specimen, and its body size is about average for this species, not visibly larger or smaller than other specimens ob-

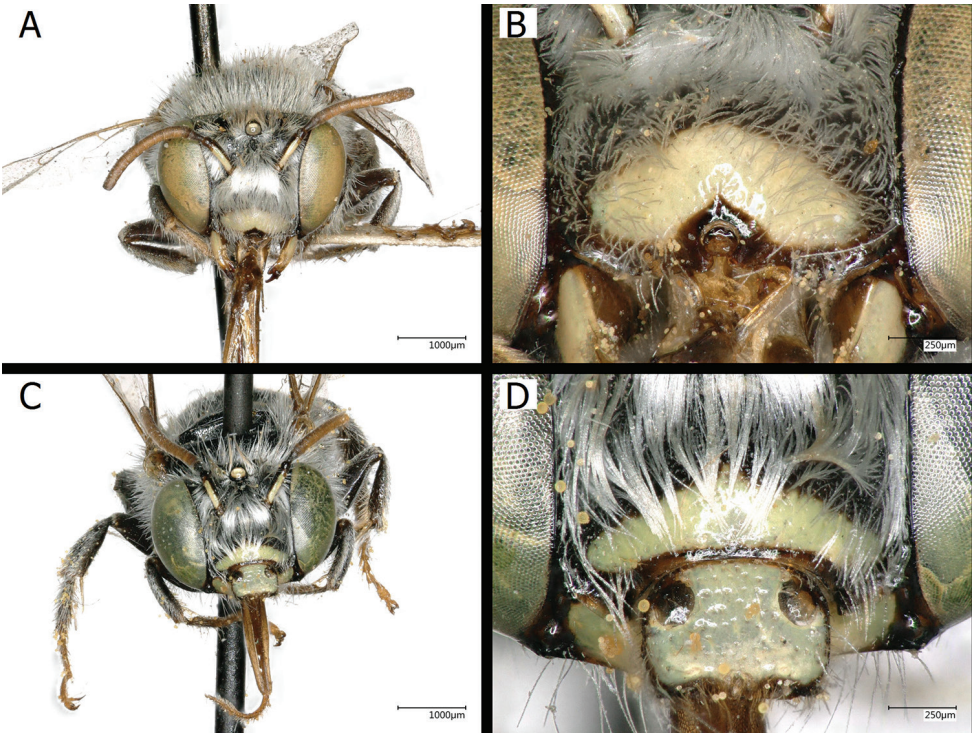

Figure 2. The deviant (UCRCENT407176) and normal (NPIC:BBSL506171) labral forms of *Anthophora petrophila*: **A** deviant, 50× magnification **B** deviant, 200× magnification **C** normal, 50× magnification **D** normal, 200× magnification. Scale bars indicate 1000µM (**A, C**) or 250µm (**B, D**).

served. Consequently, malnutrition during development appears to be an unlikely cause of this labral deformity. No Strepsiptera or other parasites were evident, suggesting the malformed labrum is also not a result of parasitic growth inhibition (Borowiec and Salata 2015; Salt 1927).

It is notable that the wings of the specimen are completely intact. Wing wear is a widely-accepted metric of adult age in bees, based upon activity, and the exceptionally rapid wingbeats and skillful flight of *Anthophora* (*Heliophila*) make this feature especially useful in this group (Foster and Cartar 2011; Kemp 2000; Michener et al. 1955; Packer and Knerer 1986). As the specimen was collected on a flower, this cannot be explained by reduction of musculature or other internal factors that would lead to an inability to fly and, thereby, preservation of the wings.

Discussion

This deformity is quite rare, as it was only seen in one of >30,000 *Anthophora* examined. This could reflect the rarity of labral deformities or suggest that such deformi-

ties are deleterious. Given the apparent use of the epipharyngeal wall as a seal on the proboscis, the wall's reduction should dampen the suction efficiency of the proboscis (Carreck et al. 2013). Another possibility is that the sensillae present on the labrum are involved in initiating or modifying food responses, and setal absence could influence feeding behaviors. It may be that the deviant specimen was unable to feed, or very inefficient at doing so.

Although the direct effects of this deformity are unclear, the lack of wing wear corroborates potential reduced feeding ability, as the bee must have either emerged recently or been discouraged from flying by the futility of attempts to eat. The effects of labrum and epipharyngeal wall reduction could be tested in future studies by using knockout methods to target genes involved in labrum development and then conducting comparative observations on the eating behaviors of normal versus deformed bees (Siemanowski et al. 2015).

Although rarely reported, deviant phenotypes can be useful for exploring developmental pathways, embryology, and potential evolutionary pathways. Changes to developmental pathways can result in new phenotypes that have selective advantages. For example, the facultative polyphenism seen in termite castes is achieved through manipulations of gene regulation in response to socio-environmental characteristics, such as the state of the colony (Korb and Hartfelder 2008). In bees, the developmental fluidity of sex-based characters provides the raw materials on which selective forces can act. Deviant phenotypes often trade female characters, such as pollen-gathering scopae and nest-constructing mandibles, for male characters, such as hairlessness and simple mandibles (Wcislo et al. 2004). Fertile individuals which lack the proper tools to build and provision their own nests may instead opt for a cleptoparasitic lifestyle and usurp others' nests, in lieu of not reproducing. If heritable, such traits could then be passed to future generations.

Abnormalities in insects are thought to arise from one of four teratogenic processes: genetic mutation, malnutrition, disruption of typical developmental pathways by external, abiotic forces (e.g., temperature changes, chemicals, radiation) or parasitism (Wcislo et al. 2004). Given the absence of evidence for malnutrition, parasitism, and the fact that bee larval environments are well-shielded from most abiotic factors, it seems plausible that this aberration is a consequence of mutation. Studies investigating the heritability of deformities are rare outside of model systems like *Drosophila*, but have also been suggested in some studies of ant gyandromorphism and intercastes (Wheeler 1937), as well as deformities of *Tenebrio molitor* L. beetles (Steinhaus and Zeikus 1968). Unfortunately, the rarity of deformed bees makes study of mutation in the group more difficult.

It is initially surprising that this anomalous specimen survived and successfully emerged as an adult. This suggests either that the labrum was functional during its larval stage or that the larva could develop and attain a normal adult body size without its function. If the labrum were also non-functional in the larva, then this suggests that the labrum is not necessary for successful larval development in non-parasitic bees. This may be due to the relatively high effort female bees exert in provisioning their

nests. As females choose and prepare the entire larval food mass, it may be that larval decision-making is of negligible importance, and that if there are contaminants (e.g., fungi) then the larvae are doomed regardless of labral and epipharyngeal functionality. However, as we cannot be certain of the developmental stage in which the deformity arose or the cause of the deformity, our inferences remain limited.

The fact that this specimen is male raises an interesting possibility. If it were female, and the labrum is indeed needed for successful foraging, it is unlikely that such a female would have been able to provision her offspring as well as a normal female could. The energetic costs of foraging and excavation of even a single cell could be too high for a deformed female, because typical members of this subgenus appear to construct a single cell over the course of a day, each in cell its own nest (Torchio and Youssef 1968; Torchio 1971; Orr unpublished nest records). As a result, the mutation would not likely be passed down by a female (if it is indeed genetic). In contrast, a lucky male may mate quite soon after it has emerged. The sex-biased inheritance patterns that this and other abnormalities may exhibit could prove to be an interesting area for future research in bees.

Conclusions

This study describes the novel morphological anomaly of bee labral reduction, while also reviewing the diversity of labral functions across bees overall. The potential implications of this aberration are also discussed, including how labrum reduction might impact feeding ability and whether fitness effects thereof affect life stages and sexes differently. Although many studies have focused on gynandromorphism in bees (Michez et al. 2009, and many others), this is one of relatively few to explore other deformities. Notably, prior papers have focused primarily on visual or antennal deformities, rather than aberrations that could impact feeding ability (Alfonsus 1931 [one central compound eye]; Engel et al. 2014 [extra ocelli]; Gibbs 2010 [ocelli reduction and slight translocation, compound eye enlargement]; Hopwood 2007 [compound eye fusion, "cyclops"]; Knerer and Atwood 1964 [metanotal anomalies]; Rodeck 1943 [one antenna lost]; Sivik 1962 [antennal segment deformation]).

Descriptive studies such as this are fundamental to bettering our knowledge of life on Earth. However, such studies seem to have gradually lost their luster in recent memory (Grimaldi and Engel 2007). It is, nonetheless, vital that we persist in describing the diversity of life and those aberrant variants which we encounter, as these lines of inquiry can uncover fundamental processes, developmental pathways, and mechanistic functions that would otherwise remain obscure. Although new methods will inevitably arise, descriptive studies and the life history information that they reveal will always valuable for both directing future research and putting the results of newer methods in a proper biological context.

Acknowledgements

We thank Douglas Yanega for access to this and other specimens of the Entomology Research Museum at University of California, Riverside. James P. Strange and Houston Judd are thanked for comments on the manuscript. Avery L. Russell, Terry Griswold, Zachary M. Portman, and Harold W. Ikerd are thanked for their input. Databasing of the specimens was supported by National Science Foundation grants DBI-0956388 to John S. Ascher and Jerome G. Rozen, Jr and DBI-0956340 to Douglas Yanega.

References

Alfonsus EC (1931) A One-Eyed Bee (*Apis Mellifica*). Annals of the Entomological Society of America 24(2): 405–408. https://doi.org/10.1093/aesa/24.2.405

Alves-dos-Santos I, Melo GA, Rozen Jr JG (2002) Biology and immature stages of the bee tribe Tetrapediini (Hymenoptera: Apidae). American Museum Novitates, 1–45. https://doi.org/10.1206/0003-0082(2002)377%3C0001:BAISOT%3E2.0.CO;2

Baker JR (1971) Development and sexual dimorphism of larvae of the bee genus *Coelioxys*. Journal of the Kansas Entomological Society, 225–235.

Borowiec L, Salata S (2015) *Pheidole symbiotica* Wasmann, 1909, an enigmatic supposed social parasite, is a nematode-infested form of *Pheidole pallidula* (Nylander, 1849) (Hymenoptera: Formicidae: Myrmicinae). Sociobiology 62: 181–186. https://doi.org/10.13102/sociobiology.v62i2.181-186

Cane JH (1996) Nesting resins obtained from *Larrea* pollen host by an oligolectic bee, *Trachusa larreae* (Cockerell) (Hymenoptera: Megachilidae). Journal of the Kansas Entomological Society 69: 99–102.

Cane JH, Payne JA (1988) Foraging ecology of the bee *Habropoda laboriosa* (Hymenoptera: Anthophoridae), an oligolege of blueberries (Ericaceae: *Vaccinium*) in the southeastern United States. Annals of the Entomological Society of America 81: 419–427. https://doi.org/10.1093/aesa/81.3.419

Carreck NL, Andree M, Brent CS, Cox-Foster D, Dade HA, Ellis JD, Hatjina F, van Englesdorp D (2013) Standard methods for *Apis mellifera* anatomy and dissection. Journal of Apicultural Research 52: 1–40. https://doi.org/10.3896/IBRA.1.52.4.03

Chapman RF (1998) The Insects: Structure and Function. Cambridge University Press, Cambridge, UK, 788 pp.

Chapman RF, de Boer G (Eds) (1995) Regulatory mechanisms in insect feeding. Chapman and Hall, New York, NY, 398 pp.

Cockerell TDA (1897) The New Mexico species of *Anthidium*. The Canadian Entomologist 29: 220–223. https://doi.org/10.4039/Ent29220b-9

Cockerell TDA (1905) The bees of Southern California VII. Bulletin of the Southern California Academy of Sciences 4: 13–15.

Cook AG (1972) The ultrastructure of the A1 sensilla on the posterior surface of the clypeo-labrum of *Locusta migratoria migratorioides* (R and F). Cell and Tissue Research 134: 539–554. https://doi.org/10.1007/BF00307673

de Brito Sanchez MG (2011) Taste perception in honey bees. Chemical Senses 36: 675–692. https://doi.org/10.1093/chemse/bjr040

Dellacasa G, Dellacasa M, Mann DJ (2010) The morphology of the labrum (epipharynx, ikrioma and aboral surface) of adult Aphodiini (Coleoptera: Scarabaeidae: Aphodiinae), and its implications for systematics. Insecta Mundi 0132: 1–21.

Ellis JD, Hepburn HR (2006) An ecological digest of the small hive beetle (*Aethina tumida*), a symbiont in honey bee colonies (*Apis mellifera*). Insectes Sociaux 53: 8–19. https://doi.org/10.1007/s00040-005-0851-8

Engel MS, Hinojosa-Díaz IA, Sagot P, Mérida J, Ayala R (2014) A pentocellar female of *Caenaugochlora inermis* from southern Mexico (Hymenoptera: Halictidae). Journal of the Kansas Entomological Society 87(4): 392–394. https://doi.org/10.2317/JKES130907.1

Erickson Jr E, Carlson SD, Garment MB (1986) A Scanning Electron Microscope Atlas of the Honey Bee. Iowa State University Press, Iowa City, IA, 292 pp.

Fabricius JC (1804) Systema Piezatorum, secundum ordines, genera, species; adjectis synonymis, locis, observationibus, descriptionibus. Reichard, Brunsvigae [Brunswick].

Foster DJ, Cartar RV (2011) What causes wing wear in foraging bumble bees? The Journal of experimental biology 214: 1896–1901. https://doi.org/10.1242/jeb.051730

Frase T, Richter S (2013) The fate of the onychophoran antenna. Development Genes and Evolution 223: 247–251. https://doi.org/10.1007/s00427-013-0436-x

Garófalo CA, Rozen Jr JG (2001) Parasitic behavior of *Exaerete smaragdina* with descriptions of its mature oocyte and larval instars (Hymenoptera: Apidae: Euglossini). American Museum Novitates 3349: 1–28. https://doi.org/10.1206/0003-0082(2001)349%3C0001:PBOESW%3E2.0.CO;2

Gibbs J (2010) An aberrant bee of the species *Lasioglossum* (*Dialictus*) *disparile* (Cresson)(Hymenoptera: Halictidae) with brief taxonomic notes on the species. Journal of the Kansas Entomological Society 83(1): 92–96. https://doi.org/10.2317/JKES0806.16.1

Grimaldi D, Engel MS (2005) Evolution of the Insects. Cambridge University Press, Cambridge, UK, 772 pp.

Grimaldi DA, Engel MS (2007) Why descriptive science still matters. BioScience 57: 646–647. https://doi.org/10.1641/B570802

Grimaldi D, Underwood BA (1986) *Megabraula*, a new genus for two new species of Braulidae (Diptera), and a discussion of braulid evolution. Systematic Entomology 11: 427–438.

Hopwood JL (2007) A "cyclops" of the bee *Lasioglossum* (*Dialictus*) *bruneri* (Hymenoptera: Halictidae). Journal of the Kansas Entomological Society 80(3): 259–261. https://doi.org/10.2317/0022-8567(2007)80[259:ACOTBL]2.0.CO;2

Kemp DJ (2000) Contest behavior in territorial male butterflies: Does size matter? Behavioral Ecology 11: 591–596. https://doi.org/10.1093/beheco/11.6.591

Knerer G, Atwood CE (1964) Metanotal anomalies in sweat bees (Hymenoptera: Halictidae). Proceedings of the Entomological Society of Washington 66(2): 111–112.

Korb J, Hartfelder K (2008) Life history and development- a framework for understanding developmental plasticity in lower termites. Biological Reviews 83: 295–313. https://doi.org/10.1111/j.1469-185X.2008.00044.x

Larabee FJ, Suarez AV (2014) The evolution and functional morphology of trap-jaw ants (Hymenoptera: Formicidae). Myrmecological News 20: 25–36.

Lee J (1998) Cranberry-pollinating bee wears a mustache. Agricultural Research 46: 16–17.

Messer AC (1984) *Chalicodoma pluto*: The world's largest bee rediscovered living communally in termite nests (Hymenoptera: Megachilidae). Journal of the Kansas Entomological Society 57: 165–168.

Michaux FA, Nuttall T (1842) The North American Sylva; Or, A Description of the Forest Trees of the United States, Canada, and Nova Scotia, Considered Particularly with Respect to Their Use in the Arts, and Their Introduction Into Commerce: To which is Added a Description of the Most Useful of the European Trees. (Vol. 3). William Amphlett, New Harmony, Indiana.

Michener CD (1944) Comparative external morphology, phylogeny, and a classification of the bees (Hymenoptera) Bulletin of the American Museum of Natural History 82: 151–326.

Michener CD, Cross EA, Daly HV, Rettenmeyer CW, Wille A (1955) Additional techniques for studying the behavior of wild bees. Insectes Sociaux 2: 237–246. https://doi.org/10.1007/BF02224384

Michener CD (1978) The parasitic groups of Halictidae (Hymenoptera: Apoidea). Los grupos parásitos de Halictidae (Hymenoptera: Apoidea). The University of Kansas Science Bulletin 51: 291–339. https://doi.org/10.5962/bhl.part.24961

Michener CD (2007) The Bees of the World. John Hopkins University Press, Baltimore, MD, 992 pp.

Michez D, Rasmont P, Terzo M, Vereecken NJ (2009) A synthesis of gynandromorphy among wild bees (Hymenoptera: Apoidea), with an annotated description of several new cases. In Annales de la Société Entomologique de France (Vol. 45, No. 3). Taylor & Francis Group, Oxford, UK, 365–375.

Mitchell BK, Itagaki H, Rivet M-P (1999) Peripheral and central structures involved in insect gustation. Microscopy Research and Technique 47: 401–415. https://doi.org/10.1002/(SICI)1097-0029(19991215)47:6<401::AID-JEMT4>3.0.CO;2-

Murao R, Tadauchi O (2005) Description of immature stages of *Colletes esakii* (Hymenoptera, Colletidae). Esakia 45: 55–60.

Norden B, Batra S (1985) Male bees sport black mustaches for picking up parsnip perfume (Hymenoptera: Anthophoridae). Proceedings Entomological Society of Washington 87: 317–322.

O'Donnell DJ (1989) A morphological and taxonomic study of first instar larvae of Aphidiinae (Hymenoptera: Braconidae). Systematic Entomology 14: 197–219. https://doi.org/10.1111/j.1365-3113.1989.tb00277.x

Ortega-Hernández J, Budd GE (2016) The nature of non-appendicular anterior paired projections in Palaeozoic total-group Euarthropoda. Arthropod Structure and Development 45: 185–199. https://doi.org/10.1016/j.asd.2016.01.006

Packer L, Knerer G (1986) An analysis of variation in the nest architecture of *Halictus ligatus* in Ontario. Insectes Sociaux 33: 190–205 https://doi.org/10.1007/BF02224597

Pitts JP, Matthews RW (2000) Description of the larva of *Sphaeropthalma pensylvanica* (Lepeletier) (Hymenoptera: Mutillidae: Sphaeropthalminae). Journal of Entomological Science 35: 334–337.

Posnien N, Bashasab F, Bucher G (2009) The insect upper lip (labrum) is a nonsegmental appendage-like structure. Evolution and Development 11: 480–488. https://doi.org/10.1111/j.1525-142X.2009.00356.x

Rebora M, Gaino E, Piersanti S (2014) The epipharyngeal sensilla of the damselfly *Ischnura elegans* (Odonata, Coenagrionidae). Micron 66: 31–36. https://doi.org/10.1016/j.micron.2014.05.003

Rodeck HG (1943) Antennal anomaly in *Nomada vicina* Cresson (Hym.: Apoidea). Entomological News 54(8): 175.

Rozen JG (2001) A taxonomic key to mature larvae of cleptoparasitic bees (Hymenoptera: Apoidea). American Museum Novitates 3309: 1–28. https://doi.org/10.1206/0003-0082(2001)309%3C0001:ATKTML%3E2.0.CO;2

Rozen Jr JG, Kamel SM (2006) Interspecific variation in immature larvae of the cleptoparasitic bee genus *Coelioxys* (Hymenoptera: Megachilidae). Journal of the Kansas Entomological Society 79: 348–358. https://doi.org/10.2317/0603.28.1

Salt G (1927) The effects of stylopization on aculeate Hymenoptera. Journal of Experimental Zoology 48: 223-331. https://doi.org/10.1002/jez.1400480107

Sandoz J-C, Hammer M, Menzel R (2002) Side-specificity of olfactory learning in the honeybee: US input side. Learning and Memory 9: 337–348. https://doi.org/10.1101/lm.50502

Say T (1838) Descriptions of new species of North American Hymenoptera, and observations on some already described. Boston Journal of Natural History 1: 362–416.

Siemanowski J, Richter T, Bucher G (2015) Notch signaling induces cell proliferation in the labrum in a regulatory network different from the thoracic legs. Developmental Biology 408: 164–177. https://doi.org/10.1016/j.ydbio.2015.09.018

Sivik F (1962) Antennal anomaly of a neotropical bee, *Augochlora pura mosieri* Cockerell, found in Florida (Hymenoptera: Apoidea). Florida Entomologist 45(4): 195. https://doi.org/10.2307/3492402

Smith FW, Angelini DR, Gaudio MS, Jockusch EL (2014) Metamorphic labral axis patterning in the beetle *Tribolium castaneum* requires multiple upstream, but few downstream, genes in the appendage patterning network. Evolution and Development 16: 78–91. https://doi.org/10.1111/ede.12066

Smith FW, Goldstein B (In press) Segmentation in Tardigrada and diversification of segmental patterns in Panarthropoda. Arthropod Structure and Development. https://doi.org/10.1016/j.asd.2016.10.005

Snodgrass RE (1985) Anatomy of the Honey Bee. Comstock Publishing Associates, Cornell University Press, Ithaca, NY.

Snodgrass RE (1993) Principles of Insect Morphology. Cornell University Press, Ithaca, NY, 768 pp.

Steinhaus EA, Zeikus RD (1968) Teratology of the beetle *Tenebrio molitor* I. Gross morphology of certain abnormality types. Journal of Invertebrate Pathology 10: 190–210. https://doi.org/10.1016/0022-2011(68)90077-3

Straka J, Bogusch P (2007) Description of immature stages of cleptoparasitic bees *Epeoloides coecutiens* and *Leiopodus trochantericus* (Hymenoptera: Apidae: Osirini, Protepeolini) with remarks to their unusual biology. Entomologica Fennica 18: 242–254.

Thorp RW (2000) The collection of pollen by bees. In: Dafni A, Hesse M, Pacini E (Eds) Pollen and Pollination. Springer-Verlag, Wien, Austria, 211–223. https://doi.org/10.1007/978-3-7091-6306-1_11

Vilhelmsen L (1996) The preoral cavity of lower Hymenoptera (Insecta): Comparative morphology and phylogenetic significance. Zoologica Scripta 25: 143–170. https://doi.org/10.1111/j.1463-6409.1996.tb00156.x

Walker K (1995) Revision of the Australian native bee subgenus *Lasioglossum* (*Chilalictus*). Part 1 of 2. Memoirs of the Museum of Victoria 55(1): 1–214.

Wcislo WT, Gonzalez VH, Arneson L (2004) A review of deviant phenotypes in bees in relation to brood parasitism, and a gynandromorph of *Megalopta genalis* (Hymenoptera: Halictidae). Journal of Natural History 38: 1443–1457.

Wheeler WM (1937) Mosaics and other anomalies among ants. Harvard University Press, Cambridge, MA, 95 pp. https://doi.org/10.4159/harvard.9780674437081

Whitehead A, Larsen J (1976) Ultrastructure of the contact chemoreceptors of *Apis mellifera* L.(Hymenoptera: Apidae). International Journal of Insect Morphology and Embryology 5: 301–315. https://doi.org/10.1016/0020-7322(76)90030-1

Whitten WM, Young AM, Williams NH (1989) Function of glandular secretions in fragrance collection by male euglossine bees (Apidae: Euglossini). Journal of Chemical Ecology 15: 1285–1295. https://doi.org/10.1007/BF01014830

Zaim A, Petit D, El Ghadraoui L (2013) Dietary diversification and variations in the number of labrum sensilla in grasshoppers: Which came first? Journal of biosciences 38: 339–349. https://doi.org/10.1007/s12038-013-9325-8

JHR 57: 103–114 (2017)
doi: 10.3897/jhr.57.12491
http://jhr.pensoft.net

RESEARCH ARTICLE

JOURNAL OF Hymenoptera RESEARCH
A peer-reviewed open-access journal
The International Society of Hymenopterists

Anthropogenic waste products as preferred nest sites for *Myrmica rubra* (L.) (Hymenoptera, Formicidae)

Michał Michlewicz[1], Piotr Tryjanowski[1]

1 *Department of Zoology, Institute of Zoology, Poznań University of Life Sciences, Wojska Polskiego 71C, 60-625 Poznań, Poland*

Corresponding author: *Michał Michlewicz* (michlewiczmichal@gmail.com)

Academic editor: *Petr Klimeš* | Received 2 March 2017 | Accepted 7 June 2017 | Published 30 June 2017

http://zoobank.org/6A065F2F-A2D0-4B90-9A53-0B4CD5242050

Citation: Michlewicz M, Tryjanowski P (2017) Anthropogenic waste products as preferred nest sites for *Myrmica rubra* (L.) (Hymenoptera, Formicidae). Journal of Hymenoptera Research 57: 103–114. https://doi.org/10.3897/jhr.57.12491

Abstract

Sites containing anthropogenic waste products or dumps are currently treated as refugia by a lot of animal groups, including ants. In this study the population structure of *Myrmica rubra* (L.) ants was compared between habitats containing and lacking anthropogenic waste products. The density of colonies and individual nests, number of queens and of workers both per colony and per nest, and queen size were analyzed. Twenty plots with waste products and 20 control (natural) plots (paired, each 10×10m in size) were established and compared. Results show a significant increase in colony and nest density on the plots with waste compare to the control plots. However, the number of workers, queens and queen size did not differ significantly between plot types. Overall number, as well as proportion of polycalic colonies was higher on plots with waste products. These results suggest that when *M. rubra* has more potential nest site opportunities created by human activity, the density of its colonies increases. Moreover, the anthropogenic waste product are strongly preferred nest sites for this species on the human-disturbed plots, as only them were used as nest loci there in contrast to control plots.

Keywords

ants, colony structure, human pressure, modified habitat, polydomy, rubbish, nesting habit

Copyright *Michail Michlewicz, Piotr Tryjanowski.* This is an open access article distributed under the terms of the Creative Commons Attribution License (CC BY 4.0), which permits unrestricted use, distribution, and reproduction in any medium, provided the original author and source are credited.

Introduction

Human-origin waste dumps are considered to be potential sources of pollution of water, soil and air, and cause the spread of parasites and of invasive animal and plant species (Ružičková et al. 1996). However, for some groups of animals, these waste dumps act as refugia (Oro et al. 2013, Baranová et al. 2015). Among these animals, important inhabitants of such sites include ants (Wiezik 2006).

Ants are ecologically very important insects, which have considerable and varied impacts on ecosystems (Wilson and Hölldobler 2005). They are very widespread, abundant and have a great influence on soil formation (Hölldobler and Wilson 1990, Folgarait 1998, Frouz and Jilková 2008). Ants also have great adaptive capacity when it comes to getting food resources. They are rather opportunistic and general predators and can modify their diet according to available resources (Wilson and Hölldobler 2005) and are also important herbivores (Rico-Gray and Oliveira 2007). Some species become domestic pests (Klotz et al. 2008), while others play an important role in conservation biology of other, threatened species of insects, such as butterflies (Buszko 2004).

Although the structure of ant colonies and their response to potential harmful human activities has received a lot of attention (e.g. Majer 1983, Krzysztofiak 1991, Pętal 1994, Holec and Frouz 2005), there is no study which would test for the effects of anthropogenic waste products as potential suitable nest sites on native ant populations to our best knowledge.

Apart from the size of colonies, the ants can react to the environmental factors such as temperature (Bishop et al. 2016) or latitude (connected with temperature) (Heinze et al. 2003) also by changing their morphology, including their body size. Taking this into account, it is good to investigate whether different density and colony structure may affect ant size.

The aim of the current study was to (a) compare the density of competing colonies, as well as individual nest density of *Myrmica rubra* (L.), a locally common ant species in Central Europe, between places containing and lacking anthropogenic waste products, (b) test if population structure (size of colonies, number of workers and of queens per colony and per nest) is different between these two habitats and (c) compare the size of queens from the two habitats in order to detect any tendencies in gyne size related to potential different densities.

This was based on hypotheses that 1) the density of colonies on plots containing anthropogenic waste products is higher, as those product can be used as nest sites and 2) the structure of colonies in both habitats is different (e.g. number of queens or workers, and the body size of queens, per colony and per nest is lower on control plots).

Materials and methods

Study species

Myrmica rubra is the most ecologically tolerant of all European *Myrmica* Latr. (Czechowski et al. 2012). It is found in a variety of habitats, as long as they are at

least partially humid. The species is also commonly found in anthropogenic habitats (Czechowski et al. 2012, Radchenko et al. 2004, Radchenko and Elmes 2010), where it sometimes uses anthropogenic waste products as nest sites (M. Michlewicz, personal observation). *Myrmica rubra* forms colonies which are generally polygynous, sometimes polycalic and consist of up to 10,0000 workers (Czechowski et al. 2012). Klotz et al. (2008) even reported colonies consisting of 20,000 workers and 600 queens. The number of nests in polycalic colonies of *M. rubra* can be large and are then called "super-colonies" (Radchenko and Elmes 2010). Because of this, aggression tests, following Roulston et al. (2003), were carried out to check how many distinct colonies were present, including possible multi-nest colonies.

Study sites

This study was undertaken in NW Poland in 2014 and 2015. Locations where study plots were established were divided into two categories: 1) "control" (20 plots) and 2) containing anthropogenic waste products (20 plots). Each plot was, according to the methods reviewed in Pętal and Pisarski (1966), 10×10m in size. Each locality has one pair of the plots – one control and one plot with waste products, at least 50 metres apart (with a maximum of 57 metres). "Experimental" plots were those considered suitable for *M. rubra* and which contained anthropogenic waste products on the ground (rubbish, empty bottles, cans, tires, clothing, rubble etc.) covering about 1/5 of the plot area (i.e. 20 m^2). Natural plots were generally similarincluding vegetation and soil structure, but lacked any anthropogenic waste products. All plots were humid grassland with whole area sparsely, but evenly covered with not very high bushes (up to ca. 3 metres) of several plant species: *Salix* sp., *Pinus sylvestris* L., *Sambucus nigra* L., *Prunus serotina* (Ehrh.). Herbaceous vegetation consist mostly of grasses [mainly *Poa* cf. *trivialis* L. and *Elymus repens* (L.)], with some herbs present, like *Perasites hybridus* (L.), *Urtica dioica* L., *Chelidonium majus* L. and others. Each plot with waste products was previously known to the first author, with a record of that rubbish has been laying there for at least three years before this study took place. Localizations, coordinates, altitude, date of examination as well as general habitat description of each of 20 localities is available in the Suppl. material 1.

Sampling techniques

Search was made for all nests of *M. rubra* at each site by the same methods, and in a similar time for each pair of the plots, to avoid seasonal differences. This species is relatively easy to identify in the field by an experienced person using a hand lens. In the field a hand lens with 10× magnification was used. Identification was subsequently confirmed in the laboratory using a stereomicroscope. Each nest was marked with small flag on which was written a unique number. Aggression tests were then carried out and actual colonies were re-marked with numbers if necessary. Aggression tests were carried

out in the field, using plastic Petri dishes (90 mm in diameter), cleaned with alcohol after each test. The arenas containing different colonies were marked with different colors. The assays include 1-1 and 5-5 battles of live worker specimens. Ants presenting aggressive behavior (biting and/or stinging) were marked as members of different colonies. Each time control test, with members of the same colony, was also carried out, but no aggressive behavior were observed in these. Whole number of workers from assays were taken in account when number of workers per colony was estimated. Every colony/nest was then excavated using a shovel and put on a white sheet (ca. 150×150 cm), then every ant from the nest was collected using an aspirator and put in a vial (or vials) containing 75% ethanol. In the laboratory the ants were counted and queens measured.

Measurements

Queen measurements were taken using Zeiss AxioCam MRc 60 N-C 2/3" 0.63× camera fitted with Zeiss SteREO Lumar.V12 stereomicroscope and AxioVision rel. 4.8 software. Measurements were taken on the base of photographs using the given software. Mesosoma length (ML) was measured as a surrogate of body size, as it is strongly correlated with queen size (Steiner et al. 2006). General aim of taking measurements was to detect any tendencies in queen size, potentially related to the different nest densities. Sixty queens from control and 60 from plots with waste products were measured, selected randomly from the whole number of queens collected from all nests.

Statistical analysis

The results were analyzed using PASW® Statistics 18 and RStudio version 3.2.3 software (R Core Team 2015). First, Shapiro-Wilk normality test was used to check normality of distributions of the variables, and because some of them have non-normal distribution a non-parametric Wilcoxon signed-rank test (comparing the effects among the paired plots) and Mann-Whitney U-test (comparing the queen size) were used. Chi-square test was used to compare proportion of polycalic colonies among the two plot kinds.

Results

Colony and nests densities

Total number of 166 colonies (47 on control and 119 on experimental plots) consisting of a total number of 196 nests (53 on control and 143 on experimental plots) was found. Statistical analysis using a Wilcoxon signed-rank test found a significant differences between both the number of colonies (Fig. 1A; $W = 16$, $P < 0.00001$) and nests (Fig. 1B; $W = 13.5$, $P < 0.00001$) between control and plots with waste products.

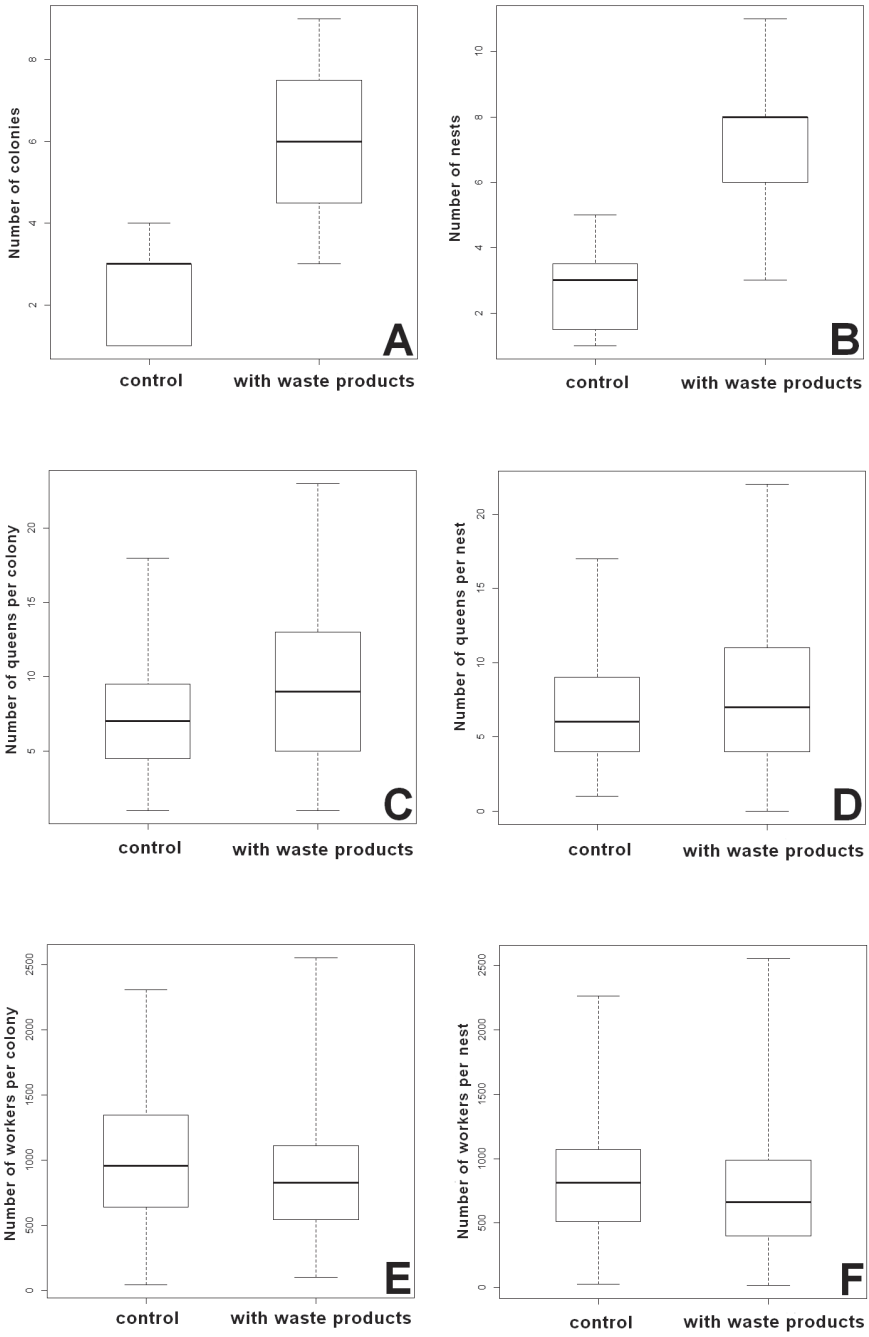

Figure 1. Variation of measured nest parameters between control plots and plots with waste products in *Myrmica rubra*. **A** colony density (P < 0.0001) **B** nest density (P < 0.0001) **C** number of queens per colony (P = 0.06) **D** number of queens per nest (P = 0.26) **E** number of workers per colony (P=0.32) **F** number of workers per nest (P = 0.06). Numbers are given as median per plot (per 100 m^2), whiskers of the boxplot represent the range of minimum and maximum values.

Overall, 26 polycalic colonies was found (5 on control and 21 on experimental plots), and chi-square test found significant difference in proportion of polycalic colonies among the two plot kinds (χ^2 = 4.6493, P = 0.03). Minimum number of nests in those colonies was two, while the maximum was four (one time, on plot with waste products). The mean number of colonies per plot (100 m^2) on control areas was 2.35±0.23 (and the mean number of nests 2.65±0.29) and on plots with waste products 5.95±0.4 for colonies and 7.25±0.44 for nests.

Colony structure and size

Number of queens

In total, 1479 queens were sampled (359 from control and 1120 from plots with waste products). No "microgyne" forms were found in any nest (i.e. recognized by eye). The difference between number of queens on control and "experimental" plots both per colony (Fig. 1C) and per nest (Fig. 1D) was statistically insignificant (W = 2269.5, P = 0.06 and W = 3438.5, P = 0.26, respectively), although there was a tendency of a higher queen numbers recorded in the plots with waste products. Mean queen number per colony was 7.6±0.6 (control) and 9.4±0.47 (plot with waste products), and per nest was 6.8±0.53 (control) and 7.7±0.39 (plot with waste products).

Number of workers

The difference between number of workers both per colony (Fig. 1E) and nest (Fig. 1F) on both plot types was statistically insignificant (W = 3076, P = 0.32 and W = 2269.5, P = 0.06), although the numbers were higher on average in the control plots this time. Mean number of workers per colony on control plots with waste products was 1024.3±85.27 and 937.5±51.35, respectively. Values for nest were 908.3±76.67 (control) and 769.1±44.82 (plots with waste products).

Queen measurements

The difference in size (based on mesosoma lenght) between queens from control (n = 60) and experimental (n = 60) plots was not statistically significant (Mann-Whitney U-test, Z = – 0.19, P = 0.8493) (Fig. 2). Mean size of ML of measured queens was 2.02±0.01 mm on control and 2.05±0.01 mm on plots with waste products.

Nest sites

Interestingly, on plots with waste products only these microhabitats were used as nest sites by ants. These include: empty bottles (both plastic and glass) and cans, jars, tires, clothing, bricks with holes, old carpets, plastic carrier bags, other pieces of metal or plastic, often partially covered with wet soil. On control plots *M. rubra* nests were always found in clumps of grass and/or under rocks or pieces of wood, but those microhabitats were not occupied by the species in plots with the waste.

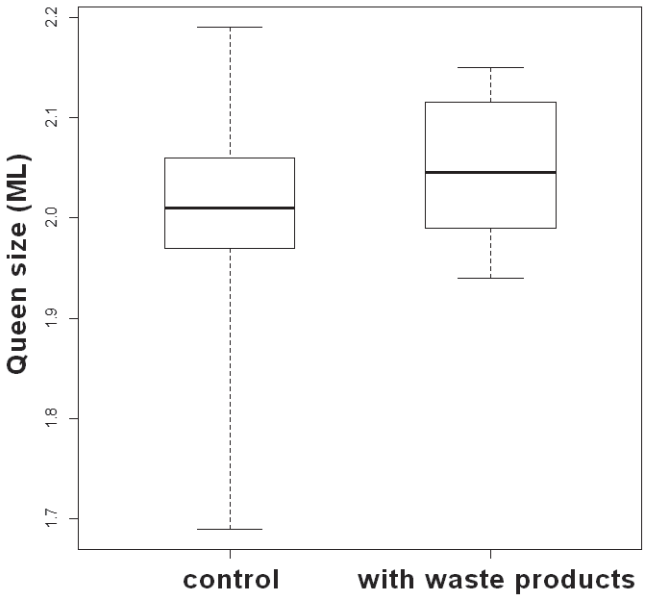

Figure 2. Variation in median queen size (mesosoma length in mm) between control plots and plots with waste products in *Myrmica rubra*. Difference is statistically insignificant. Whiskers of the boxplot represents the range of minimum and maximum values.

Discussion

Previous studies show that in suitable humid grassland ecosystems the density of *M. rubra* nests is limited more by the number of appropriate nest sites than by the availability of food resources. When one nest site is, for some reason, abandoned by one colony, it is quickly recolonized by another of (in most cases) the same *Myrmica* species (Radchenko and Elmes 2010).

Concerning densities of *M. rubra*, only grassland habitats with no substantial volume of waste products have been studied before (e.g. Parapura and Pisarski 1971, Pętal 1980, Seppä and Walin 1996, Radchenko and Elmes 2010 and references therein, Huszár et al. 2014). Our effort is, to our knowledge, hence the first comparing nest and colonies densities, as well as workers and queens numbers (and size of the latter), on plots with and without anthropogenic waste product in order to investigate, whether those pieces of rubbish may be used by ants as nest sites and affect their populations. We showed, that anthropogenic waste products (listed in Results) can act as preferred nest loci. On plots with high level of anthropogenic waste products, only those are used as nest sites. However, increase of food resources (especially a higher quantity of small invertebrates there) may also probably affect the establishment and survival of the ant colonies in habitats with anthropogenic waste products (M. Michlewicz, personal observation), although we did not measure these parameters in our

plots. Among studied variables, only number of colonies and number of nests on both plot types showed significant differences. Previous studies, also conducted in Poland (Czechowski et al. 2012 and references therein) showed, that densities of *M. rubra* nests vary greatly depending on habitat type. Therefore, it is crucial to properly choose both "experimental" and control plot within the same habitat and time to control, also for microenvironmental and seasonal characteristics, as done in this study.

To our knowledge, highest density of *M. rubra* in Poland was reported in the Carpathian alder forest in Pieniny National Park and equals 100 nests per 100 m^2 (Czechowska 1976). Some other studies also report rather high densities, e.g. 26.0 (Parapura and Pisarski 1971), 20.5 ± 19.3 (Babik et al. 2009) and 20.0 (Czechowski 1985). Although, some studies did not show such high densities, e.g. 1.0±0.31 (mean±SD) (Rzeszowski et al. 2013), 6.0 (Czechowski et al. 1990), 0.05, 3.0 and 14.0 (Pętal 1980) (all given in number of nests per 100 m^2). Despite the fact that our results from plots with waste products (mean 7.25±0.44 nests/100 m^2) are not as high as some literature data, this density significantly varies from results from control plots (mean 2.65±0.29 nests/100 m^2). Notably, the "control-experimental" plot pairs were chosen in the very similar habitats (see Suppl. material 1), but only waste products were used as nest sites in the latter plots. This is a strong evidence that the increased nest and colony densities observed here were caused by the human-deposited waste, and that *M. rubra* ants prefer these waste products as nest sites, whenever available.

As some studies document, number of queens both per colony and per nest, as well as number of workers can also widely differ in *Myrmica* ants. Seppä and Walin (1996) report colonies consisting of mean number of 7.56 queens and 961–828 workers. Elmes (1980) reports mean number of 15.89 queens per colony and Elmes and Pętal (1990) write about overall number of workers per colony between 1,000 and 2,000. Our results on both worker and queen numbers fit those ranges. However, differences in those numbers between both plot types were insignificant. This might indicate, that living in higher densities makes *M. rubra* ants more tolerant to other colonies of the same species, but those colonies does not have to be necessary smaller (both in respect the number of workers and queens). This is in agreement with our observation of also more polycalic colonies to be established on the plots with waste products, as those colonies act behaviorally and ecologically as a single nest.

Differences in queen size between the two plot types were not statistically significant. Similar results were found by Huszár et al. (2014). This shows that living at higher density probably does not necessarily lead to changes in gyne morphology. Moreover, no "microgyne" form queens were found during the study process. However, although the queen size did not differ, there was slight tendency (insignificant) to a higher number of queens but lower number of workers per nest in the plots containing waste, which is in agreement with strategy of the ants to invest more to sexuals and to establishment of the new nest satellites, where enough "empty" nest sites is available (Oster and Wilson 1978, Poitrineau et al. 2009).

Some research showed, that where *M. rubra* forms polycalic nest systems, the number of other species of ants is significantly lower (Seppä and Pamilo 1995, Seppä and

Walin 1996, Huszár et al. 2014). Future studies are needed to test if similar results will be found on habitats where *M. rubra* live in higher density because of presence of anthropogenic waste products and consider also the effects of its population increase on the other ant species. Such further insight is needed given the ongoing damage of the natural environments by humans, which can influence, however, positively some insect populations, as demonstrated here for the case of *M. rubra* and waste products.

Acknowledgements

PT was supported by the NCN grant N N304 294240. Queen measurements were made at the Division of Apidology, Institute of Zoology, Poznań University of Life Sciences with the kind help of Dr Aleksandra Łangowska. Our sincere thanks go to Professor Tim Sparks from Coventry University, England, for language check and other comments. We also thank to the reviewers Dr Pavel Pech (Department of Biology, University of Hradec Králové, Czech Republic), Professor Wojciech Czechowski (Museum and Institute of Zoology, Polish Academy of Sciences, Poland), and to editor Dr Petr Klimeš (Institute of Entomology, Biology Centre of the Czech Academy of Sciences, Czech Republic) for valuable and critical comments on the previous version of the manuscript.

References

Babik H, Czechowski W, Włodarczyk T, Sterzyńska M (2009) How does a strip of clearing affect the forest community of ants (Hymenoptera: Formicidae)? Fragmenta Faunistica 52: 125–141. https://doi.org/10.3161/00159301FF2009.52.2.125

Baranová B, Manko P, Jászay T (2015) Waste dumps as local biodiversity hotspots for soil macrofauna and ground beetles (Coleoptera: Carabidae) in the agricultural landscape. Ecological Engineering 81: 1–13. https://doi.org/10.1016/j.ecoleng.2015.04.023

Bishop TR, Robertson MP, Gibb H, van Rensburg BJ, Braschler B, Chown SL, Foord SH, Munyai TC, Okey I, Tshivhandekano PG, Werenkraut V, Parr CL (2016) Ant assemblages have darker and larger members in cold environments. Globe Ecology and Biogeography 25: 1489–1499. https://doi.org/10.1111/geb.12516

Buszko J (2004) *Maculinea arion* (Linnaeus, 1758), *Maculinea teleius* (Bergsträsser, 1779), *Maculinea nausithous* (Bergsträsser, 1779), *Maculinea alcon* (Denis et Schiffermüller, 1775). In: Głowacki Z, Nowacki J (Eds) Polish Red Data Book of Animals – Invertebrates. Instytut Ochrony Przyrody PAN, Akademia Rolnicza w Poznaniu, Kraków – Poznań, 248–252.

Czechowska W (1976) Myrmekofauna Pienińskiego Parku Narodowego (Hymenoptera, Formicoidea). Fragmenta Faunistica 21: 115–144. https://doi.org/10.3161/00159301FF1976.21.5.115

Czechowski W (1985) Competition between *Myrmica laevinodis* Nyl. and *Lasius niger* (L.) (Hymenoptera, Formicoidea). Annales Zoologici 39: 153–173

Czechowski W, Pisarski B, Czechowska W (1990) Ants (Hymenoptera, Formicoidea) of moist meadows on the Mazovian Lowland. Fragmenta Faunistica 34: 47–60. https://doi.org/10.3161/00159301FF1990.34.4.047

Czechowski W, Radchenko A, Czechowska W, Vepsäläinen K (2012) The ants of Poland with reference to the myrmecofauna of Europe – Fauna Poloniae 4. Natura Optima Dux Foundation, Warszawa, 496 pp.

Elmes GW (1980) Queen numbers in colonies of ants of the genus *Myrmica*. Insectes Sociaux 27: 43–60. https://doi.org/10.1007/BF02224520

Elmes GW, Pętal J (1990) Queen number as an adaptable trait: evidence from wild populations of two red ant species (genus *Myrmica*). Journal of Animal Ecology 59: 675–690. https://doi.org/10.2307/4888

Folgarait PJ (1998) Ant biodiversity and its relationship to ecosystem functioning: a review. Biodiversity and Conservation 7: 1221–1244. https://doi.org/10.1023/A:1008891901953

Frouz J, Jilková V (2008) The effect of ants on soil properties and processes (Hymenoptera: Formicidae). Myrmecological News 11: 191–199.

Heinze J, Foitzik S, Fischer B, Wanke T, Kipyatkov VE (2003) The significance of latitudinal variation in body size in a Holarctic ant, *Leptothorax acervorum*. Ecography 26: 349–355. https://doi.org/10.1034/j.1600-0587.2003.03478.x

Holec M, Frouz J (2005) Ant (Hymenoptera: Formicidae) communities in reclaimed and unreclaimed brown coal mining spoil dumps in the Czech Republic. Pedobiologia 49: 345–357. https://doi.org/10.1016/j.pedobi.2005.03.001

Hölldobler B, Wilson EO (1990) The Ants. Harvard University Press, Cambridge, 732 pp. https://doi.org/10.1007/978-3-662-10306-7

Huszár DB, Larsen RS, Carlsen S, Boomsma JJ, Pedersen JS (2014) Convergent development of ecological, genetic, and morphological traits in native supercolonies of the red ant *Myrmica rubra*. Behavioral Ecology and Sociobiology 68: 1859–1870. https://doi.org/10.1007/s00265-014-1795-7

Klotz J, Hansen L, Pospischil R, Rust M (2008) Urban Ants of North America and Europe. Identification, biology and management. Cornell University Press, Cornell, 196 pp.

Krzysztofiak L (1991) The effect of habitat pollution with heavy metals on ant populations and ant-hill soil. Ekologia Polska 39: 181–202.

Majer JD (1983) Ants: bio-indicators of minesite rehabilitation, land-use, and land conservation. Environmental management 7: 375–383. https://doi.org/10.1007/BF01866920

Oro D, Genovart M, Tavecchia G, Fowler MS, Martínez-Abraín A (2013) Ecological and evolutionary implications of food subsidies from humans. Ecology Letters 16(12): 1501–1514. https://doi.org/10.1111/ele.12187

Oster GF, Wilson EO (1978) Caste and ecology in the social insects. Princeton University Press, Princeton, 352 pp.

Parapura E, Pisarski B (1971) Mrówki (Hymenoptera, Formicidae) Bieszczadów. Fragmenta Faunistica 17: 319–356. https://doi.org/10.3161/00159301FF1971.17.13.319

Pętal J (1980) Ant populations, their regulation and effect on soil in meadows. Ekologia Polska 28: 297–326.

Pętal J (1994) Reaction of ant communities to degradation of forest habitats in the Karkonosze Mountains. Memorabilia Zoologica 48: 171–179.

Pętal J, Pisarski B (1966) Metody ilościowe stosowane w badaniach myrmekologicznych. Ekologia Polska B 12: 363–376.

Poitrineau K, Mitesser O, Poethke HJ (2009) Workers, sexuals, or both? Optimal allocation of resources to reproduction and growth in annual insect colonies. Insectes Sociaux 56: 119–129. https://doi.org/10.1007/s00040-009-0004-6

R Core Team (2015) R: A language and environment for statistical computing. R Foundation for Statistical Computing, Vienna, Austria. https://www.R-project.org/

Radchenko A, Czechowska W, Czechowski W (2004) Błonkówki – Hymenoptera. Mrówkowate – Formicidae. Klucze do Oznaczania Owadów Polski, XXIV, Toruń, 138 pp.

Radchenko A, Elmes GW (2010) *Myrmica* ants (Hymenoptera: Formicidae) of the Old World – Fauna Mundi 3. Natura Optima Dux Foundation, Warszawa, 789 pp.

Rico-Gray V, Oliveira PS (2007) The ecology and evolution of ant-plant interactions. University of Chicago Press, 320 pp. https://doi.org/10.7208/chicago/9780226713540.001.0001

Roulston TH, Buczkowski G, Silverma J (2003) Nestmate discrimination in ants: effect of bioassay on aggressive behavior. Insectes Sociaux 50: 151–15. https://doi.org/10.1007/s00040-003-0624-1

Ružičková H, Halada L, Jedlička L, Kalivodová E (1996) Biotopes of Slovakia. Guide-book for Mapping and the Biotopes Catalogue. Institute of Landscape Ecology, Slovak Academy of Sciences, Stimul, Bratislava, 92 pp.

Rzeszowski K, Babik H, Czechowski W, Markó B (2013) Ants (Hymenoptera: Formicidae) of Chełmowa Góra in the Świętokrzyski National Park. Fragmenta Faunistica 56: 1–15. https://doi.org/10.3161/00159301FF2013.56.1.001

Seppä P, Pamilo P (1995) Gene flow and population viscosity in *Myrmica* ants. Heredity 74: 200–209. https://doi.org/10.1038/hdy.1995.28

Seppä P, Walin L (1996) Sociogenetic organization of the red ant *Myrmica rubra*. Behavioral Ecology and Sociobiology 38: 207–217. https://doi.org/10.1007/s002650050234

Steiner FM, Schlick-Steiner BC, Konrad H, Moder K, Christian E, Seifert B, Crozier RH, Stauffer C, Buschinger A (2006) No sympatric speciation here: multiple data sources show that the ant *Myrmica microrubra* is not a separate species but an alternate reproductive morph of *Myrmica rubra*. Journal of Evolutionary Biology 19: 777–787. https://doi.org/10.1111/j.1420-9101.2005.01053.x

Wiezik M (2006) Historical municipal waste dump in Banská Štiavnica as ants refugia in urban environment. Wastes-Bio-Degradable, Energetic and Material Utilization. Conference Text-book, Brno. [in Slovak]

Wilson EO, Hölldobler B (2005) The rise of the ants: A phylogenetic and ecological explanation. Proceedings of the National Academy of Sciences of the United States of America 102: 7411–7414. https://doi.org/10.1073/pnas.0502264102

Supplementary material 1

Study sites

Authors: Michał Michlewicz, Piotr Tryjanowski

Data type: species data

Explanation note: General description of study localities, including the dates of investigation.

Copyright notice: This dataset is made available under the Open Database License (http://opendatacommons.org/licenses/odbl/1.0/). The Open Database License (ODbL) is a license agreement intended to allow users to freely share, modify, and use this Dataset while maintaining this same freedom for others, provided that the original source and author(s) are credited.

Link: https://doi.org/10.3897/jhr.57.12491.suppl1

JHR 57: 115–121 (2017)
doi: 10.3897/jhr.57.12462
http://jhr.pensoft.net

RESEARCH ARTICLE

JOURNAL OF Hymenoptera RESEARCH
A peer-reviewed open-access journal
The International Society of Hymenopterists

Description of *Aphelopus fuscoflavus*, a new species of Dryinidae from Thailand (Hymenoptera, Chrysidoidea)

Adalgisa Guglielmino[1], Massimo Olmi[2], Alessandro Marletta[3], Zai-fu Xu[4]

1 *Department of Agriculture and Forestry Sciences (DAFNE), University of Tuscia, Viterbo, Italy* **2** *Tropical Entomology Research Center, Viterbo, Italy* **3** *Department of Biological, Geological and Environmental Sciences, Animal Biology section, University of Catania, Catania, Italy* **4** *Department of Entomology, College of Agriculture, South China Agricultural University, Guangzhou, P.R. China*

Corresponding author: *Zai-fu Xu* (xuzaifu@scau.edu.cn)

Academic editor: *Michael Ohl* | Received 28 February 2017 | Accepted 7 April 2017 | Published 30 June 2017

http://zoobank.org/7F135A17-F735-4A56-9721-99135D774EF5

Citation: Guglielmino A, Olmi M, Marletta A, Xu Z-f (2017) Description of *Aphelopus fuscoflavus*, a new species of Dryinidae from Thailand (Hymenoptera, Chrysidoidea). Journal of Hymenoptera Research 57: 115–121. https://doi.org/10.3897/jhr.57.12462

Abstract

A new species of *Aphelopus* Dalman is described from Thailand, Sakon Nakhon: *A. fuscoflavus* **sp. n.** Morphologically the new species is similar to *A. zonalis* Xu, Olmi & He, 2013, known from China, Hainan, but it is clearly different in having the basivolsella fused with the paramere, while the basivolsella is not fused with the paramere in *A. zonalis*. Published identification keys to the Oriental species of *Aphelopus* are modified to include the new species.

Keywords

Aphelopinae, *Aphelopus*, new species, Oriental region, key, Thailand

Introduction

Dryinidae (Hymenoptera, Chrysidoidea) are parasitoids of leafhoppers, planthoppers and treehoppers (Hemiptera, Auchenorrhyncha) (Guglielmino and Virla 1998; Guglielmino and Bückle 2003, 2010; Guglielmino et al. 2006, 2013, 2015). *Aphelopus* Dalman, 1823 is a genus that is present in all zoogeographical regions (Olmi 1984; Xu et al. 2013; Olmi and Virla 2014; Olmi and Xu 2015). In total 78 species have been described from all continents (Olmi and Xu 2015) and the genus was revised at

Copyright *Adalgisa Guglielmino et al.* This is an open access article distributed under the terms of the Creative Commons Attribution License (CC BY 4.0), which permits unrestricted use, distribution, and reproduction in any medium, provided the original author and source are credited.

world level by Olmi (1984, 1991) and in the Oriental, Neotropical and Eastern Palaearctic regions by Xu et al. (2013), Olmi and Virla (2014) and Olmi and Xu (2015), respectively. The species of *Aphelopus* inhabiting the Oriental region have been recently studied by Xu et al. (2013); they listed 31 species in total.

Aphelopus species are parasitoids of leafhoppers belonging to Typhlocybinae (Cicadellidae) (Guglielmino et al. 2013). Contrarily to almost all dryinids, females of *Aphelopus* do not have chelae and do not feed on their hosts; they grasp the body of their hosts between the two fore legs, with or without the help of their mandibles (Olmi 1984, 1994).

In 2016 we examined additional specimens of *Aphelopus* from Thailand and discovered a new species described in this paper.

Materials and methods

The descriptions follow the terminology used by Olmi (1984) and Xu et al. (2013). The measurements reported are relative, except for the total length (head to abdominal tip, without the antennae), which is expressed in millimetres. The following abbreviations are used in the descriptions: POL is the distance between the inner edges of the two lateral ocelli; OL is the distance between the inner edges of a lateral ocellus and the median ocellus; OOL is the distance from the outer edge of a lateral ocellus to the compound eye; OPL is the distance from the posterior edge of a lateral ocellus to the occipital carina; TL is the distance from the posterior edge of an eye to the occipital carina.

The term "metapectal-propodeal complex" is here used in the sense of Kawada et al. (2015). It corresponds to the term "propodeum" *sensu* Olmi (1984, 1994), Olmi and Virla (2014), Olmi and Xu (2015) and Xu et al. (2013). The term "ADO's" is here used in the sense of Riolo et al. (2016). It corresponds to the term "rhinaria" *sensu* Olmi (1984, 1994), Olmi and Virla (2014), Olmi and Xu (2015) and Xu et al. (2013).

The types of all Oriental species of *Aphelopus* have been previously examined by the authors.

The type specimen described in this paper is deposited in the collection of the Queen Sirikit Botanic Garden, Chiang Mai, Thailand (QSBG).

Results

Genus *Aphelopus* Dalman, 1823

Aphelopus Dalman, 1823: 8. Type species: *Dryinus atratus* Dalman, 1823, by subsequent designation of Westwood (1839).

Diagnosis. Female: Fully winged; epistomal suture not touching antennal toruli; occipital carina complete; antenna without ADO's; palpal formula 5/2; forewing with cos-

tal cell enclosed by pigmented veins, with pterostigma; stigmal vein long and regularly curved; course of forewing veins not marked by dark stripes; hind wing hyaline, with costal cell, without dark medial longitudinal stripe; protarsus not chelate; tibial spurs 1/1/2. Male: fully winged; epistomal suture not touching antennal toruli; occipital carina complete; palpal formula 5/2; forewing with costal cell enclosed by pigmented veins, with pterostigma; stigmal vein long and regularly curved; course of forewing veins not marked by dark stripes; hind wing hyaline, with costal cell, without dark medial longitudinal stripe; basivolsella situated completely below distivolsella apex; tibial spurs 1/1/2.

***Aphelopus fuscoflavus* sp. n.**
http://zoobank.org/FF150F3A-F60D-4702-B992-08DE179813E9
Figs 1–3

Diagnosis. Male with antenna filiform; head testaceous, except large brown spot on vertex; mesosoma testaceous, except area of scutum between notauli darkened, scutellum and metanotum brown, metapectal-propodeal complex black; notauli complete, posteriorly separated; basivolsella with one subdistal bristle, fused with paramere.

Description. *Male*. Fully winged (Fig. 1). Length 1.7 mm. Head testaceous, except large brown spot on vertex. Antenna yellow, except segments 4–10 darkened. Mesosoma testaceous, except area of scutum between notauli darkened, scutellum and metanotum brown, metapectal-propodeal complex black. Metasoma brown. Legs yellow. Antenna filiform. Antennal segments in following proportions: 3:3:4:4:5:6:6:6:6:9. Head dull, granulated. Frontal line incomplete, present in anterior half of face. Occipital carina complete. POL = 7; OL = 3; OOL = 2; OPL = 2.5; TL = 2; greatest breadth of posterior ocelli shorter than OL (2:3). Scutum, scutellum and metanotum dull, granulated. Notauli complete, posteriorly separated; minimum distance between notauli longer than greatest breadth of posterior ocelli (3:2). Metapectal-propodeal complex with dorsal surface (i.e. metapostnotum) dull, reticulate rugose; posterior surface (i.e. first abdominal tergum) reticulate rugose, with median area shiny, unsculptured. Forewing hyaline, without dark transverse bands. Basivolsella (Fig. 2) fused with paramere and with one subdistal bristle. Tibial spurs 1/1/2.

Female. Unknown.

Material examined. Holotype: male, Thailand, Sakon Nakhon Province, Phu Phan National Park, Nam Hom Waterfall, Sao Hi, 17°07.340'N 104°20.788'E, 344 m, 25–31.III.2007,Malaise trap, T2377, Sailom Tonqboonchai leg. (QSBG).

Hosts. Unknown.

Etymology. The name *fuscoflavus* derives from the Latin adjectives "*fuscus*" (dark) and "*flavus*" (yellow), because of the partly testaceous and partly brown colour.

Remarks. Because of the head testaceous, except large brown spot on vertex, the mesosoma partly testaceous and partly brown, the complete notauli, the basivolsella with one subdistal bristle, the new species is similar to *Aphelopus zonalis* Xu, Olmi & He, 2013, described from China, Hainan. The main difference between *A. fuscoflavus*

Figure 1. *Aphelopus fuscoflavus* sp. n.: male holotype in dorsal view. Length 1.7 mm.

and *A. zonalis* is centered on the structure of the basivolsella; fused with the paramere (Fig. 2) in *A. fuscoflavus*, not fused in *A. zonalis* (Fig. 3). In the key to the males of the Oriental *Aphelopus* species published by Xu et al. (2013), the new species can be included by replacing couplets 1–4 as follows:

1 Mesosoma and metasoma totally testaceous, except petiole black..... .....***A. borneanus*** **Olmi**
– Mesosoma and metasoma partly or totally black or brown.....**2**
2 Head testaceous, at most with ocellar region, or vertex, or part of face darkened **3**
– Head mostly or totally black or brown.....**8**
3 Notauli absent .....***A. maculiceps*** **Bergman**
– Notauli distinct **4**
4 Basivolsella with one subdistal bristle (Figs 2, 3) .....**4'**
– Basivolsella with two subdistal bristles **5**
5 Basivolsella not fused with paramere (Fig. 3) ..... ***A. zonalis*** **Xu, Olmi & He**
– Basivolsella fused with paramere (Fig. 2).....***A. fuscoflavus*** **sp. n.**

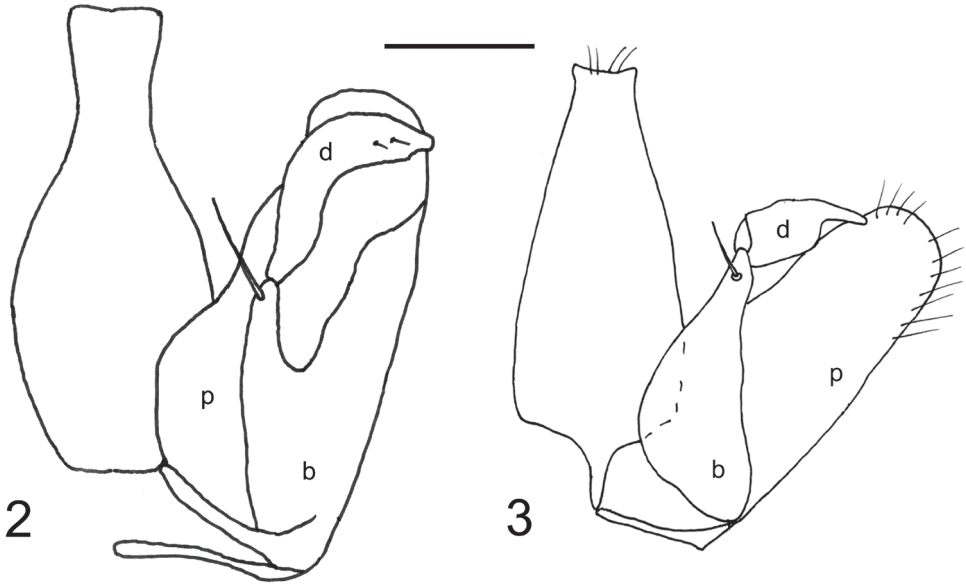

Figures 2–3. Male genitalia, holotypes, left half removed. **2** *Aphelopus fuscoflavus* sp. n. **3** *A. zonalis* Xu, Olmi & He, 2013 (from Xu et al. 2013) (**b** = basivolsella; **d** = distivolsella; **p** = paramere). Scale bars = 0.09 mm (**2**), 0.10 mm (**3**).

Conclusion

Xu et al. (2013) recorded 71 species of Dryinidae from Thailand. Subsequently, Olmi et al. (2015) added an additional species: *Anteon huettingeri* Olmi, Xu & Guglielmino, 2015. Dryinidae of Thailand belong to the following genera: *Aphelopus* Dalman, 1823 (seven species), *Crovettia* Olmi, 1984 (one species), *Anteon* Jurine, 1807 (27 species), *Deinodryinus* Perkins, 1907 (two species), *Bocchus* Ashmead, 1893 (three species), *Thaumatodryinus* Perkins, 1905 (two species), *Dryinus* Latreille, 1804 (13 species), *Pseudodryinus* Olmi, 1991 (one species), *Neodryinus* Perkins, 1905 (five species), *Echthrodelphax* Perkins, 1903 (three species), *Haplogonatopus* Perkins, 1905 (one species) and *Gonatopus* Ljungh, 1810 (seven species). With the description of the above new species the number of species now known from Thailand is 73.

In comparison with the 193 species recorded in China by He and Xu (2002) and the 62 and 40 listed respectively in India and Laos (Xu et al. 2013), the dryinid fauna of Thailand is poorly known. Some genera such as *Gonatopus* (with only seven species listed) are clearly understudied.

However, the dryinids of Thailand will be better understood in the future. In fact, during the three year period 2006–2009, an intensive survey of the terrestrial arthropod fauna of Thailand was conducted by the Queen Sirikit Botanic Garden, The Thai Forestry Group, The Hymenoptera Institute and The Natural History Museum of Los Angeles County (TIGER: Thailand Inventory Group for Entomological Research,

coordinated by Michael Sharkey) (http://sharkeylab.org/tiger/). This survey resulted in the collection of about 5000 specimens of Dryinidae, which are actually in study in the authors' laboratories. The new species described herein is one of the first results of this study.

Acknowledgements

Many thanks to Dr. Michael Sharkey (Department of Entomology, University of Kentucky, Lexington, Kentucky, USA) for sending the specimen of *Aphelopus* described in the present paper. We are also grateful to all curators of collections who have sent us type material on loan. We are very indebted to Michael Ohl and Denis Brothers for their useful comments and suggestions to improve the manuscript. This paper was supported by the National Natural Science Foundation of China (No. 31472027).

References

Ashmead WH (1893) Monograph of the North American Proctotrypidae. Bulletin of the United States National Museum, 45: 1–472. https://doi.org/10.5479/si.03629236.45.1

Dalman CR (1823) Analecta entomologica. Typis Lindhianis, Holmiae, Sweden, 104 pp. https://doi.org/10.5962/bhl.title.66069

Guglielmino A, Bückle C (2003) Description of larval instars of *Neodryinus typhlocybae* (Ashmead, 1893) (Hymenoptera Dryinidae), with remarks on its biology. Mitteilungen aus dem Museum fuer Naturkunde in Berlin. Deutsche Entomologische Zeitschrift, 50(1): 143–150. https://doi.org/10.1002/mmnd.20030500114

Guglielmino A, Bückle C (2010) Description of larval instars of *Mystrophorus formicaeformis* Ruthe (Hymenoptera: Dryinidae). Zootaxa, 2602: 57–66.

Guglielmino A, Virla EG (1998) Postembryonic development of *Gonatopus lunatus* Klug (Hymenoptera: Dryinidae: Gonatopodinae), with remarks on its biology. Annales de la Société entomologique de France (N. S.), 34(3): 321–333.

Guglielmino A, Bückle C, Moya-Raygoza G (2006) Description of the larval instars of *Gonatopus bartletti* Olmi, 1984 (Hymenoptera: Dryinidae). Zootaxa, 1226: 51–60.

Guglielmino A, Olmi M, Bückle C (2013) An updated host-parasite catalogue of world Dryinidae (Hymenoptera: Chrysidoidea). Zootaxa, 3740: 1–113. https://doi.org/10.11646/zootaxa.3740.1.1

Guglielmino A, Parise G, Bückle C (2015) Description of larval instars of *Dryinus tarraconensis* Marshall, 1868 and *Gonatopus baeticus* (Ceballos, 1927) (Hymenoptera: Chrysidoidea: Dryinidae), parasitoids of the genus *Dictyophara* Germar, 1833 (Hemiptera: Auchenorrhyncha: Dictyopharidae). Zootaxa, 4032(1): 42–54. https://doi.org/10.11646/zootaxa.4032.1.2

He JH, Xu ZF (2002) Hymenoptera Dryinidae (Fauna Sinica 29). Science Press, Beijing, China, 464 pp.

Jurine L (1807) Nouvelle méthode de classer les Hyménoptères et les Diptères, 1. Hyménoptères. Paschoud, Genève, Switzerland, 326 pp+14 plates.

Kawada R, Lanes GO, Azevedo CO (2015) Evolution of metapostnotum in flat wasps (Hymenoptera, Bethylidae): implications for homology assessments in Chrysidoidea. PLoS ONE, 10(10): e0140051. https://doi.org/10.1371/journal.pone.0140051

Latreille PA (1804) Nouvelle dictionnaire d'Histoire naturelle, 24. F. Dufart, Paris, France, 104 pp.

Ljungh SJ (1810) *Gonatopus*, novum insectorum genus. Beiträge zur Naturkunde, 2: 161–163.

Olmi M (1984) A revision of the Dryinidae (Hymenoptera). Memoirs of the American Entomological Institute, 37: 1–1913.

Olmi M (1991) Supplement to the revision of the world Dryinidae (Hymenoptera Chrysidoidea). Frustula entomologica (1989) (N. S.), 12 (25): 109–395.

Olmi M (1994) The Dryinidae and Embolemidae (Hymenoptera: Chrysidoidea) of Fennoscandia and Denmark (Fauna Entomologica Scandinavica 30). E. J. Brill, Leiden, Netherlands, 100 pp.

Olmi M, Virla EG (2014) Dryinidae of the Neotropical Region (Hymenoptera: Chrysidoidea). Zootaxa, 3792 (1): 1–534. https://doi.org/10.11646/zootaxa.3792.2.1

Olmi M, Xu ZF (2015) Dryinidae of the Eastern Palaearctic region (Hymenoptera: Chrysidoidea). Zootaxa, 3996(1): 1–253. https://doi.org/10.11646/zootaxa.3996.1.1

Olmi M, Xu ZF, Guglielmino A (2015) A new species of the genus *Anteon* Jurine (Hymenoptera, Dryinidae) from Thailand. ZooKeys, 504: 141–147. https://doi.org/10.3897/zookeys.504.9333

Perkins RCL (1903) The leafhopper of the sugar cane. Territory of Hawaii, Board of Agriculture and Forest, Division of Entomology, Bulletin, 1: 1–38.

Perkins RCL (1905) Leafhoppers and their natural enemies (Pt. i. Dryinidae). Report of Work of the Experiment Station of the Hawaiian Sugar Planters' Association, Division of Entomology, Bulletin, 1(I): 1–69.

Perkins RCL (1907) Parasites of leaf-hoppers. Report of Work of the Experiment Station of the Hawaiian Sugar Planters' Association, Division of Entomology, Bulletin, 4: 5–59.

Riolo P, Isidoro N, Ruschioni S, Minuz RL, Bin F, Romani R (2016) Anatomy of the antennal dorsal organ in female of *Neodryinus typhlocybae* (Hymenoptera: Dryinidae): a peculiar sensory structure possibly involved in perception of host vibration. Journal of Morphology, 277: 128–137. https://doi.org/10.1002/jmor.20485

Westwood JO (1839) Synopsis of the genera of the British Insects. In: An Introduction to the Modern Classification of Insects, vol. 2. Longman, Orme, Brown, Green and Longmans, London, p. 76.

Xu ZF, Olmi M, He JH (2013) Dryinidae of the Oriental region (Hymenoptera: Chrysidoidea). Zootaxa, 3614: 1–460. https://doi.org/10.11646/zootaxa.3900.1.1

JHR 57: 123–134 (2017)
doi: 10.3897/jhr.57.11766
http://jhr.pensoft.net

RESEARCH ARTICLE

JOURNAL OF Hymenoptera RESEARCH
A peer-reviewed open-access journal
The International Society of Hymenopterists

The genus *Nipponopius* Fischer (Hymenoptera, Braconidae, Opiinae) new for China, with description of a new species

Tong Zhou[1], Cornelis van Achterberg[1], Zi-Sheng Guo[1]

1 *Shaanxi Key Laboratory for Animal Conservation / Key Laboratory of Resource Biology and Biotechnology in Western China, College of Life Sciences, Northwest University, 229 North Taibai Road, Xi'an, Shaanxi 710069, China*

Corresponding author: *Zi-Sheng Guo* (zishengguo@nwu.edu.cn)

Academic editor: *G. Broad* | Received 11 January 2017 | Accepted 18 April 2017 | Published 30 June 2017

http://zoobank.org/C55DE47E-92C0-489D-9E7C-7FF93B7D55B0

Citation: Zhou T, van Achterberg C, Guo Z-S (2017) The genus *Nipponopius* Fischer (Hymenoptera, Braconidae, Opiinae) new for China, with description of a new species. Journal of Hymenoptera Research 57: 123–134. https://doi.org/10.3897/jhr.57.11766

Abstract

Nipponopius glabricaudatus **sp. n.** from Shaanxi and Ningxia (NW China) is described and illustrated (Hymenoptera: Braconidae: Opiinae). A key to the species of *Nipponopius* Fischer, 1963, is added and for the first time the male is described and illustrated. The genus is reported for the second time from outside Japan and is new for China. The position of *Nipponopius* Fischer is discussed and it is accepted as a valid genus.

Keywords

Braconidae, Opiinae, *Nipponopius*, new species, Palaearctic, China, Shaanxi, Ningxia, Japan

Introduction

Nipponopius Fischer, 1963, belongs to the large subfamily Opiinae (Hymenoptera, Braconidae), with 2,063 valid species in 39 genera according to Yu et al. (2016). It is a common group containing generally small (2–5 mm) parasitoid wasps, but *Nipponopius* Fischer is rarely collected. Opiinae occur worldwide and the world fauna has been reviewed by Fischer (1972, 1977, 1986, 1987). Wharton (1988, 1997), van Achterberg

Copyright *Tong Zhou et al.* This is an open access article distributed under the terms of the Creative Commons Attribution License (CC BY 4.0), which permits unrestricted use, distribution, and reproduction in any medium, provided the original author and source are credited.

(1997, 2004a, 2004b), van Achterberg and Salvo (1997), van Achterberg and Chen (2004) and Tan et al. (2016) published updates or some additions for the existing keys to the genera of the Opiinae, but the number of genera and the limits of several genera remain still a matter of discussion.

Wharton (1997) synonymised the monotypic genus *Nipponopius* Fischer with *Utetes* Foerster, 1863, because both share the curved basal carinula at the inner side of the hind tibia. We disagree with including all opine species with this character into one large genus *Utetes* Foerster s.l. The resulting group is too diverse and provisional DNA data show that probably several lineages are involved (Li et al. 2013). The morphology of *Nipponopius* Fischer differs distinctly from that of *Utetes* Foerster s.s.; best exemplified by the morphology of the hind leg, the position of the dorsope of the first metasomal tergite and the incised female hypopygium. Therefore, we concur with Tobias (2000) that *Nipponopius* Fischer should be treated as a separate genus.

Nipponopius can be recognised from all other opiines by the aberrant legs of both sexes (hind coxa ventrally angularly produced (Figs 9, 19, 20), the second-fourth tarsal segments very robust (Figs 8, 15, 17, 18), the telotarsi enlarged (Figs 8, 15, 17) but less so in males (Fig. 18) and the deeply incised hypopygium of females (Figs 13, 14, 17).

Nothing is known about the biology of *Nipponopius* species, but all Opiinae are solitary koinobiont endoparasitoids of larvae of cyclorraphous Diptera. The oviposition may take place in the egg of the host (ovo-larval parasitoid) or in an early instar larva. The parasitoid larva has it final development when the host larva made its puparium and the adult emerges from this puparium. Opiinae may play an important role in the control of dipterous pests as fruit-infesting Tephritidae and mining Agromyzidae.

Material and methods

The specimens were collected by using a sweep net and directly killed and preserved in 70% alcohol. The specimens were chemically treated with a mixture of xylene + alcohol 96% and amyl acetate, respectively (AXA-method; van Achterberg 2009; van Achterberg et al. 2010). For identification of the subfamily Opiinae, see van Achterberg (1990, 1993), for identification of *Nipponopius* Fischer, see Fischer (1972) and the diagnosis in this paper, for references to the Opiinae, see Yu et al. (2016) and for the terminology used in this paper, see van Achterberg (1988, 1993). Measurements are taken as indicated by van Achterberg (1988): for the length and the width of a body part the maximum length and width is taken, unless otherwise indicated. The length of the mesosoma is measured from the anterior border of the mesoscutum till the apex of the propodeum and of the first tergite from the posterior border of the adductor till the medio-posterior margin of the tergite. Observations and descriptions were made with an Olympus SZX11 stereomicroscope and fluorescent lamps. Photographic images were made with the Keyence VHX-5000 digital microscope. The examined specimens are deposited in the American Entomological Institute, Gainesville, USA (AEI) and in the College of Life Sciences, Northwest University, Xi'an, China (NWUX).

Systematics

***Nipponopius* Fischer, 1963**
Figures 1–41

Nipponopius Fischer, 1963: 283, 1972b: 481; Tobias, 1998: 563. Type species (by monotypy): *Nipponopius incisus* Fischer, 1963 [examined].

Diagnosis. Hind tibia with basal carinula (Fig. 41); mandible triangular with two subequal teeth and hardly twisted, without or a weak ventral carina (Figs 10, 26, 36); apex of antenna with distinct spine (Figs 16, 30, 40); mesopleuron with one groove (= precoxal sulcus) and sternaulus absent (Figs 5, 22, 32); postpectal carina absent; vein CU1b of fore wing as long as vein 3-CU1 (Fig. 1) or somewhat shorter (Figs 17, 31); first subdiscal cell of fore wing distinctly widened apically; vein m-cu of fore wing converging to vein 1-M posteriorly and vein 1-M curved (Figs 1, 17, 31); vein 1-SR+M distinctly sinuate; hind coxa submedially angularly produced ventrally (Figs 5, 9, 19, 20); second-fourth tarsal segments of ♀ very robust (Figs 8, 17, 25), but less of ♂ (Figs 18, 35); telotarsi and arolium enlarged (Figs 8, 15, 17, 18); dorsope rather small, removed from lateral margin of first tergite (Figs 7, 23, 34); hypopygium of ♀ large, strongly sclerotized parts deeply incised (Figs 13, 14, 25), basally punctate, laterally and apico-medially with membranous parts.

Notes. According to Wharton (1997) *Nipponopius* Fischer is a junior synonym of *Utetes* Foerster, 1863, because of the possession of the hind tibial carinula. We agree with Tobias (2000) that *Nipponopius* deserves a separate status, not the least because of the presence of a rather small dorsope removed from the lateral margin of the first tergite (Figs 7, 23, 34), the angularly protruding hind coxa ventrally (Figs 8, 9, 19, 20) and the long vein CU1b of fore wing combined with apically widened first subdiscal cell (Fig. 1), features absent in *Utetes* Foerster s.s.

Biology. Unknown.

Distribution. East Palaearctic: Japan, Far East Russia, China. Two species.

Key to species of the genus *Nipponopius* Fischer

1 Anterior tentorial pits rather large (Figs 26, 36); precoxal sulcus remain far removed from anterior margin of mesopleuron (Figs 22, 32) and remainder of mesopleuron smooth antero-dorsally; ovipositor sheath glabrous apically (Fig. 25); vein CU1b of fore wing shorter than vein 3-CU1 (Figs 21, 31); first metasomal tergite largely smooth (Figs 23, 24, 34) ..... ***N. glabricaudatus* sp. n.**

– Anterior tentorial pits small (Fig. 2); precoxal sulcus reaching anterior margin of mesopleuron (Fig. 5) and mesopleuron partly crenulate antero-dorsally; ovipositor sheath distinctly setose apically (Fig. 5); vein CU1b of fore wing as long as vein 3-CU1 (Fig. 1); first tergite rather finely punctate-rugose (Fig. 7)..... ***N. incisus* Fischer, 1963**

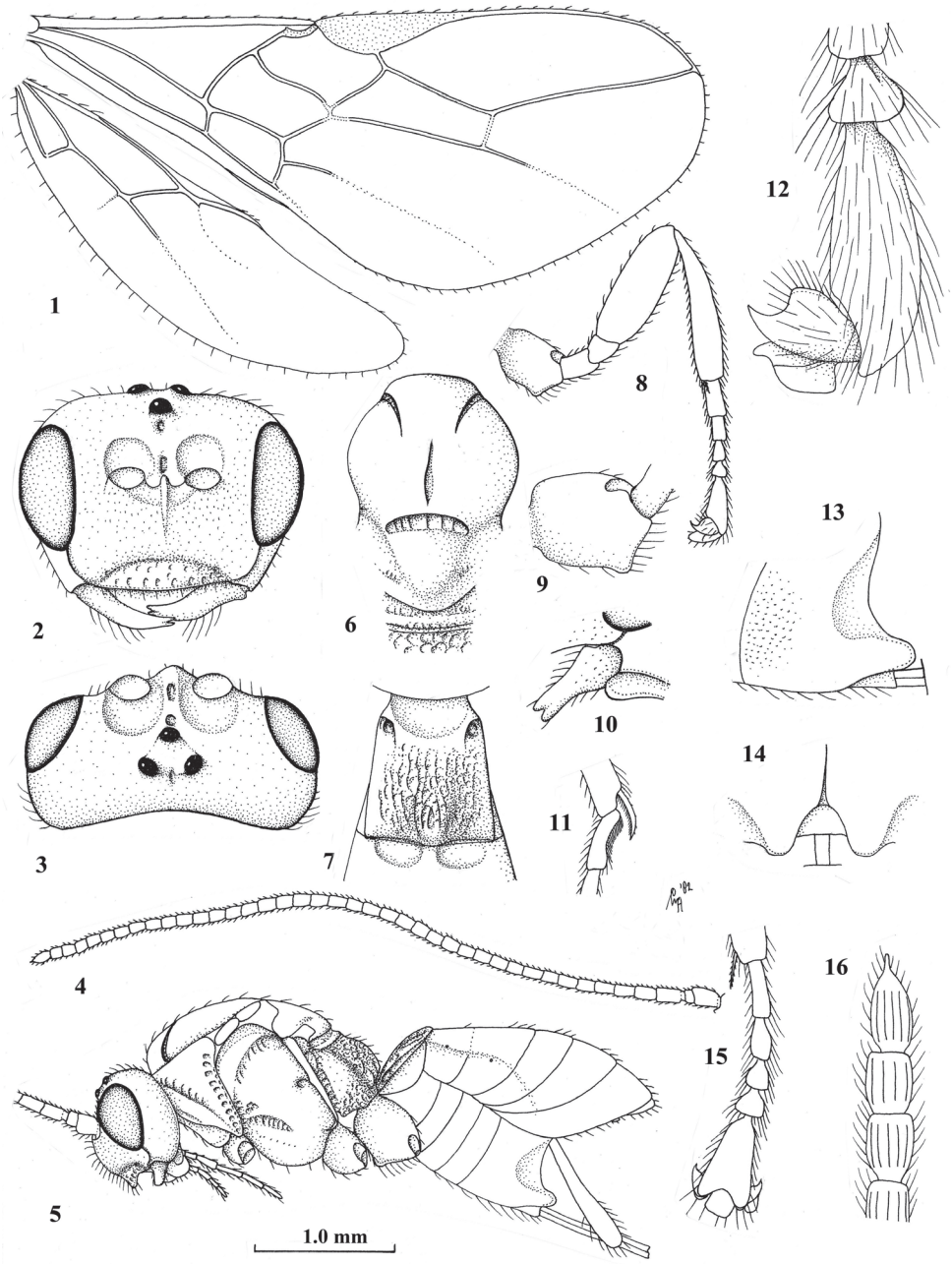

Figures 1–16. *Nipponopius incisus* Fischer, ♀, holotype. **1** wings **2** head anterior **3** head dorsal **4** antenna **5** habitus lateral **6** mesosoma dorsal **7** first metasomal tergite dorsal **8** hind leg lateral **9** hind coxa lateral **10** mandible and occipital carina latero-ventral **11** fore tibial spur **12** outer hind claw lateral **13** hypopygium lateral **14** hypopygium ventral **15** hind tarsus dorsal **16** apical segments of antenna.

***Nipponopius glabricaudatus* Zhou & van Achterberg, sp. n.**
http://zoobank.org/0899D6C7-24E8-4206-9B76-148601CF4CE9
Figures 17–41

Type material. Holotype, ♀ (NWUX), "NW. **China: Ningxia**, Jingyuan, Mt. Liupan, Erlonghe For[estry] Farm, 23°24'N 106°20'E, c. 1800 m, 2.viii.2015, Jiangli Tan". Paratype: 1 ♂ (NWUX), "NW. China: **Shaanxi**, Ningshan, Mt. Qin, Xunyangba, 33°33'N, 108°32'E, c. 1300 m, vii.2014, Jiangli Tan".

Diagnosis. Very similar to the only other known species, *N. incisus* Fischer, but differs especially by the large anterior tentorial pits, the reduced precoxal sulcus, the shorter vein CU1b of fore wing and the apically glabrous ovipositor sheath.

Description. Holotype, ♀, length of body 3.1 mm; of fore wing 4.0 mm.

Head. Head slightly transverse, width 1.8 times its median length in dorsal view and temple directly narrowed behind eyes (Fig. 27); antenna with 40 segments, 1.1 times as long as fore wing, third segment 1.3 times as long as fourth segment, length of third, fourth and penultimate segments 1.7, 1.5 and 1.8 times their width, respectively (Figs 29, 30); maxillary palp as long as height of head; labial palp segments slender; occipital carina far separated from hypostomal carina and carina dorsally absent; hypostomal carina wide, protruding (Fig. 28); length of eye in dorsal view 2.7 times temple; temple and vertex sparsely punctate and with long setae; stemmaticum weakly convex, with small depression behind stemmaticum; OOL: diameter of ocellus: POL = 28:10:11; frons distinctly depressed behind antennal sockets, glabrous medially, finely punctate and setose laterally; face punctate, medially elevated (Figs 26, 27), extending as a median carina to level of posterior margin of antennal sockets; width of clypeus 3.0 times its maximum height and 0.6 times width of face; anterior tentorial pits rather large (Fig. 26); clypeus moderately convex, punctate and protruding, ventrally slightly curved and thin; hypoclypeal depression narrow (Figs 26, 28); malar suture largely absent; length of malar space 0.5 times basal width of mandible; mandible triangular and with narrow ventral carina (Fig. 28).

Mesosoma. Mesosoma 1.3 times longer than high; dorsal pronope large, elliptical (Fig. 27); pronotal side smooth, only anteriorly and postero-ventrally crenulated (Fig. 22); epicnemial area largely smooth except anterior margin shortly crenulate; precoxal sulcus remain far removed from anterior margin of mesopleuron, moderately wide and distinctly crenulate (Fig. 23); remainder of mesopleuron mostly smooth; episternal scrobe large; pleural sulcus only ventrally finely crenulate (Fig. 22); mesosternal sulcus medium-sized and moderately crenulate, posteriorly smooth; anterior metapleural sulcus crenulate and widened ventrally (Fig. 22), metapleuron largely smooth dorsally, but coarsely reticulate ventrally (Fig. 22); notauli short, crenulated anteriorly and absent posteriorly; medio-posterior depression of mesoscutum long and narrow elliptical; lateral lobes of mesoscutum mostly glabrous, smooth and shiny, with few setae at middle lobe and near notauli; scutellar sulcus deep and with 3 distinct longitudinal carinae, 0.2 times as long as scutellum; scutellum convex, largely smooth except some punctures and with few setae; side of scutellum smooth except some crenulation (Fig. 23); metanotum

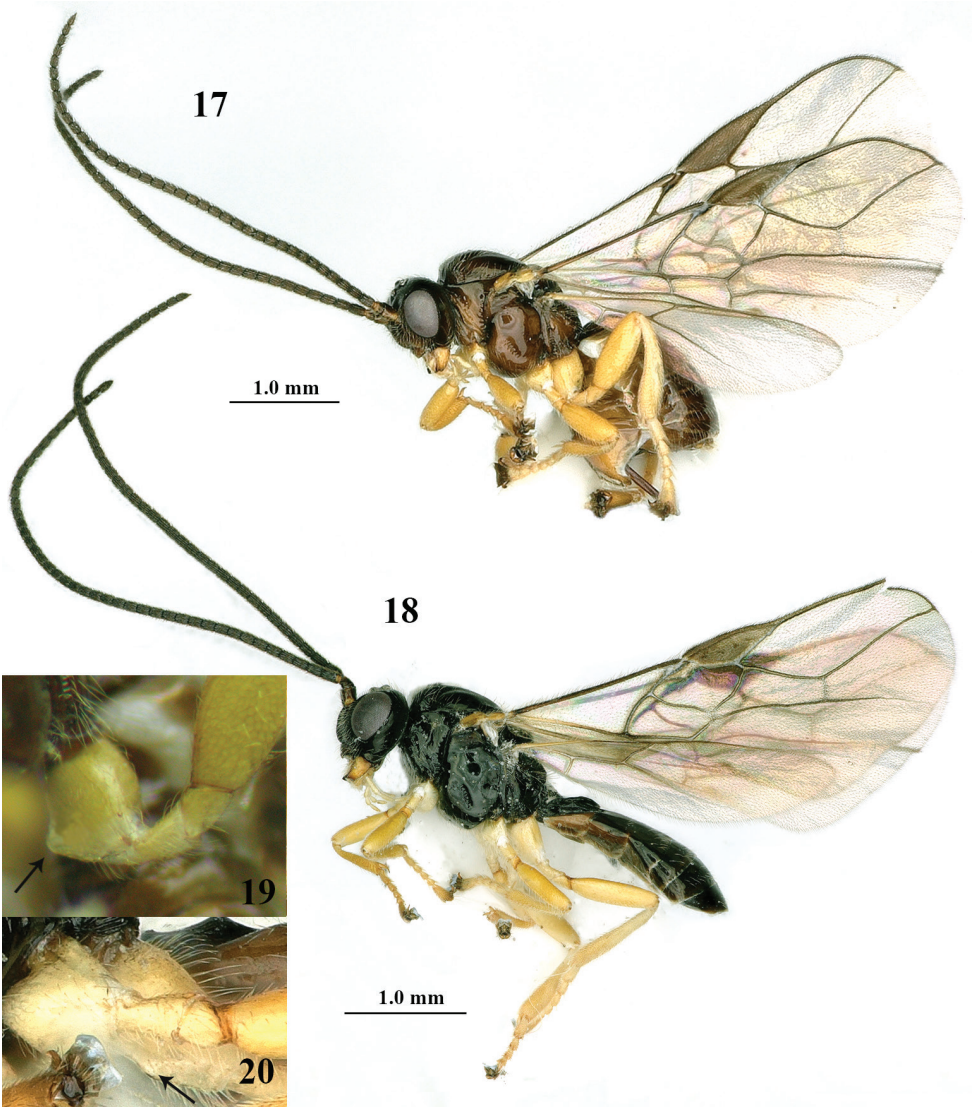

Figures 17–20. *Nipponopius glabricaudatus* sp. n., ♀, holotype, but 18 and 20 of ♂, paratype. **17, 18** habitus lateral **19, 20** hind coxa lateral (arrow pointing to coxal protuberance).

smooth except posterior margin shortly crenulate; dorsal surface of propodeum short, punctate-rugose, and with a short medio-longitudinal carina connected to an irregular transverse carina, its posterior surface largely punctate-reticulate (Fig. 23).

Wings. Fore wing: pterostigma elliptical; vein r issued just before middle of pterostigma (Fig. 21); r:2-SR:3-SR:SR1 = 3:15:21:36; SR1 slightly curved;1-CU1:2-CU1 = 1:6; CU1b shorter than 3-CU1; m-cu postfurcal;1-CU1 hardly widened. Hind wing: M+CU:1-M:1r-m = 21:21:14; cu-a straight (Fig. 21).

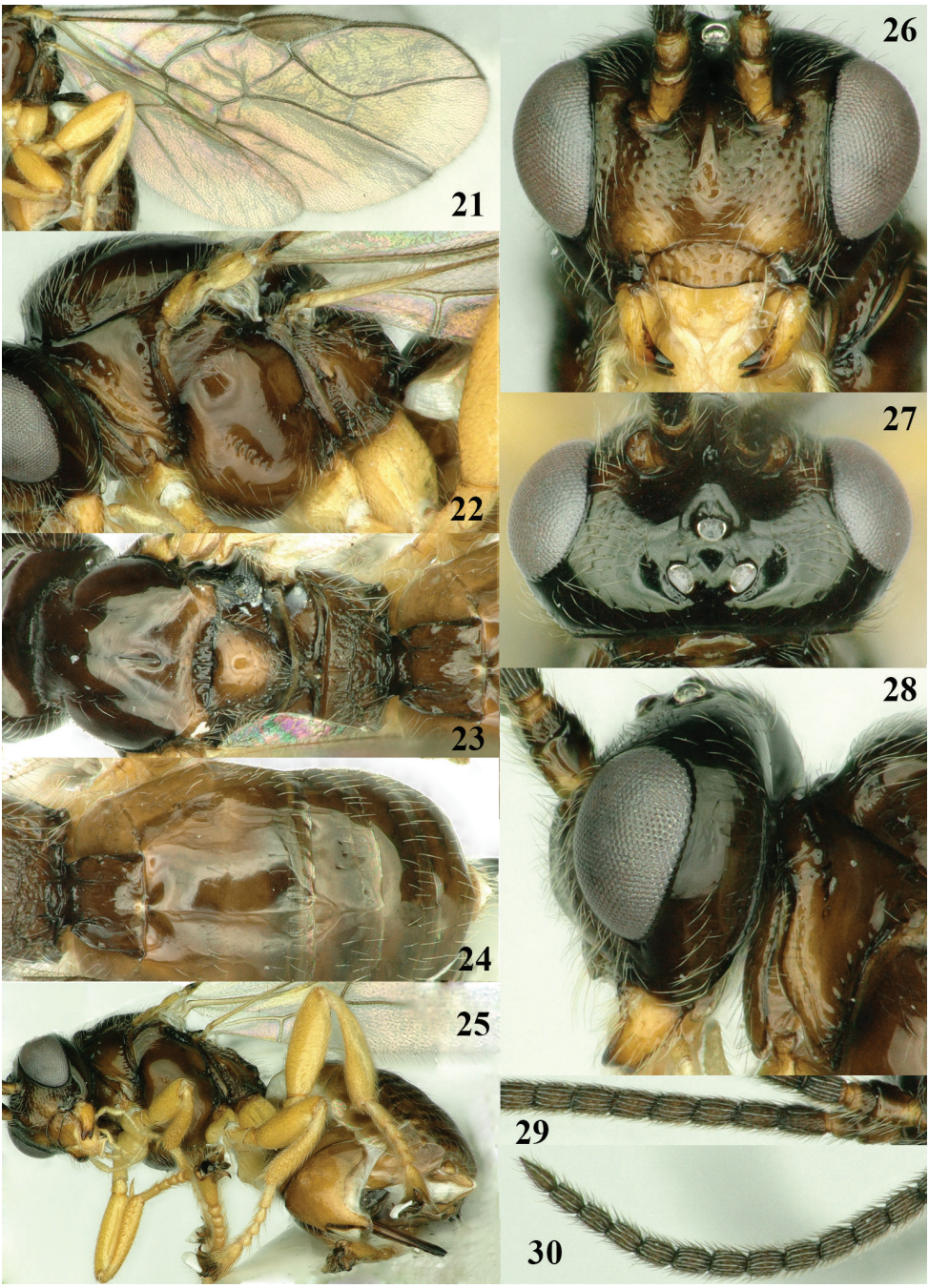

Figures 21–30. *Nipponopius glabricaudatus* sp. n., ♀, holotype. **21** wings **22** mesosoma lateral **23** mesosoma and first metasomal tergite dorsal **24** metasoma dorsal **25** legs and hypopygium antero-ventral **26** head anterior **27** head dorsal **28** head lateral **29** basal antennal segments **30** apical antennal segments.

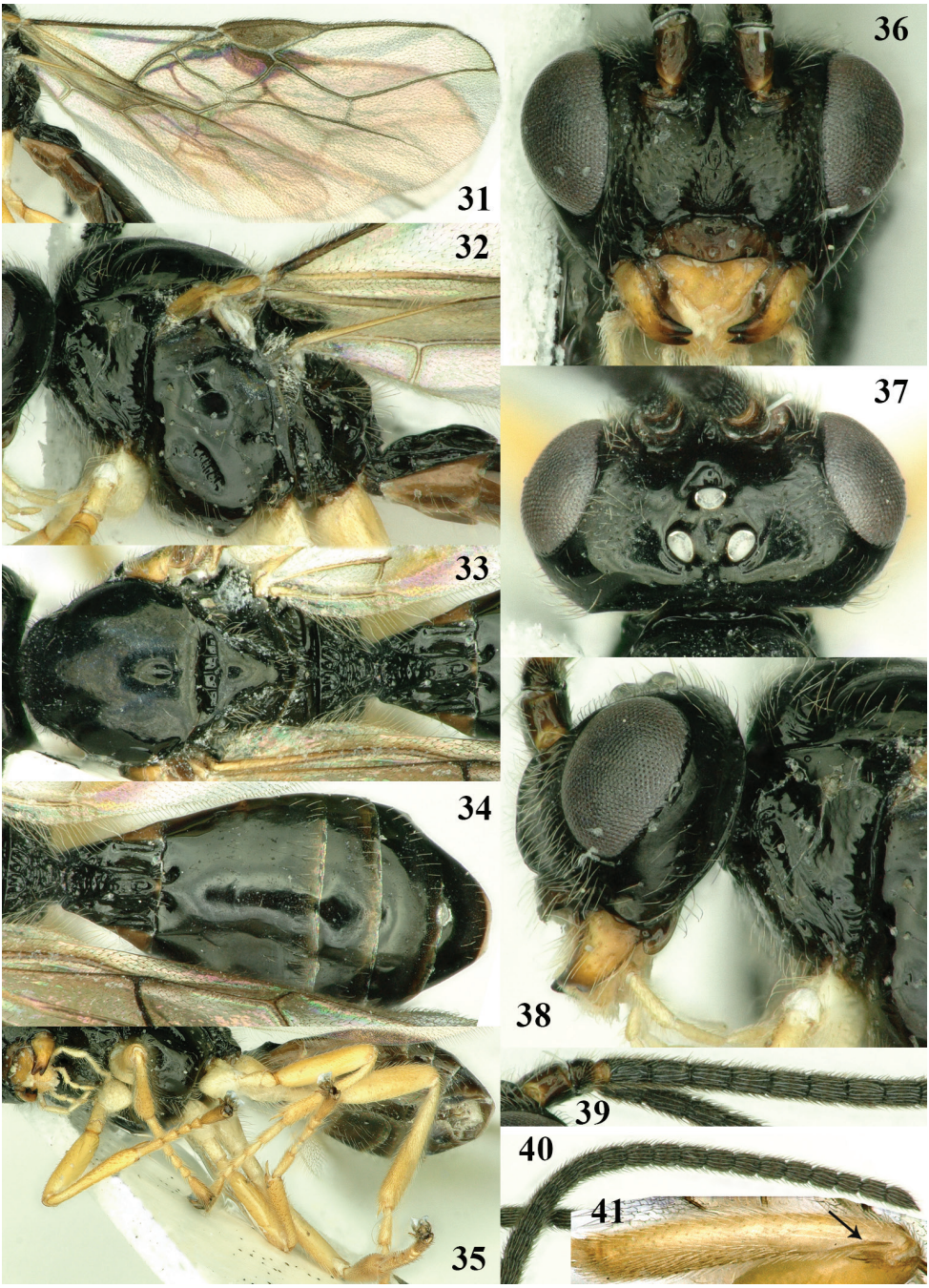

Figures 31–41. *Nipponopius glabricaudatus* sp. n., ♂, paratype. **31** wings **32** mesosoma and first metasomal tergite lateral **33** id. dorsal **34** metasoma dorsal **35** legs antero-ventral **36** head anterior **37** head dorsal **38** head lateral **39** basal antennal segments **40** apical antennal segments **41** inner side of hind tibia lateral (arrow pointing to carinula).

Legs. Hind coxa smooth, with long setae, and distinctly protruding ventro-medially (Figs 19, 25); femora widened (Fig. 25); carinula of hind tibia long, sinuate and area behind it largely glabrous (Fig. 41); tarsal claws medium-sized (Fig. 25); length of femur, tibia and basitarsus of hind leg 2.7, 4.6 and 2.0 times their width, respectively.

Metasoma. Length of first metasomal tergite 1.1 times its apical width, its surface evenly convex, shiny, largely smooth, with dorsal carinae converging basally and parallel extending to its posterior half (Figs 23, 24), with laterope large and deep (Fig. 22); second suture obsolescent; second to sixth tergites smooth and sparsely setose posteriorly; combined length of second and third tergites 0.4 times total length of metasoma (Fig. 24); ovipositor sheath glabrous, sheath 0.16 times as long as fore wing and 0.6 times as long as hind tibia (Fig. 25).

Colour. Irregularly dark brown or brown; mandible (except dark brown apices), palpi, tegulae and legs yellow; wing membrane subhyaline; veins M+CU1 and C+SC+R of both wings partly pale yellowish.

Male. Fore wing length 3.7 mm, body length 4.1 mm (Fig. 18). Antenna with 47 segments; mesosternal sulcus medium-sized and completely crenulated; propodeum strongly sculptured, its dorsal surface areolate and reticulate posteriorly (Figs 33, 34); hind coxa with a relatively small protuberance ventro-medially (Fig. 20); hind femur and tibia less robust, with its length 3.4 times and 6.5 times their width, respectively (Fig. 35); first metasomal tergite distinctly convex, with relatively strong rugae between dorsal carina anteriorly (Figs 33, 34) and laterope deep (Fig. 32); body generally black or blackish brown, but mandible (except dark apices), palpi, tegulae and legs pale yellow (Figs 18, 35).

Distribution. China (Ningxia, Shaanxi).

Etymology. The name is derived from "glaber" (Latin for "hairless") and "cauda" (Latin for "tail"), because of the glabrous ovipositor sheath of the holotype.

Nipponopius incisus **Fischer, 1963**

Figures 1–16

Nipponopius incisus Fischer, 1963: 283, 1972b: 481; Tobias, 1998: 563.

Type material. Holotype, ♀ (AEI), "Kami Kochi, Jap[an], 24.vii.1954, Townes Family", "Holotype", "*Nipponopius incisus* n. sp., ♀, det. Fischer", "Type No. 260", "*Nipponopius incisus* Fischer, Type".

Diagnosis. For the differences see the key to species and the diagnosis of *N. glabricaudatus* sp. n.

Redescription. Holotype, ♀, length of body 4.3 mm; of fore wing 4.8 mm.

Head. Temple gradually narrowed behind eyes (Fig. 3); antenna with 41 segments, 1.1 times as long as fore wing, third segment 1.2 times as long as fourth segment, length of third, fourth and penultimate segments 2.2, 1.8 and 1.3 times their width,

respectively (Figs 4, 16); maxillary palp as long as height of head; labial palp segments slender; occipital carina far separated from hypostomal carina and carina dorsally absent; hypostomal carina wide, protruding (Figs 5, 10); length of eye in dorsal view 1.4 times temple; temple and vertex sparsely punctate and with long setae; stemmaticum weakly convex, with small depression behind stemmaticum (Fig. 3); OOL: diameter of ocellus: POL = 25:8:10; frons distinctly depressed behind antennal sockets, glabrous medially, punctulate and setose laterally, with two deep pits in front of anterior ocellus (Fig. 3); face punctulate, medially elevated (Fig. 2), extending as a median carina to level of posterior margin of antennal sockets; width of clypeus 4.0 times its maximum height and 0.7 times width of face; anterior tentorial pits small (Fig. 2); clypeus moderately convex, punctate and protruding, ventrally slightly curved and thin; hypoclypeal depression narrow (Fig. 2); malar suture curved, deep and short; length of malar space 0.7 times basal width of mandible; mandible triangular and with narrow ventral carina (Figs 5, 10).

Mesosoma 1.3 times longer than high; dorsal pronope absent, except for transverse groove; pronotal side smooth, only oblique groove and posteriorly crenulated (Fig. 5); epicnemial area and mesopleuron dorsally narrowly crenulate; precoxal sulcus reaching anterior margin of mesopleuron, moderately wide and distinctly crenulate (Fig. 5); remainder of mesopleuron mostly smooth; episternal scrobe large; pleural sulcus largely smooth (Fig. 5); anterior metapleural sulcus crenulate and widened ventrally (Fig. 5), metapleuron largely smooth dorsally, except rugosity ventrally (Fig. 5); notauli short, finely crenulated anteriorly and absent posteriorly; medio-posterior depression of mesoscutum long and narrow droplet-shaped; lateral lobes of mesoscutum mostly glabrous, smooth and shiny, with few setae at middle lobe and near notauli; scutellar sulcus deep and with 6 distinct longitudinal carinae, 0.2 times as long as scutellum; scutellum convex, largely smooth and with few setae; side of scutellum smooth except some indistinct crenulation (Fig. 6); metanotum largely smooth but posterior margin narrowly crenulate; dorsal surface of propodeum coarsely reticulate, and without medio-longitudinal or transverse carinae, its posterior surface hardly differentiated (Fig. 5).

Wings. Fore wing: pterostigma elliptical; M+CU1 entirely sclerotized; 1-SR long; r issued just before middle of pterostigma (Fig. 1); r:2-SR:3-SR:SR1 = 3:14:23:41; SR1 straight;1-CU1:2-CU1 = 2:15; CU1b equal to 3-CU1; m-cu postfurcal;1-CU1 hardly widened. Hind wing: M+CU:1-M:1r-m = 21:21:14; cu-a straight (Fig. 1).

Legs. Hind coxa smooth, with long setae, and angularly protruding ventro-medially (Figs 8, 9); femora widened; tarsal claws robust basally and slender apically (Fig. 12); length of femur, tibia and basitarsus of hind leg 2.6, 5.6 and 2.0 times their width, respectively.

Metasoma. Length of first metasomal tergite 1.1 times its apical width, medially strongly convex, shiny, rather finely punctate-rugose, with dorsal carinae only near dorsope, and with laterope deep and elliptical (Fig. 5); second suture obsolescent; second to sixth tergites smooth and their apical half setose; combined length of second and third tergites 0.4 times total length of metasoma (Fig. 5); apical third of ovipositor

sheath distinctly setose, sheath 0.18 times as long as fore wing and 0.8 times as long as hind tibia (Figs 5, 8).

Colour. Black; palpi pale yellowish, mandible (except dark brown apices), clypeus, scapus ventrally, annellus, inner orbits above level of antennal sockets, tegulae largely (humeral plate partly dark brown) and legs yellowish-brown; face, temple, metasoma (except first tergite), pterostigma and veins dark brown; wing membrane subhyaline.

Distribution. Japan (Honshu, including garden of Imperial Palace in Tokyo; Konishi and Maetô 2000), Far East Russia (Sakhalin oblast).

Acknowledgements

The second author gratefully acknowledge the kindness of the late Dr Henry K. Townes (AEI, Gainesville) to loan him the holotype of *Nipponopius incisus*. The research was supported jointly by the National Natural Science Foundation of China (NSFC, No. 31201732, 31572300), and the Northwest University Undergraduate Training Program for Innovation and Entrepreneurship, China (No. 2017155).

References

Fischer M (1963) Über paläarktische Opiinae (Hym., Braconidae). Annalen des Naturhistorischen Museums in Wien 66: 283–305.

Fischer M (1972) Hymenoptera Braconidae (Opiinae I). (Paläarktische Region). Das Tierreich 91: i–xii + 1–620.

Fischer M (1977) Hymenoptera Braconidae (Opiinae II). (Amerika). Das Tierreich 96: 1–1001.

Fischer M (1986) Neue Bestimmungsschlüssel für paläarktische Opiinae, neue Subgenera, Redeskriptionen und eine neue Art (Hymenoptera, Braconidae). Annalen des Naturhistorischen Museums in Wien 88/89: 607–662.

Fischer M (1987) Hymenoptera Braconidae (Opiinae III) - äthiopische, orientalische, australische und ozeanische Region. Das Tierreich 104: 1–734.

Konishi K, Maetô K (2000) [Ichneumonoidea, Evanioidea, Trigonaloidea and Ibaliidae (Hymenoptera) from the Imperial Palace, Tokyo.] Memoirs of the National Science Museum 36: 307–323. [in Japanese]

Li X-Y, van Achterberg C, Tan J-C (2013) Revision of the subfamily Opiinae (Hymenoptera, Braconidae) from Hunan (China), including thirty-six new species and two new genera. ZooKeys 268: 1–168. http://doi.org/10.3897/zookeys.268.4071

Tan J-L, Tan Q-Q, van Achterberg C, Chen X-X (2016) A new genus *Carinopius* gen. n. of the subfamily Opiinae (Hymenoptera, Braconidae) from China and Vietnam, with description of a new species. Zootaxa 4061(5): 569–574. http://doi.org/10.11646/zootaxa.4061.5.6

Tobias VI (1998) In: Ler PA (Ed.) Key to the insects of Russian Far East. 4. Neuropteroidea, Mecoptera, Hymenoptera 3: 1–706. Dal'nauka, Vladivostok, Opiinae, 558–655.

Tobias VI (2000) New data on subfamily Opiinae (Hymenoptera, Braconidae) from the Russian Far East. Far Eastern Entomologist 83: 1–16.

van Achterberg C (1988) Revision of the subfamily Blacinae Foerster (Hymenoptera, Braconidae). Zoologische Verhandelingen Leiden 249: 1–324.

van Achterberg C (1993) Illustrated key to the subfamilies of the Braconidae (Hymenoptera: Ichneumonoidea). Zoologische Verhandelingen Leiden 283: 1–189.

van Achterberg C (1997) Revision of the Haliday collection of Braconidae (Hymenoptera). Zoologische Verhandelingen Leiden 314: 1–115.

van Achterberg C, Salvo A (1997) Reared Opiinae (Hymenoptera: Braconidae) from Argentina. Zoologische Mededelingen Leiden 71(18): 189–214.

van Achterberg C (2004a) New Indo-Australian subgenera and species of the genera *Xynobius* Foerster and *Ademoneuron* Fischer (Hymenoptera: Braconidae: Opiinae). Zoologische Mededelingen Leiden 78(20): 313–329.

van Achterberg C (2004b) *Bitomoides* gen. nov. (Hymenoptera: Braconidae: Opiinae) from Europe. Zoologische Mededelingen Leiden 78(21): 331–335.

van Achterberg C, Chen X-X (2004) Six new genera of Braconidae (Hymenoptera) from China. Zoologische Mededelingen Leiden 78(2): 77–100.

van Achterberg C (2009) Can Townes type Malaise traps be improved? Some recent developments. Entomologische Berichten Amsterdam 69: 129–135.

van Achterberg C, Grootaert P, Shaw MR (2010) Chapter 17. Flight interception traps for arthropods: 423–462. In: Eymann J, Degreef J, Häuser C, Monje JC, Samyn Y, VandenSpiegel D (Eds) Manual on field recording techniques and protocols for All Taxa Biodiversity Inventories and Monitoring. ABC Taxa 1/2: 1–652.

Wharton RA (1988) Classification of the Braconid subfamily Opiinae (Hymenoptera). Canadian Entomologist 120: 333–360. https://doi.org/10.4039/Ent120333-4

Wharton RA (1997) Generic relationships of opiine Braconidae (Hymenoptera) parasitic on fruit-infesting Tephritidae (Diptera). Contributions of the American Entomological Institute 30(3): 1–53.

Yu DS, van Achterberg C, Horstmann K (2016) Taxapad 2016, Ichneumonoidea 2015. Database on flash-drive. http://www.taxapad.com, Nepean, Ontario, Canada.

JHR 57: 135–142 (2017)
doi: 10.3897/jhr.57.12555
http://jhr.pensoft.net

RESEARCH ARTICLE

JOURNAL OF Hymenoptera RESEARCH
A peer-reviewed open-access journal
The International Society of Hymenopterists

First report of the genus *Coeliniaspis* Fischer (Hymenoptera, Braconidae, Alysiinae) from China and Russia

Min-Lin Zheng[1], Jia-Hua Chen[1], Cornelis van Achterberg[2]

1 *Beneficial Insects Institute, Fujian Agriculture and Forestry University, Fuzhou, Fujian Province, 350002, China* **2** *Key Laboratory of Resource Biology and Biotechnology in Western China (Northwest University), Ministry of Education; School of Life Sciences, Northwest University, 229 North Taibai Road, Xi'an, Shanxi 710069, China*

Corresponding author: *Cornelis van Achterberg* (c.vanachterberg@xs4all.nl)

Academic editor: *J. Fernandez-Triana* | Received 6 March 2017 | Accepted 3 April 2017 | Published 30 June 2017

http://zoobank.org/431D3114-7299-4CFF-8B8B-C2D489E19006

Citation: Zheng M-L, Chen J-H, van Achterberg C (2017) First report of the genus *Coeliniaspis* Fischer (Hymenoptera, Braconidae, Alysiinae) from China and Russia. Journal of Hymenoptera Research 57: 135–142. https://doi.org/10.3897/jhr.57.12555

Abstract

Coeliniaspis Fischer, 2010 (Braconidae, Alysiinae, Dacnusini) is recorded from China and Russia for the first time. *Coeliniaspis insularis* (Tobias, 1998) is reported from China (Fujian), redescribed and illustrated. A key to the species of the genus *Coeliniaspis* Fischer is added. *Coeliniaspis insularis* (Tobias, 1998) and *C. rufiventris* (Tobias, 1998) are new combinations.

Keywords

Taxonomy, parasitoids, new combination, Oriental, China, Fujian, Russia, Dacnusini, *Coeliniaspis insularis*

Copyright *Min-Lin Zheng et al.* This is an open access article distributed under the terms of the Creative Commons Attribution License (CC BY 4.0), which permits unrestricted use, distribution, and reproduction in any medium, provided the original author and source are credited.

Introduction

The genus *Coeliniaspis* Fischer, 2010 (Hymenoptera, Braconidae, Alysiinae, Dacnusini) is a monotypic genus described from Cambodia, with *C. kohkongensis* Fischer, 2010, as type species. According to Griffith's (1964) diagnosis, this genus belongs to the *Coelinius* genus-group. Its biology is unknown, but related genera contain (ovo-) larval parasitoids of Chloropidae (Diptera).

Coeliniaspis is reported here for the first time from China and Far Eastern Russia; it is also the first record outside Cambodia. The species found in China, *C. insularis* comb. n., is redescribed and illustrated. Keys to the genera of *Coelinius* genus-group and the species of *Coeliniaspis* Fischer are provided.

Material and methods

The Chinese specimens were collected in Fujian (southeast China) by sweep-netting in August 2001. For the terminology of morphological features and sculpture, measurements and wing venation nomenclature, see van Achterberg (1988, 1993). The morphological characters were examined and photographed using a Leica M205C digital stereomicroscope. The specimens are deposited in the Beneficial Insects Institute, Fujian Agriculture and Forestry University (Fuzhou, China).

Taxonomy

Coeliniaspis Fischer, 2010

Coeliniaspis Fischer, 2010: 646. Type species (by original designation): *Coeliniaspis kohkongensis* Fischer, 2010 (examined).

Diagnosis. Flagellomeres of antenna densely setose; clypeus flattened, with ventral lamella or more or less depressed medially and sublaterally protruding (Fig. 7; see arrow); mandible with four teeth, additional (= fourth) tooth dorso-basally on middle tooth (Fig. 10); vein r of fore wing arising from or before middle of pterostigma (Fig. 1); second metasomal tergite coarsely sclerotized, distinctly sculptured and with complete sharp lateral crease.

Remarks. *Coeliniaspis* is included in the *Coelinius* genus-group because of the presence of the longitudinal sculpture on the second metasomal tergite, similar to that of the first tergite, the mandible with an additional tooth between first and second teeth, the metapleuron with rugose sculpture and sparsely pubescent, and the first subdiscal cell of fore wing elongate (Fig. 1). For the differences within the *Coelinius* genus-group, see the key below.

Distribution. Oriental (Cambodia, China (new record)), Russia (Far East, new record).

Key to the genera of *Coelinius* genus-group

(modified after van Achterberg, 2014)

1 Dorsope absent or nearly so; mesosternum with triangular reticulate-rugose area medio-posteriorly; first metasomal tergite more than 2.3 times as long as its apical width; vein 2-R1 of fore wing frequently rather long [pterostigma usually about as long as vein 1-R1; clypeus strongly protruding forwards] **2**

– Dorsope present; mesosternum with only a narrow crenulate suture medio-posteriorly; first tergite usually less than 2.3 times as long as its apical width; vein 2-R1 of fore wing short or absent **3**

2 Vein 1-SR+M of fore wing absent; scutellar sulcus chevron-shaped; pterostigma distinctly longer than vein 1-R1 (= metacarp); clypeus moderately protruding forwards.....***Neocoelinius*** **Granger, 1949**

– Vein 1-SR+M of fore wing present; scutellar sulcus transverse; pterostigma usually about as long as vein 1-R1; clypeus strongly protruding forwards [fourth metasomal tergite smooth; second tergite not carapace-like and second tergite without complete sharp lateral crease; clypeus without pair of ventral protuberances] .....***Coelinidea*** **Viereck, 1913**

3 Dorso-posterior half of pronotal side distinctly protruding posteriorly; metasoma of female blade-like compressed posteriorly; head nearly square in dorsal view; vein r of fore wing issued distinctly behind middle of pterostigma.....**4**

– Dorso-posterior half of pronotal side truncate, at most dorso-apically protruding; metasoma of female less compressed; head transverse in dorsal view; vein r of fore wing usually issued between base and middle of pterostigma or from its middle **5**

4. Vein r of fore wing strongly oblique; first metasomal tergite elongate; entire dorsal half of pronotal side protruding posteriorly .....***Coelinius*** **Nees, 1818**

– Vein r of fore wing subvertical; first tergite short; dorsal half of pronotal side less protruding posteriorly [face short, sharp-angularly protruding] .... ***Eucoelinidea*** **Tobias, 1979**

5 Clypeus medio-ventrally depressed (arrow in Fig. 7) and sublaterally protruding or emarginate medio-ventrally and with a pair of small ventral lobes [head cubical (Fig. 8); second metasomal tergite with complete sharp lateral crease (Fig. 5) and third tergite evenly setose] ..... ***Coeliniaspis*** **Fischer, 2010**

– Clypeus medio-ventrally straight or weakly convex and no ventral protuberances or lamella; sharp lateral crease of second tergite variable, e.g. complete in most *Sarops* spp. **6**

6 Third to sixth metasomal tergites densely setose; tarsal claws lamelliform, widened apically in dorsal view; third tergite usually partly or largely sculptured [vein r of fore wing issued near middle of pterostigma; parasitoid of *Lipara* spp. in *Phragmites*-galls] .....***Polemochartus*** **Schulz, 1911**

– Third to sixth tergites sparsely setose; tarsal claws normal, cylindrical apically in dorsal view; third tergite smooth.....**7**

7 Ventro-lateral corners of clypeus angled; vein r of fore wing issued subbasally from pterostigma; first tergite widened apically; clypeus distinctly protruding in lateral view.....***Laotris*** **Nixon, 1943**

– Ventro-lateral corners of clypeus rounded; vein r of fore wing issued medially from pterostigma; first tergite subparallel-sided apically; clypeus slightly protruding in lateral view.....***Sarops*** **Nixon, 1942**

Key to species of *Coeliniaspis* Fischer

1 First metasomal tergite 4.9–5.0 times as long as wide apically and about 4.0 times as long as its maximum width (Fig. 4); apical half of second tergite gradually narrowed posteriorly and 6.0 times longer than its apical width (Fig. 6); third tergite smooth; apical half of notauli widely crenulate and connected to medio-posterior depression of mesoscutum (Fig. 3); vertex and frons distinctly remotely punctate (Fig. 8) ..... ***C. insularis*** **(Tobias, 1998) comb. n.**

– First tergite 1.8–2.5 times as long as wide apically and about twice longer than its maximum width; second tergite parallel-sided and 1.5 times longer than its apical width; third tergite more or less sculptured; notauli developed on anterior half of mesoscutum and absent near medio-posterior depression; vertex and frons finely punctulate [clypeus distinctly emarginate medio-ventrally, resulting in a pair of small ventral lobes] **2**

2 Posterior half of notauli present, crenulate and nearly reaching scutellar sulcus; in dorsal view, temple and eye almost equal in length; head in dorsal view 1.5 times wider than long medially; antenna, hind coxa and femur, and apical half of metasoma brownish yellow ..... ***C. rufiventris*** **(Tobias, 1998) comb. n.**

– Posterior half of notauli absent, remaining far from scutellar sulcus; temple in dorsal view 1.4 times as long as eye; head in dorsal view 1.2 times wider than long medially; antenna black (except for yellow scapus); hind coxa and femur dark brown; apical half of metasoma reddish brown .... ***C. kohkongensis*** **Fischer, 2010**

Coeliniaspis insularis **(Tobias, 1998), comb. n.**
Figs 1–10

Coelinius (Sarops) insularis Tobias, 1998: 308–309.
Sarops insularis; Fischer, 2001: 45–47 (redescription).

Description. Female (from Mt. Wuyi): Body length 7.5 mm; fore wing length 4.0 mm.

Head. Antenna with 49 segments present and apical part missing, according to original description with 46–56 segments. First flagellomere 1.1 times as long as second flagellomere, second flagellomere as long as third flagellomere. First and second

flagellomeres 1.8 and 1.7 times as long as their maximum width, respectively. Head in dorsal view subquadrate, 1.4 times as wide as its median length. Eye 1.1 times as long as temple (Fig. 8). OOL:OD:POL = 21:8:6. Mandible with 4 teeth, tooth somewhat curved outwards. Additional tooth between first tooth and middle tooth on base of middle tooth. Middle tooth acute and long, other teeth obtuse and shorter (Fig. 10). Face somewhat protruding, strongly punctate, conspicuously setose, with a weak medio-longitudinal crest on its lower half and a depressed medio-dorsally (Fig. 7). Frons setose, somewhat depressed and rugulose medio-anteriorly (Fig. 8). Clypeus slightly convex dorsally, hardly protruding beyond face in lateral view and medio-ventrally distinctly depressed and without ventral lobes (Fig. 7).

Mesosoma. Length of mesosoma 2.3 times its height. Pronotum with a deep and nearly round pronope (Fig. 8), side of pronotum moderately punctate (Fig. 2). Propleuron largely crenulate-rugose. Mesoscutum conspicuously setose (Figs 2, 3). Notauli complete, wide posteriorly and strongly crenulate. Medio-posterior depression at posterior half of mesoscutum narrow, deep and crenulate (Fig. 3). Scutellar sulcus deep and distinctly crenulate. Scutellum somewhat convex, densely setose. Metanotum with a relatively weak median spine, not protruding beyond scutellum. Propodeum relatively long, largely reticulate-rugose and sparsely setose, medio-longitudinal carina restricted to anterior fifth of propodeum. Mesopleuron mainly glabrous and smooth. Precoxal sulcus long, almost transverse and nearly complete, rugulose (Fig. 2). Mesopleural furrow relatively narrow, curved and evenly crenulate. Metapleuron mainly reticulate-rugose and sparsely setose (Fig. 2).

Wings. Fore wing: pterostigma ellipitical, 0.8 times as long as vein 1-R1; vein r arises from middle of pterostigma; vein r:3-SR+SR1:2-SR = 10:64:21; vein 1-SR+M nearly straight; vein 3-SR+SR1 distinctly sinuate (Fig. 1); vein cu-a postfurcal, almost perpendicular to vein 2-CU1 and 2-1A; vein 1-CU1:2-CU1 = 1:7; first subdiscal cell more or less elongate. Hind wing: 1-1A distinctly curved (Fig. 1); vein M+CU:1-M = 3:2.

Legs. Hind femur 4.0 times as long as wide. Hind tibia as long as its tarsus. Outer and inner hind tibial spurs 0.2 and 0.3 times as long as basitarsus, respectively. Hind basitarsus 2.0 times as long as second tarsal segment. Hind telotarsus 0.8 times as long as third tarsal segment.

Metasoma. Tergites very elongate (Figs 4–6). First tergite 4.0 times as long as its maximum width (5.0 times its apical width), parallel-sided, coarsely longitudinally striate and sparsely setose (Fig. 4). Dorsope relatively large and deep (Fig. 4). Laterope large and finely rugose. Second tergite narrow rectangular and with coarse longitudinal striae, 0.85 times as long as first tergite, and its apical half gradually narrowed posteriorly in dorsal view (Fig. 6), its apical width 0.6 times its basal width, largely glabrous and 6.1 times longer than its apical width. Third and following tergites blade-like compressed (Fig. 5), third tergite smooth and setose. Ovipositor widened and distinctly projecting beyond apex of metasoma (Fig. 9), its setose part 0.2 times as long as first tergite.

Colour. Black. Antenna dark reddish brown. Clypeus black, labrum reddish brown, palpi yellow, mandible reddish brown but edge of teeth black. Pterostigma and most veins of hind wing yellowish brown. Fore and middle legs mainly brownish

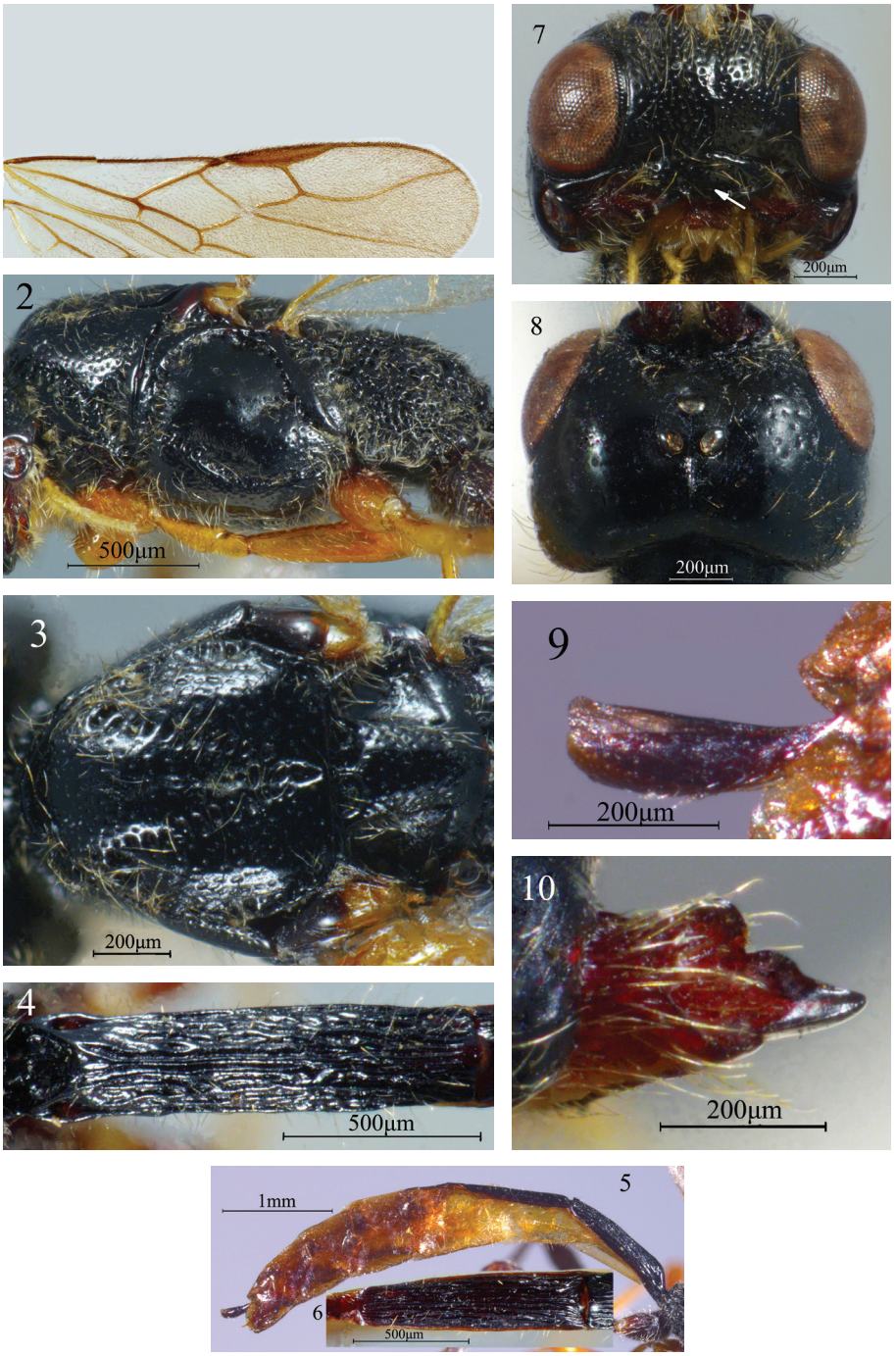

Figures 1–10. *Coeliniaspis insularis* (Tobias), ♀, China, Mt. Wuyi. **1** wings **2** mesosoma, lateral aspect **3** mesonotum, dorsal aspect **4** first metasomal tergite, dorsal aspect **5** metasoma, lateral aspect **6** second metasomal tergite, dorsal aspect **7** head, anterior aspect (arrow indicates clypeal depression) **8** head, dorsal aspect **9** ovipositor sheath, lateral aspect **10** mandible, full sight on second tooth.

yellow, hind leg dark reddish brown but trochanter brownish yellow. First and second tergites mainly black, third and following tergites yellowish brown, ovipositor sheath largely dark brown (Fig. 9).

Male. Similar to female, but body 7.0 mm long, antenna with 69 segments and head, in dorsal view, 1.4 times as wide as its median length. According to the original description, antenna of paratype male with 59 segments.

Biology. Unknown.

Material examined. 1 ♀, China, Fujian, Mt. Wuyi, 3.VII.1981, leg. Yihua Liu; 1 ♂, same data but leg. Juchang Huang.

Distribution. Known only from the type locality in Far East Russia (Sakhalin Obl.) and from China (Fujian). The species and genus are new for China.

Coeliniaspis rufiventris (Tobias, 1998), comb. n.

Coelinius (*Sarops*) *rufiventris* Tobias, 1998: 311.
Sarops insularis; Fischer 2001: 48–49 (redescription).

Notes. The redescription by Fischer (2001) clearly stated that the clypeus is ventrally indented ("eingedellt") and is similar to the type species of the genus *Coeliniaspis* Fischer, 2010. Therefore, we transfer this species (only known from Far Eastern Russia) to the latter genus; the genus is new for Russia.

Acknowledgements

We wish to express our gratitude to Dr Junling Geng of FPDEP (Fujian Provincal Department of Environmental Protection) for her helpful advice on taking photographs. This study was supported by grant No. 2016J01114 of the Fujian Province Science Foundation.

References

van Achterberg C (1988) Revision of the subfamily Blacinae (Hymenoptera: Braconidae). Zoologische Verhandelingen Leiden 249: 1–324.

van Achterberg C (1993) Illustrated key to the subfamilies of the Braconidae (Hymenoptera: Ichneumonoidea). Zoologische Verhandelingen Leiden 283: 1–189, 1–66.

van Achterberg C (2014) Notes on the checklist of Braconidae (Hymenoptera) from Switzerland. Mitteilungen der Schweizerischen Entomologischen Gesellschaft 87: 191–213.

Fischer M (2001) Genauere Studien an jüngst beschriebenen Dacnusini aus dem Fernen Osten Russlands und weiteren Formen aus der Paläarktis (mit einem Anhang über Alysiini) (Hymenoptera, Braconidae, Alysiinae). Linzer Biologische Beiträge 33(1): 35–82.

Fischer M (2010) Einige neue Taxa der Kieferwespen aus der Sammlung des Biologiezentrums des Oberösterreichischen Landesmuseums in Linz (Hymenoptera, Braconidae, Alysiinae). Linzer Biologische Beiträge 42(1): 635–657.

Griffiths GCD (1964) The Alysiinae (Hym. Braconidae) parasites of the Agromyzidae (Diptera) I. General questions of taxonomy, biology and evolution. Beiträge zur Entomologie 14(7–8): 823–914.

Nixon GEJ (1943) A revision of the European Dacnusini (Hym., Braconidae, Dacnusinae). Entomologist's Monthly Magazine 79: 20–34.

Tobias VI (1998) Alysiinae (Dacnusini) and Opiinae. In: Ler PA (Ed.) Key to the insects of Russian Far East. Vol. 4. Neuropteroidea, Mecoptera, Hymenoptera. Pt 3. Dal'nauka, Vladivostok, 299–411, 558–655.

Wharton RA (1994) New genera, species and records of new world Alysiinae (Hymenoptera: Braconidae). Proceedings of the Entomological Society of Washington 96 (4): 630–664.

Yu DSK, van Achterberg C, Horstmann K (2012) Taxapad 2012, Ichneumonoidea 2011. Database on flash-drive. Ottawa, Ontario. http://www.taxapad.com

Zheng ML, Chen JH, van Achterberg C (2013) The discovery of the rare genus *Epimicta* Foerster (Hymenoptera: Braconidae) in China, with a description of a new species. Zootaxa 3613(2): 190–194. https://doi.org/10.11646/zootaxa.3613.2.7

JHR 57: 143–153 (2017)
doi: 10.3897/jhr.57.12517
http://jhr.pensoft.net

RESEARCH ARTICLE

JOURNAL OF Hymenoptera RESEARCH
A peer-reviewed open-access journal
The International Society of Hymenopterists

First record of *Aphidius ericaphidis* (Hymenoptera, Braconidae) in Europe: North American hitchhiker or overlooked Holarctic citizen?

Andjeljko Petrović[1], Jelisaveta Čkrkić[1], Aiman Jamhour[1], Olivera Petrović-Obradović[2], Milana Mitrović[3], Petr Starý[4], Barbro Nedstam[5], Željko Tomanović[1]

1 *Institute of Zoology, Faculty of Biology, University of Belgrade, Studentski trg 16, 11000 Belgrade, Serbia* **2** *Department of Plant Protection, Faculty of Agriculture, University of Belgrade, Nemanjina 6, 11081 Zemun, Serbia* **3** *Department of Plant Pests, Institute for Plant Protection and Environment, Banatska 33, 11080 Zemun, Serbia* **4** *Laboratory of Aphidology, Institute of Entomology, Biology Centre, Academy of Sciences of the Czech Republic, Branišovská 31, 37005 České Budějovice, Czech Republic* **5** *Plant Protection Centre, Swedish Board of Agriculture, Alnarp, Sweden (ret.)*

Corresponding author: *Andjeljko Petrović* (andjeljko@bio.bg.ac.rs)

Academic editor: *J. Fernandez-Triana* | Received 3 March 2017 | Accepted 21 April 2017 | Published 30 June 2017

http://zoobank.org/1F9074E9-6DC6-4326-A392-727C492E5F2F

Citation: Petrović A, Čkrkić J, Jamhour A, Petrović-Obradović O, Mitrović M, Starý P, Nedstam B, Tomanović Ž (2017) First record of *Aphidius ericaphidis* (Hymenoptera, Braconidae) in Europe: North American hitchhiker or overlooked Holarctic citizen? Journal of Hymenoptera Research 57: 143–153. https://doi.org/10.3897/jhr.57.12517

Abstract

Aphidius ericaphidis, an aphid parasitoid originally described from North America, is recorded in Europe for the first time, based on morphological and molecular analyses. The species is recorded in Serbia, the Netherlands, Sweden and the United Kingdom. It was formerly recorded as *Aphidius* sp./*Ericaphis latifrons*/*Vaccinium uliginosum* from the Alps (France). The possible origin of *A. ericaphidis*, as well as its likely distribution, is discussed in relation to its host. As it is a specific parasitoid of *Ericaphis* aphids, especially the invasive aphid *Ericaphis scammelli* on blueberries, its potential as a biocontrol agent is also discussed.

Keywords

Alien species, *Aphidius ericaphidis*, *Ericaphis scammelli*, blueberries, biological control

Copyright *Andjeljko Petrović et al.* This is an open access article distributed under the terms of the Creative Commons Attribution License (CC BY 4.0), which permits unrestricted use, distribution, and reproduction in any medium, provided the original author and source are credited.

Introduction

Growing of highbush blueberry started with the experiments of Coville (1910) in the first decade of the 20th century in the United States. The first successful attempts to grow blueberries in Europe were made in Germany in the 1930s (Heermann 1932). They resulted in the first commercial plantation of 50 ha in 1951 (Pliszka 1997). World blueberry production has been significantly expanding in recent years, owing to the fruit's numerous health benefits. Between 1994 and 2014, the world area under commercial blueberries almost doubled, while production rose four times (FAOSTAT Database). With their high antioxidant capacity, long shelf life and minimal preparation prior to consumption, blueberries are considered a "superfruit" (Clarke 2016).

One of the economically most important blueberry pathogens is the blueberry scorch virus (BlScV), which was first observed in Washington, USA, in commercial blueberry fields (Martin and Bristow 1988). After that it was reported in British Columbia, Canada (Hudgins 2000) and has since spread to Europe (Ciuffo et al. 2005, Paduch-Cichal et al. 2011, Richert-Pöggeler et al. 2015, EPPO 2016). Most of the records are from the commercially grown highbush blueberry (*Vaccinium corymbosum* L.), and according to EPPO there are still no data on the susceptibility of native European *Vaccinium* species (EPPO 2005). Symptoms caused by BlScV differ depending on the cultivar of blueberry. In sensitive cultivars, infection can lead to complete necrosis (blighting) of flowers and young leaves and twig dieback followed by severe yield loss, while tolerant cultivars can show little or no visible symptoms of infection (Bristow et al. 2000, Martin et al. 2012).

The blueberry scorch virus is transmitted mainly by *Ericaphis fimbriata* (Richards) in a nonpersistent manner (Bristow et al. 2000). *Ericaphis fimbriata* is probably synonymous with *E. scammelli* (Mason), based on morphological and molecular analyses (Blackman and Eastop 1984, Foottit et al. 2008, G. Bosio – pers. comm. 2001, V. Eastop – pers. comm. 2002) and will be referred to as *E. scammelli* in this paper. The aphid is most likely native to North America and was probably introduced into Europe with plant material (Barbagallo et al. 1998), with the first record for Europe from the UK in 1964 (Cœur d'acier et al. 2010). In Britain it was described as *E. fimbriata* ssp. *pernettyae*, monoecious holocyclic on *Pernettya mucronata* but probably also holocyclic on *Vaccinium* species (Prior 1971), Italian populations are referred to as *E. scammelli* and are monoecious holocyclic on *Vaccinium* spp. (Blackman and Eastop 1984, Barbagallo et al. 1998, Pansa and Tavela 2008). Besides those two countries, it has also been recorded in the Netherlands, France (Nieto Nafria 2013) and Sweden (Nedstam 2008).

The braconid parasitoid complex of *E. scammelli* (=*E. fimbriata*) in North America consists of 10 species (Hymenoptera: Aphidiinae), among which the most common are *Praon unicum* Smith, 1944 and *Aphidius ericaphidis* Pike & Starý, 2011 (Raworth et al. 2008, Pike et al. 2011, Mathur et al. 2013). Here we present the first records of *A. ericaphidis* from Europe and discuss its potential as a biocontrol agent in European blueberry orchards.

Methods

During the last several years, the Aphidiinae fauna on different fruit species was investigated throughout Europe. Samples of *Vaccinium* spp. leaves with aphids and mummies were collected. The samples were kept under laboratory conditions until parasitoid emergence. After emergence, parasitoids were immersed in 96% ethanol and preserved for later examination. External morphology of the specimens was studied using a ZEISS Discovery V8 stereomicroscope. Scanning electron micrographs were obtained using a JEOL JSM-6390 scanning electron microscope. All specimens are deposited in the collection of the Institute of Zoology, Faculty of Biology, University of Belgrade and the collection of P. Starý, České Budějovice, Czech Republic.

Molecular analysis

Three *A. ericaphidis* specimens from Scotland were used for molecular analysis. DNA was extracted from individual adult wasps using the Qiagen DNeasy Blood & Tissue Kit (Qiagen Inc., Valencia, CA) following the manufacturer's instructions. The barcoding region of the mitochondrial cytochrome oxidase subunit I (COI) gene was amplified using the primers LCO1490 and HCO2198 (Folmer et al. 1994).

DNA amplification was performed in a final volume of 20 µl containing 1 µl of DNA, 11.8 µl of H_2O, 2 µl of High Yield Reaction Buffer A with 1 x Mg, 1.8 µl of $MgCl_2$ (2.25 mM), 1.2 µl of dNTP (0.6 mM), 1 µl of each primer (0.5 µM) and 0.2 µl of KAPATaq DNA polymerase (0,05U/µl) (Kapa Biosystems Inc., USA). PCR was conducted in an Eppendorf Mastercycler® (Hamburg, Germany) using the following thermal profile: initial denaturation at 95°C for 5 min, followed by 35 cycles of 94°C for 60 s, 54°C for 60 s, 72°C for 90 s and a final extension step at 72°C for 7 min. Purification of PCR products and DNA sequencing in both directions was performed by Macrogen Inc. (Seoul, Korea).

Sequences of *A. ericaphidis* specimens from North America and other *Aphidius* species were obtained from GenBank and used in phylogenetic analysis. Those *Aphidius* species were chosen because of their morphological similarity to *A. ericaphidis* or because they parasitize *E. scammelli*. An *Ephedrus* sp. sequence from GenBank (acc. number KR787408) was used as an outgroup taxon. Sampling data for specimens used in this study are given in Table 1.

Sequences were edited using FinchTV ver 1.4.0 (http://www.geospiza.com). Alignment was conducted using CLUSTAL W integrated in MEGA 5 software (Tamura et al. 2011). Sequences were trimmed to a length of 611 bp. The sequences of analysed *A. ericaphidis* specimens were deposited in GenBank under accession numbers KY513289–KY513291. Calculation of average genetic distances between sequences was performed using Kimura's two-parameter method (K2P) of base substitution (Kimura 1980).

A phylogenetic tree was constructed using the MEGA 5 software (Tamura et al. 2011) and the Maximum likelihood method with 1000 bootstrap replicates.

Table 1. Sampling data for Aphidiinae specimens used in the molecular analysis.

Parasitoid	Code	Geographic origin	Aphid host	Plant	Accession number
Aphidius ericaphidis	IM50	Scotland	*Ericaphis scammelli*	*Vaccinium corymbosum*	KY513289
Aphidius ericaphidis	IM51	Scotland	*Ericaphis scammelli*	*Vaccinium corymbosum*	KY513290
Aphidius ericaphidis	IM52	Scotland	*Ericaphis scammelli*	*Vaccinium corymbosum*	KY513291
Aphidius ericaphidis		Canada/USA	*Ericaphis fimbriata*	*Vaccinium corymbosum*	KC211024
Aphidius ericaphidis		Canada/USA	*Ericaphis fimbriata*	*Vaccinium corymbosum*	EU574902
Aphidius avenaphis		USA	*Sitobion avenae*	*Triticum aestivum*	JN164784
Aphidius matricariae		Canada			KR888554
Aphidius urticae		UK			JX507436
Aphidius ervi		Canada/USA			KC211026
Ephedrus sp.					KR787408

Results

Aphids infesting *Vaccinium corymbosum* in Serbia, Sweden and Scotland were identified as *E. scammelli.* Rearing parasitoids from *E. scammelli* resulted in finding the species *A. ericaphidis* for the first time in Europe. *Aphidius ericaphidis* is recorded in Serbia, Sweden and the United Kingdom (Scotland). Additional re-examination of collections (P. Starý) led to identification of *A. ericaphidis* in France and the Netherlands as well, the re-examined specimens from both countries having been previously identified as *Aphidius* sp. (Starý et al. 1971, P. Starý unpubl.). In total 24 females and 19 males were found.

As the original differential diagnosis of *A. ericaphidis* referred to North American congeners (Pike et al. 2011), it is advisable to relate it also to those in Europe as follows: *Aphidius ericaphidis* (Fig. 1) is most similar to *Aphidius matricariae* Haliday 1834. It can be easily distinguished from the latter by the number of maxillary and labial palpomeres [*A. matricariae* has 3-segmented maxillary palps and 2-segmented labial palps vs. 4-segmented maxillary palps and 3-segmented labial palps in *A. ericaphidis*] and by pterostigma length / R1 forewing vein ratio [*A. matricariae* = 1.1 (range 1–1.2) vs. *A. ericaphidis* = 2.1 (range 1.7–2.7)].

Aphidius ericaphidis

Fig. 1

Serbia, Mladenovac, 10 VI 2015, 7 females and 4 males reared from *Ericaphis scammelli* on *Vaccinium corymbosum*; 23 VI 2015, 3 males reared from *Ericaphis scammelli* on *Vaccinium corymbosum.* United Kingdom, Scotland, 19 VI 2014, 9 females and 5 males reared from *Ericaphis scammelli* on *Vaccinium corymbosum*. Sweden,

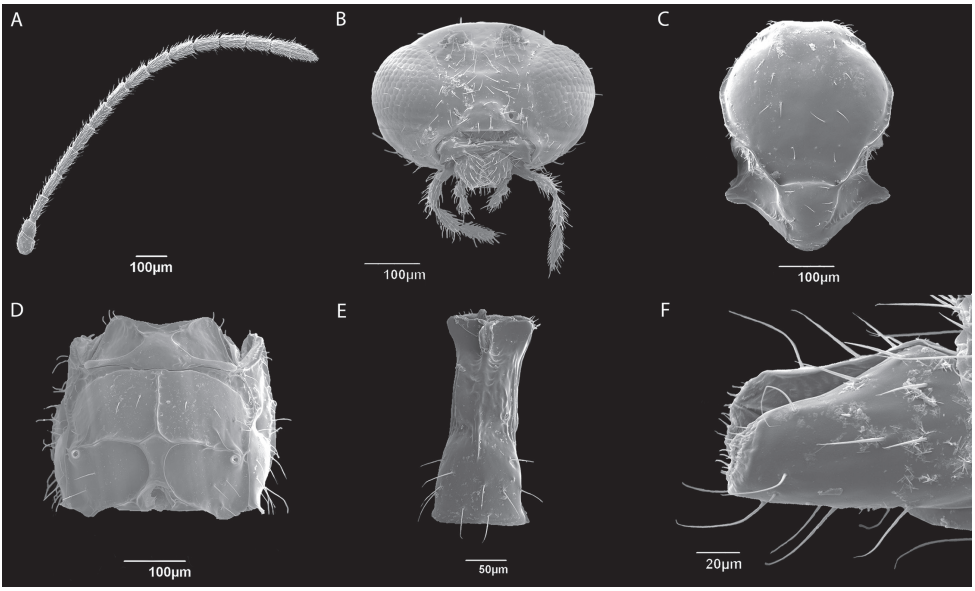

Figure 1. *Aphidius ericaphidis* female: **A** antenna **B** head **C** mesonotum – dorsal aspect **D** propodeum – dorsal aspect **E** petiole – dorsal aspect **F** ovipositor – lateral aspect.

Glemmingebro, Scania, 24 VI 2008, 1 female and 1 male from *Ericaphis scammelli* on *Vaccinium corymbosum*; 30 VI 2008, 5 females and 5 males from *Ericaphis scammelli* on *Vaccinium corymbosum*, greenhouse. Netherlands, Kootwijk, 8 VI 1965, 1 female from *Ericaphis latifrons* on *Empetrum nigrum.* France, Lognan (Hte-Savoie), 12 VIII 1968, 1 female and 1 male from *Ericaphis latifrons* on *Vaccinium uliginosum*.

Molecular analysis of *Aphidius ericaphidis*

Three barcoding sequences of *A. ericaphidis* originating from Scotland were compared with two sequences of *A. ericaphidis* from the USA and were determined to be identical, with no variable sites detected.

Topology of the phylogenetic tree shows clear separation of *A. ericaphidis* from other *Aphidius* species used in the analysis (Fig. 2). Though morphologically more similar to it than to the other *Aphidius* species, *A. ericaphidis* did not cluster with *A. matricariae*, and the mean K2P distance between the two species was 8.1% (Table 2). Divergence rates in relation to other species morphologically similar to *A. ericaphidis* or parasitizing *E. scammelli* were as follows: *A. urticae* – 8.9%, *A. avenaphis* – 10.4% and *A. ervi* – 8.3% (Table 2). Those distances are greater than what is considered to be enough for the separation of Aphidiinae species (Derocles et al. 2012, Tomanović et al. 2014). Thus, after morphological description, we here support the status of this taxon with molecular analysis.

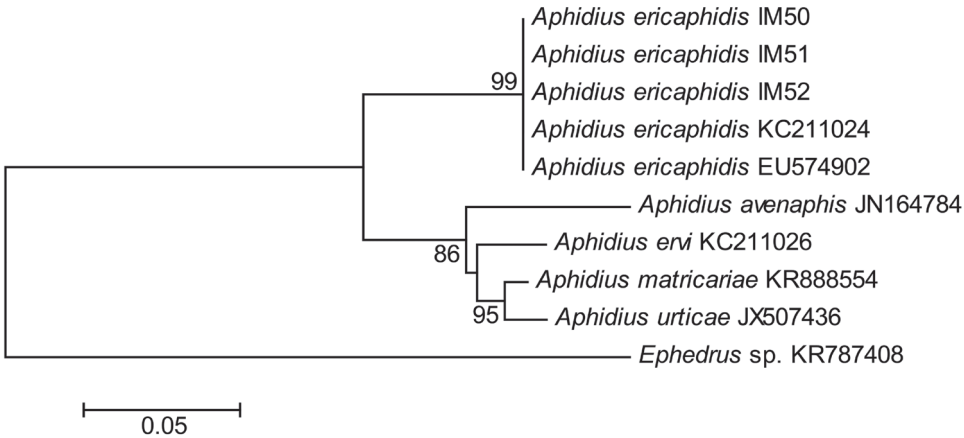

Figure 2. Phylogenetic tree based on COI sequences inferred by Maximum Likelihood (ML) method. Bootstrap values over 80% are shown.

Table 2. Mean K2P distances between COI sequences of *Aphidius* species used in this study.

	A. ericaphidis	***A. matricariae***	***A. urticae***	***A. avenaphis***
A. ericaphidis				
A. matricariae	0.081			
A. urticae	0.089	0.018		
A. avenaphis	0.104	0.058	0.063	
A. ervi	0.083	0.034	0.037	0.065

Discussion

Highbush blueberry production has been on the rise in the world, and as a consequence of increased international trade of planting material, plant pathogens and pests are also being spread to new areas. In the last 15 years, two exotic *Vaccinium* pathogens with North American origin (*Monilinia vaccinii-corymbosi* and BlScV) were detected in Europe, and it is assumed that both were imported with plant material (Gosch 2003, Ciuffo et al. 2005, Munda 2011, Paduch-Cichal et al. 2011, Richert-Pöggeler et al. 2015). The situation is the same with at least two pest species, blueberry gall midge *Dasineura oxycoccana* and the aphid *Ericaphis scammelli*, which most likely also have a North American origin (Bosio et al. 1998, Barbagallo et al. 1998). Although *E. scammelli* (under different names) has been present in Europe for over half a century (Cœur d'acier et al. 2010), *A. ericaphidis* is its first parasitoid detected in Europe (in Serbia, Sweden, the Netherlands, France and the United Kingdom). While most alien Aphidiinae species reported in Europe were introduced intentionally as biocontrol agents (Roy et al. 2011, Petrović et al. 2013), for *A. ericaphidis* this is not the case. Some *A. ericaphidis* populations were most likely founded by specimens introduced accidentally with *Vaccinium* plant material "hitchhiking" in *E. scammelli*. This is the

most obvious scenario for the records from Serbia and Sweden. Intensive research of Aphidiinae in Serbia has been ongoing for more than 20 years, and one of the main focuses has been on the Aphidiinae fauna of high mountain plants (including native *Vaccinium* species). Until recently (2015), there was no evidence of either *E. scammelli* or *A. ericaphidis* (Kavallieratos et al. 2004, Žikić et al. 2012). Both the aphid and the parasitoid were detected for the first time on a commercial *V. corymbosum* plantation with material imported from the Netherlands (probably originating from North America). *Aphidius ericaphidis* from *E. scammelli*/*V. corymbosum* in a greenhouse in Sweden might also be a result of an accidental introduction from North America via blueberry nurseries in Germany. The same year when *A. ericaphidis* was recorded (2008), a detailed survey of aphids on blueberries (native and highbush plantations) was conducted, and the parasitoid was found only in one greenhouse situated about 30 km from the nearest forest woodland and surrounded by farmland (B. Nedstam unpubl.).

However, our revision of material from earlier collections from France and the Netherlands showed that the parasitoid has been present in Europe at least as long as *E. scammelli* (if not longer). At the time of the records, blueberry production in Europe wasn't as extensive as it is today, and the import of plants from North America was limited to a few countries. The record from France suggests that those populations of *A. ericaphidis* had enough time to spread and establish, especially since the record is from a native high mountain ecosystem (*Vaccinium uliginosum*/*Ericaphis latifrons*/*Aphidius ericaphidis*).

The lack of any genetic differences shows that analysed European and North American populations of *A. ericaphidis* are very closely related. This can suggest that the analysed specimens were from a recent introduction or that they represent a species with no genetic differentiations based on the COI gene, as has been recorded before for some other *Aphidius* species (*A. uzbekistanicus* and *A. avenaphis*) (Tomanović et al. 2013).

Since molecular and morphological analyses of the target parasitoid populations revealed no significant differences, it might be concluded that *A. ericaphidis* is a member of the Holarctic forest tundra faunistic complex (Starý 1970) associated with different *Ericaphis* aphids in both Europe and North America. Although it is a very common parasitoid of *Ericaphis* in North America (at least in the Pacific Northwest) (Pike et al. 2011), in Europe it is quite rare, with only two records prior to 2008 (Starý et al. 1971, P. Starý unpubl.). There are two main factors contributing to the spread of *A. ericaphidis* in Europe during the last decade. The first one involves probable multiple introductions from North America with planting material and *E. scammelli*; the second one consists of a possible new adaptation of European populations of *A. ericaphidis* to this introduced aphid.

The current known host range of European populations of *A. ericaphidis* is similar to that of North American populations, with the vast majority of records reported from *Ericaphis* aphids (Pike et al. 2011). Although three out of 10 parasitoid species (*Aphidius ervi*, *Aphidius matricariae* and *Lysiphlebus testaceipes*) that parasitize *E. scammelli* in North America also occur in Europe, *A. ericaphidis* is the only species recorded that successfully parasitizes *E. scammelli* (Suppl. material 1: Table S1.). In this respect, there is potential

in biological control of these aphids, which can serve as vectors of the blueberry scorch virus if populations are left uncontrolled. Since the virus has spread to Europe recently, the possibility of using *A. ericaphidis* as a biocontrol agent should be investigated thoroughly. It can then be added to the list of already tested European Aphidiinae species for which the ability to control *E. scammelli* in field conditions has been determined (Dassonville et al. 2013). Of course, this requires very careful additional testing, since there are several parasitoid species that were introduced as biocontrol agents and then became widespread (Roy et al. 2011) and broadened their host range in non-native areas (Mitrović et al. 2013, Petrović et al. 2013). On the other hand, Pike et al. (2011) report rare occurrences of parasitization of *Macrosiphum parvifolii* Richards by *A. ericaphidis*, which implies its potential to parasitize other species.

The current distribution of *A. ericaphidis* and that of its host *Ericaphis scammelli* in Europe are most likely much broader than those recorded so far, and field surveys should therefore be conducted in all *Vaccinium* growing areas to monitor the spread of *A. ericaphidis* in Europe and possible changes of its host range.

Acknowledgements

This study was supported by the Ministry of Education, Science and Technological Development of the Republic of Serbia (project III43001). The participation of P. Starý was funded by the Institute of Entomology, while that of B. Nedstam (ret.) was funded by the Swedish Board of Agriculture. We thank the Viridaxis company for the loan of *A. ericaphidis* specimens from Scotland.

References

Barbagallo S, Bosio G, Brussino G, Scarpelli F (1998) Gli afidi infestanti le colture del mirtillo gigante americano in Italia. Informatore Fitopatologico 48: 65–71. http://www.verdeeparesaggio.it/2008/02/04/afidi-infestanti-le-colture-del-mirtillo-gigante-americano-in-italia/

Blackman RL, Eastop VF (1984) Aphids on the world's crops: an identification and information guide. Wiley, New York, 466 pp.

Bosio G, Bogetti C, Brussino G, Gremo F, Scarpelli F (1998) *Dasineura oxycoccana*, a new pest of blueberry (*Vaccinium corymbosum*) in Italy. Informatore Fitopatologico 11: 36–41.

Bristow PR, Martin RR, Windom GE (2000) Transmission, field spread, cultivar response, and impact on yield in highbush blueberry infected with *Blueberry scorch virus*. Phytopathology 90(5): 474–479. http://dx.doi.org/10.1094/PHYTO.2000.90.5.474

Ciuffo M, Pettiti D, Gallo S, Masenga V, Turina M (2005) First report of *Blueberry Scorch Virus* in Europe. Plant Pathology 54: 565. http://dx.doi.org/10.1111/j.1365-3059.2005.01198.x

Clarke S (2016) Blueberries in the European Union. Agriculture and Agri-Food Canada. http://www.agr.gc.ca/resources/prod/Internet-Internet/MISB-DGSIM/ATS-SEA/PDF/6719-eng.pdf

Cœur d'acier A, Pérez Hidalgo N, Petrović-Obradović O (2010) Aphids (Hemiptera, Aphididae). In: Roques A, Kenis M, Lees D, Lopez-Vaamonde C, Rabitsch W, Rasplus JY, Roy D (Eds) Alien terrestrial arthropods of Europe. Biorisk 4(1): 435–474. http://dx.doi.org/10.3897/biorisk.4.57

Coville FV (1910) Experiments in blueberry culture. U.S. Department of Agriculture Bulletin 193.

Dassonville N, Thiellemans T, Gosset V (2013) FresaProtect and BerryProtect: mixes of parasitoids to control all common aphid species on protected soft fruit crops: Product development and case studies from three years of experience. Aspects of Applied Biology 119: 79–81. http://www.viridaxis.com/wp-content/uploads/emr_case_studies.pdf

Derocles SA, Le Ralec A, Plantegenest M, Chaubet B, Cruaud C, Cruaud A, Rasplus JY (2012) Identification of molecular markers for DNA barcoding in the Aphidiinae (Hymenoptera: Braconidae). Molecular Ecology Resources 12: 197–208. http://dx.doi.org/10.1111/j.1755-0998.2011.03083.x

EPPO [European and Mediterranean Plant Protection Organisation] (2005) First report of Blueberry scorch carlavirus in Europe: addition to the EPPO Alert List. https://gd.eppo.int/reporting/article-1433 [accessed on 10.1.2017]

EPPO [European and Mediterranean Plant Protection Organisation] (2016) *Blueberry scorch virus* (BLSCV0). https://gd.eppo.int/taxon/BLSCV0/distribution [accessed on 10.1.2017]

Food and Agriculture Organization of the United Nations (2012) FAOSTAT Database. FAO, Italy, Rome. http://faostat3.fao.org/home/E [January 25, 2017]

Folmer O, Black M, Hoeh W, Lutz R, Vrijenhoek R (1994) DNA primers for amplification of mitochondrial cytochrome c oxidase subunit I from diverse metazoan invertebrates. Molecular Marine Biology and Biotechnology 3: 294–299. https://www.ncbi.nlm.nih.gov/pubmed/7881515

Foottit RG, Maw HEL, von Dohlen CD, Hebert PDN (2008) Species identification of aphids (Insecta: Hemiptera: Aphididae) through DNA barcodes. Molecular Ecology Resources 8: 1189–1201. http://dx.doi.org/10.1111/j.1755-0998.2008.02297.x

Gosch C (2003) *Monilinia vaccinii-corymbosi* on Highbush Blueberries (*Vaccinium corymbosum* L.): Also in Europe! European Journal of Horticultural Science 68(5): 238–241.

Heermann W (1932) Witere Beiträge zur Heidelbeerzüchtung. Der Züchter 4(1): 1–8.

Hudgins E (2000) Survey of *Blueberry Scorch Virus* in highbush blueberries in British Columbia. Canadian Plant Disease Survey 81:144–147.

Kavallieratos NG, Tomanović Ž, Starý P, Athanassiou CG, Sarlis GP, Petrović O, Niketić M, Veroniki MA (2004) A survey of aphid parasitoids (Hymenoptera: Braconidae: Aphidiinae) of Southeastern Europe and their aphid-plant associations. Applied Entomology and Zoology 39(3): 527–563. http://dx.doi.org/10.1303/aez.2004.527

Kimura M (1980) A simple method for estimating evolutionary rate of base substitutions through comparative studies of nucleotide sequences. Journal of Molecular Evolution 16: 111–120. http://dx.doi.org/10.1007/bf01731581

Mathur S, Raworth DA, Pike KS, Fitzpatrick SM (2013) Diagnostic molecular markers to detect and identify primary parasitoids (Hymenoptera: Braconidae) of *Ericaphis fimbriata* on highbush blueberry. Journal of the Entomological Society of British Columbia 110: 19–26. http://journal.entsocbc.ca/index.php/journal/article/view/289

Martin RR, Bristow PR (1988) A Carlavirus associated with Blueberry Scorch Disease. Phytopathology 78(12): 1636–1640. http://dx.doi.org/10.1094/Phyto-78-1636

Martin RR, Polashock JJ, Tzanetakis IE (2012) New and emerging viruses of blueberry and cranberry. Viruses 4: 2831–2852. http://dx.doi.org/10.3390/v4112831

Mitrović M, Petrović A, Kavallieratos NG, Starý P, Petrović-Obradović O, Tomanović Ž, Vorburger C (2013) Geographic structure with no evidence for host-associated lineages in European populations of *Lysiphlebus testaceipes*, an introduced biological control agent. Biological Control 66(3): 150–158. http://dx.doi.org/10.1016/j.biocontrol.2013.05.007

Munda A (2011) *Monilinia* pathogens of cultivated and native *Vaccinium* species in Slovenia. Acta Agriculturae Slovenica 97: 99–104. http://dx.doi.org/10.2478/v10014-011-0005-9

Nedstam B (2008) Some pest problems and solutions in Swedish organic greenhouse production. Integrated Control in Protected Crops, Temperate Climate, IOBC/wprs Bulletin 32: 155–157. http://www.iobc-wprs.org/pub/bulletins/iobc-wprs_bulletin_2008_32.pdf#page=171

Nieto Nafria JM (2013) Fauna Europaea: Hemiptera, Aphididae. Fauna Europaea version 2.6.2. http://www.faunaeur.org

Paduch-Cichal E, Kalinowska E, Chodorska M, Sala-Rejczak K, Nowak B (2011) Detection and identification of viruses of highbush blueberry and cranberry using serological ELISA test and PCR technique. Acta Scientiarum Polonorum, Hortorum Cultus 10(4): 201–215. http://wydawnictwo.up.lublin.pl/acta/hortorum_cultus/2011/4/18.pdf

Pansa MG, Tavella L (2008) Aphid population dynamics on highbush blueberry in relation to the spread of *Blueberry scorch virus* in Piedmont (NW Italy). Bulletin of Insectology 61(1): 205–206. http://www.bulletinofinsectology.org/pdfarticles/vol61-2008-205-206pansa.pdf

Petrović A, Mitrović M, Starý P, Petrović-Obradović O, Žikić V, Tomanović Ž, Vorburger C (2013) *Lysiphlebus orientalis* (Hymenoptera, Braconidae), a new invasive aphid parasitoid in Europe – evidence from molecular markers. Bulletin of Entomological Research 103: 451–457. http://dx.doi.org/10.1017/S0007485313000035

Pike KS, Starý P, Graf G, Raworth DA, Mathur S, Tanigoshi LK, Murray T (2011) A new *Aphidius* Nees (Hymenoptera, Braconidae, Aphidiinae) of *Ericaphis fimbriata* (Richards) (Hemiptera, Aphididae) and key to parasitoids of blueberry aphid in the Pacific Northwest. Zootaxa 2802: 58–62. http://www.mapress.com/j/zt/article/view/10775

Pliszka K (1997) Overview on *Vaccinium* production in Europe. Acta Horticulturae 446: 49–52. http://dx.doi.org/10.17660/ActaHortic.1997.446.5

Prior RNB (1971) Some notes on new or uncommon aphids recently found in Britain. Zoological Journal of the Linnaean Society 50: 397–430. http://dx.doi.org/10.1111/j.1096-3642.1971.tb00768.x

Raworth DA, Pike KS, Tanigoshi LK, Mathur S, Graf G (2008) Primary and secondary parasitoids (Hymenoptera) of aphids (Hemiptera: Aphididae) on blueberry and other *Vaccinium* in the Pacific Northwest. Community and Ecosystem Ecology 37(2): 472–477. http://dx.doi.org/10.1093/ee/37.2.472

Richert-Pöggeler KR, Turhal AK, Schuhmann S, Maaß C, Blockus S, Zimmermann E, Eastwell KC, Martin RR, Lockhart B (2015) *Carlavirus* biodiversity in horticultural host plants: Effi-

cient virus detection and identification combining electron microscopy and molecular biology tools. Acta Horticulturae 1072: 37–45. http://dx.doi.org/10.17660/ActaHortic.2015.1072.3

Roy HE, Roy DB, Roques A (2011) Inventory of terrestrial alien arthropod predators and parasites established in Europe. BioControl 56: 477–504. http://dx.doi.org/10.1007/s10526-011-9355-9

Starý P (1970) Biology of aphid parasitoids (Hymenoptera, Aphidiidae) with respect to integrated control. Dr. W. Junk, The Hague, 1–643.

Starý P, Remaudière G, Leclant F (1971) Les Aphidiidae (Hym.) de France et leurs hôtes (Hom. Aphididae): description d'espèces nouvelles, ècologie, lutte biologique. Entomophaga, Mémoire Hors-série 5: 1–72.

Tamura K, Peterson D, Peterson N, Stecher G, Nei M, Kumar S (2011) MEGA5: Molecular evolutionary genetics analysis using maximum likelihood, evolutionary distance and maximum parsimony methods. Molecular Biology and Evolution 28: 2731–2739. http://dx.doi.org/10.1093/molbev/msr121

Tomanović Ž, Kos K, Petrović A, Starý P, Kavallieratos NG, Žikić V, Jakše J, Trdan S, Ivanović A (2013) The relationship between molecular variation and variation in the wing shape of three aphid parasitoid species: *Aphidius uzbekistanicus* Luzhetzki, *Aphidius rhopalosiphi* De Stefani Perez and *Aphidius avenaphis* (Fitch) (Hymenoptera: Braconidae: Aphidiinae). Zoologischer Anzeiger 252(1): 41–47. https://doi.org/10.1016/j.jcz.2012.03.003

Tomanović Ž, Petrović A, Mitrović M, Kavallieratos NG, Starý P, Rakhshani E, Rakhshanipour M, Popović A, Shukshuk AH, Ivanović A (2014) Molecular and morphological variability within the *Aphidius colemani* group with redescription of *Aphidius platensis* Brethes (Hymenoptera: Braconidae: Aphidiinae). Bulletin of Entomological Research 104: 552–565. http://dx.doi.org/10.1017/S0007485314000327

Žikić V, Ilić-Milošević M, Stanković S, Petrović A, Petrović-Obradović O, Kavallieratos N, Starý P, Tomanović Ž (2012) Aphidiinae (Hymenoptera: Braconidae) of Serbia and Montenegro – tritrophic interactions. Acta Entomologica Serbica 17(1/2): 83–105. http://www.eds.org.rs/AES/Vol17/Zikic%20et%20al%20(2012).pdf

Supplementary material 1

Table S1. Parasitoids of *Ericaphis* aphids from North America and Europe

Authors: Andjeljko Petrović, Jelisaveta Čkrkić, Aiman Jamhour, Olivera Petrović-Obradović, Milana Mitrović, Petr Starý, Barbro Nedstam, Željko Tomanović

Data type: species data

Copyright notice: This dataset is made available under the Open Database License (http://opendatacommons.org/licenses/odbl/1.0/). The Open Database License (ODbL) is a license agreement intended to allow users to freely share, modify, and use this Dataset while maintaining this same freedom for others, provided that the original source and author(s) are credited.

Link: https://doi.org/10.3897/jhr.57.12517.suppl1

JHR 57: 155–166 (2017)
doi: 10.3897/jhr.57.12990
http://jhr.pensoft.net

RESEARCH ARTICLE

JOURNAL OF Hymenoptera RESEARCH
A peer-reviewed open-access journal
The International Society of Hymenopterists

Host-Dryinidae (Hymenoptera) interactions on edge grasses of maize agroecosystem throughout winter in Mexico

Iskra M. Becerra-Chiron[1], Gustavo Moya-Raygoza[1], Alejandro Muñoz-Urias[2]

1 *Departamento de Botánica y Zoología, CUCBA, Universidad de Guadalajara, km 15.5 carretera Guadalajara-Nogales, Las Agujas, Zapopan, C.P. 45110, Apdo. Postal 139, Jalisco, México* **2** *Departamento de Ecología, CUCBA, Universidad de Guadalajara, km 15.5 carretera Guadalajara-Nogales, Las Agujas, Zapopan, C.P. 45110, Apdo. Postal 139, Jalisco, México*

Corresponding author: *Gustavo Moya-Raygoza* (moyaraygoza@gmail.com)

Academic editor: *J. Neff* | Received 31 March 2017 | Accepted 3 May 2017 | Published 30 June 2017

http://zoobank.org/9B5E8065-CCA9-42F2-AE0C-286A6B6A7653

Citation: Becerra-Chiron IM, Moya-Raygoza G, Muñoz-Urias A (2017) Host-Dryinidae (Hymenoptera) interactions on edge grasses of maize agroecosystem throughout winter in Mexico. Journal of Hymenoptera Research 57: 155–166. https://doi.org/10.3897/jhr.57.12990

Abstract

Little is known about the host-parasitoid interactions on the edges of crops during winter. Our objective was to determine the parasitoid species that attack nymphs and adults of leafhoppers and planthoppers, and evaluate the interactions that occur during winter on maize edges. Between January and June of 2014 and 2015 leafhoppers and planthoppers with evidence of parasitism by Dryinidae (Hymenoptera) were collected on grasses that grow in maize fields margins in Mexico and were maintained alive until parasitoid adult emergence. Dryinids such as *Gonatopus huggerti* (Olmi), *Gonatopus mimoides* (Perkins), *Gonatopus breviforceps* (Kieffer), and *Gonatopus caraibicus* (Olmi) were the most common parasitoids. They attacked several leafhopper species such as *Dalbulus maidis* (DeLong), *Balclutha incisa* (Matsumura), *Exitianus picatus* (Gibson), and *Stirellus bicolor* (Van Duzee). The connection of the net was of 31%. The presence of parasitoids in winter margins highlights the importance of conserving maize edges for biological control.

Keywords

Chrysidoidea, Auchenorrhyncha, Cicadellidae, biological control, Host-parasitoid interactions

Copyright *Iskra M. Becerra-Chiron et al.* This is an open access article distributed under the terms of the Creative Commons Attribution License (CC BY 4.0), which permits unrestricted use, distribution, and reproduction in any medium, provided the original author and source are credited.

Introduction

Edges in agroecosystems form a habitat hosting herbivore insects and their predators and parasitoids (Marshall and Moonen 2002, Ramsden et al. 2015). In addition, edges where perennial plants live, offer green resources during winter and become places with high insect biodiversity (Dennis and Fry 1992, Vollhardt et al. 2008). In addition, edges are important during winter when the crop is absent because they offer food, refuge, and sites for reproduction that help in the survival of herbivores and their natural enemies (Rabb et al. 1976, Marshall and Moonen 2002, Ramsden et al. 2015). Most of the edges in agroecosystems are formed by grasses (Marshall and Moonen 2002, Moya-Raygoza and Becerra-Chiron 2014), which contain a large number of herbivore leafhoppers (Hemiptera: Cicadellidae) (Hamilton and Whitcomb 2010).

Many leafhopper species are efficient vectors of viruses and bacteria to plants (Nault and Bradfute 1979, Weintraub and Beanland 2006). For example, in maize, which is one of the most important cereals in the world (Buckler et al. 2001), the leafhopper *Exitianus* sp. and *Exitianus obscurinervis* (Stål) (Hemiptera: Cicadellidae) transmit the bacterium Corn Stunt Spiroplasma (CSS) *Spiroplasma kunkelii* (Virla 2000, Carloni et al. 2011). Also, the leafhopper *Stirellus bicolor* (Van Duzee)(Hemiptera: Cicadellidae) transmits CSS, the Maize Rayado Fino Virus (MRFV), and the Maize Chlorotic Dwarf Virus (MCDV) (Nault and Bradfute 1979, Nault 1980, Wayadande and Nault 1993). Another vector is the corn leafhopper *Dalbulus maidis* (DeLong) (Hemiptera: Cicadellidae), considered the most important leafhopper pest of maize throughout Latin America, because it can transmit efficiently CSS, Maize Bushy Stunt Phytoplasma (MBSP), and MRFV (Nault 1990). In addition, leafhopper species that do not transmit plant pathogens inhabit edge grasses such as *Balclutha incisa* (Matsumura) (Hemiptera: Cicadellidae) (Narhardiyati and Bailey 2005) and *Amblysellus* sp. (Hemiptera: Cicadellidae). Leafhoppers that occur during the winter season on perennial grasses bordering maize fields are diverse with *S. bicolor*, *Graminella sonora* (Ball), *Dalbulus elimatus* (Ball), *D. maidis*, *B. incisa*, and *Exitianus picatus* (Gibson) (Hemiptera: Cicadellidae) being the most abundant species (Pinedo-Escatel and Moya-Raygoza 2015). However, none of the previous species were found to be positive for CSS or MBSP, suggesting that these two bacteria do not pass the winter in leafhoppers that overwinter on edge grasses (Torres-Moreno et al. 2015).

On the other hand, leafhoppers that inhabit edge grasses of maize fields were parasitized by dryinids and strepsipterans during the dry season (Moya-Raygoza and Becerra-Chiron 2014). Leafhoppers such as *Stirellus bicolor*, *G. sonora*, *E. picatus*, *Ambysellus* sp. and *D. maidis* are attacked by parasitoids. However, the species that attack these leafhoppers have not been investigated. Therefore, the objective of the present study was to search for adult parasitoids that attack nymphs and adult leafhoppers throughout the winter season on perennial grasses that border harvested maize agroecosystems and build a net between host species and parasitoid species to know the link among them.

Methods

The study was conducted in the region of Zapopan, state of Jalisco, Mexico 20°44'49"N, 103°30'48"W; 1,662 m above sea level. This region was selected because it represents the environmental condition in which maize is cultivated in most of the tropics. Maize is seeded there in June, when the wet season starts. Maize plants dry out in November and are harvested in December. From December to May grasses grow and have green foliage in the maize edges. This study was conducted during two consecutive winter seasons in 2014 and 2015, starting in January and ending in May. Sampling was done three times per week, using a sweep net for one hour between 11 am. and noon and performing 1,200 sweeps per sampling.

The collected hopper (leafhoppers or planthoppers) nymphs or adults with evidence of parasitism were maintained alive. Parasitized hoppers show on the thorax or abdomen a black sac hosting a larva of a parasitoid (Rios-Reyes and Moya-Raygoza 2004, Kathirithamby 2005). The live parasitized hoppers were transferred to leaf-cages on live grasses (*Brachiaria plantaginea* (Link) or *Digitaria ciliaris* (Retz) (Cyperales: Poaceae)), were grown in pots in a greenhouse. Each leaf-cage was 4.0 by 5.5 by 2.0 cm, with a small hole covered with fine mesh. Each hopper was maintained in a rearing room at 25 ± 2 °C, 50 % relative humidity, with a photoperiod of 12: 12 h (L:D) for a 45 days period. After 45 days each leaf-cage was reviewed to collect the emerged adult parasitoid and the hopper host, which were collected and stored in 70% ethanol for future identification. Parasitoids and hoppers were identified to genus or species level by different specialists in taxonomy. Voucher specimens were deposited in the entomological collection (CAJAPE) of the University of Guadalajara, Jalisco, Mexico and in the entomological collection (MOLC) of the University of Tuscia, Viterbo, Italy.

Network size, link density, dependence, and connectance were performed with Package bipartite (Dormann et al. 2008) of R software, and nestedness was conducted with ANINHADO (Guimarães and Guimarães 2006).

Results

The grasses found bordering the harvested maize fields during the 2014 and 2015 winter season were the following Cyperales-Poaceae: *Brachiaria plantaginea* , *Rhynchelytrum repens* (Willd), *Cynodon plectostachyus* (Schum.), *Sorgum vulgare* (Pers), and *Digitaria ciliaris*. They showed green foliage throughout the winter-dry season from January to May. Hoppers without and with parasitism evidence were found on these grasses.

Leafhopper (Hemiptera: Cicadellidae) nymphs and adults of the subfamily Deltocephalinae were parasitized mainly by wasps (Hymenoptera: Dryinidae) of the subfamily Gonatopodinae during two consecutive winter seasons of 2014 and 2015. Most of the leafhoppers with evidence of parasitism were collected in March, April, and May, when compared with those collected in January and February ($\chi^2 = 65.15$, $P < 0.05$).

Nymphs of *Exitianus* sp. and adults of *E. picatus* were parasitized in January and February by the following Dryinidae species: *Gonatopus huggerti* (Olmi), *Gonatopus mimoides* (Perkins) and *Gonatopus* sp. In addition, an undetermined species of Delphacidae was parasitized by an undetermined strepsipteran of the genus *Elenchus* (Strepsiptera: Elenchidae). In March, April, and May, more species of leafhoppers were parasitized. Nymphs and adults of *B. incisa*, *E. picatus*, *Amblysellus* sp., *D. maidis*, and *S. bicolor* were parasitized by the following Dryinidae: *G. huggerti*, *G. mimoides*, *Gonatopus breviforceps* (Kieffer), *Gonatopus caraibicus* (Olmi), and *Gonatopus* sp. (Table 1).

Dryinids of the genus *Gonatopus* attacked leafhoppers belonging to different tribes throughout the 2014 and 2015 winter seasons. For example, *G. mimoides* attacked leafhoppers of different tribes almost the whole winter season, parasitizing *D. maidis* and *B. incisa* (Macrostelini), *E. picatus* (Chiasmini), and *Amblysellus* sp. (Deltocephalini), whereas species such as *G. caraibicus* parasitized *Amblysellus* sp. (Deltocephalini) and *S. bicolor* (Stenometopiini) (Fig. 1).

Host (hopper)-parasitoid interactions are indicated by a qualitative network of species that occur on winter perennial grasses bordering harvested fields of maize. The network comprises 13 species (six parasitoid species and seven hopper host taxa) (Fig. 2). Every hopper species was parasitized by two species of parasitoids. *Gonatopus mimoides* and *G. huggerti* parasitize the largest proportion of the hopper species (four and three species respectively) while *G. breviforceps* parasitizes only one. Although *G. mimoides* was the species with the highest density of interactions, it shows a marked dependence (0.60) on *E. picatus*, in contrast with *G. huggerti* which showed three interactions, but with the same dependence (0.33) on each of them. The connectance was less than 0.31. The nestedness was 0.65; however, it was not significantly lower than expected by chance ($P > 0.05$).

Discussion

The present study is a report on the grass species (first trophic level), the herbivore hoppers and their nymphs (second trophic level), and adult parasitoids (third trophic level), that live during the winter-dry season on the edges of maize fields once the crop is harvested. Our results agree with those of Altieri and Letourneau (1982), Tscharntke (2000), Marshall and Moonen (2002) and Ramsden et al. (2015), who found that edge vegetation is a key factor in the maintenance of parasitoids. Natural enemies abundance and diversity is increased by the vegetation on the edges in crops such as maize (Moya-Raygoza and Becerra-Chiron 2014), grapes (Nicholls et al. 2001, Altieri et al. 2005) and rice (Lou et al. 2013). In addition, edges not only function as habitat, but also as a site that provides hosts, food, and overwintering places for insect natural enemies (Sotherton 1985, Morris and Webb 1987).

Little is known about herbivore leafhopper vectors during winter season on the edges when the crop is absent. In maize, edge grasses host high diversity of leafhoppers, among which *Exitianus* sp. *B. incisa*, *S. bicolor*, *G. sonora*, *Amblysellus* sp., *E. picatus* and

Table 1. Adult parasitoids emerged (♀ or ♂) from the hopper in nymphal (N) or adult (A) stage collected on grasses during the winter seasons (January to May) of 2014 and 2015.

Parasitoid species	January	February	March	April	May
Gonatopus huggerti ♀	*Exitianus* sp. (N) *Exitianus picatus* (A)		*Balclutha incisa* (N)		
Gonatopus mimoides ♂ ♀		*Exitianus picatus* (A)	*Balclutha incisa* (A) *Exitianus picatus* (N)	*Exitianus picatus* (N) *Amblysellus* sp. (N) *Exitianus picatus* (A)	*Exitianus picatus* (A) *Exitianus picatus* (N) *Balclutha incisa* (A) *Dalbulus maidis* (A)
Gonatopus breviforceps ♀			*Balclutha incisa* (A)		*Balclutha incisa* (A)
Gonatopus caraibicus ♀				*Stirellus bicolor* (A) *Amblysellus* sp. (N) *Stirellus bicolor* (A)	*Stirellus bicolor* (A) *Amblysellus* sp. (A)
Gonatopus sp.♂	*Exitianus* sp. (N)			*Amblysellus* sp. (N)	*Amblysellus* sp. (A)
Elenchus sp.	Planthopper (A)				
Total with evidence of parasitism	5	2	29	27	28

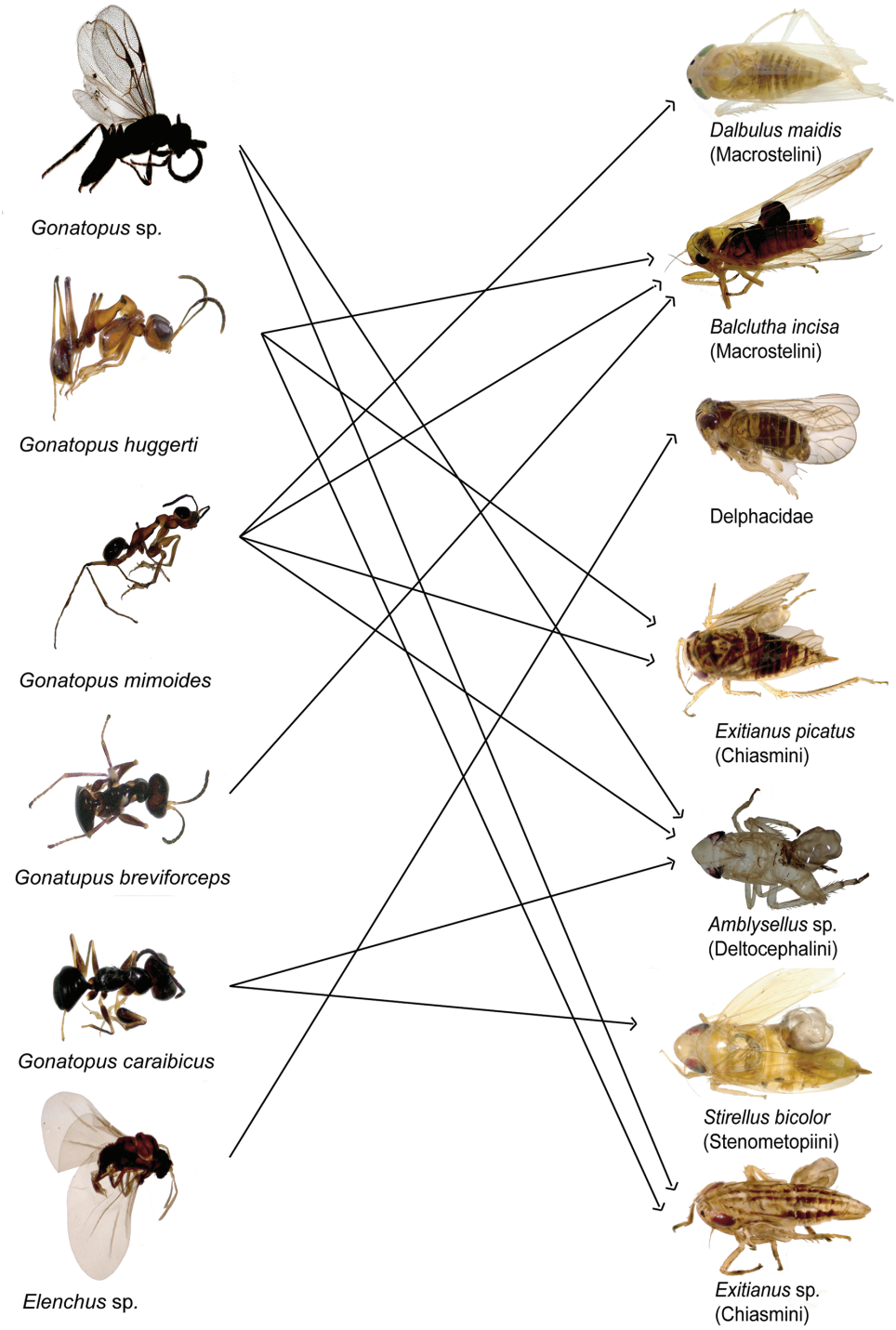

Figure 1. Total of parasitoid-host interactions found on the edges of maize agroecosystem in the winter seasons of 2014 and 2015. Name in parenthesis show the name of the host tribe.

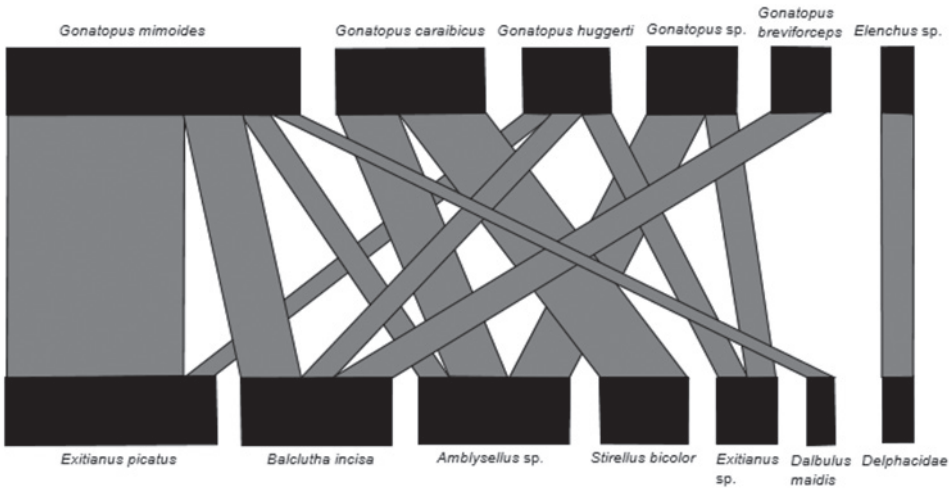

Figure 2. Quantitative food web of parasitoid-host interaction found on the edges of maize agroecosystem in the winter seasons of 2014 and 2015. Top names are the parasitoid species and bottom names are the host species.

D. elimatus are the most abundant species (Pinedo-Escatel and Moya-Raygoza 2015). Among the previous species, the literature indicates that the leafhopper *Exitianus* sp. transmits CSS (Virla 2000), *S. bicolor* transmits CSS, MRFV, and MCDV (Nault and Bradfute 1979, Nault and DeLong 1980), and *D. maidis* transmits CSS, MBSP, and MRFV (Nault 1990). Fortunately during winter edge grasses host leafhoppers that do not carry plant pathogenic bacteria and virus (Torres-Moreno et al. 2015). Results of the present study indicate grasses are green all the time bordering maize field and during the winter are a green food resource for leafhoppers free of plant pathogenic bacteria and viruses, but hosting nymph and adult parasitoids.

Six parasitoids species develop and emerge from nymph or adult hoppers. The most abundant leafhopper species were attacked by dryinids, among which most species are reported for first time on edge grasses. Previously, *G. caraibicus* was reported as a parasitoid of the leafhoppers *Amplicephalus simpliciusculus* (Linnavuori), *Haldorus sexpunctatus* (Berg), *Chlorotettix* sp., *Planicephalus flavicosta* (Stål), *Exitianus obscurinervis* (Stål) and *Graminella stelliger* (Berg) (Guglielmino et al. 2013, Olmi and Virla 2014). In the present study *S. bicolor* and *Amblysellus* sp. leafhoppers are parasitized by *G. caraibicus* in April and May on edge grasses. For the first time *G. huggerti* is reported to attack *E. picatus* and *B. incisa* on grasses during winter. This parasitoid was found previously attacking *Exitianus* sp., *Polyamia tolteca* Kramer, *Polyamia satur* (Ball), *Planicephalus flavicosta* (Stål) and *Graminella comata* (Ball) in Mexico, Peru, Paraguay and Puerto Rico (Olmi et al. 2000, Garcete-Barret 2001, Moya-Raygoza and Olmi 2010, Olmi and Virla 2014). For the first time leafhopper hosts of *G. mimoides* are reported in Mexico: *E. picatus*, *B. incisa*, *D. maidis*, and *Amblysellus* sp. (for the USA see also Guglielmino et al. 2013). In addition, *G. breviforceps*, which has a Neo-

tropical distribution, is reported for the second time attacking *B. incisa* (see for the first time Moya-Raygoza and Olmi 2010). Most of the above new records were obtained because previous studies have not been focused on the edge grasses and the leafhopper-parasitoid interactions that occur on these winter grasses with green foliage.

Parasitoids attacked, developed and emerged from nymphs and adult leafhoppers belonging to different tribes. This report indicates that most parasitoids that live on the edge grasses during winter are generalists. Egg parasitoids, i.e *Anagrus breviphragma* Soyka (Hymenoptera: Mymaridae), *Paracentrobia* sp. and *Pseudoligosita* sp. (Hymenoptera: Trichogrammatidae), also were generalists. They are the most common parasitoids attacking the eggs of *D. maidis* during the maize growing season in Mexico (Moya-Raygoza et al. 2012). These egg parasitoids attack not only the corn leafhopper but also the eggs of several species of cicadellids and delphacids (Moya-Raygoza et al. 2012).

Generalist parasitoids are important because a wide host range is a vital parameter with regard to a natural enemy´s quality as a control agent (Salvo and Valladares 1997). Also generalist parasitoids show more plastic behavior and they have the ability to use a wide diversity of host resources, in which host availability changes through time (Raymond et al. 2015), particularly when abiotic factors such as temperature and humidity change during the winter-dry season on the maize edges. In central Mexico the lowest temperatures occur in January and February reaching 5 °C in January. Between March and May the lowest temperature was between 12 and 19 °C (Pinedo-Escatel and Moya-Raygoza 2015). Host-parasitoid food webs are altered by habitat modification in agriculture systems (Tylianakis et al. 2007) but no study has investigated the food web in field margins or edges of maize agroecosystems. This study shows that the food web on edges of maize fields supports the presence of herbivore leafhoppers and their parasitoids. The connection found in this study was less than 31%. Also the nesting index was of 0.65 indicating the network is not nested (Dunne et al. 2002).

Edges with reduced management intensity show an increase in immigration of insects, particularly natural enemies (Batáry et al. 2012). In our case, edges of maize fields are unmanaged, so they conserve the biodiversity of leafhoppers and their dryinid parasitoids, as found in the present study. A similar result was obtained by Moya-Raygoza and Becerra-Chiron (2014), concerning leafhopper egg parasitoids. This biodiversity occurs in part because grasses are green, resulting in food available for leafhoppers, which depend on a liquid diet. These grasses thus are a perennial habitat for leafhoppers and their parasitoids. Perennial edges also increase biodiversity (Altieri 1999, Werling et al. 2011). In addition, predation of pests in crops by different arthropods increases when perennial habitats such as grasslands and forests are found in the agricultural landscape (Dix et al. 1995, Werling et al. 2011). Conserving biodiversity on edges during winter is important for the natural enemies because they could colonize the new maize plants seeded in the wet season in June. Traditionally maize edges are considered sites for overwintering of insect pests (Free and Williams 1979) and local farms burn the edges and stubble. However burning the maize edges and stubble before seeding maize generates high level of carbon dioxide, affecting global warming (Li et al. 2007, Tylianakis et al. 2008).

In conclusion, edges that surround maize agroecosystem during winter hold leafhoppers from different tribes, which are attacked by generalist parasitoids. A food web of leafhoppers-parasitoids is presented for the first time for maize field edges formed by grasses. It is important to conserve this biodiversity of parasitoids for the conservation of natural biological control in maize edges.

Acknowledgments

We thanks Massimo Olmi (Tropical Entomology Research Center) for the identification of dryinids, Jeyaraney Kathirithamby (University of Oxford) for the identification of the Strepsipteran taxon, Christopher Dietrich (Illinois National History Survey Museum) and Adilson Pinedo-Escatel (CUCBA, Universidad de Guadalajara) for the identification of leafhoppers. Also we thank Liberato Portillo (CUCBA, Universidad de Guadalajara) for the suggestions during the study and Jose Luis Villalpando Prieto (SAGARPA) for the grasses determination.

References

Altieri MA (1999) The ecological role of biodiversity in agroecosystems. Agriculture, Ecosystems & Environment 74: 19–31. https://doi.org/10.1016/S0167-8809(99)00028-6

Altieri MA, Letourneau DK (1982) Vegetation management and biological control in agroecosystems. Crop Protection 1: 405–430. https://doi.org/10.1016/0261-2194(82)90023-0

Altieri MA, Ponti L, Nicholls CI (2005) Manipulating vineyard biodiversity for improved insect pest management: case studies from northern California. International Journal of Biodiversity Science & Management 1: 191–203. https://doi.org/10.1080/17451590509618092

Batáry P, Holzschuh A, Orci KM, Samu F, Tscharntke T (2012) Responses of plant, insect and spider biodiversity to local and landscape scale management intensity in cereal crops and grasslands. Agriculture, Ecosystems & Environment 146: 130–136. https://doi.org/10.1016/j.agee.2011.10.018

Buckler ES, Thornsberry JM, Kresovich S (2001) Molecular diversity, structure and domestication of grasses. Genetical Research 77: 213–218. https://doi.org/10.1017/S0016672301005158

Carloni E, Virla EG, Paradell S, Carpane P, Nome C, Laguna I, Giménez Pecci MP (2011) *Exitianus obscurinervis* (Hemiptera: Cicadellidae), a new experimental vector of *Spiroplasma kunkelii*. Journal of Economic Entomology 104: 1793–1799. https://doi.org/10.1603/EC11156

Dennis P, Fry GL (1992) Field margins: can they enhance natural enemy population densities and general arthropod diversity on farmland?. Agriculture, Ecosystems & Environment 40: 95–115. doi.org/10.1016/0167-8809(92)90086-Q

Dix ME, Johnson RJ, Harrell MO, Case RM, Wright RJ, Hodges L, Young LJ (1995) Influences of trees on abundance of natural enemies of insect pests: a review. Agroforestry Systems 29: 303–311. https://doi.org/10.1007/BF00704876

Dormann CF, Gruber B, Fründ J (2008) Introducing the bipartite package: analysing ecological networks. R news 8: 8–11.

Dunne JA, Williams RJ, Martinez ND (2002) Food-web structure and network theory: the role of connectance and size. Proceedings of the National Academy of Sciences of the United States of America 99: 12917–12922. https://doi.org/10.1073/pnas.192407699

Free JB, Williams IH (1979) The distribution of insect pests on crops of oil-seed rape (*Brassica napus* L.) and the damage they cause. The Journal of Agricultural Science 92: 139–149. https://doi.org/10.1017/S0021859600060597

Garcete-Barret BR (2001) Adendo al catálogo de los Dryinidae (Hymenoptera: Chrysidoidea) del Paraguay. Boletin del Museo Nacional de Historia Natural del Paraguay 13: 53–55. www.faunaparaguay.com/bmnhnpy2001garcete7.pdf

Guglielmino A, Olmi M, Bückle C (2013) An updated host-parasite catalogue of word Dryinidae (Hymenoptera: Chrysidoidea). Zootaxa 3740: 1–113. https://doi.org/10.11646/zootaxa.3740.1.1

Guimarães PR, Guimarães P (2006) Improving the analyses of nestedness for large sets of matrices. Environmental Modelling & Software 21: 1512–1513. https://doi.org/10.1016/j.envsoft.2006.04.002

Hamilton KGA, Whitcomb RF (2010) Leafhoppers (Homoptera: Cicadellidae): a major family adapted to grassland habitats. In: Shorthouse JD, Floate KD (Eds) In arthropods of canadian grasslands. Biological Survey of Canada (Ottawa): 169–197. https://doi.org/10.3752/9780968932148.ch8

Kathirithamby J (2005) Strepsiptera (Insecta) of Mexico–A Review. In: Julio SB, Refugio LF (Eds) Monograph No. 12, Vedalia, México, 103–118. http://www.smcb-mx.org/Documentos%20Vedalia/vol_12b/VedaliaVol12_2C.pdf

Li X, Wang S, Duan L, Hao J, Li C, Chen Y, Yang L (2007) Particulate and trace gas emissions from open burning of wheat straw and corn stover in China. Environmental, Science & Technology 41: 6052–6058. https://doi.org/10.1021/es0705137

Lou Y-G, Zhang G-R, Zhang W-Q, Hu Y, Zhang J (2013) Biological control of rice insect pests in China. Biological Control 67: 8–20. https://doi.org/10.1016/j.biocontrol.2013.06.011

Marshall EJP, Moonen AC (2002) Field margins in northern Europe: their functions and interactions with agriculture. Agriculture, Ecosystems & Environment 89: 5–21. https://doi.org/10.1016/S0167-8809(01)00315-2

Morris MG, Webb NR (1987) The importance of field margins for the conservation of insects. In: Way JM, Grieg-Smith PW (Eds) Field margins. Monograph No. 35, Thornton Heath, London, 53–65.

Moya-Raygoza G, Albarracin EL, Virla EG (2012) Diversity of egg parasitoids attacking *Dalbulus maidis* (Hemiptera: Cicadellidae) populations at low and high elevation sites in Mexico and Argentina. Florida Entomologist 95: 105–112. https://doi.org/10.1653/024.095.0117

Moya-Raygoza G, Becerra-Chiron IM (2014) Overwintering biology of egg parasitoids of *Dalbulus maidis* (Hemiptera: Cicadellidae) on perennial grasses, volunteer maize, stubble, and drip-irrigated maize. Annals of the Entomological Society of America 107: 926–932. https://doi.org/10.1603/AN14003

Moya-Raygoza G, Olmi M (2010) A catalogue of Dryinidae of Mexico with descriptions of the opposites sexes of same species (Hymenoptera Chrysidoidea). Frustula Entomologica New Series 31: 77–112.

Narhardiyati M, Bailey WJ (2005) Biology and natural enemies of the leafhopper *Balclutha incisa* (Matsumura) (Hemiptera: Cicadellidae: Deltocephalinae) in south-western Australia. Australian Journal of Entomology 44: 104–109. https://doi.org/10.1111/j.1440-6055.2005.00460.x

Nault LR (1980) Maize bushy stunt and corn stunt: a comparison of disease symptoms, pathogen host ranges, and vectors. Phytopathology 70: 659–662. https://doi.org/10.1094/Phyto-70-659

Nault LR (1990) Evolution of an insect pest: maize and the corn leafhopper, a case study. Maydica 35: 165–175.

Nault LR, Bradfute OE (1979) Corn stunt: involvement of a complex of leafhopper-borne pathogens. In: Maramorosch K, Harris KF (Eds) Leafhopper vectors and plant disease agents. Academic Press, London, 561–586. https://doi.org/10.1016/B978-0-12-470280-6.50021-0

Nault LR, DeLong DM (1980) Evidence for co-evolution of leafhoppers in the genus *Dalbulus* (Cicadellidae: Homoptera) with maize and its ancestors. Annals of the Entomological Society 73: 349–353. https://doi.org/10.1093/aesa/73.4.349

Nicholls CI, Parrella M, Altieri MA (2001) The effects of a vegetational corridor on the abundance and dispersal of insect biodiversity within a northern California organic vineyard. Landscape Ecology 16: 133–146. https://doi.org/10.1023/A:1011128222867

Olmi M, Virla EG (2014) Dryinidae of the Neotropical region (Hymenoptera: Chrysidoidea). Zootaxa 3792: 1–534. doi.org/10.11646/zootaxa.3792.2.1

Olmi M, Virla EG, Fernández F (2000) Las avispas Dryinidae de la región neotropical (Hymenoptera: Chrysidoidea). Biota Colombiana 1: 141–163.

Pinedo-Escatel JA, Moya-Raygoza G (2015) Diversity of leafhoppers during the winter dry season on perennial grasses bordering harvested fields of maize. Southwestern Entomologist 40: 263–272. https://doi.org/10.3958/059.040.0203

Rabb RL, Stinner RE, Van den Bosch R (1976) Conservation and augmentation of natural enemies. In: Huffaker CB, Messenger PS (Eds) Theory and practice of biological control. Academic Press, New York, 233–249.

Ramsden MW, Menéndez R, Leather SR, Wäckers F (2015) Optimizing field margins for biocontrol services: the relative role of aphid abundance, annual floral resources, and overwinter habitat in enhancing aphid natural enemies.Agriculture, Ecosystems & Environment 199: 94–104. https://doi.org/10.1016/j.agee.2014.08.024

Raymond L, Ortiz-Martínez SA, Lavandero B (2015) Temporal variability of aphid biological control in contrasting landscape contexts. Biological Control 90: 148–156. https://doi.org/10.1016/j.biocontrol.2015.06.011

Rios-Reyes AV, Moya-Raygoza G (2004) Ciclo biológico, parasitismo y depredación de *Gonatopus bartletti* Olmi 1984 (Hymenoptera: Dryinidae), un enemigo natural de la chicharrita *Dalbulus maidis* (Delong y Wolcott 1923) (Hemiptera: Cicadellidae). Folia Entomologica Mexicana 43: 249–255. http://bio-nica.info/Biblioteca/Rios2004Gonatopus.pdf

Salvo A, Valladares GR (1997) An analysis of leaf-miner and plant host ranges of three *Chrysocharis* species (Hym.: Eulophidae) from Argentina. Entomophaga 42: 417–426. https://doi.org/10.1007/BF02769835

Sotherton NW (1985) The distribution and abundance of predatory Coleoptera overwintering in field boundaries. Annals of Applied Biology 106: 17–21. https://doi.org/10.1111/j.1744-7348.1985.tb03089.x

Torres-Moreno R, Moya-Raygoza G, Pérez-López E (2015) Absence of corn stunt spiroplasma and maize bushy stunt phytoplasma in leafhoppers (Hemiptera: Cicadellidae) that inhabit edge grasses throughout winter in Jalisco, Mexico. Florida Entomologist 98: 967–969. https://doi.org/10.1653/024.098.0325

Tscharntke T (2000) Parasitoid populations in the agricultural landscape. In: Hochberg ME, Ives AR (Eds) Parasitoid Population Biology. Princeton University Press (Princeton, USA) 235–253.

Tylianakis JM, Tscharntke T, Lewis OT (2007) Habitat modification alters the structure of tropical host–parasitoid food webs. Nature 445: 202–205. https://doi.org/10.1038/nature05429

Tylianakis JM, Didham RK, Bascompte J, Wardle DA (2008) Global change and species interactions in terrestrial ecosystems. Ecology Letters 11: 1351–1363. https://doi.org/10.1111/j.1461-0248.2008.01250.x

Virla EG (2000) Aportes al conocimiento del complejo de enemigos naturales de *Exitianus obscurinervis*(Insecta-Cicadellidae). Boletín de sanidad vegetal, Plagas, Madrid España 26: 365–375. www.bio-nica.info/biblioteca/Virla2001Cicadellidae.pdf

Vollhardt IM, Tscharntke T, Wäckers FL, Bianchi FJ, Thies C (2008) Diversity of cereal aphid parasitoids in simple and complex landscapes. Agriculture, Ecosystems & Environment 126: 289–292. https://doi.org/10.1016/j.agee.2008.01.024

Wayadande AC, Nault LR (1993) Leafhopper probing behavior associated with maize chlorotic dwarf virus transmission to maize. Phytopathology 83: 522–526. https://doi.org/10.1094/Phyto-83-522

Weintraub PG, Beanland L (2006) Insect vectors of phytoplasmas. Annual Review of Entomology 51: 91–111. https://doi.org/10.1146/annurev.ento.51.110104.151039

Werling BP, Meehan TD, Gratton C, Landis DA (2011) Influence of habitat and landscape perenniality on insect natural enemies in three candidate biofuel crops. Biological Control 59: 304–312. https://doi.org/10.1016/j.biocontrol.2011.06.014

JHR 57: 167–177 (2017)
doi: 10.3897/jhr.57.13506
http://jhr.pensoft.net

CORRIGENDA

JOURNAL OF Hymenoptera RESEARCH
A peer-reviewed open-access journal
The International Society of Hymenopterists

Corrigenda: Revision of the *asychis* species group of *Aphelinus* (Hymenoptera, Aphelinidae). Journal of Hymenoptera Research 54: 1–32. https://doi.org/10.3897/jhr.54.10457

Xanthe A. Shirley[1], James B. Woolley[1], Keith R. Hopper[2]

1 *Department of Entomology, Texas A&M University, College Station, TX, 77843 USA* **2** *USDA-ARS-BIIRL, Newark, DE, 19713 USA*

Corresponding author: *Xanthe A. Shirley* (xanthe.shirley@gmail.com)

Academic editor: *H. Baur* | Received 2 May 2017 | Accepted 3 May 2017 | Published 30 June 2017

http://zoobank.org/5E60F2AE-1C1E-4C5E-81AD-0C73650DB20D

Citation: Shirley XA, Woolley JB, Hopper KR (2017) Corrigenda: Revision of the *asychis* species group of *Aphelinus* (Hymenoptera, Aphelinidae). Journal of Hymenoptera Research 54: 1–32. https://doi.org/10.3897/jhr.54.10457. Journal of Hymenoptera Research 57: 167–177. https://doi.org/10.3897/jhr.57.13506

It has come to our attention that the above-referenced article was published with an older version of the plates, which results in numerous mismatches between figure numbers cited in the text, and figure numbers on the plates themselves. Below are corrected plates for all figures, with correct figure numbers that correspond to the citations of figures in the text. For convenience, the figure captions are also included below. Readers should use these corrected plates in combination with the original paper.

Copyright *Xanthe A. Shirley et al.* This is an open access article distributed under the terms of the Creative Commons Attribution License (CC BY 4.0), which permits unrestricted use, distribution, and reproduction in any medium, provided the original author and source are credited.

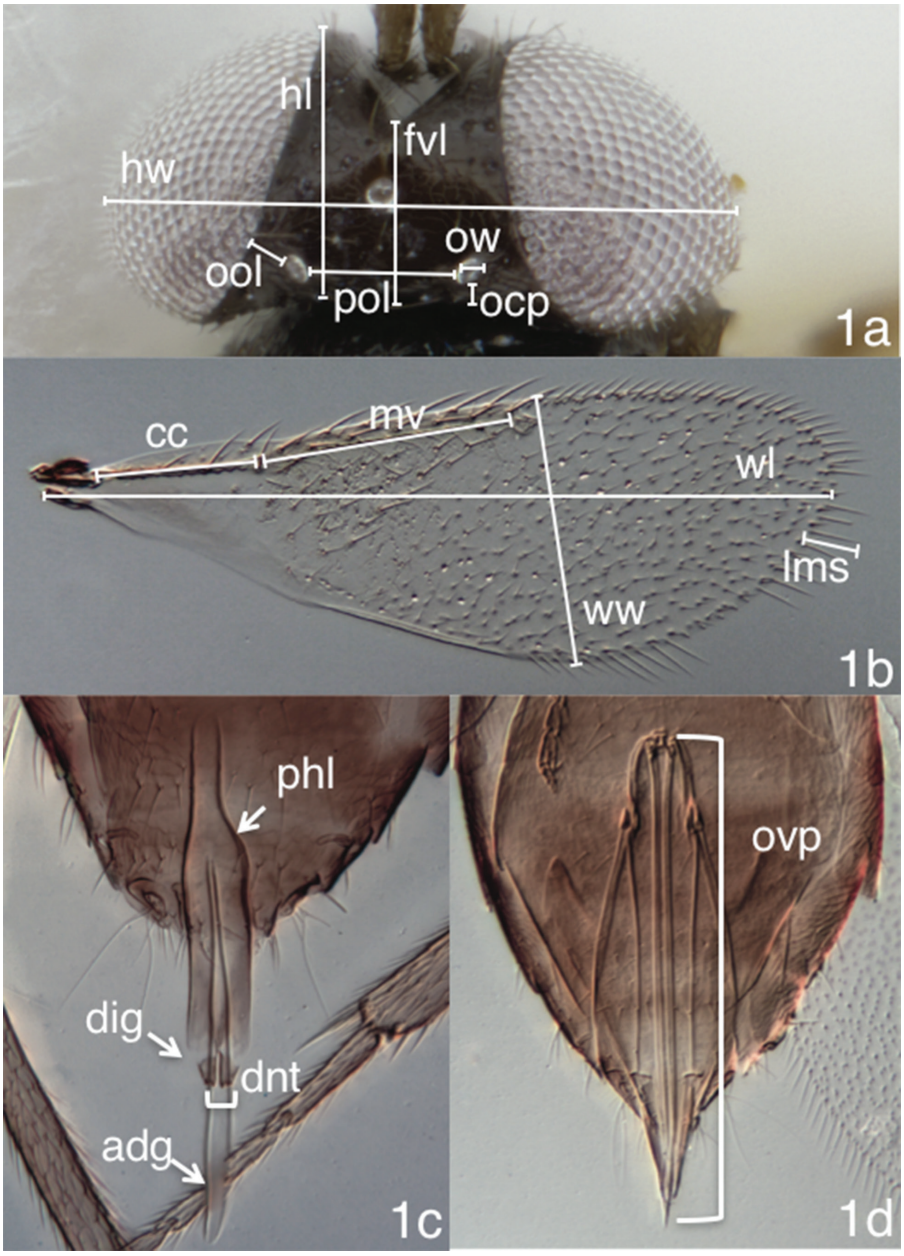

Figure 1. Measurements and terminology. **a** *Aphelinus kazakhstanensis* sp. n. female, head, dorsal view (TAMU-ENTO X0856040) (fvl: frontovertex length; hl: head length; hw: head width; ocp: posterior ocellus to occipital margin distance; ool: posterior ocellus to eye margin distance; ow: posterior ocellus width; pol: posterior interocellar distance) **b** *Aphelinus sinensis* sp. n. female, fore wing, dorsal view (TAMU-ENTO X0852875) (cc: costal cell length; mv: marginal vein length; wl: wing length; ww: wing width; lms: longest marginal seta length) **c** *Aphelinus certus* male genitalia, ventral view (TAMU-ENTO X0616479) (adg = aedeagus; dig = digiti; dnt = denticles; phl = phallobase) **d** *Aphelinus atriplicis* female, metasoma, ventral view (TAMU-ENTO X0616471) (ovp = ovipositor).

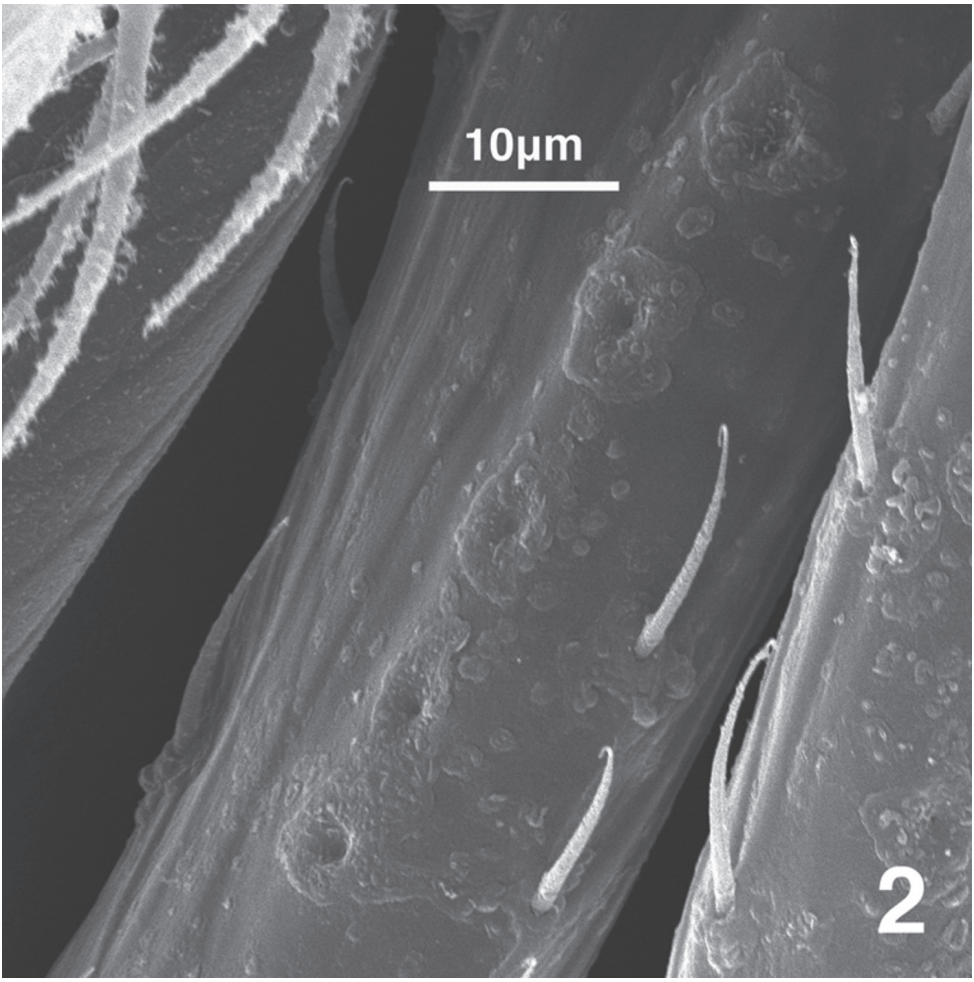

Figure 2. *Aphelinus sinensis* sp. n., male, scape, ventral view. Note the five linearly arranged exocrine gland pores.

Figure 3. *Aphelinus asychis*, card-mounted specimens. **a** male, antennae and head, lateral view (BMNH 1038770) **b** female, antennae and face, anterior view (BMNH 1038772) **c** male, habitus, lateral view (BMNH 1038770) **d** female, habitus, lateral view (BMNH 1038772) **e** male, habitus, dorsal view (BMNH 1038770) **f** female, habitus, dorsal view (BMNH 1038772).

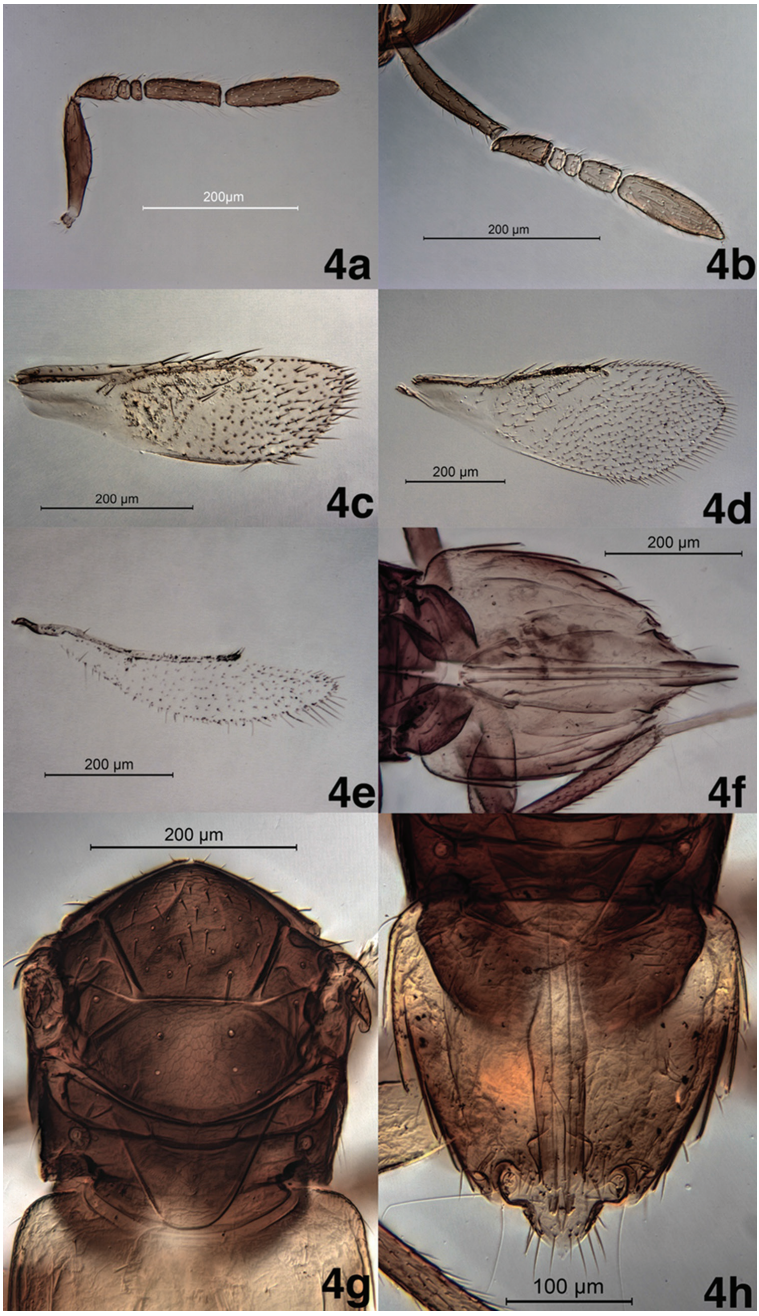

Figure 4. *Aphelinus asychis*, slide-mounted specimens. **a** male, antenna, lateral view (BMNH 1039637) **b** female, antenna, lateral view (TAMU-ENTO X0856569) **c** male, fore wing, dorsal view (TAMU-ENTO X0856303) **d** female, fore wing, dorsal view (TAMU-ENTO X0856301) **e** female, hind wing, dorsal view (TAMU-ENTO X0856301) **f** female, metasoma, ventral view (TAMU-ENTO X0856301) **g** female, mesosoma, dorsal view (TAMU-ENTO X0856301) **h** male, genitalia, ventral view (TAMU-ENTO X0856303).

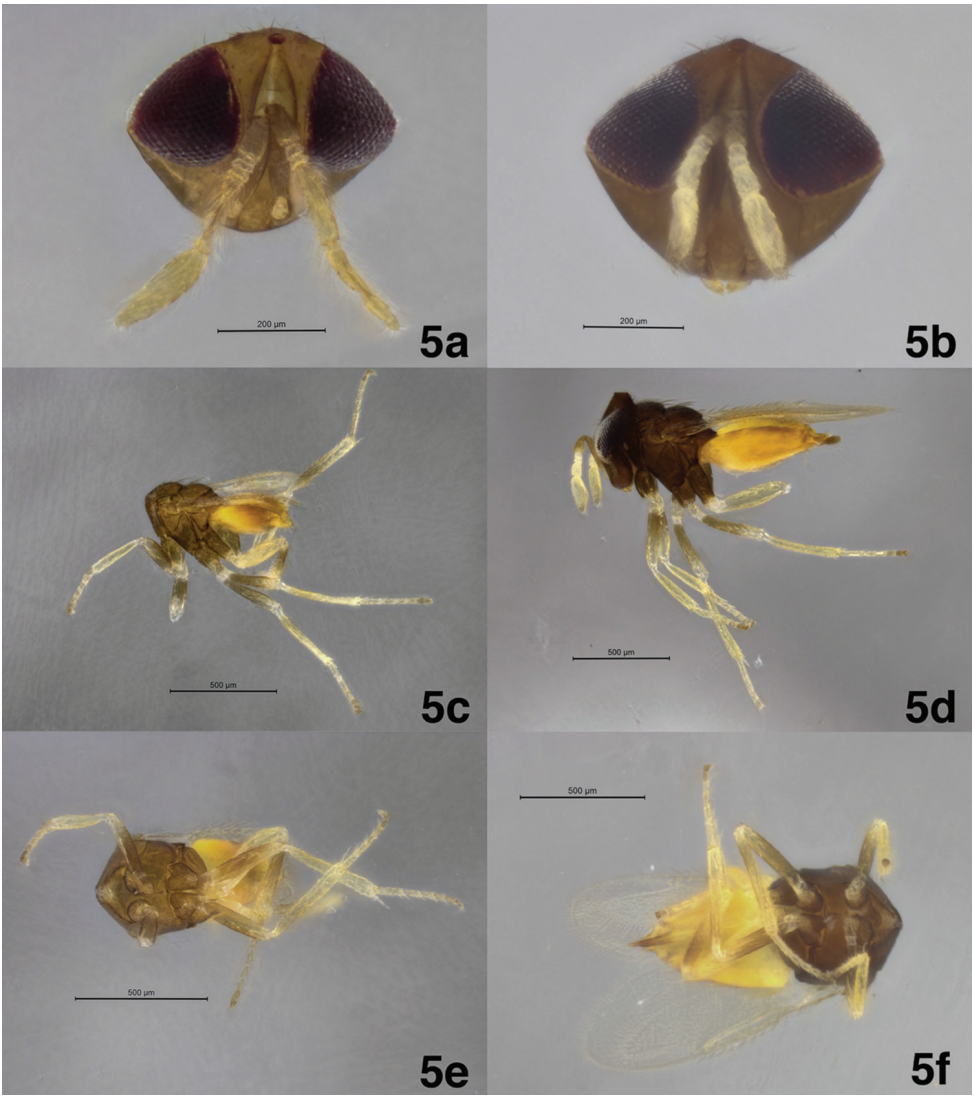

Figure 5. *Aphelinus kazakhstanensis*, paratypes in 95% ethanol. **a** male, antennae and face, anterior view (TAMU-ENTO X0856689) **b** female, antennae and face, anterior view (TAMU- ENTO X0856403) **c** male, habitus, lateral view (TAMU-ENTO X0856689) **d** female, habitus, lateral view (TAMU-ENTO X0856400) **e** male, habitus, ventral view (TAMU-ENTO X0856689) **f** female, habitus, ventral view (TAMU-ENTO X0856403).

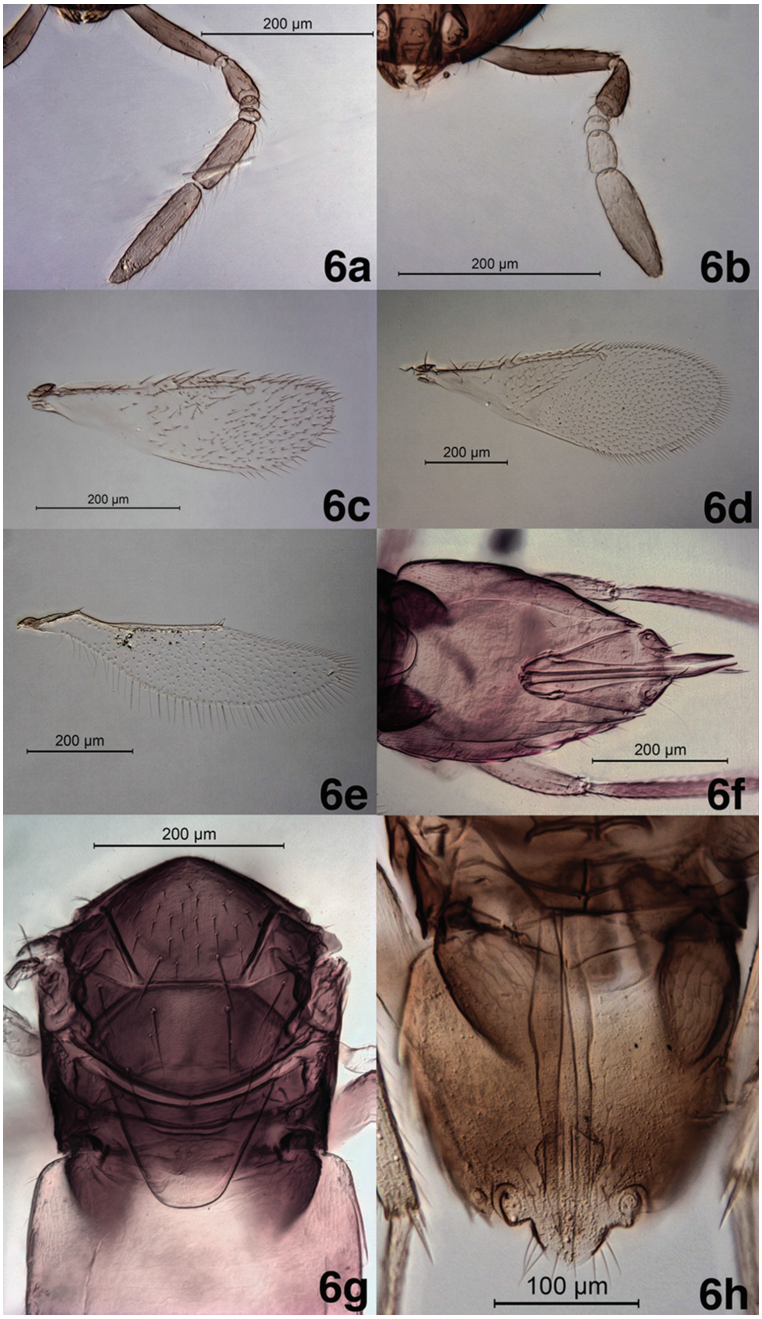

Figure 6. *Aphelinus kazakhstanensis*, slide-mounted paratypes. **a** male, antenna, lateral view (TAMU-ENTO X0856044) **b** female, antenna, lateral view (TAMU-ENTO X0855782) **c** male, fore wing, dorsal view (TAMU-ENTO X0856072) **d** female, fore wing, dorsal view (TAMU-ENTO X0616386) **e** female, hind wing, dorsal view (TAMU-ENTO X0852956) **f** female, metasoma, ventral view (TAMU-ENTO X0616386) **g** female, mesosoma, dorsal view (TAMU-ENTO X0852880) **h** male, genitalia, ventral view (TAMU-ENTO X0856075).

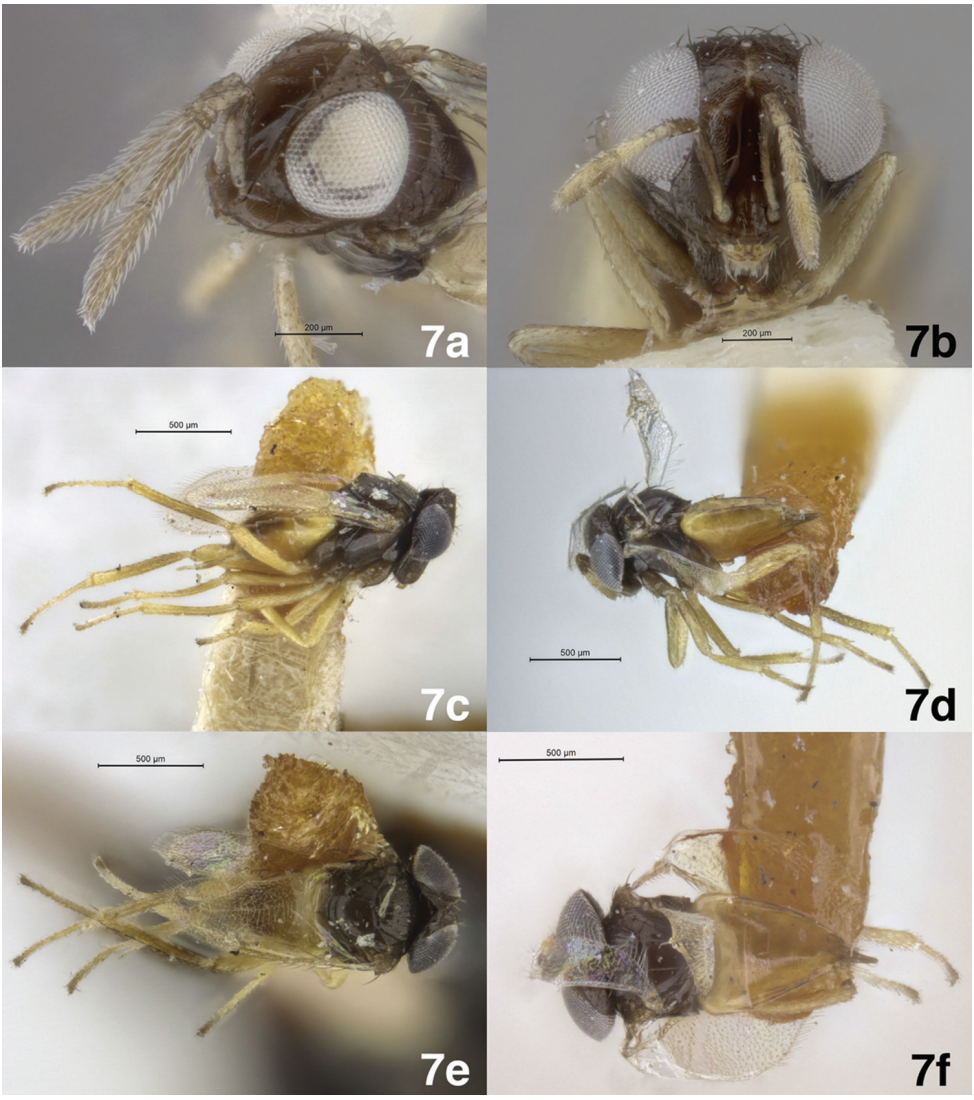

Figure 7. *Aphelinus semiflavus*, point-mounted specimens. **a** male, antennae and face, lateral view (CNC 00122807) **b** female, antennae and face, anterior view (CNC 00122818) **c** male, habitus, lateral view (USNM ENT 2076436) **d** female, habitus, lateral view (paralectotype) **e** male, habitus, dorsal view (USNM ENT 2076436) **f** female, habitus, dorsal view (paralectotype).

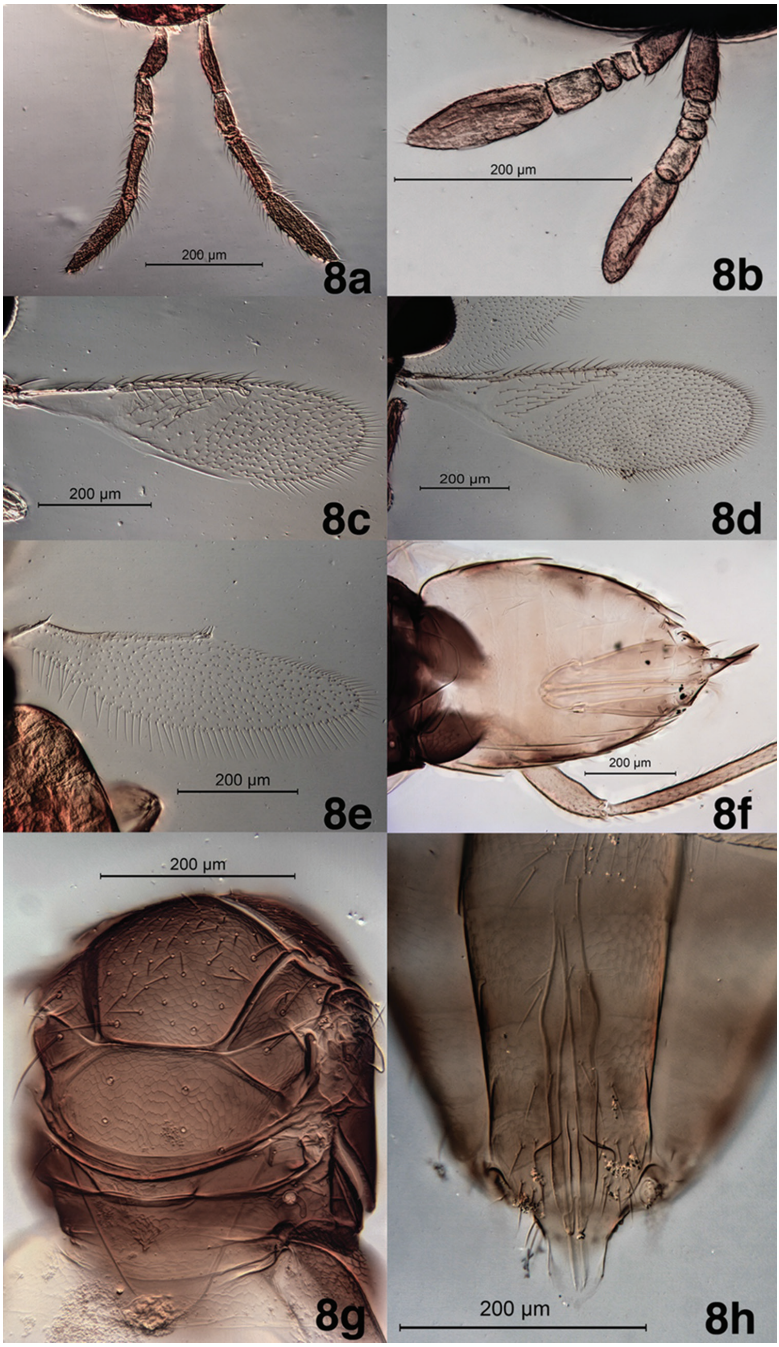

Figure 8. *Aphelinus semiflavus*, slide-mounted specimens. **a** male, antenna, lateral view (paralectotype) **b** female, antenna, lateral view (paralectotype) **c** male, fore wing, dorsal view (paralectotype) **d** female, fore wing, dorsal view (paralectotype) **e** female, hind wing, dorsal view (paralectotype) **f** female, metasoma, ventral view (UCRC ENT 326827) **g** female, mesosoma, dorsal view (CNC 00122803) **h** male, genitalia, ventral view (UCRC ENT 326826).

Figure 9. *Aphelinus sinensis* sp. n., paratypes in 95% ethanol. **a** male, antennae and face, anterior view (TAMU-ENTO X0856562) **b** female, antennae and face, anterior view (TAMU- ENTO X0856563) **c** male, habitus, lateral view (TAMU-ENTO X0856562) **d** female, habitus, lateral view (TAMU-ENTO X0856563) **e** male, habitus, ventral view (TAMU-ENTO X0856562) **f** female, habitus, ventral view (TAMU-ENTO X0856563).

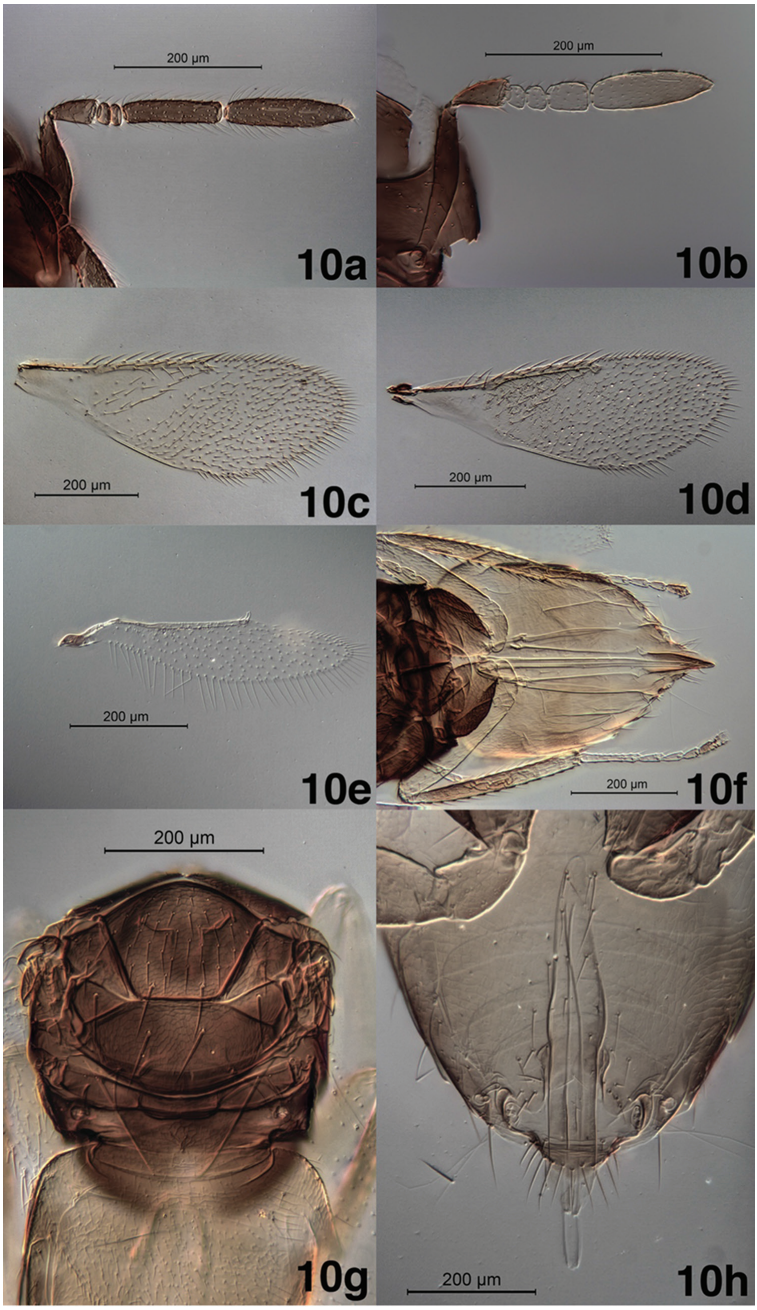

Figure 10. *Aphelinus sinensis* sp. n., slide-mounted paratypes. **a** male, antenna, lateral view (TAMU-ENTO X0852885) **b** female, antenna, lateral view (TAMU-ENTO X0852877) **c** male, fore wing, dorsal view (TAMU-ENTO X0852885) **d** female, fore wing, dorsal view (TAMU-ENTO X0852875) **e** female, hind wing, dorsal view (TAMU-ENTO X0852869) **f** female, metasoma, ventral view (TAMU-ENTO X0852880) **g** female, mesosoma, dorsal view (TAMU-ENTO X0852880) **h** male, genitalia, ventral view (TAMU-ENTO X0852885).